Dynamic System Multivariate Calibration for Optimal Primary Output Estimation

Rolf Ergon
Telemark College
Department of Technology
Porsgrunn, Norway

Thesis submitted to the
Norwegian University of Science and Technology
for the degree of Dr.ing.
July 1999

To Frida
- my granddaughter

Abstract

In industrial plants and other types of dynamic systems, it is a common situation that measurements of primary system outputs are not available on-line. The primary outputs may for example be quality properties, that can be determined only through costly laboratory analyses, i.e. they can be measured only at a low sampling rate and with a considerable time delay. Since the primary outputs give vital information on the system performance, and in fact may be the sole purpose of the system, it is of interest to estimate them continuously or at a high sampling rate. This can be done by use of a system model utilizing all available information in both the known system inputs and the secondary system outputs that often are available at a high sampling rate.

The thesis considers the identification of optimal primary output estimators for this purpose from experimental data, using known system inputs and secondary measurements as estimator inputs. The estimators are based on underlying Kalman filters, and the identification can be done by use of an ordinary prediction error method. However, an optimal utilization of the secondary output information may require that an output error (OE) model structure is specified. This is one of the major new insights provided by the thesis.

With low noise secondary measurements, it is in some cases possible to use estimators of reduced complexity. This is found from an analysis of perfect measurement cases, and further developed into a systematic method for finding a parsimonious estimator with a minimized mean-squared validation error.

The experimental data must include primary output measurements. It is, however, shown in the thesis that also low and even irregular primary output sampling rate data may be used for the purpose, provided that the prediction error method is appropriately modified. This is a direct consequence of the OE structure used, including the use of secondary measurements as estimator inputs, and it is considered to be of significant practical and economical importance.

It is also shown in the thesis that the ordinary least squares (LS) estimator for static systems is a special case of the general current (a posteriori) OE estimator for dynamic systems. This also forms a link from Kalman filtering to principal component analysis (PCA), and to the chemometrical principal component regression (PCR) and partial least squares regression (PLSR) methods based on data

compression into latent variables. These methods make use of data weighting matrices, and assuming a latent variable data structure, the optimal weighting matrix is shown to be a transposed Kalman gain. It is further shown that in cases with a few independent and many dependent and collinear regressor variables, the best solution may be obtained by use of a two-step PCA/PLSR+LS solution, where the independent variables are used only in the second step.

The static latent variables methods are finally combined with the developed methods for identification of dynamic primary output estimators, leading to two-step PCA+OE and PLSR+OE methods, where the known inputs are used only in the second step.

The theory and methods developed are tested on simulated data. They are also tested on data from industrial plants and experimental test rigs, primarily with operator support applications in mind.

Further applications in e.g. failure detection and feedback control are given a preliminary discussion.

Preface and acknowledgments

This thesis will hopefully help to bridge the gap between the scientific communities of automatic control and chemometrics. The first part is clearly rooted in the fields of dynamic systems theory and system identification. It is intentionally written in a detailed fashion, in order to ease the reading for interested chemometricians, and an appendix gives a short introduction to Kalman filtering theory. The chemometrical part emphasizes the relation to dynamic systems theory, and only short introductions to the chemometrical algorithms are given in an appendix. All the interesting and valuable methods related to latent variables interpretation are, however, omitted, and readers that are not familiar with this are encouraged to spend some time with the references given.

The thesis and the accompanying course exams (one full time year curriculum) are the results of six years of work in parallel with my lecturing position at the Department of Technology at Telemark College, Norway. In this period the board of the college granted me two semesters leave of absence, and both the department and the board deserves an acknowledgment for that.

Several of my colleagues at the department also deserves an acknowledgment. Professor Jens I. Ytreeide agreed to act as formal supervisor, while professor Kim H. Esbensen has been formal co-supervisor. Although none of them has been deeply involved in my work, I want to thank them both for encouragement and fruitful discussions on the basic aim and parts of the thesis. Associate professor David Di Ruscio encouraged me to present my results internationally at conferences and in journals. He was also the co-author of the first of my six papers on the subject of the thesis, and I thank him for that cooperation. Associate professor Bernt Lie introduced me to Scientific WorkPlace and Visio Technical, and deserves sincere thanks for his general helpfulness.

A number of M.Sc. students at Telemark College have collected industrial data and applied my methods as part of their project and thesis work, and I want to thank them all for their efforts. They were: Cecilie Gjermundbo, Harald Faanes, Vidar B. Gundersen, Bjørn Karlstad, Evy Kristine Karstensen, Getahun Melka, Jan-Ole Omland, Egil Romberg, Ragnar Røstad, Espen Sæter, Kenneth Tvedt and Jørn Owe Wilhelmsen. As they worked on the basis of my theoretical results and under my supervision, I have felt free to use some of their practical results

in the thesis. I also want to express my sincere thanks to the companies involved in these student assignments. My main contact persons and the companies were: Kjetil L. Børve, Kristian Helland, Ulf A. Stendal and Eric Wilsher at Borealis AS, Lammert J. Altena at Icopal AS, Terje Karstang at Norsk Hydro ASA and Ketil Svinning at Norcem AS. All these companies have vital parts of their industrial activities located in the county of Telemark.

Some experiments were performed at the acoustic test rig of the Applied Chemometrics Group at Telemark College and the Tel-Tek research foundation. The group is initiated and led by Kim Esbensen, and Ph.D. student Maths Halstensen is acknowledged for his helpfulness with these experiments.

During the six years that I have been engaged in this Ph.D. program, I have had the pleasure to see both my daughter and my son entering Ph.D. programs of their own. Åshild has now received her degree in plant pathology at the Agricultural University of Norway, while Torbjørn is deeply involved in a zoological ecology project at the University of Oslo in cooperation with the University of Aberdeen. I found these parallel developments quite inspiring, and I want to thank them both for interesting discussions on general scientific subjects.

Finally, I want to thank my wife Målfrid for moral support during less bright periods of my work, and for a great deal of patience during the entire project. Her insistence on keeping up a variety of outdoor and other weekend activities has been good for my body as well as for my often far too narrow mid-week mind. In the final stage she also corrected a number of errors in my American English.

Porsgrunn, July 1999

Rolf Ergon

Contents

Nomenclature

Abbreviations and acronyms

ARMAX	AutoRegressive Moving Average with eXogenous inputs
ARMAXP	Reference to ARMAX prediction estimator
ARMAXC	Reference to ARMAX current estimator
$ARMAX_2$	Reference to ARMAX model not using primary output information
$ARMAX_2P$	Reference to $ARMAX_2$ prediction estimator
$ARMAX_2C$	Reference to $ARMAX_2$ current estimator
ARX	AutoRegressive with eXogenous inputs
Cov, Var	Covariance/variance
$\det(\cdot)$	Determinant of a matrix
$\dim(\cdot)$	Dimension of vector/matrix
FDI	Fault Detection and Isolation
FIR	Finite Impulse Response (model)
KF	Kalman Filter
LS	Least Squares
MAE	Mean Absolute Error
MSE	Mean Squared Error
OE	Output Error
OEC	Output Error Current (estimator)
OEP	Output Error Prediction (estimator)
PCA	Principal Component Analysis
PCR	Principal Component Regression
PEM	Prediction Error Method
PLSR	Partial Least Squares Regression
RMSE	Root Mean Square Error
PRBS	Pseudo-Random Binary Sequence
PT	Pressure Transmitter
QT	Quality Transmitter
SI	System Identification
SVD	Singular Value Decomposition
TT	Temperature Transmitter

Latin letters

Symbol	Description
a, a_i	scalar parameter or gain factor
a, a_2	number of components in PCA/PCR/PLSR
A^c, A^c_{ij}, A, A_{ij}	transition matrix or block part of transition matrix (continuous-time/discrete-time system)
$A\left(q^{-1}\right)$, $B\left(q^{-1}\right)$ etc.	polynomial in the unit time delay operator
b, b_i	scalar parameter or gain factor
b, b_1, b_2	theoretical parameter vector in linear regression
$\hat{b}$, $\hat{b}_1$, $\hat{b}_2$	data based parameter vector in linear regression
B^c, B	input matrix (continuous-time/discrete-time system)
B^{LS}, B^{KF}, B^{PCR}, B^{PLSR}	theoretical parameter matrix in linear regression
$\hat{B}^{\mathrm{LS}}$, $\hat{B}^{\mathrm{KF}}$, $\hat{B}^{\mathrm{PCR}}$, $\hat{B}^{\mathrm{PLSR}}$	data based parameter matrix in linear regression
C, C_1, C_2	output matrix (general/primary output/secondary output)
$d, d(t), d_k$	plant disturbance (general/continuous-time/discrete-time)
dT	dead time in discrete-time system
D, D_1, D_2	direct input-output matrix (general/primary output/secondary output)
e, $e(t)$, e_k	white innovations (general/continuous-time/discrete-time system)
E	residual matrix
Ex	mathematical expectation of random variable x
f, f_i	scalar parameter
G^c, G	white process noise input matrix (continuous-time/discrete-time system)
G_d	process disturbance input matrix
$G(q^{-1}, \theta)$, $H(q^{-1}, \theta)$	transfer function for discrete-time system
h	scalar function in PEM criterion function
h_i	Markov parameter vector in Hankel matrix
H_n	Hankel matrix of order n
I	unity matrix
j	discrete time step number
$J_N(\theta)$	PEM criterion function
k	discrete time step number
k^c, k^c_{ij}, k, k_{ij}	vector/element in Kalman gain (continuous-time/discrete-time system)

K^c, K	Kalman gain (continuous-time/discrete-time system)
K^{ARMAX}, K^{OE}	Kalman gain in ARMAX/OE estimator
K_2^{OE}	Kalman gain in OEC and OEP estimators
K_a	Krylov matrix of order a
L	FIR model summation limit
$\mathcal{L}$	Laplace transform operator
m	number of primary measurements
M	number of Monte Carlo runs
$(\cdot)_M$	subscript in Martens PLSR algorithm
n	model order
n_u, n_v, n_{w_2}, n_{y_2}	number of known inputs etc.
nn	row vector specifying PEM model
N, N_1, N_2	number of samples
p	time steps between observations
p	number of variables in regression problem
p_{ij}^c, p_{ij}	element in state estimation error covariance matrix (continuous-time/discrete-time system)
P^c, P	state estimation error covariance matrix (continuous-time/discrete-time system)
P	loading matrix in PCA/PCR factorization
q	vector in iterative PLSR algorithm
q	shift operator
q^{-1}	unit time delay operator
r	number of known inputs
r_v^c, r_v, r_w^c, r_w	process/measurement noise variance (continuous-time/discrete-time)
r_{ij}^c, r_{ij}	element in noise covariance matrix (continuous-time/discrete-time)
R_v^c, R_v, R_w^c, R_w	process/measurement noise covariance matrix (continuous-time/discrete-time)
R_{ij}^c, R_{ij}	block element in noise covariance matrix (continuous-time/discrete-time)
S	singular value matrix in SVD factorization $X = USV^T$
S_{s}, S_{noise}	signal/noise part of singular value matrix
t	continuous time
T_i	time constant
T	sampling interval
T	score matrix in PCA/PCR/PLSR factorization
$u(t)$, u_k	known input (continuous-time/discrete-time)

U	matrix of known inputs
U	orthogonal matrix in SVD factorization $X = USV^T$
U_s, U_{noise}	signal/noise part of orthogonal SVD matrix
$v(t)$, v_k	white process noise (continuous-time/discrete-time)
V	orthogonal matrix in SVD factorization $X = USV^T$, or other orthogonal matrix
V_s, V_{noise}	signal/noise part of orthogonal SVD matrix
$V_N(\theta)$	PEM criterion function
w	mass flow
$w(t)$, w_k	white measurement noise (continuous-time/discrete-time)
W	weighting matrix in regularized regression
$(\cdot)_W$	subscript in Wold PLSR method
x, $x(t)$, x_k	state vector (general/continuous-time/discrete-time)
$\dot{x}$, $\dot{x}(t)$	time derivative of continuous-time state vector
$\hat{x}$, $\hat{x}(t)$, $\hat{x}_k$	state estimate (general/continuous-time/discrete-time system)
$\hat{x}_{k\|k-1}$, $\hat{x}_{k\|k}$	prediction (a priori)/current (a posteriori) state estimate
$\tilde{x}(t)$, $\tilde{x}_k$	state estimation error (continuous-time/discrete-time system)
$X(s)$	Laplace transformed state vector
X	data matrix in PCA/PCR/PLSR
y_1, $y_1(t)$, $y_{1,k}$	primary output (general/continuous-time/discrete-time)
$\hat{y}_1$, $\hat{y}_1(t)$, $\hat{y}_{1,k}$	primary output estimate (general/continuous-time/discrete-time system)
$\hat{y}_{1,k\|k-1}$	prediction (a priori) primary output estimate
$\hat{y}_{1,k\|k}$	current (a posteriori) primary output estimate
$y^{\text{pred}}_{k\|k-1}$, $y^{\text{pred}}_{1,k\|k-1}$	predictor output before minimization (general/primary output)
y_2, $y_2(t)$, $y_{2,k}$	secondary output (general/continuous-time/discrete-time)
$\hat{Y}_1(s)$	Laplace transformed primary output estimate
Y_1	matrix of primary observations
$Y_2(s)$	Laplace transformed secondary output
Y_2	matrix of secondary observations
z, $z(t)$, z_k	primary property (general/continuous-time/discrete-time)
$\hat{z}$, $\hat{z}(t)$, $\hat{z}_k$	primary property estimate (general/continuous-time/discrete-time)
$\hat{z}_{k\|k-1}$	prediction (a priori) primary property estimate
$\hat{z}_{k\|k}$	current (a posteriori) primary property estimate
$z^{\text{pred}}_{k\|k-1}$	predictor output before minimization
$\hat{Z}(s)$	Laplace transformed primary property estimate

Greek letters

Symbol	Description
α	PRBS filtering parameter
α_k	binary factor (0 or 1) in PEM criterion function for low rate primary sampling case
β, β_0	parameters in regression analysis ($\hat{y}_{1,j\|j} = \beta_0 + \beta y_{2,j}$)
$\gamma(t)$, γ_k	non-white estimation error (continuous-time/discrete-time)
$\delta(t)$	Dirac impulse function
ε_k, $\varepsilon_{1,k}$, $\varepsilon_{2,k}$	prediction error (general/primary output/secondary output)
ζ	relative damping factor
η_k	non-white discrete-time estimation error
θ^{init}, θ, $\hat{\theta}$, θ_0, θ^*	parameter vector (initial/general/estimate/exact/biased)
ϑ_k	non-white discrete-time estimation error
λ, λ_i	eigenvalue
μ	factor in perfect measurement analysis
μ	statistical mean value
ξ_i^T	row vector in data matrix X
ς_k	joint input-output time series
τ_k	latent variable
τ_i^T	row vector in score matrix T
$\hat{\tau}_{k\|k-1}$	prediction estimate of latent variable
$\hat{\tau}_{k\|k}$	current estimate of latent variable
φ_k^T	row data vector in LS method for dynamic systems
ψ_k	non-white discrete-time estimation error
Γ_n	observability matrix for discrete-time system
Δ	innovation process covariance matrix
Σ	theoretical covariance matrix
$\hat{\Sigma}$	sampled data covariance matrix
Ψ	PCR residual matrix
Ω_n	reachability matrix for discrete-time system

Chapter 1

Introduction and overview

This chapter gives an introduction to the problem treated and a fairly detailed overview over the thesis. The main new insights and other contributions are summarized.

1.1 Introduction to problem area

1.1.1 Basic industrial problem

In many industrial plants, measurements of primary system outputs are not available on-line. Such outputs are typically product quality properties, that for practical and economical reasons are measured only at a fairly low and possibly irregular sampling rate, often through laboratory analyses of physical samples. For operator support and other purposes, it is of interest to estimate these primary outputs more or less continuously, and that can be done by use of the known inputs and a deterministic model of the plant. Such estimates will fail to capture the influence of unmeasured plant disturbances, and may therefore be far from satisfactory.

In typical cases, however, the plant is equipped with a number of sensors that give secondary output information at a high sampling rate intended for operator support and local control. In such cases the primary outputs may be estimated at the high sampling rate, utilizing all available information contained in the known inputs, either manipulated or measured, and in the secondary plant measurements. The problem is illustrated in Fig. 1.1.

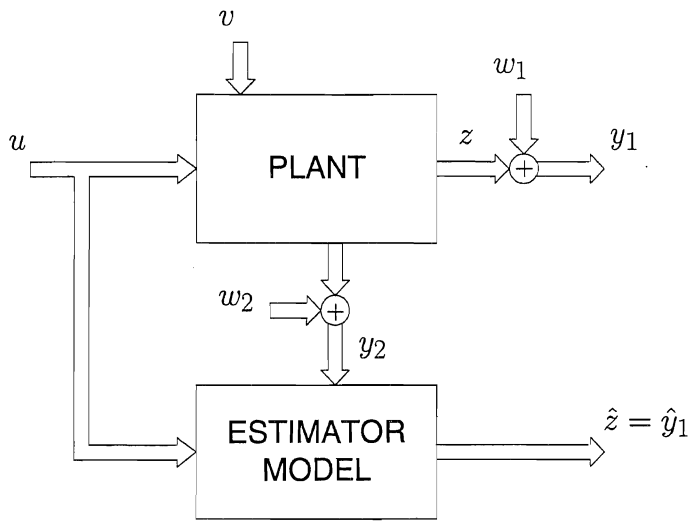

Figure 1.1 Basic principle for estimation of primary properties z and primary system outputs y_1 from known inputs u and secondary outputs y_2 in presence of process noise v and measurement noise w_1 and w_2.

Note that the primary properties are denoted z in Fig. 1.1, and our main interest is accordingly to determine an estimate $\hat{z}$. We will, however, assume that w_1 is white noise, and the best estimate of z will thus in many cases be the best estimate of y_1 (also assuming that w_2 is white noise uncorrelated with w_1), i.e. $\hat{z} = \hat{y}_1$. In the following we will use both the $\hat{z}$ and the $\hat{y}_1$ notations.

The insight behind the use of the y_2 measurements as inputs to the estimator model is that they may carry valuable information about the stationary process noise v, which it should be possible to utilize when estimating z. The y_2 measurements may in fact also carry information about plant disturbances that cannot be modeled as a stationary stochastic process. The industrial use of primary property/output estimators may be operator support, failure detection, and feedback control.

In the special case that the plant in Fig. 1.1 can be adequately modeled by static input-output relations, we have a linear regression problem with a straightforward least squares solution, assuming a large enough number of observations. With a limited number of observations and a large number of y_2 variables, it may then be necessary to use some form of regularization. We will return to the static case later.

In the general dynamical case, the estimator model in Fig. 1.1 may be obtained by mechanistic modeling. The basic aim of the thesis is, however, to develop the theoretical basis and practical methods for *identification of the optimal estimator from experimental data.* This data must then also include y_1 measurements, although not necessarily at a high sampling rate.

Example 1.1

Consider the continuous-time system in Fig. 1.2, where

- u is a manipulated and known input
- v is an unmeasured white process noise source
- the transfer function with time constant T_3 is a process noise model, i.e. x_3 is the physical noise
- $x = \begin{bmatrix} x_1 & x_2 & x_3 \end{bmatrix}^T$ is the state vector
- w_1, w_{21}, w_{22} and w_{23} are white measurement noise sources
- y_1 is the primary measurement
- y_{21}, y_{22} and y_{23} are secondary measurements.

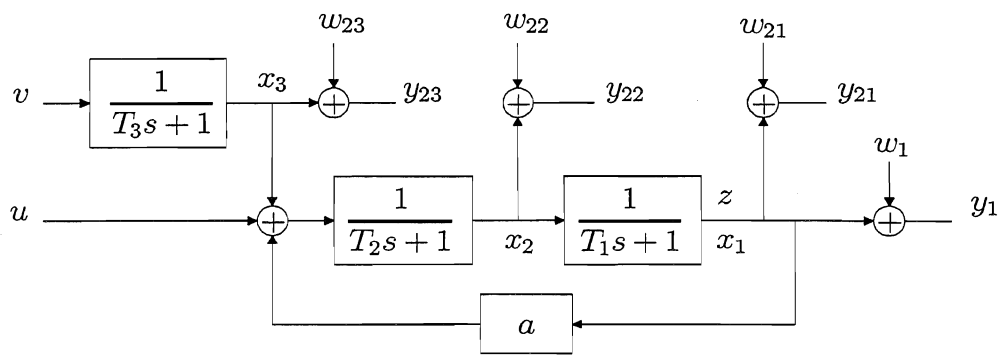

Figure 1.2 Theoretical continuous-time system with second-order plant, first-order process noise model, known input u, primary measurement y_1 and secondary measurements $y_2 = \begin{bmatrix} y_{21} & y_{22} & y_{23} \end{bmatrix}^T$.

If the plant model including the noise covariances were known, the optimal z estimator would in the present case (with y_1 not normally available) be a Kalman filter driven by u and y_2, but not by y_1 (see Appendix A for an introduction to Kalman filtering and further references). When the model is not known, we are left with the opportunity to identify the estimator, or in other words to identify the underlying Kalman filter. From the figure we can directly see that

- with a low noise output $y_{21} \approx x_1 = z$ it is possible to use the simple zero-order estimator $\hat{y}_1 = \hat{z} = y_{21}$

- with a low noise output $y_{22} \approx x_2$ it is possible to identify a good deterministic first-order model with y_{22} as input and y_1 as output
- with a low noise output $y_{23} \approx x_3$ it is possible to identify a good deterministic second-order model with u and y_{23} as inputs and y_1 as output, i.e. without use of the noise model.

With noise corrupted y_2 measurements it is theoretically possible to find an estimator that makes use of all available information in u, y_{21}, y_{22} and y_{23} in an optimal way. Whether this theoretically optimal estimator or a reduced estimator as indicated above is to be preferred, depends on the noise levels and the number of sampled observations in the identification experiment, and has to be decided on the basis of validation against independent data.

■

1.1.2 Industrial example

Fig. 1.3 shows an experimental twin-screw extruder at the Borealis polyolefine plant in Bamble, Norway. In an experiment this extruder was used to produce hard polypropylene foam, with the measured foam density as the primary quality output $y_{1,k}$ (see Chapter 10 for results). The manipulated u_k inputs were a common temperature setpoint for some heating zones along the extruder and a gas injection pressure, while the secondary $y_{2,k}$ outputs were the outlet pressure and temperature measurements along the extruder.

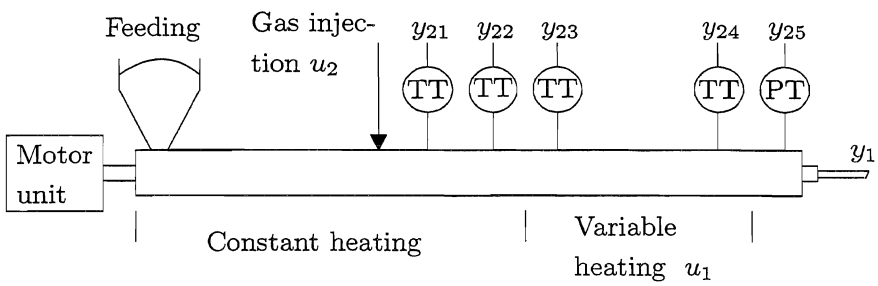

Figure 1.3 Experimental extruder with variable heating setpoint u_1 [°C], gas injection pressure u_2 [bar], temperature measurements y_{21} to y_{24} [°C], outlet pressure y_{25} [bar] and foam density y_1 [g/cm^3].

Industrial example with multivariate data

The system in Fig. 1.3 above has two inputs and five outputs, and it is thus a multivariable system. The data generated by the system must then be said to be

multivariate, although the number of variables is not very high. We would have a more typical multivariate case if a near-infrared (NIR) spectroscopic measurement was included, with for example 4096 additional variables (frequencies).

Related examples

Although the main focus of the thesis is on the type of industrial problems indicated above, there may well exist interesting and important examples related to for example environmental or ecological problems. Such applications are, however, not further discussed in the thesis.

1.1.3 Terminology

Although the primary property z is directly measured through the output y_1 only at a low sampling rate (except possibly in an experiment), information about z may to a large extent be contained in the y_2 measurements. The plant itself thus acts as an instrument for indirect measurement of z, and the process of finding the relation between y_2 and z can therefore be seen as a form of calibration. Since the plant generally is dynamic in nature, and since the available data may be highly multivariate, it has been considered appropriate to use the terminology *dynamic system multivariate calibration* (Ergon and Di Ruscio, 1997, Ergon, 1998a,b,c and Ergon and Halstensen, 1999).

As indicated by this terminology, the work presented in the thesis has its roots in two different scientific fields. One is the broad field concerning *dynamic systems*, more specifically *system identification*, while the other is the field of *chemometrics*, specifically *multivariate calibration*. Both system identification and multivariate calibration have, however, a common root in *linear regression* and *least squares estimation*.

A comment on the use of the terms multivariable and multivariate is also in place. Inspired by Belsley (1991) and Johansson (1993), we relate the term multivariable to multiple-input, multiple-output systems that may exist either as abstract concepts without context or as physical real-world entities. The term multivariate, on the other hand, is used to denote real-life data (or simulations of real-life data) in a given context with meaning and units and perhaps some statistical distribution properties. In short, real-world or simulated *multivariable systems* generate *multivariate data*.

1.1.4 General background

A basic background for the present work is the statistical theory of regression related to static systems. In the notation of the thesis, linear regression is concerned with the estimation of primary dependent variables y_1 on the basis of information provided by known independent variables u and measured secondary dependent

variables y_2. Again using the extruder in Fig. 1.3 as an example, we could make an attempt to estimate the primary output y_1 by use of a static model with u_1 and u_2 as independent regressor variables and y_{21} to y_{25} as dependent regressor variables, and assuming that the feed quality as well as the manipulated inputs u_1 and u_2 are slowly varying, a useful estimator could then be found by use of the least squares (LS) method. The discovery of the LS method is generally attributed to Gauss in 1795 (Grewal and Andrews, 1993), and it has since then been successfully used in numerous practical cases in a wide field of application areas.

When the number of regressor variables is large and the number of observations is limited, the ordinary solution to the LS problem may have very large variance due to overfitting, and some form of regularization is then called for (e.g. Tikhonov and Arsenin, 1977). In many such cases, fortunately, the estimator variables are strongly collinear, and most of the information can thus be compressed into a few latent variables within a subspace of the variable space. Basic tools for this data compression are singular value decomposition (SVD) and principal component analysis (PCA), and the regression method directly based on this is principal component regression (PCR), while partial least squares regression (PLSR) combines data compression and regression in an iterative approach. Detailed presentations of PCR and PLSR are given in Martens and Næs (1989) and Høskuldsson (1996) (see also Appendix C for an introduction and further references). The PCA, PCR and PLSR tools for multivariate data analysis are used in many cases of great practical interest, also when the estimator variables far outnumber the observations at hand. An example is product quality characterization by use of near infrared spectroscopy, with several thousand estimator variables (frequencies) and often less than one hundred observations.

In parallel with the development of the static PCR and PLSR methods, the field of dynamic system identification (SI) has been developed into a sophisticated set of methods and practical tools. Classical SI is summarized in comprehensive books, e.g. Ljung (1987,1999) and Söderström and Stoica (1989), and a short introduction to the prediction error method (PEM) used throughout the thesis is given in Appendix B. At present, subspace identification methods attract a great deal if interest, see e.g. Van Overschee and De Moor (1996) and Di Ruscio (1997). A short discussion on the use of direct subspace methods in the present context is given in Chapter 11. In all forms of SI, one finds that LS estimation is used as a basic tool. It is, however, refined by use of for example prediction optimization methods in order to account for the noise influence in a proper way. With overparametrized models, or data that is not informative enough, there may also in SI be a need for regularization (see e.g. Sjöberg et al., 1993). The need for this may, however, be reduced by an appropriate model reduction, i.e. by use of a parsimonious model with as few parameters as possible.

Through the use of innovation models, system identification is closely linked to the Kalman filtering theory (Appendix A). The different process and measurement

noise sources are then replaced by the white innovations in an underlying Kalman filter.

1.1.5 Preliminary comparison of static and dynamic estimators

From a system identification and Kalman filtering point of view, it is intuitively evident that the classical LS linear regression and the modern PCR and PLSR multivariate calibration methods may be seen as special static cases of the more general parametric SI methods for dynamic systems. When these similarities are to be investigated, four basic facts have to be acknowledged:

1. The LS, PCR and PLSR methods are used to find models for estimation of unknown output variables y from both independent and dependent known variables x. In SI terminology this means methods for estimation of unknown system outputs y_1 from both independent system inputs u and dependent system outputs y_2. The basic observation here is that also dependent outputs y_2 ought to be used as inputs in the SI procedure. This is not a new observation (see e.g. Ljung, 1995), but a theoretical treatment of appropriate methods for optimal utilization of the y_2 information still appears necessary.

2. When the multivariate calibration models are used for estimation, the y_1 outputs are of course not known, and this will also be the case for the corresponding dynamic models found by SI. We are therefore lead to consider output error (OE) models and not the qualitatively different ARMAX (AutoRegressive Moving Average with eXogenous inputs) type of models based on known past y_1 outputs. This is necessary since identification of an ARMAX model would result in the wrong underlying Kalman filter, considering that neither past nor present y_1 outputs are available. This insight is a central contribution of the thesis (see also Ergon, 1999).

3. The known input and secondary measurement sampling rate must be high enough to capture the plant dynamics. However, since the optimal estimators are based on OE models, they may be identified by use of experimental data with a low and even irregular primary output sampling rate. This insight is another main contribution of the thesis (see also Ergon, 1998b).

4. In order to find the optimal y_1 estimate at a specific sampling instant, also current (a posteriori) information must be utilized. The underlying Kalman filter must therefore be of the predictor-corrector form, which is normally not the case for innovation models used in system identification.

These basic facts must be reflected in the theoretical analysis of the relations between SI and LS, PCR and PLSR, and this is quite independent of the specific SI methods considered.

1.1.6 Previous work related to inferential control schemes

The primary output estimation problem outlined above has earlier been discussed in the context of inferential control schemes. Joseph and Brosilow (1978) assumed constant known inputs $u(t)$ to a continuous-time system, and split the estimator into static and dynamic parts. Assuming known noise covariances and the plant dynamics known from impulse or step response tests, the Kalman filter based optimal dynamic estimator was then developed. However, no attempt was made to identify the optimal estimator entirely from recorded plant data. Mejdell and Skogestad (1989) applied a static PLSR solution to a distillation column for estimation of composition, using tray temperatures as secondary information, but made no attempt to extend the solution to the dynamical case. Budman et al. (1992) compared the approaches of Joseph and Mejdell when applied to an experimental fixed bed methanation reactor, and found the PLSR approach superior when the nonlinear system was operated in a wide range of operating points. Wise (1991) described the theoretical bases for using PCA to model dynamic systems within a state-space framework, and Harnett et al. (1998) used this approach in a simulation of an overheads condensor and reflux drum model for a distillation column. The limitations of this PCA approach is further discussed in Chapter 9.

1.1.7 Questions raised and answered

The following questions are raised and answered in the thesis:

- How should optimal primary output estimators be designed, assuming a known and linear plant model?
- How should the optimal estimators be identified, in the case the plant model is not known?
- How should noise free and low noise secondary measurements be handled?
- How should the optimal estimator structure be determined?
- Can the industrially interesting case with a low and possibly irregular primary output sampling rate be handled?
- What is the theoretical connection between dynamic estimator solutions and the static LS, PCR and PLSR methods?
- What should dynamical PCR and PLSR methods look like?

The theoretical answers to these questions are supported by simulations throughout the thesis, and by real data examples presented in Chapter 10.

1.2 Theoretical primary output estimators

Assuming that a reliable deterministic-stochastic linear model of the plant in Fig. 1.1 is known (from mechanistic modeling or system identification), optimal estimators for the primary properties z and outputs y_1 can be realized as Kalman filters driven by the known inputs u and the secondary y_2 measurements. The optimal continuous-time estimator as well as optimal discrete-time estimators are developed in Chapter 2, which is a basis for the following chapters dealing with the estimator identification problem. A summary of Chapter 2 is given below.

Basic discrete-time model

The basic discrete-time model used in the thesis is

$$\begin{aligned} x_{k+1} &= Ax_k + Bu_k + Gv_k \\ y_{1,k} &= C_1 x_{1,k} + D_1 u_k + w_{1,k} \\ y_{2,k} &= C_2 x_{2,k} + D_2 u_k + w_{2,k}, \end{aligned} \tag{1.1}$$

where x_k is the state vector, and where v_k, $w_{1,k}$ and $w_{2,k}$ are white noise sequences.

Optimal prediction (a priori) estimator

Utilizing the information in past $y_{2,k}$ values as well as past and present u_k values, and assuming that v_k and $w_k = \begin{bmatrix} w_{1,k}^T & w_{2,k}^T \end{bmatrix}^T$ are independent white noise sequences uncorrelated with u_k, the theoretically optimal prediction (a priori) estimator is

$$\begin{aligned} \hat{z}_{k|k-1} &= \hat{y}_{1,k|k-1} = C_1 \left[qI - A + AK_2^{\mathrm{OE}} C_2 \right]^{-1} \\ &\quad \times \left[\left(B - AK_2^{\mathrm{OE}} D_2 \right) u_k + AK_2^{\mathrm{OE}} y_{2,k} \right] + D_1 u_k \\ &= F_p^{-1}(q^{-1}) \left[B_{p,1}(q^{-1}) u_k + B_{p,2}(q^{-1}) y_{2,k} \right], \end{aligned} \tag{1.2}$$

where K_2^{OE} is the gain in a Kalman filter driven by u_k and $y_{2,k}$, while $F_p(q^{-1})$, $B_{p,1}(q^{-1})$, and $B_{p,2}(q^{-1})$ are polynomials in the unit time delay operator q^{-1}. The estimate $\hat{z}_{k|k-1}$ is here a linear combination of past estimates, past and present values of u_k and past values of $y_{2,k}$, where the horizon into the past is determined by the model order n.

The notation K_2^{OE} is used since the estimator corresponds to the output error (OE) model

$$y_{1,k} = F_p^{-1}(q^{-1}) \left[B_{p,1}(q^{-1}) u_k + B_{p,2}(q^{-1}) y_{2,k} \right] + \vartheta_k, \tag{1.3}$$

where ϑ_k as explained in Chapter 2 is a none-white noise sequence. The reason for using this OE model, and not the deterministic part (considering $y_{2,k}$ as an input) of an ARMAX model, is simply that only the OE model will give the correct Kalman gain, considering that y_1 is not normally available. This is contrary to the ordinary case with only u_k as input, where the deterministic part of the ARMAX model is identical with the deterministic part of the OE model. The details of this is shown in Chapter 2, and also in Ergon (1999).

Optimal current (a posteriori) estimator

When present $y_{2,k}$ values are used as well, the theoretical current (a posteriori) estimator becomes

$$\begin{aligned}\hat{z}_{k|k} &= \hat{y}_{1,k|k} = C_1\left(I - K_2^{\mathrm{OE}}C_2\right)\left[qI - A + AK_2^{\mathrm{OE}}C_2\right]^{-1} \\ &\quad \times \left[\left(B - AK_2^{\mathrm{OE}}D_2\right)u_k + AK_2^{\mathrm{OE}}y_{2,k}\right] \\ &\quad + C_1K_2^{\mathrm{OE}}\left(y_{2,k} - D_2u_k\right) + D_1u_k \\ &= F_c^{-1}(q^{-1})\left[B_{c,1}(q^{-1})u_k + B_{c,2}(q^{-1})y_{2,k}\right], \end{aligned} \tag{1.4}$$

corresponding to the OE model

$$y_{1,k} = F_c^{-1}(q^{-1})\left[B_{c,1}(q^{-1})u_k + B_{c,2}(q^{-1})y_{2,k}\right] + \psi_k, \tag{1.5}$$

where also ψ_k is a non-white sequence.

1.3 Identification of primary output estimators

The OE estimators (1.2) and (1.4) can be consistently identified from input-output data from a controlled experiment, where u_k, $y_{1,k}$ and $y_{2,k}$ for $k = 1, 2, \ldots, N$ are available at a sufficiently high sampling rate, with u_k persistently exciting and N sufficiently large. The theoretical basis for this is developed in Chapter 3, where also practical identification methods are discussed, and where examples and Monte Carlo simulations that support the theoretical results are included.

It follows from the analysis in Chapter 2 that the OE estimators above may not be derived by modifying ARMAX estimators, as can be done in the ordinary case with only u_k used as estimator input. This has important consequences when it comes to the identification of asymptotically ($N \to \infty$) optimal estimators.

The main results in Chapter 3 are published in Ergon and Di Ruscio (1997), Ergon (1998a,c) and Ergon (1999), and a summary is given below.

Identification of optimal prediction estimators

The optimal prediction estimator (1.2) can be found by identification of the system (1.3), with the non-white noise sequence ϑ_k. The identification can be done by use of a standard prediction error method (PEM) based on Kalman filtering formalism (see Appendix B). The basic principle in PEM is to use an OE prediction model in parallel with the plant itself. The output $z^{\text{pred}}_{k|k-1}(\theta) = y^{\text{pred}}_{1,k|k-1}(\theta)$ from this model is based on past $y_{2,k}$ values as well as past and present u_k values, and the resulting prediction error is

$$\varepsilon_{1,k}(\theta) = y_{1,k} - y^{\text{pred}}_{1,k|k-1}(\theta), \tag{1.6}$$

where θ is the parameter vector used in the prediction model. In Chapter 3 it is shown that minimization of a scalar criterion function

$$V_N(\theta) = \mathrm{h}\left[\frac{1}{N}\sum_{k=1}^{N}\varepsilon_{1,k}(\theta)\varepsilon^T_{1,k}(\theta)\right] \tag{1.7}$$

asymptotically (for $N \to \infty$) results in the optimal output error prediction (OEP) estimator (1.2). This means that $\theta \to \hat{\theta} = \theta_0$, where θ_0 is the exact parameter vector that for the sake of the theoretical analysis is assumed to exist, and at the same time $\frac{1}{N}\sum_{k=1}^{N}\varepsilon_{1,k}(\theta)\varepsilon^T_{1,k}(\theta) \to \frac{1}{N}\sum_{k=1}^{N}\vartheta_k\vartheta_k^T$, which according to the underlying Kalman filter theory is a minimized expression. In (1.7), the scalar function may be $\mathrm{h}[\cdot] = \det[\cdot]$ or $\mathrm{h}[\cdot] = \mathrm{trace}[\cdot]$. The minimization is performed by use of a numerical Gauss-Newton procedure, and in order to avoid local minima this normally requires an initial model that basically can be found by ordinary least squares estimation (Ljung, 1987,1999).

Identification of optimal current estimators

The optimal output error current (OEC) estimator is found in a similar way by identification of the system (1.5), where the polynomials are defined by (1.4).

1.4 Perfect measurement cases

From Example 1.1 and Fig. 1.2 it is obvious that simultaneous use of several perfect noise free secondary measurements theoretically may cause a conflict between different perfect models. If, for example, both y_{22} and y_{23} are perfect measurements, we must make a choice between a first-order model using only y_{22} and a second-order model using u and y_{23} as inputs, and the natural choice would then be the more parsimonious first-order model with only T_1 as unknown parameter. We will then find that the rest of the system will be decoupled, and that a, T_2 and T_3 cannot be identified by use of only the y_{22} and y_1 output data.

More detailed discussions of an in the context of the thesis interesting theoretical perfect measurement case are given in Chapter 4, where some new perfect measurement Kalman filtering results are also presented (see also Ergon and Di Ruscio, 1997). Identification of pure deterministic systems with neither process nor measurement noise is also discussed in Chapter 4.

1.5 Determination of estimator structure

As in other practical system identification cases, there is also in the present context a need to find a parsimonious estimator that captures the essential plant characteristics using as few parameters as possible (Ljung, 1987,1999). The main points are to determine

- the appropriate model order n
- which inputs u_k and secondary measurements $y_{2,k}$ to use.

The final answers to these questions are found by validation against independent experimental data. In many cases with a limited number of observations as a basis for the estimator identification, the smallest root-mean-square validation error (RMSE) in the estimation of $y_{1,k}$ may then very well be obtained by use of a reduced and asymptotically ($N \rightarrow \infty$) biased estimator with a parameter vector $\theta^* \neq \theta_0$, where θ_0 is the exact parameter vector that is assumed to exist. To reduce the bias one basically has to employ larger end more flexible model structures, requiring more parameters and possibly increasing the estimation covariance. We thus want to find a good trade-off between the bias and variance contributions to the total RMSE. A systematic method for this model structure determination is presented in Chapter 5 (see also Ergon and Di Ruscio, 1997).

1.6 The low primary output sampling rate case

In many practical cases it is not feasible to perform an experiment with high rate sampling of the primary system outputs, and there is thus a need for methods based on low and possibly irregular sampling rate y_1 data. This case is studied in Chapter 6, extending the theory and the methods presented in Chapter 3 (see also Ergon, 1998b). The basic insight here is that it is not quite necessary to minimize the criterion function (1.7) as a function of $\varepsilon_{1,k}(\theta)$ for all samples at $k = 1, 2, \ldots, N$. It is in fact sufficient to minimize

$$V_{N_1}(\theta) = \mathrm{h}\left[\frac{1}{N_1}\sum_{k=1}^{N}\alpha_k\varepsilon_{1,k}(\theta)\,\varepsilon_{1,k}^T(\theta)\right] = \mathrm{h}\left[\frac{1}{N_1}\sum_{j=1}^{N_1}\varepsilon_{1,j}(\theta)\,\varepsilon_{1,j}^T(\theta)\right], \qquad (1.8)$$

where

$$\alpha_k = \begin{cases} 1, \text{ at the time instants } k \text{ where } y_1 \text{ is sampled} \\ 0, \text{ at the time instants } k \text{ where } y_1 \text{ is not sampled,} \end{cases}$$

and where thus $\varepsilon_{1,j}(\theta)$ are the prediction errors that can be obtained from the $y_{1,j}$ measurements that are available at a low and possibly also irregular sampling rate. The minimization will then be based on a reduced number, $N_1 < N$, of the predictor outputs $z^{\text{pred}}_{k|k-1} = y^{\text{pred}}_{1,k|k-1}$, corresponding in time with the available $y_{1,j}$ samplings. The practical and theoretical requirements are only that

- the u_k and $y_{2,k}$ sampling rate is high enough to capture the plant dynamics
- the plant is persistently excited
- the number N_1 of available $y_{1,j}$ samples is sufficiently large
- the y_1 samples are representative, i.e. that $y_{1,j}$ has the same statistical distribution as $y_{1,k}$ would have.

In this case, however, an initial model for the numerical minimization cannot be found by ordinary least squares estimation, and solutions to this problem are therefore also presented in Chapter 6, together with Monte Carlo simulations that verify the feasibility of the proposed methods.

1.7 Ordinary linear regression as special case

As mentioned earlier, we may as a special case have a static plant in Fig. 1.1. The model (1.1) is then simplified to

$$\begin{aligned} x_{k+1} &= v_k \\ y_{1,k} &= C_1 x_k + D_1 u_k + w_{1,k} \\ y_{2,k} &= C_2 x_k + D_2 u_k + w_{2,k}, \end{aligned} \tag{1.9}$$

where x_k is the vector of latent variables explaining $y_{1,k}$ and $y_{2,k}$. The theoretical current estimator model (1.5) is then simplified to

$$\begin{aligned} y_{1,k} &= C_1 K_2^{\text{OE}} (y_{2,k} - D_2 u_k) + D_1 u_k + e_k \\ &= B_1^T u_k + B_2^T y_{2,k} + e_k, \end{aligned} \tag{1.10}$$

where u_k are known independent regressor variables, while $y_{2,k}$ are known but dependent and noise corrupted regressor variables and e_k is white noise.

We find the corresponding data based estimator by collecting the observations u_k^T, $y_{1,k}^T$ and $y_{2,k}^T$ for $k = 1, 2, \ldots, N$ in data matrices U, Y_1 and Y_2, and solving the overdetermined set of equations

$$Y_1 = \begin{bmatrix} U & Y_2 \end{bmatrix} \begin{bmatrix} B_1 \\ B_2 \end{bmatrix} + E. \tag{1.11}$$

The classical unbiased LS solution is then

$$\begin{bmatrix} \hat{B}_1^{\mathrm{LS}} \\ \hat{B}_2^{\mathrm{LS}} \end{bmatrix} = \left(\begin{bmatrix} U^T \\ Y_2^T \end{bmatrix} \begin{bmatrix} U & Y_2 \end{bmatrix} \right)^{-1} \begin{bmatrix} U^T \\ Y_2^T \end{bmatrix} Y_1, \tag{1.12}$$

or without known input variables

$$\hat{B}^{\mathrm{LS}} = \left(Y_2^T Y_2 \right)^{-1} Y_2^T Y_1. \tag{1.13}$$

The theoretical relation between the OE model (1.5) and the static form (1.10), with the LS solution (1.12) or (1.13), is developed in Chapter 7. As (1.5) is related to an underlying Kalman filter, this also forms a theoretical link between Kalman filtering and ordinary linear regression. The results in Chapter 7 are previously reported in Ergon (1998a,c).

1.8 Multivariate static case

In many cases of great practical interest we have a large number of collinear variables y_2 in (1.10), which for a realistic number of observations may cause very large variance in the parameter estimates. The solution to this problem is some form of regularization, e.g. PCR or PLSR, where u_k and $y_{2,k}$ (or only $y_{2,k}$) are replaced by a low number of estimated latent variables $\hat{\tau}_k$. Assuming a data structure in accordance with the model (1.9), the latent variables τ_k are then the state variables x_k.

The theoretical connection from Kalman filtering via the optimal current estimator (1.4) and least squares regression to PCR and PLSR is presented in Chapter 8, and part of this is also previously reported in Ergon (1998a,c). An early and less general attempt to look into these relations were given in Berntsen (1988).

In PCR and PLSR the regularization is obtained by use of a weighting matrix W, and the data based estimator (1.13) is then replaced by

$$\hat{B} = \hat{W} \left(\hat{W}^T Y_2^T Y_2 \hat{W} \right)^{-1} \hat{W}^T Y_2^T Y_1, \tag{1.14}$$

where $\hat{W}_{\mathrm{PCR}}$ and $\hat{W}_{\mathrm{PLS}}$ are found from the data as shown in Appendix C. However, as shown in Chapter 8 the optimal weighting matrix is a transposed Kalman gain, i.e.

$$\hat{B}_{opt.} = \left(K_2^{\mathrm{OE}} \right)^T \left(K_2^{\mathrm{OE}} Y_2^T Y_2 \left(K_2^{\mathrm{OE}} \right)^T \right)^{-1} K_2^{\mathrm{OE}} Y_2^T Y_1, \tag{1.15}$$

which is considered to be a theoretically interesting result.

Another and more practically interesting result presented in Chapter 8 is related to problems with a few known inputs u_k and a large number of collinear y_2 measurements. The best regression model may then be obtained by use of two-step PCA/PLSR+LS solutions, where the u_k information is used only in the second LS step.

Other forms of regularization, e.g. ridge regression (Hoerl and Kennard, 1970) or neural networks with restricted training (Sjöberg and Ljung, 1995), are not treated in the thesis.

1.9 Multivariate dynamical cases

In Chapter 9, the multivariate static estimators are combined with the dynamic current estimator (1.4), resulting in PCA+OE and PLSR+OE methods. This may be practical solutions when some or all of the secondary y_2 measurements are collinear. The resulting estimators will then become of the type shown in (1.4), with past and present values of $y_{2,k}$ partly or altogether replaced by the corresponding estimates $\hat{\tau}_k$ of latent variables. Monte Carlo simulations are included in order to show the feasibility of the proposed methodology. The basic idea in Chapter 9 is previously presented in Ergon (1998a,c), and an acoustic chemometry application is presented in Ergon and Halstensen (1999).

1.10 Real data examples

The theory and methods developed in the thesis are to some extent tested on real data. These cases include an experimental research extruder at the Borealis polyolefine plant in Bamble, Norway, a polyethylene civil engineering pipe production extruder at the Icopal plant in Drangedal, Norway, a complex industrial plant run by Norsk Hydro, Norway, and an acoustic chemometrics experimental setup at Telemark Institute of Technology, Porsgrunn, Norway. These applications are presented in Chapter 10.

1.11 Further research areas

The thesis focuses on the basic problem of estimating primary output properties that are not normally measured on-line, and the immediate industrial application of this is in operator support systems. Basic issues related to e.g. closed loop identification, use of prior knowledge, estimator validation, estimator robustification, estimator updating and possible applications in fault detection and isolation (FDI) and closed loop control are briefly discussed in Chapter 11, but are otherwise left for further research.

1.12 Main contributions of the thesis

The main new insights and results presented in the thesis are the following:

- In order to utilize the information in the secondary output measurements in an optimal way in primary property estimators, we must use OE structures and not ARMAX structures (Chapter 2 and Chapter 3). This is also presented in Ergon and Di Ruscio (1997) and Ergon (1998a,c), and a more detailed discussion is given in Ergon (1999).

- The optimal OE estimators may be identified also when the primary output is sampled at a low and possibly also irregular rate (Chapter 6). This was first presented in Ergon (1998a), and further discussed in Ergon (1998b).

- Assuming a latent variable data structure, the ordinary LS estimator is a special static case of the optimal current OE estimator (Chapter 7). Since PCR and PLSR are again special cases of the least squares method (Chapter 8), it readily follows how dynamic PCA+OE and PLSR+OE estimators should be developed (Chapter 9). These relations are also discussed in Ergon (1998a,c).

- The dynamic PCA+OE estimators may be identified also in the low primary output sampling rate case. An acoustic chemometrics example of that is given in Chapter 10, and another example is presented in Ergon and Halstensen (1999).

Other contributions are as follows:

- Theoretical development of the optimal OE prediction (a priori) and current (a posteriori) primary output estimators in the high y_1 sampling rate case, including asymptotic estimation covariance results (Chapter 2), and a detailed clarification concerning consistent identification of these estimators using the secondary measurements as inputs in a prediction error method (Chapter 3).

- Some new asymptotic perfect measurement Kalman filtering results (Chapter 4 and Ergon and Di Ruscio, 1997).

- A systematic method for selection of model order and relevant known inputs and secondary measurements (Chapter 5 and Ergon and Di Ruscio, 1997).

- Methods for finding initial parameter values in the low y_1 sampling rate case (Chapter 6).

- A theoretical result showing that the optimal weighting matrix for the chemometrical PCR/PLSR methods is a transposed Kalman gain (Chapter 8).

- Proposed two-step PCA+LS and PLSR+LS methods for static problems with both independent and dependent regressor variables (Chapter 8).
- A proposed fault detection scheme (Chapter 11).
- Some clarifications concerning estimator properties essential for feedback control applications (Chapter 11).
- Some proposed feedback control structures (Chapter 11).

Chapter 2

Theoretical primary output estimators

This chapter serves as an introduction to the discrete-time estimator identification problem discussed in the following chapters. Under the assumption of a reliable plant model from either mechanistic modeling or system identification, we develop theoretical primary output estimators and estimation covariances, both for the continuous-time and the discrete-time cases. The main point in the chapter is that in order to utilize the secondary y_2 measurement information in an optimal way, we must use OE models. It is also shown that these models cannot be seen as special cases of ARMAX models, which is contrary to the ordinary case with only the known independent variables u used as input. The chapter is based on well known Kalman filtering theory.

2.1 The optimal continuous-time estimator

Although we will later focus on identification of discrete-time estimators, it is instructive to start with the continuous-time case.

2.1.1 Statement of continuous-time estimator problem

Assume the known continuous-time plant model

$$\begin{aligned} \frac{dx(t)}{dt} &= A^c x(t) + B^c u(t) + G^c v(t) \\ z(t) &= C_1 x(t) + D_1 u(t) \\ y_1(t) &= z(t) + w_1(t) \\ y_2(t) &= C_2 x(t) + D_2 u(t) + w_2(t), \end{aligned} \tag{2.1}$$

where $x(t)$ is the state vector, and where in the general multivariable case $u(t)$, $v(t)$, $z(t)$, $y_1(t)$, $y_2(t)$, $w_1(t)$ and $w_2(t)$ are vectors as well. Here,

- $u(t)$ is a known input signal
- $v(t)$ is a formal zero mean white noise stochastic process with covariance function given by the expectation $Ev(t_1)v^T(t_2) = R_v^c\delta(t_1 - t_2)$, where $\delta(t)$ is the Dirac impulse function
- $w(t) = \begin{bmatrix} w_1^T(t) & w_2^T(t) \end{bmatrix}^T$ is a formal zero mean white noise stochastic process with covariance function given by the expectation $Ew(t_1)w^T(t_2) = R_w^c\delta(t_1 - t_2) = \begin{bmatrix} R_{11}^c & R_{12}^c \\ R_{21}^c & R_{22}^c \end{bmatrix} \delta(t_1 - t_2)$
- R_w^c is positive definite (see Chapter 4 for a special perfect measurement case)
- $v(t)$ and $w(t)$ are uncorrelated, i.e. $Ev(t_1)w^T(t_2) = 0$ for all t_1 and t_2 (may be ralaxed, see Subsection 2.2.6)
- both $v(t)$ and $w(t)$ are uncorrelated with the input $u(t)$, i.e. $Eu(t_1)v^T(t_2) = 0$ and $Eu(t_1)w^T(t_2) = 0$ for all t_1 and t_2
- only the output $y_2(t)$ is normally available (which may, however, also include more or less noisy measurements of $z(t)$)
- (C_2, A^c) is detectable (see Appendix A)
- $(A^c, G^c\sqrt{R_v^c})$ is stabilizable (see Appendix A).

These assumptions make it possible to apply the Kalman filtering theory (Appendix A). Note that noise components that are not white must be modeled as filtered white noise, with the filter model included in the plant model (2.1). Also note that some or all of the secondary y_2 measurements may be collinear, and also collinear with some or all of the known inputs u and/or some or all of the primary y_1 measurements.

The problem is now to determine the optimal linear $\hat{z}(t)$ estimator based on $u(t)$ and $y_2(t)$. With an optimal estimator we here mean an unbiased and minimum variance estimator.

2.1.2 Continuous-time Kalman filter solution

The optimal solution to the problem stated above is to use a continuous-time Kalman filter driven by the known inputs $u(t)$ and the available secondary $y_2(t)$ measurements. Introducing the state estimate $\hat{x}(t)$, the Kalman filter is given by

$$\begin{aligned} \frac{d\hat{x}(t)}{dt} &= A^c\hat{x}(t) + B^c u(t) + K_2^c e_2(t) \\ \hat{y}_2(t) &= C_2\hat{x}(t) + D_2 u(t) \\ e_2(t) &= y_2(t) - \hat{y}_2(t), \end{aligned} \tag{2.2}$$

where $e_2(t)$ is the formally white innovations representation.

In order to determine K_2^c we solve the algebraic Riccati equation

$$0 = A^cP^c + (A^cP^c)^T + G^cR_v^c(G^c)^T - P^cC_2^T(R_{22}^c)^{-1}C_2P^c, \tag{2.3}$$

where $P^c = E\left(x(t) - \hat{x}(t)\right)\left(x(t) - \hat{x}(t)\right)^T$ is the minimized state estimation covariance matrix (Appendix A). We then find

$$K_2^c = P^cC_2^T(R_{22}^c)^{-1}. \tag{2.4}$$

Elimination of $\hat{y}_2(t)$ and $e_2(t)$ from (2.2) and use of the z and y_1 output equations in (2.1) result in

$$\begin{aligned} \frac{d\hat{x}(t)}{dt} &= \left(A^c - K_2^cC_2\right)\hat{x}(t) + \left(B^c - K_2^cD_2\right)u(t) + K_2^cy_2(t) \\ \hat{z}(t) &= \hat{y}_1(t) = C_1\hat{x}(t) + D_1u(t). \end{aligned} \tag{2.5}$$

This estimator is shown in the block diagram in Fig. 2.1.

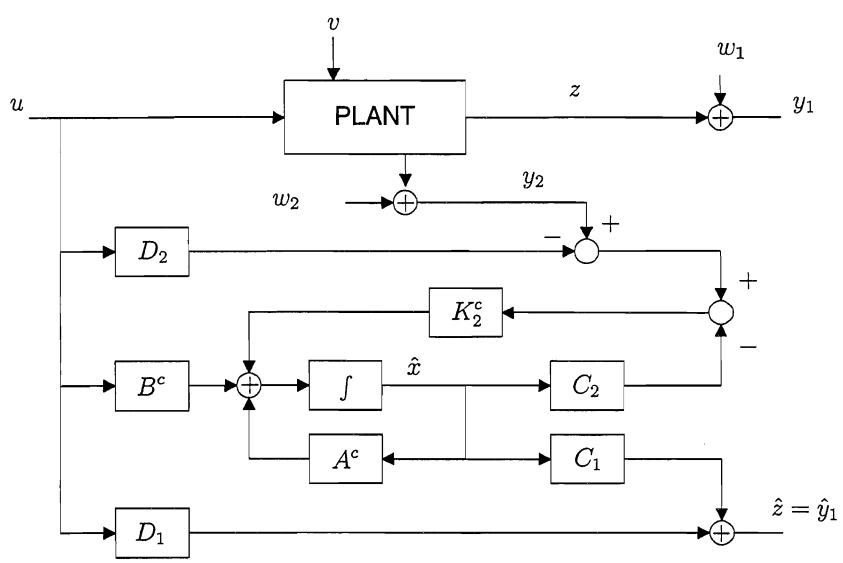

Figure 2.1 Block diagram for optimal continuous-time z and y_1 estimator.

The y_1 estimation error becomes

$$\gamma(t) = y_1(t) - \hat{y}_1(t) = C_1 \left[x(t) - \hat{x}(t)\right] + w_1(t), \tag{2.6}$$

which is a colored noise signal (not a white innovations representation, since it is not an internal feedback signal in the Kalman filter).

The estimator (2.5) may also be expressed by Laplace transformation assuming $\hat{x}(0) = 0$, and after elimination of $\hat{X}(s)$ we then find the optimal $Z(s)$ and $Y_1(s)$ estimator

$$\begin{aligned} \hat{Z}(s) &= \hat{Y}_1(s) = C_1 \left[sI - A^c + K_2^c C_2\right]^{-1} \left[\left(B^c - K_2^c D_2\right) U(s) + K_2^c Y_2(s)\right] \\ &\quad + D_1 U(s), \end{aligned} \tag{2.7}$$

and the optimal $z(t)$ and $y_1(t)$ estimator

$$\hat{z}(t) = \hat{y}_1(t) = \mathcal{L}^{-1}\left\{\hat{Z}(s)\right\}. \tag{2.8}$$

Remark 1 *If the measurement noise sources $w_1(t)$ and $w_2(t)$ are correlated, i.e. if $Ew_1(t)w_2^T(t) \neq 0$, the Kalman filter will not give the optimal $y_1(t)$ estimate. The Kalman filter will, however, still give the optimal estimate of the primary property $z(t) = C_1 x(t) + D_1 u(t)$, and that is the important issue in the context of the thesis.*

Continuous estimator covariances

The theoretical $\hat{z}(t)$ and $\hat{y}_1(t)$ estimation covariances follow directly from (2.6) and the definition $P^c = E\left(x(t) - \hat{x}(t)\right)\left(x(t) - \hat{x}(t)\right)^T$ as

$$\mathrm{Cov}\left(\hat{z}(t)\right) = C_1 P^c C_1^T \tag{2.9}$$

and

$$\mathrm{Cov}\left(\hat{y}_1(t)\right) = E\gamma(t)\gamma^T(t) = C_1 P^c C_1^T + R_{11}^c, \tag{2.10}$$

where P^c is given by (2.3).

The development of the optimal continuous-time estimator and its covariance properties are summarized in Proposition 2.1:

Proposition 2.1 - Optimal continuous-time estimator

For the system (2.1), the optimal continuous-time $z(t)$ and $y_1(t)$ estimator based on $u(t)$ and $y_2(t)$ is given by (2.5) or (2.7) and (2.8). The estimator covariances are given by (2.9) and (2.10).

■

Example 2.1

Consider the system in Example 1.1, with $T_1 = 10$, $T_2 = 0$, $T_3 = 100$, $a = 0$ and $y_2 = y_{23}$. This might be a stirred-tank heating system with constant holdup as shown in Fig. 2.2a, with a first-order process noise model. The block diagram is shown in Fig. 2.2b. Note that the system is not observable from the y_2 output, i.e. that (C_2, A^c) is only detectable (the non-observable part is asymptotically stable, as required by the Kalman filtering theory, see Appendix A).

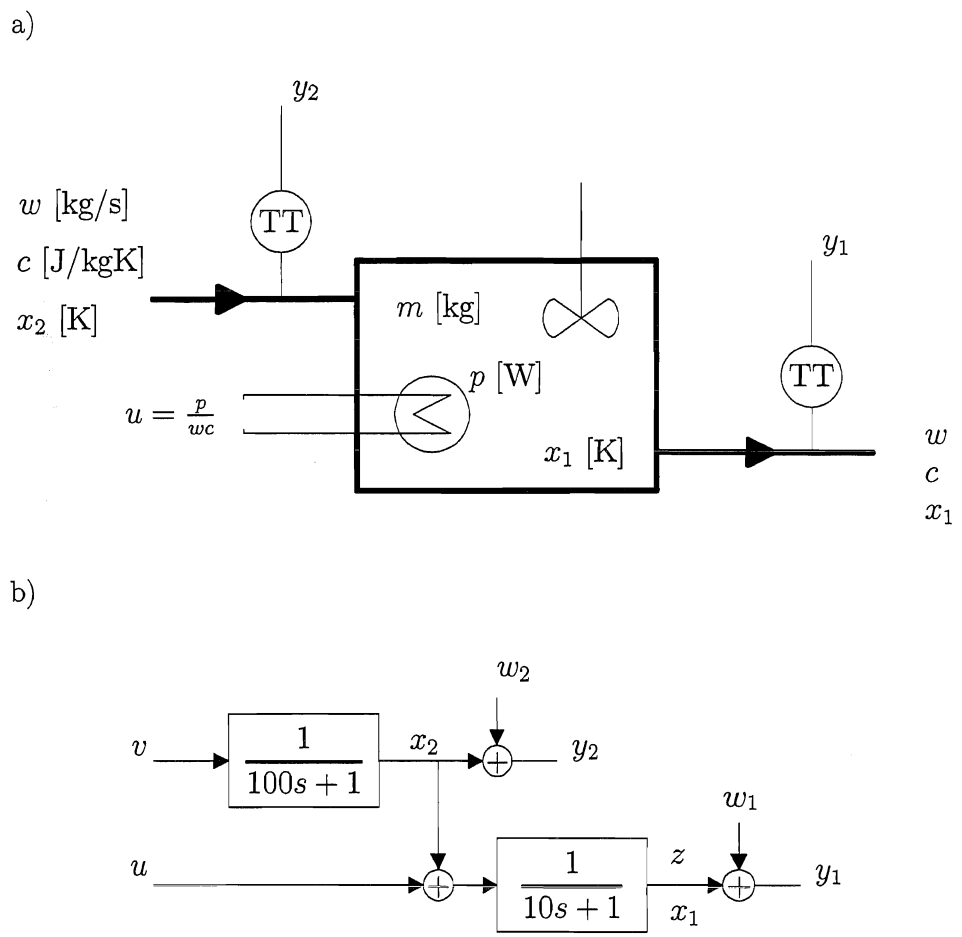

Figure 2.2 Stirred-tank heating system with constant holdup and variable temperatures, and the corresponding block diagram assuming a first-order noise model.

With $w/m = 0.1$, the system is modeled as

$$\begin{aligned} \dot{x}_1 &= -0.1x_1 + 0.1x_2 + 0.1u \\ \dot{x}_2 &= -0.01x_2 + 0.01v \\ z &= x_1 \\ y_1 &= z + w_1 \\ y_2 &= x_2 + w, \end{aligned} \tag{2.11}$$

where the noise variances are so far not specified.

We thus have $A^c = \begin{bmatrix} -0.1 & 0.1 \\ 0 & -0.01 \end{bmatrix}$, $B^c = \begin{bmatrix} 0.1 \\ 0 \end{bmatrix}$, $G^c = \begin{bmatrix} 0 \\ 0.01 \end{bmatrix}$, $C_1 = \begin{bmatrix} 1 & 0 \end{bmatrix}$ and $C_2 = \begin{bmatrix} 0 & 1 \end{bmatrix}$, and a straightforward solution of (2.3) then gives

$$P^c = \begin{bmatrix} \frac{0.1r_{22}^c p_{22}^c}{0.11r_{22}^c + p_{22}^c}\left(1 - \frac{0.5p_{22}^c}{0.11r_{22}^c + p_{22}^c}\right) & \frac{0.1r_{22}^c p_{22}^c}{0.11r_{22}^c + p_{22}^c} \\ \frac{0.1r_{22}^c p_{22}^c}{0.11r_{22}^c + p_{22}^c} & p_{22}^c \end{bmatrix}, \tag{2.12}$$

with p_{22}^c determined by

$$(p_{22}^c)^2 + 0.02r_{22}^c p_{22}^c - 10^{-4} r_{22}^c r_v^c = 0. \tag{2.13}$$

From (2.4) we further find

$$K_2^c = \begin{bmatrix} k_{12}^c \\ k_{22}^c \end{bmatrix} = \begin{bmatrix} 0.1\frac{\sqrt{(\cdot)}-1}{\sqrt{(\cdot)}+10} \\ 0.01\left(\sqrt{(\cdot)} - 1\right) \end{bmatrix}, \tag{2.14}$$

where $\sqrt{(\cdot)} = \sqrt{1 + r_v^c / r_{22}^c}$. The estimator (2.7) is then obtained as

$$\begin{aligned} \hat{Z}(s) &= \hat{Y}_1(s) = \begin{bmatrix} 1 & 0 \end{bmatrix} \begin{bmatrix} s + 0.1 & k_{12}^c - 0.1 \\ 0 & s + k_{22}^c + 0.01 \end{bmatrix}^{-1} \\ &\quad \times \left(\begin{bmatrix} 0.1 \\ 0 \end{bmatrix} U(s) + \begin{bmatrix} k_{12}^c \\ k_{22}^c \end{bmatrix} Y_2(s) \right) \\ &= \frac{0.1}{s + 0.1} U(s) + \frac{k_{12}^c (s + k_{22}^c + 0.01) + k_{22}^c (0.1 - k_{12}^c)}{(s + 0.1)(s + k_{22}^c + 0.01)} Y_2(s). \end{aligned} \tag{2.15}$$

A block diagram for the system and the estimator is shown in Fig. 2.3.

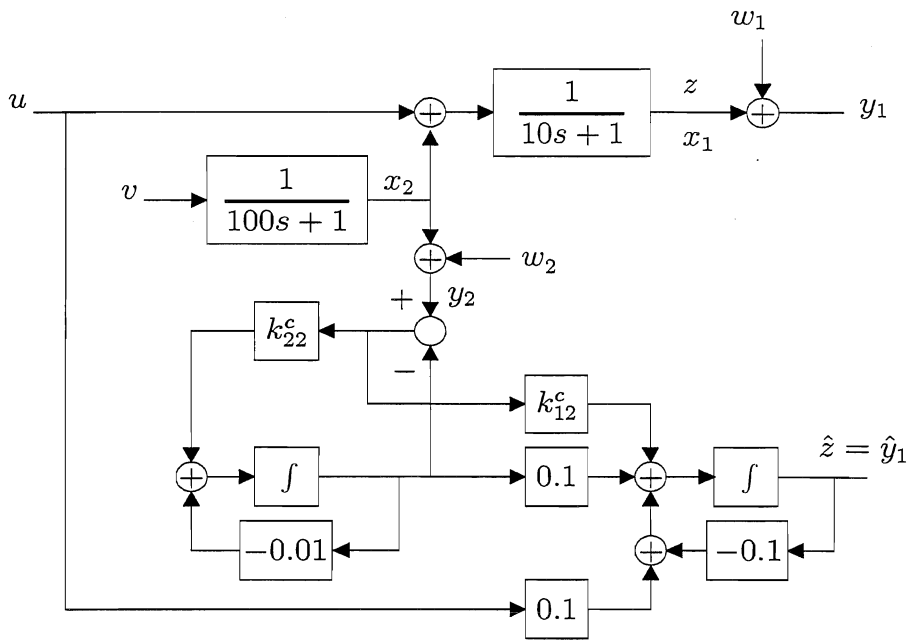

Figure 2.3 Block diagram for the system in Fig. 2.2 and the corresponding primary property estimator.

From (2.15) we find two extreme cases with expected results:

- An extremely noisy y_2 measurement, i.e. $r_v^c/r_{22}^c \to 0$, results in $K_2^c \to \begin{bmatrix} 0 & 0 \end{bmatrix}^T$ and

$$\hat{Z}(s) = \hat{Y}_1(s) \to \frac{1}{10s+1} U(s), \tag{2.16}$$

while (2.12) and (2.13) with $p_{22}^c/r_{22}^c \to 0$ give $p_{22}^c = 0.005 r_v^c$, and thus from (2.9)

$$\text{Var}\,(\hat{z}(t)) = p_{11}^c \to \frac{0.1 p_{22}^c}{0.11} = \frac{0.0005}{0.11} r_v^c. \tag{2.17}$$

- A perfect y_2 measurement, i.e. $r_v^c/r_{22}^c \to \infty$, results in $K_2^c \to \begin{bmatrix} 0.1 & \infty \end{bmatrix}^T$,

$$\hat{Z}(s) = \hat{Y}_1(s) \to \frac{1}{10s+1} \left[U(s) + Y_2(s) \right], \tag{2.18}$$

and

$$\text{Var}\,(\hat{z}(t)) \to 0. \tag{2.19}$$

With the assumptions made, we find a perfect deterministic estimator using u and y_2 as inputs, while the process noise model is decoupled.

■

2.2 Optimal discrete-time estimators

We now develop the discrete-time optimal estimators that we in Chapter 3 will identify from sampled input-output data. We consider both the prediction (a priori) estimator based on past and present known inputs u_k and past secondary measurements $y_{2,k}$, and the current (a posteriori) estimator based also on present $y_{2,k}$ measurements.

2.2.1 Statement of discrete-time estimator problem

Consider the known discrete-time plant model

$$\begin{aligned} x_{k+1} &= Ax_k + Bu_k + Gv_k \\ z_k &= C_1 x_k + D_1 u_k \\ y_{1,k} &= z_k + w_{1,k} \\ y_{2,k} &= C_2 x_k + D_2 u_k + w_{2,k}, \end{aligned} \tag{2.20}$$

where x_k is the state vector, and where in the general multivariable case u_k, v_k, z_k, $y_{1,k}$, $y_{2,k}$, $w_{1,k}$ and $w_{2,k}$ are vectors as well. Here,

- u_k is a known input signal
- v_k is a zero mean white noise sequence, with a covariance matrix determined by the expectation $R_v = Ev_k v_k^T$
- $w_k = \begin{bmatrix} w_{1,k}^T & w_{2,k}^T \end{bmatrix}^T$ is a zero mean white noise sequence, with a covariance matrix determined by the expectation $R_w = \begin{bmatrix} R_{11} & R_{12} \\ R_{21} & R_{22} \end{bmatrix} = Ew_k w_k^T$
- R_w is positive definite (see Chapter 4 for a special perfect measurement case)
- v_k and w_k are uncorrelated, i.e. $Ev_j w_k^T = 0$ for all j and k (may be relaxed, see Subsection 2.2.6)
- both v_k and w_k are uncorrelated with the input u_k, i.e. $Eu_j v_k^T = 0$ and $Eu_j w_k^T = 0$ for all j and k
- only the output $y_{2,k}$ is normally available (which may, however, also include more or less noisy measurements of z_k)
- (C_2, A) is detectable (see Appendix A)
- $(A, G\sqrt{R_v})$ is stabilizable (see Appendix A).

These assumptions make it possible to apply the Kalman filtering theory (Appendix A). Note that noise components that are not white must be modeled as filtered white noise, with the filter model included in the system model (2.20). Also note that some or all of the secondary y_2 measurements may be collinear, and also collinear with some or all of the known inputs u and/or some or all of the primary y_1 measurements.

Time delays may be included by use of extra state variables in the plant model (Franklin et al., 1990), or they may be accounted for by appropriately shifting the input and/or output data.

The problem is now to determine the optimal linear one-step-ahead prediction (a priori) estimator $\hat{z}_{k|k-1}$ based on past and present u_k and past $y_{2,k}$ values, and the optimal linear current (a posteriori) estimator $\hat{z}_{k|k}$ based also on present $y_{2,k}$ values. With an optimal estimator we here mean an unbiased and minimum variance estimator.

Note that it is a part of the problem that neither past nor present $y_{1,k}$ values are available as a basis for the z_k estimates. This is a common situation in industrial applications, e.g. in polymer extruding, where product quality measurements involve costly laboratory analyses. Product samples are then collected at a rather low sampling rate, and product quality estimates at a higher rate may thus be valuable for operator support and other applications.

2.2.2 General discussion on ARMAX and OE models

As a background for the development and later identification of optimal discrete-time estimators, it is suitable to look at some model alternatives. We will then find a principal and important difference between the ordinary case using only u as estimator input, and the present case using also y_2 as input.

The ordinary case

In the ordinary case with u_k as input and y_k as output, the discrete-time predictor form Kalman filter driven by u_k and y_k will be given by the equations

$$\begin{aligned} \hat{x}_{k+1|k} &= A\hat{x}_{k|k-1} + Bu_k + AKe_k \\ \hat{z}_{k|k-1} &= \hat{y}_{k|k-1} = C\hat{x}_{k|k-1} + Du_k \\ e_k &= y_k - \hat{y}_{k|k-1}, \end{aligned} \tag{2.21}$$

where $\hat{x}_{k|k-1}$ is the prediction (a priori) state estimate and e_k is the white innovations process, while K is the Kalman gain (Appendix A).

Remark 2 *The subscript $(\cdot)_{k|k-1}$ notation is used to mark variables estimated at time step k on the basis of y_k data up to time step $k-1$.*

From (2.21) follows the innovations model

$$\begin{aligned} \hat{x}_{k+1|k} &= A\hat{x}_{k|k-1} + Bu_k + AKe_k \\ y_k &= C\hat{x}_{k|k-1} + Du_k + e_k. \end{aligned} \tag{2.22}$$

OE model From (2.22) we find the OE (Output Error) model

$$y_k = \left[C(qI - A)^{-1}B + D\right] u_k + \eta_k, \tag{2.23}$$

where $\eta_k = \left[C(qI - A)^{-1}K + I\right] e_k$ is a non-white sequence. The optimal z_k and y_k estimator when past values of y_k are not known is thus

$$\hat{z}_k^{\mathrm{OE}} = \hat{y}_k^{\mathrm{OE}} = \left[C(qI - A)^{-1}B + D\right] u_k. \tag{2.24}$$

The z_k estimation error covariance is then determined by the process noise propagated through the plant, given by the solution of the Lyapunov equation

$$P^{\mathrm{OEU}} = AP^{\mathrm{OEU}}A^T + GR_vG^T, \tag{2.25}$$

where $P^{\mathrm{OEU}} = E(x_k - \hat{x}_{1,k}^{\mathrm{OE}})(x_k - \hat{x}_{1,k}^{\mathrm{OE}})^T$, and the result is

$$\mathrm{Cov}(\hat{z}_k^{\mathrm{OE}}) = CP^{\mathrm{OEU}}C^T. \tag{2.26}$$

ARMAX model As an alternative we may eliminate e_k from (2.22) and arrive at the ARMAX (AutoRegressive Moving Average with eXtra inputs) model

$$y_k = C(qI - A + AKC)^{-1}\left[(B - AKD)u_k + AKy_k\right] + Du_k + e_k. \tag{2.27}$$

This is the basis for optimal z_k and y_k estimation when past y_k measurements are available.

Comparison of OE and ARMAX models From (2.23) and (2.27) we see that the deterministic part of the OE model is equal to the deterministic part of the ARMAX model with $K = 0$. This fact may be utilized when the ordinary OE model is to be identified from input-output data (see Chapter 3).

The present case

OE model When we use also $y_{2,k}$ as an input to the estimator, the Kalman filter driven by u_k and $y_{2,k}$ (and not $y_{1,k}$, since it is assumed not to be available) will be given by

$$\begin{aligned} \hat{x}_{k+1|k}^{\mathrm{OE}} &= A\hat{x}_{k|k-1}^{\mathrm{OE}} + Bu_k + AK_2^{\mathrm{OE}}e_{2,k}^{\mathrm{OE}} \\ \hat{y}_{2,k|k-1} &= C_2\hat{x}_{k|k-1}^{\mathrm{OE}} + D_2u_k \\ e_{2,k}^{\mathrm{OE}} &= y_{2,k} - \hat{y}_{2,k|k-1}. \end{aligned} \tag{2.28}$$

From this follows the innovations model

$$\begin{aligned} \hat{x}^{\mathrm{OE}}_{k+1|k} &= A\hat{x}^{\mathrm{OE}}_{k|k-1} + Bu_k + AK_2^{\mathrm{OE}} e^{\mathrm{OE}}_{2,k} \\ y_{2,k} &= C_2\hat{x}^{\mathrm{OE}}_{k|k-1} + D_2u_k + e^{\mathrm{OE}}_{2,k}, \end{aligned} \tag{2.29}$$

which after elimination of $\hat{x}^{\mathrm{OE}}_{k|k-1}$ and combined with the primary output equations in (2.20) gives the OE model

$$\begin{aligned} y_{1,k} &= C_1\left[qI - A + AK_2^{\mathrm{OE}}C_2\right]^{-1} \\ &\quad \times \left[\left(B - AK_2^{\mathrm{OE}}D_2\right)u_k + AK_2^{\mathrm{OE}}y_{2,k}\right] + D_1u_k + \vartheta_k, \end{aligned} \tag{2.30}$$

where

$$\vartheta_k = C_1(x_k - \hat{x}^{\mathrm{OE}}_{k|k-1}) + w_{1,k} \tag{2.31}$$

is a non-white sequence (not an innovations representation, since it is not an internal feedback signal in the Kalman filter).

ARMAX model When we use also $y_{1,k}$ as an input to the Kalman filter, the innovations model (2.29) is altered to

$$\begin{aligned} \hat{x}^{\mathrm{ARMAX}}_{k+1|k} &= A\hat{x}^{\mathrm{ARMAX}}_{k|k-1} + Bu_k \\ &\quad + AK_1^{\mathrm{ARMAX}} e^{\mathrm{ARMAX}}_{1,k} + AK_2^{\mathrm{ARMAX}} e^{\mathrm{ARMAX}}_{2,k} \\ y_{1,k} &= C_1\hat{x}^{\mathrm{ARMAX}}_{k|k-1} + D_1u_k + e^{\mathrm{ARMAX}}_{1,k} \\ y_{2,k} &= C_2\hat{x}^{\mathrm{OE}}_{k|k-1} + D_2u_k + e^{\mathrm{ARMAX}}_{2,k}, \end{aligned} \tag{2.32}$$

which after elimination of $e^{\mathrm{ARMAX}}_{2,k}$ and $\hat{x}^{\mathrm{ARMAX}}_{k|k-1}$ gives the ARMAX model

$$\begin{aligned} y_{1,k} &= C_1\left[qI - A + AK_1^{\mathrm{ARMAX}}C_1 + AK_2^{\mathrm{ARMAX}}C_2\right]^{-1} \\ &\quad \times \begin{bmatrix} \left(B - AK_1^{\mathrm{ARMAX}}D_1 - AK_2^{\mathrm{ARMAX}}D_2\right)u_k \\ +AK_1^{\mathrm{ARMAX}}y_{1,k} + AK_2^{\mathrm{ARMAX}}y_{2,k} \end{bmatrix} \\ &\quad + D_1u_k + e^{\mathrm{ARMAX}}_{1,k}. \end{aligned} \tag{2.33}$$

Comparison of OE and ARMAX models A comparison of the OE and ARMAX models above shows that the deterministic part (considering $y_{2,k}$ as an input) of the OE model (2.30) has the same structure as the deterministic part (again considering $y_{2,k}$ as an input) of the ARMAX model (2.33) with $K_1^{\mathrm{ARMAX}} = 0$. Note, however, that the Kalman gains K_2^{OE} and K_2^{ARMAX} are not the same, except for special cases with perfect $y_{2,k}$ measurements and/or very noisy $y_{1,k}$ measurements. Use of K_2^{ARMAX} in (2.28) will thus be the same as using an observer

with a non-optimal gain instead of the Kalman filter driven by u_k and $y_{2,k}$, and it will therefore generally not give the optimal prediction of z_k and $y_{1,k}$. This has significant importance when it comes to the problem of estimator identification (see Chapter 3).

2.2.3 Optimal output error prediction (OEP) estimator

It follows from the discussion above, that the optimal prediction (a priori) estimator for z_k and $y_{1,k}$ when past $y_{1,k}$ values are not known is derived from (2.30) as

$$\begin{aligned} \hat{z}^{\mathrm{OE}}_{k|k-1} &= \hat{y}^{\mathrm{OE}}_{1,k|k-1} = C_1 \left[qI - A + AK_2^{\mathrm{OE}} C_2\right]^{-1} \\ &\quad \times \left[\left(B - AK_2^{\mathrm{OE}} D_2\right) u_k + AK_2^{\mathrm{OE}} y_{2,k}\right] + D_1 u_k, \end{aligned} \tag{2.34}$$

i.e. based on a Kalman filter driven by u_k and $y_{2,k}$. The Kalman gain is then found from the algebraic Riccati equation

$$\begin{aligned} P^{\mathrm{OEP}} &= AP^{\mathrm{OEP}} A^T + GR_v G^T \\ &\quad -AP^{\mathrm{OEP}} C_2^T \left(C_2 P^{\mathrm{OEP}} C_2^T + R_{22}\right)^{-1} C_2 P^{\mathrm{OEP}} A^T \end{aligned} \tag{2.35}$$

and

$$K_2^{\mathrm{OE}} = P^{\mathrm{OEP}} C_2^T \left(C_2 P^{\mathrm{OEP}} C_2^T + R_{22}\right)^{-1}, \tag{2.36}$$

where $P^{\mathrm{OEP}} = E(x_k - \hat{x}^{\mathrm{OE}}_{k|k-1})(x_k - \hat{x}^{\mathrm{OE}}_{k|k-1})^T$ is the minimized prediction state estimation covariance (see Appendix A).

This prediction estimator is shown in the block diagram in Fig. 2.4.

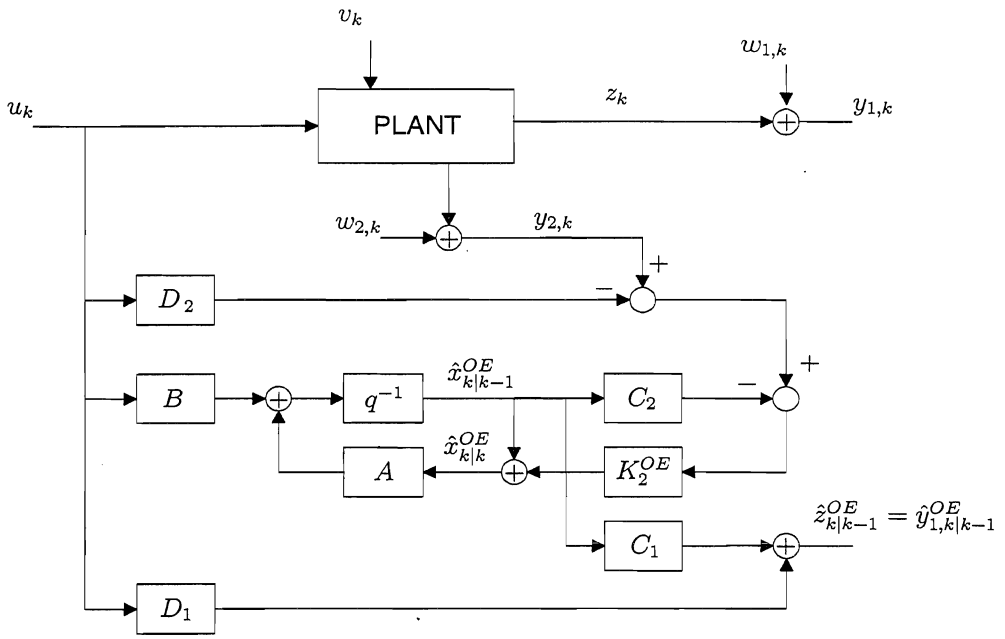

Figure 2.4 Block diagram for optimal discrete-time primary property prediction estimator.

Prediction estimator covariances

The theoretical $\hat{z}^{\mathrm{OE}}_{k|k-1}$ and $\hat{y}^{\mathrm{OE}}_{1,k|k-1}$ estimation covariances follow directly from (2.30), (2.31) and (2.34) and the fact that $z_k = y_{1,k} - w_{1,k}$ as

$$Cov\left(\hat{z}^{\mathrm{OE}}_{k|k-1}\right) = C_1 P^{\mathrm{OEP}} C_1^T \tag{2.37}$$

and

$$Cov\left(\hat{y}^{\mathrm{OE}}_{1,k|k-1}\right) = E\vartheta(t)\vartheta^T(t) = C_1 P^{\mathrm{OEP}} C_1^T + R_{11}, \tag{2.38}$$

where P^{OEP} is given by (2.35).

The development of the optimal prediction estimator and its covariance properties are summarized in Proposition 2.2:

Proposition 2.2 - Optimal discrete-time prediction estimator

For the system (2.20), the optimal discrete-time prediction z_k and $y_{1,k}$ estimator based on past and present u_k and past $y_{2,k}$ values is given by (2.34). The estimator covariances are given by (2.37) and (2.38).

■

2.2.4 Optimal output error current (OEC) estimator

In the discrete-time Kalman filter given by (2.28), the current (a posteriori) state estimate is formed by

$$\hat{x}^{\mathrm{OE}}_{k|k} = (I - K^{\mathrm{OE}}_2 C_2)\hat{x}^{\mathrm{OE}}_{k|k-1} + K^{\mathrm{OE}}_2 (y_{2,k} - D_2 u_k) \tag{2.39}$$

(see Fig. 2.4 and Appendix A).

Remark 3 *The subscript $(\cdot)_{k|k}$ notation is used to mark variables estimated at time step k on the basis of $y_{2,k}$ data up to time step k.*

From the innovations model (2.29) we obtain

$$\hat{x}^{\mathrm{OE}}_{k|k-1} = \left[qI - A + AK^{\mathrm{OE}}_2 C_2\right]^{-1} \left[(B - AK^{\mathrm{OE}}_2 D_2)u_k + AK^{\mathrm{OE}}_2 y_{2,k}\right], \tag{2.40}$$

and thus from (2.39) and the z and $y_{1,k}$ output equations in (2.20) the optimal current estimator

$$\begin{aligned} \hat{z}^{\mathrm{OE}}_{k|k} \;=\; & \hat{y}^{\mathrm{OE}}_{1,k|k} = C_1(I - K^{\mathrm{OE}}_2 C_2)\left[qI - A + AK^{\mathrm{OE}}_2 C_2\right]^{-1} \\ & \times \left[(B - AK^{\mathrm{OE}}_2 D_2)u_k + AK^{\mathrm{OE}}_2 y_{2,k}\right] \\ & + C_1 K^{\mathrm{OE}}_2 (y_{2,k} - D_2 u_k) + D_1 u_k. \end{aligned} \tag{2.41}$$

The block diagram for this estimator is the same as shown in Fig. 2.4, only that we now use the output $\hat{z}^{\mathrm{OE}}_{k|k} = \hat{y}^{\mathrm{OE}}_{1,k|k} = C_1 \hat{x}^{\mathrm{OE}}_{k|k} + D_1 u_k$, i.e. based on the current state estimate $\hat{x}^{\mathrm{OE}}_{k|k}$.

The y_1 estimation error then becomes

$$\psi_k = y_{1,k} - \hat{y}^{\mathrm{OE}}_{1,k|k} = C_1 \left(x_k - \hat{x}^{\mathrm{OE}}_{k|k}\right) + w_{1,k}, \tag{2.42}$$

which just as ϑ_k in (2.31) is a non-white sequence.

Remark 4 *As in the continuous-time case, the Kalman filter will not give the optimal current estimate $\hat{y}^{OE}_{1,k|k}$ if the measurement noise sources $w_{1,k}$ and $w_{2,k}$ are correlated, i.e. if $Ew_1(k)w_2^T(k) \neq 0$. The Kalman filter will, however, still give the optimal estimate of the output property $z_k = C_1 x_k + D_1 u_k$.*

Current estimator covariances

The theoretical $\hat{z}^{\mathrm{OE}}_{k|k}$ and $\hat{y}^{\mathrm{OE}}_{1,k|k}$ estimation covariances follow from (2.42) and the fact that $z_k = y_{1,k} - w_{1,k}$ as

$$Cov\left(\hat{z}^{\mathrm{OE}}_{k|k}\right) = C_1 P^{\mathrm{OEC}} C_1^T \tag{2.43}$$

and

$$\mathrm{Cov}(\hat{y}^{\mathrm{OE}}_{1,k|k}) = E\psi_k\psi_k^T = C_1 P^{\mathrm{OEC}} C_1^T + R_{11}, \tag{2.44}$$

with $P^{\mathrm{OEC}} = E(x_k - \hat{x}^{\mathrm{OE}}_{k|k})(x_k - \hat{x}^{\mathrm{OE}}_{k|k})^T$ determined from

$$\begin{aligned} P^{\mathrm{OEC}} &= (I - K_2^{\mathrm{OE}} C_2) P^{\mathrm{OEP}} \left(I - K_2^{\mathrm{OE}} C_2\right)^T \\ &\quad + K_2^{\mathrm{OE}} R_{22} \left(K_2^{\mathrm{OE}}\right)^T, \end{aligned} \tag{2.45}$$

where P^{OEP} is given by (2.35) (see also Appendix A).

The optimal current estimator and its covariance properties are summarized in Proposition 2.3:

Proposition 2.3 - Optimal discrete-time current estimator

For the system (2.20), the optimal discrete-time current z_k and $y_{1,k}$ estimator based on past and present u_k and $y_{2,k}$ values is given by (2.41). The estimator covariances are given by (2.43) and (2.44).

■

2.2.5 A note on observability

Note that we do not assume that (C_2, A) is observable, only that it is detectable (see Appendix A for definitions). In many practical cases it is quite reasonable to expect the system structure

$$\begin{aligned} \begin{bmatrix} x_1 \\ x_2 \end{bmatrix}_{k+1} &= \begin{bmatrix} A_{11} & A_{12} \\ 0 & A_{22} \end{bmatrix} \begin{bmatrix} x_1 \\ x_2 \end{bmatrix}_k + \begin{bmatrix} B_1 \\ B_2 \end{bmatrix} u_k + \begin{bmatrix} G_1 \\ G_2 \end{bmatrix} v_k \\ z_k &= C_1 x_{1,k} + D_1 u_k \\ y_{1,k} &= z_k + w_{1,k} \\ y_{2,k} &= C_2 x_{2,k} + D_2 u_k + w_{2,k}, \end{aligned} \tag{2.46}$$

which means that the primary output state $x_{1,k}$ is not observable from the secondary $y_{2,k}$ outputs. As long as the system $\left(A_{11}, \begin{bmatrix} A_{12} & B_1 \end{bmatrix}, C_1, D_1\right)$ is asymptotically stable, however, (C_2, A) is still detectable, and the Kalman filtering formalism may thus be applied. A continuous-time example of this is already given in Example 2.1.

The most extreme case occurs when not even (C_2, A_{22}) is observable. This will result in $K_2^{\mathrm{OE}} = 0$, and the prediction and current estimators (2.34) and (2.41) are then reduced to

$$\hat{z}^{\mathrm{OE}}_{k|k-1} = \hat{z}^{\mathrm{OE}}_{k|k} = \hat{y}^{\mathrm{OE}}_{1,k|k-1} = \hat{y}^{\mathrm{OE}}_{1,k|k} = C_1(qI - A)^{-1}Bu_k + D_1 u_k. \tag{2.47}$$

This is the ordinary deterministic OE estimator (2.24).

2.2.6 Relaxed noise constraints

In the problem statement in Subsection 2.2.1 it was assumed that the white process and measurement noise sequences v_k and $w_k = \begin{bmatrix} w_{1,k}^T & w_{2,k}^T \end{bmatrix}^T$ are uncorrelated, i.e. that $Ev_j w_k^T = 0$ for all j and k. We may relax this constraint by still assuming that v_k and w_k are white sequences, but allowing for $Ev_k w_{2,k}^T = R_{vw} \neq 0$. As given in Åström and Wittenmark (1990), the algebraic Riccati equation (2.35) will then be replaced by

$$\begin{aligned} P_{vw}^{\mathrm{OEP}} &= AP_{vw}^{\mathrm{OEP}}A^T + GR_vG^T \\ &\quad - \left(AP_{vw}^{\mathrm{OEP}}C_2^T + GR_{vw}\right)\left(C_2P_{vw}^{\mathrm{OEP}}C_2^T + R_{22}\right)^{-1} \\ &\quad \times \left(AP_{vw}^{\mathrm{OEP}}C_2^T + GR_{vw}\right)^T. \end{aligned} \tag{2.48}$$

Optimal prediction estimator with relaxed noise constraints

We further find that AK_2^{OE} is replaced by the predictor Kalman filter gain

$$K_{p,2}^{\mathrm{OE}} = \left(AP_{vw}^{\mathrm{OEP}}C_2^T + GR_{vw}\right)\left(C_2P_{vw}^{\mathrm{OEP}}C_2^T + R_{22}\right)^{-1}, \tag{2.49}$$

and the optimal prediction estimator (2.34) is thus altered to

$$\begin{aligned} \hat{z}_{k|k-1}^{\mathrm{OE}} &= \hat{y}_{1,k|k-1}^{\mathrm{OE}} = C_1\left[qI - A + K_{p,2}^{\mathrm{OE}}C_2\right]^{-1} \\ &\quad \times \left[\left(B - K_{p,2}^{\mathrm{OE}}D_2\right)u_k + K_{p,2}^{\mathrm{OE}}y_{2,k}\right] + D_1u_k. \end{aligned} \tag{2.50}$$

Optimal current estimator with relaxed noise constraints

In this case K_2^{OE} is replaced by the predictor-corrector Kalman filter gain

$$K_{c,2}^{\mathrm{OE}} = P_{vw}^{\mathrm{OEP}}C_2^T\left(C_2P_{vw}^{\mathrm{OEP}}C_2^T + R_{22}\right)^{-1}, \tag{2.51}$$

i.e. the same expression as (2.36), only that P^{OEP} is replaced by P_{vw}^{OEP} given by (2.48). The optimal current estimator (2.41) is thus replaced by

$$\begin{aligned} \hat{z}_{k|k}^{\mathrm{OE}} &= \hat{y}_{1,k|k}^{\mathrm{OE}} = C_1\left(I - K_{c,2}^{\mathrm{OE}}C_2\right)\left[qI - A + K_{p,2}^{\mathrm{OE}}C_2\right]^{-1} \\ &\quad \times \left[\left(B - K_{p,2}^{\mathrm{OE}}D_2\right)u_k + K_{p,2}^{\mathrm{OE}}y_{2,k}\right] + C_1K_{c,2}^{\mathrm{OE}}(y_{2,k} - D_2u_k) + D_1u_k. \end{aligned} \tag{2.52}$$

2.2.7 Examples of optimal estimators

Example 2.2

Consider the pure delay system

$$\begin{aligned} x_{1,k+1} &= x_{2,k} \\ x_{2,k+1} &= u_k + v_k \\ z_k &= x_{1,k} \\ y_{1,k} &= z_k + w_{1,k} \\ y_{21,k} &= z_k + w_{21,k} \\ y_{22,k} &= x_{2,k} + w_{22,k}, \end{aligned} \tag{2.53}$$

with $A = \begin{bmatrix} 0 & 1 \\ 0 & 0 \end{bmatrix}$, $B = G = \begin{bmatrix} 0 \\ 1 \end{bmatrix}$, $C_1 = C_{21} = \begin{bmatrix} 1 & 0 \end{bmatrix}$, $C_{22} = \begin{bmatrix} 0 & 1 \end{bmatrix}$ and $D_1 = D_{21} = D_{22} = 0$. This is a pure delay system as shown in Fig. 2.5, where (C_{22}, A) is not observable.

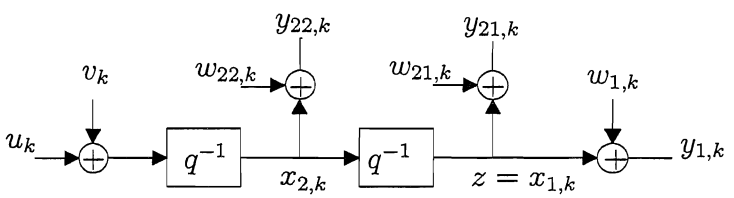

Fig. 2.5 Pure delay second-order system.

No y_{21} measurement We start by looking at the case when the y_{21} measurement is not used. The theoretical predictor for this system can be determined by first finding AK_2^{OE} from (2.35) and (2.36). We then obtain

$$P^{\mathrm{OEP}} = \begin{bmatrix} r_v r_{22}/(r_v + r_{22}) & 0 \\ 0 & r_v \end{bmatrix}, \tag{2.54}$$

$$K_2^{\mathrm{OE}} = \begin{bmatrix} 0 \\ r_v/(r_v + r_{22}) \end{bmatrix} \tag{2.55}$$

and

$$AK_2^{\mathrm{OE}} = \begin{bmatrix} r_v/(r_v + r_{22}) \\ 0 \end{bmatrix}, \tag{2.56}$$

which inserted into (2.34) and (2.41) result in equal prediction and current estimators (since $C_1 K_2^{\mathrm{OE}} = 0$ and thus $C_1 (I - K_2^{\mathrm{OE}} C_{22}) = C_1$)

$$\begin{aligned} \hat{z}_{k|k-1}^{\mathrm{OE}} &= \hat{z}_{k|k}^{\mathrm{OE}} = \left(\frac{1}{r_v} + \frac{1}{r_{22}}\right)^{-1} \left(\frac{u_{k-2}}{r_v} + \frac{y_{22,k-1}}{r_{22}}\right) \\ &= \frac{1}{1 + r_v/r_{22}} u_{k-2} + \frac{r_v/r_{22}}{1 + r_v/r_{22}} y_{22,k-1}, \end{aligned} \tag{2.57}$$

where r_v and r_{22} are the variances of v_k and $w_{22,k}$. Considering that the actual input to the system is $u+v$, this shows that the information in u and y_2 is utilized in an optimal way given the noise levels (according to the generalized form of Millmans theorem, see Lewis (1986)).

From (2.37) and (2.43) we also find the estimator variances

$$\mathrm{Var}\left(\hat{z}_{k|k-1}^{\mathrm{OE}}\right) = \mathrm{Var}\left(\hat{z}_{k|k}^{\mathrm{OE}}\right) = C_1 P^{\mathrm{OEP}} C_1^T = \frac{r_v}{1 + r_v/r_{22}}. \tag{2.58}$$

Special cases occur when

- $r_v/r_{22} \to 0$, resulting in $\hat{z}_{k|k-1}^{\mathrm{OE}} = \hat{z}_{k|k}^{\mathrm{OE}} \to u_{k-2}$ and $\mathrm{Var}\left(\hat{z}_{k|k-1}^{\mathrm{OE}}\right)$ $= \mathrm{Var}\left(\hat{z}_{k|k}^{\mathrm{OE}}\right) \to r_v$.

- $r_v/r_{22} \to \infty$, resulting in $\hat{z}_{k|k-1}^{\mathrm{OE}} = \hat{z}_{k|k}^{\mathrm{OE}} \to y_{22,k-1}$ and $\mathrm{Var}\left(\hat{z}_{k|k-1}^{\mathrm{OE}}\right)$ $= \mathrm{Var}\left(\hat{z}_{k|k}^{\mathrm{OE}}\right) \to 0$. Note that this is a reduced estimator, where the inputs u_k and v_k are decoupled by the use of the perfect y_{22} measurement (see a further discussion of such cases in Chapter 4).

All measurements used When also the y_{21} measurement is used, the prediction estimator is still the same as in (2.57), while the current estimator is altered to

$$\hat{z}_{k|k}^{\mathrm{OE}} = \frac{r_{21} r_{22} u_{k-2} + r_{21} r_v y_{22,k-1} + r_{22} r_v y_{21,k}}{r_{21} r_{22} + r_{21} r_v + r_{22} r_v}, \tag{2.59}$$

where r_{21} is the $w_{21,k}$ variance.

For two special cases we obtain the following results:

- When $r_v = r_{21} = r_{22}$ we find

$$\hat{z}_{k|k}^{\mathrm{OE}} = \frac{u_{k-2} + y_{22,k-1} + y_{21,k}}{3}, \tag{2.60}$$

while the current estimator variance becomes

$$\mathrm{Var}\left(\hat{z}_{k|k}^{\mathrm{OE}}\right) = \frac{r}{3}. \tag{2.61}$$

Using all information in u_k, $y_{22,k}$ and $y_{21,k}$ will thus in this case give only a third of the estimator variance as compared with use of only $y_{21,k}$.

- When $r_{21}/r_v \to 0$ and $r_{21}/r_{22} \to 0$ we find $\hat{z}^{\mathrm{OE}}_{k|k} \to y_{21,k}$ and $\mathrm{Var}\left(\hat{z}^{\mathrm{OE}}_{k|k}\right) \to r_{21}$.

■

Example 2.3

Consider the second-order system

$$\begin{aligned} x_{1,k+1} &= a_{11}x_{1,k} + a_{12}x_{2,k} + b_1u_k \\ x_{2,k+1} &= a_{21}x_{1,k} + a_{22}x_{2,k} + b_2u_k + v_k \\ z_k &= x_{1,k} \\ y_{1,k} &= z_k + w_{1,k} \\ y_{2,k} &= x_{2,k} + w_{2,k}. \end{aligned} \tag{2.62}$$

This will generally lead to the second-order prediction estimator

$$\begin{aligned} \hat{z}^{\mathrm{OE}}_{k|k-1} &= \hat{y}^{\mathrm{OE}}_{1,k|k-1} = -a_1\hat{y}^{\mathrm{OE}}_{1,k-1|k-2} - a_2\hat{y}^{\mathrm{OE}}_{1,k-2|k-3} \\ &\quad + b_{11}u_{k-1} + b_{12}u_{k-2} + b_{21}y_{2,k-1} + b_{22}y_{2,k-2}. \end{aligned} \tag{2.63}$$

Two special cases can be easily calculated:

- Very noisy y_2 measurements, i.e. $r_v/r_{22} \to 0$, will result in $K_2^{\mathrm{OE}} = 0$. With u as input and y_1 as output, we will then obtain the second-order prediction estimator

$$\begin{aligned} \hat{x}^{\mathrm{OE}}_{1,k+1|k} &= a_{11}\hat{x}^{\mathrm{OE}}_{1,k|k-1} + a_{12}\hat{x}^{\mathrm{OE}}_{2,k|k-1} + b_1u_k \\ \hat{x}^{\mathrm{OE}}_{2,k+1|k} &= a_{21}\hat{x}^{\mathrm{OE}}_{1,k|k-1} + a_{22}\hat{x}^{\mathrm{OE}}_{2,k|k-1} + b_2u_k \\ \hat{z}^{\mathrm{OE}}_{k|k-1} &= \hat{y}^{\mathrm{OE}}_{1,k|k-1} = \hat{x}^{\mathrm{OE}}_{1,k|k-1}. \end{aligned} \tag{2.64}$$

  This is an ordinary OE estimator, and the theoretical z_k prediction variance will thus be determined by (2.26).

- With perfect $y_{2,k}$ measurements , i.e. $r_v/r_{22} \to \infty$, the system (2.62) is reduced to the first-order deterministic system

$$\begin{aligned} x_{1,k+1} &= a_{11}x_{1,k} + a_{12}y_{2,k} + b_1u_k \\ z_k &= x_{1,k}, \end{aligned} \tag{2.65}$$

  i.e. the state variable $x_{2,k}$ is decoupled from the primary output. The resulting optimal estimator then becomes

$$\hat{z}^{\mathrm{OE}}_{k|k-1} = \hat{y}^{\mathrm{OE}}_{1,k|k-1} = (q - a_{11})^{-1}(b_1u_k + a_{12}y_{2,k}), \tag{2.66}$$

while the prediction variance according to (2.37) becomes

$$\mathrm{Var}(\hat{z}^{\mathrm{OE}}_{k|k-1}) = 0. \tag{2.67}$$

The form of estimator reduction due to perfect $y_{2,k}$ measurements that we find in this example, is more generally treated in Chapter 4.

■

2.3 Discrete-time ARMAX estimators

In Subsection 2.2.2 we have shown that primary output estimators based on ARMAX models are not optimal in the present case. The reason for this is that they are based on underlying Kalman filters that make use of past and present $y_{1,k}$ measurements, and the gain related to the $y_{2,k}$ measurements will then not be optimal when the $y_{1,k}$ measurements are not available. There are, however, still some reasons to study this type of estimators, especially since we assume that the estimators are to be identified from experimental data with a limited number of samplings:

- With near perfect y_2 measurements it may be advantageous to use a parsimonious though biased ARMAX estimator with y_2 as ordinary known inputs. This will then result in the same deterministic estimator as if the parsimonious estimator was determined by use of an OE model, but the estimation covariance for the identified estimator will generally be less (e.g. Söderstöm and Stoica, 1989). Such cases are already discussed in Example 2.1, 2.2 and 2.3.

- When a direct measurement of the primary property z is included in the y_2 measurements, we may choose to ignore the y_1 measurements and use a z estimator using only u and y_2. Such a case is discussed in Example 3.5 in Chapter 3.

- It is of general theoretical interest to study estimators based on ARMAX models, especially since the possibility to use the secondary y_2 measurements as ordinary inputs to such a model may be tempting. As we found in Subsection 2.2.2, this will theoretically lead to non-optimal primary output estimators in the present case with non-available y_1 measurements.

2.3.1 Optimal ARMAX estimators with $y_{1,k}$ available

Optimal ARMAX prediction estimator

The ARMAX model based on a Kalman filter driven by u_k, $y_{1,k}$ and $y_{2,k}$ is given by (2.33), from which follows the optimal prediction estimator

$$\begin{aligned}\hat{z}_{k|k-1}^{\mathrm{ARMAX}} &= \hat{y}_{1,k|k-1}^{\mathrm{ARMAX}} = C_1\hat{x}_{k|k-1}^{\mathrm{ARMAX}} + D_1u_k = C_1\left[qI - \tilde{A}\right]^{-1} \\ &\quad \times \left[\tilde{B}u_k + AK_1^{\mathrm{ARMAX}}y_{1,k} + AK_2^{\mathrm{ARMAX}}y_{2,k}\right] + D_1u_k,\end{aligned} \tag{2.68}$$

where $\tilde{A} = A - AK_1^{\mathrm{ARMAX}}C_1 - AK_2^{\mathrm{ARMAX}}C_2$ and $\tilde{B} = B - AK_1^{\mathrm{ARMAX}}D_1 - AK_2^{\mathrm{ARMAX}}D_2$.

The Kalman gain $K^{\mathrm{ARMAX}} = \begin{bmatrix} K_1^{\mathrm{ARMAX}} & K_2^{\mathrm{ARMAX}} \end{bmatrix}$ is here found from the algebraic Riccati equation

$$\begin{aligned}P^{\mathrm{ARMAXP}} &= AP^{\mathrm{ARMAXP}}A^T + GR_vG^T \\ &\quad -AP^{\mathrm{ARMAXP}}C^T(CP^{\mathrm{ARMAXP}}C^T + R_w)^{-1}CP^{\mathrm{ARMAXP}}A^T\end{aligned} \tag{2.69}$$

and

$$K^{\mathrm{ARMAX}} = P^{\mathrm{ARMAXP}}C^T(CP^{\mathrm{ARMAXP}}C^T + R_w)^{-1}, \tag{2.70}$$

where $C = \begin{bmatrix} C_1^T & C_2^T \end{bmatrix}^T$, and where $P^{\mathrm{ARMAXP}} = E(x_k - \hat{x}_{k|k-1}^{\mathrm{ARMAX}})(x_k - \hat{x}_{k|k-1}^{\mathrm{ARMAX}})^T$ is the minimized prediction state estimation covariance.

Assuming that y_1 is available, (2.68) is the optimal linear one-step-ahead predictor if v_k and w_k have arbitrary statistics, and the best of all predictors (including nonlinear predictors) assuming that v_k and w_k are normally distributed (Lewis, 1986).

The asymptotic prediction covariances is in this case determined by the expectations

$$\mathrm{Cov}\left(\hat{z}_{k|k-1}^{\mathrm{ARMAX}}\right) = C_1P^{\mathrm{ARMAXP}}C_1^T \tag{2.71}$$

and

$$\mathrm{Cov}\left(\hat{y}_{1,k|k-1}^{\mathrm{ARMAX}}\right) = C_1P^{\mathrm{ARMAXP}}C_1^T + R_{11}. \tag{2.72}$$

Optimal ARMAX current estimator

If also current $y_{1,k}$ and $y_{2,k}$ measurements are utilized, the optimal current estimator becomes

$$\begin{aligned}\hat{z}_{k|k}^{\mathrm{ARMAX}} &= C_1\left(I - K_1^{\mathrm{ARMAX}}C_1 - K_2^{\mathrm{ARMAX}}C_2\right)\left[qI - \tilde{A}\right]^{-1} \\ &\quad \times \left[\tilde{B}u_k + AK_1^{\mathrm{ARMAX}}y_{1,k} + AK_2^{\mathrm{ARMAX}}y_{2,k}\right] \\ &\quad +C_1K_1^{\mathrm{ARMAX}}(y_{1,k} - D_1u_k) \\ &\quad +C_1K_2^{\mathrm{ARMAX}}(y_{2,k} - D_2u_k) + D_1u_k.\end{aligned} \tag{2.73}$$

With $y_{1,k}$ available, the best estimate of $y_{1,k}$ would obviously be $\hat{y}_{1,k|k}^{\mathrm{ARMAX}} = y_{1,k}$, but such unfiltered measurements would often be of less interest.

Assuming that y_1 is available, (2.73) is the optimal linear estimator if v_k and w_k have arbitrary statistics, and the best of all estimators assuming that v_k and w_k are normally distributed (Lewis, 1986).

The asymptotic covariances for the current estimator is determined by the expectation

$$\mathrm{Cov}\left(\hat{z}_{k|k}^{\mathrm{ARMAX}}\right) = C_1 P^{\mathrm{ARMAXC}} C_1^T, \tag{2.74}$$

where

$$\begin{aligned} P^{\mathrm{ARMAXC}} &= \left(I - K^{\mathrm{ARMAX}} C\right) P^{\mathrm{ARMAXP}} \left(I - K^{\mathrm{ARMAX}} C\right)^T \\ &\quad + \left(K^{\mathrm{ARMAX}}\right) R_w \left(K^{\mathrm{ARMAX}}\right)^T, \end{aligned} \tag{2.75}$$

with P^{ARMAXP} given by (2.69) (see also Appendix A).

2.3.2 Non-optimal ARMAX estimators when $y_{1,k}$ is not available

In the main case of the thesis, neither past nor present y_1 measurements are available as a basis for the primary output estimate. In the ordinary case with only one output vector y_k, we would then set $K = 0$ in the optimal ARMAX estimator and arrive at the optimal OE estimator utilizing only the information in u_k. A natural choice in the present case is therefore to set $K_1^{\mathrm{ARMAX}} = 0$ in (2.68) and (2.73). As K_2^{ARMAX} is not the optimal gain when only the u_k an $y_{2,k}$ information is available, this will give non-optimal results. For comparison purposes we develop these non-optimal primary output estimators and their covariances.

Non-optimal ARMAX prediction estimator

With $K_1^{\mathrm{ARMAX}} = 0$ we find from (2.68) the prediction estimator

$$\begin{aligned} \hat{z}_{k|k-1}^{\mathrm{ARMAX_2}} &= \hat{y}_{1,k|k-1}^{\mathrm{ARMAX_2}} = C_1 \left[qI - A + AK_2^{\mathrm{ARMAX}} C_2\right]^{-1} \\ &\quad \times \left[(B - AK_2^{\mathrm{ARMAX}} D_2) u_k + AK_2^{\mathrm{ARMAX}} y_{2,k}\right] + D_1 u_k. \end{aligned} \tag{2.76}$$

From (2.20) and (2.32) with $K_1^{\mathrm{ARMAX}} = 0$ we find that the state estimation error $\tilde{x}_{k|k-1}^{\mathrm{ARMAX_2}} = x_k - \hat{x}_{k|k-1}^{\mathrm{ARMAX_2}}$ is governed by

$$\tilde{x}_{k+1|k}^{\mathrm{ARMAX_2}} = (A - AK_2^{\mathrm{ARMAX}} C_2) \tilde{x}_{k|k-1}^{\mathrm{ARMAX_2}} + G v_k - AK_2^{\mathrm{ARMAX}} w_{2,k}, \tag{2.77}$$

and the prediction state estimation covariance $P^{\mathrm{ARMAX_2P}} = E\tilde{x}_{k|k-1}^{\mathrm{ARMAX_2}} \left(\tilde{x}_{k|k-1}^{\mathrm{ARMAX_2}}\right)^T$ is thus determined by the Lyapunov equation

$$\begin{aligned} P^{\mathrm{ARMAX_2P}} &= \left(A - AK_2^{\mathrm{ARMAX}} C_2\right) P^{\mathrm{ARMAX_2P}} \left(A - AK_2^{\mathrm{ARMAX}} C_2\right)^T \\ &\quad + G R_v G^T + AK_2^{\mathrm{ARMAX}} R_{22} \left(AK_2^{\mathrm{ARMAX}}\right)^T. \end{aligned} \tag{2.78}$$

This is the basis for finding

$$Cov\left(\hat{z}_{k|k-1}^{\mathrm{ARMAX_2}}\right) = C_1 P^{\mathrm{ARMAX_2P}} C_1^T, \tag{2.79}$$

and

$$Cov\left(\hat{y}_{1,k|k-1}^{\mathrm{ARMAX_2}}\right) = C_1 P^{\mathrm{ARMAX_2P}} C_1^T + R_{11}. \tag{2.80}$$

Non-optimal ARMAX current estimator

With $K_1^{\mathrm{ARMAX}} = 0$ we find from (2.73) the current estimator

$$\begin{aligned} \hat{z}_{k|k}^{\mathrm{ARMAX_2}} &= \hat{y}_{1,k|k}^{\mathrm{ARMAX_2}} = C_1\left(I - K_2^{\mathrm{ARMAX}} C_2\right)\left[qI - A + AK_2^{\mathrm{ARMAX}} C_2\right]^{-1} \\ &\quad \times \left[\left(B - AK_2^{\mathrm{ARMAX}} D_2\right) u_k + AK_2^{\mathrm{ARMAX}} y_{2,k}\right] \\ &\quad + C_1 K_2^{\mathrm{ARMAX}}(y_{2,k} - D_2 u_k) + D_1 u_k. \end{aligned} \tag{2.81}$$

Defining $\tilde{x}_{k|k}^{\mathrm{ARMAX_2}} = x_k - \hat{x}_{k|k}^{\mathrm{ARMAX_2}}$ and $P^{\mathrm{ARMAX_2C}} = E\tilde{x}_{k|k}^{\mathrm{ARMAX_2}}\left(\tilde{x}_{k|k}^{\mathrm{ARMAX_2}}\right)^T$, we find

$$\begin{aligned} P^{\mathrm{ARMAX_2C}} &= \left(I - K_2^{\mathrm{ARMAX}} C_2\right) P^{\mathrm{ARMAX_2P}} \left(I - K_2^{\mathrm{ARMAX}} C_2\right)^T \\ &\quad + K_2^{\mathrm{ARMAX}} R_{22} \left(K_2^{\mathrm{ARMAX}}\right)^T, \end{aligned} \tag{2.82}$$

where $P^{\mathrm{ARMAX_2P}}$ is given by (2.78). The estimator covariances then become

$$\mathrm{Cov}\left(\hat{z}_{k|k}^{\mathrm{ARMAX_2}}\right) = C_1 P^{\mathrm{ARMAX_2C}} C_1^T, \tag{2.83}$$

and

$$\mathrm{Cov}\left(\hat{y}_{1,k|k}^{\mathrm{ARMAX_2}}\right) = C_1 P^{\mathrm{ARMAX_2C}} C_1^T + R_{11}. \tag{2.84}$$

Example 2.4

Consider the system

$$\begin{aligned} x_{k+1} &= 0.8x_k + bu_k + v_k \\ z_k &= x_k \qquad (2.85) \\ y_{1,k} &= z_k + w_{1,k} \qquad (2.86) \\ y_{2,k} &= z_k + w_{2,k}, \end{aligned}$$

with $r_{11} = Ew_{1,k}^2 = 0.0001$ and $r_{22} = Ew_{2,k}^2 = 0.01$. This is a somewhat special system, in that both $y_{1,k}$ and $y_{2,k}$ are direct measurements of the primary property.

For different process noise variances $r_v = Ev_k^2$, the theoretical primary property estimation variances $\mathrm{Var}(\hat{z}_k)$ are determined by use of the *dlqe.m* and *dlyap.m* functions in the Control System Toolbox for use with Matlab (Grace et al., 1992). The results are given in Table 2.1.

Table 2.1: Primary output estimator variances for different estimators and different levels of process noise.

Estimator type	$r_v = 0.01$	$r_v = 0.1$	$r_v = 1$
Direct use of $\hat{z}_k = y_{2,k}$	0.0100	0.0100	0.0100
OE estimator (2.24) using only u_k as input	0.0156	0.1563	1.5625
Optimal OEP estimator (2.34)	0.0137	0.1058	1.0063
Optimal OEC estimator (2.41)	0.0058	0.0091	0.0099
Non-optimal ARMAX prediction estimator (2.76)	0.0268	0.2684	2.6838
Non-optimal ARMAX current estimator (2.81)	0.0263	0.2631	2.6309

We see from this that the optimal current estimator (2.41) theoretically is the best choice, although direct use of $y_{2,k}$ is almost as good for high process noise levels. Since $y_{2,k}$ is a direct measurement of z_k, the OEC estimator is much better than the OEP estimator. Due to the fact that $r_{11} << r_{22}$ we obtain $K_2^{\mathrm{ARMAX}} \approx 0$, and this is why the non-optimal ARMAX estimators are so inferior. These differences may be much less pronounced for more general types of models, with different state variables measured by y_1 and y_2 (see e.g. Example 3.2).

■

Example 2.5

Assume a general system with perfect $y_{1,k}$ measurements, i.e. $R_{11} \to 0$. This gives $C_1 K_1^{\mathrm{ARMAX}} \to I$ and $C_1 K_2^{\mathrm{ARMAX}} \to 0$, and the current ARMAX estimator (2.73) will then as expected be simplified to $\hat{z}_{k|k}^{\mathrm{ARMAX}} \to y_{1,k}$. With $y_{1,k}$ not available we will then find $\hat{z}_{k|k}^{\mathrm{ARMAX}} = 0$, i.e. very far from optimal.

■

2.4 Disturbance sensitivity

The assumption that the process noise is white or filtered white noise may in many industrial cases be a rather rough approximation, which also means that R_v in (2.35) and K_2^{OE} in (2.36) are approximations. The developed estimators (2.34) and (2.41) will then no longer be optimal, but they may nevertheless give useful practical results.

For a discussion of this, we choose the optimal current estimator (2.41). For this estimator the estimation error due to process noise is

$$\tilde{z}^v_{k|k} = z^v_k - \hat{z}^v_{k|k}, \tag{2.87}$$

where from (2.20)

$$z^v_k = C_1 (qI - A)^{-1} G v_k. \tag{2.88}$$

With

$$y^v_{2,k} = C_2 (qI - A)^{-1} G v_k \tag{2.89}$$

and use of (2.41), we then find

$$\begin{aligned} \hat{z}^v_{k|k} &= C_1 \left(I - K_2^{\mathrm{OE}} C_2\right) \left(qI - A + AK_2^{\mathrm{OE}} C_2\right)^{-1} AK_2^{\mathrm{OE}} C_2 (qI - A)^{-1} G v_k \\ &\quad + C_1 K_2^{\mathrm{OE}} C_2 (qI - A)^{-1} G v_k. \end{aligned} \tag{2.90}$$

This results in

$$\tilde{z}^v_{k|k} = C_1 \left(I - K_2^{\mathrm{OE}} C_2\right) \left(qI - A + AK_2^{\mathrm{OE}} C_2\right)^{-1} G v_k. \tag{2.91}$$

If in addition to v_k we also have a constant disturbance d acting on the plant via the matrix G_d, we find the corresponding constant estimation error

$$\Delta z|_{u,y_2} = C_1 \left(I - K_2^{\mathrm{OE}} C_2\right) \left(I - A + AK_2^{\mathrm{OE}} C_2\right)^{-1} G_d d. \tag{2.92}$$

This should be compared with the estimation error without use of the y_2 information,

$$\Delta z|_u = C_1 (I - A)^{-1} G_d d. \tag{2.93}$$

Example 2.6

Assume the system in Example 1.1 with $y_2 = y_{23}$, and $a = 0$, $T_1 = T_2 = 1$, $T_3 = 10$, $r^c_v = 0.1$ and $r^c_{22} = 0.01$. Further assume discretization by use of a zero-order hold at the u input and direct sampling of the y_1 and y_2 outputs, with a sampling interval $T = 0.1$. We then find the approximate discrete-time noise variances $r_v = r^c_v/T = 1$ and $r_{22} = r^c_{22} = 0.01$ (Franklin et al., 1990). Finally assume that a constant disturbance d is acting on the system in the same way as the process noise. Determining K_2^{OE} by use of the *dlqe.m* function in the Control System Toolbox for use with Matlab (Grace et al., 1992), we then find the following:

- With use of the y_2 information, the static disturbance results in the static estimation error $\Delta z|_{u,y_2} = 0.0565d$.

- Without use of the y_2 information, the static disturbance results in the static estimation error $\Delta z|_u = d$.

A considerable reduction in the disturbance sensitivity is thus obtained.

■

Chapter 3

Identification of primary output estimators

This chapter deals with the problem of identifying the optimal discrete-time primary output estimators that were theoretically developed in Chapter 2. It is a basic assumption that although the primary outputs normally are sampled and measured only at a low rate, there exists high sampling rate y_1 data from an informative experiment. In Chapter 6 it will be shown that this assumption may be relaxed, i.e. that low and even irregular sampling rate y_1 experimental data is sufficient. The main point in the present chapter is that the optimal OE estimators can be consistently identified by use of the iterative prediction error method (PEM) summarized in Appendix B.

3.1 Methodological discussion

There are three different approaches to the problem of identifying the discrete-time optimal z and y_1 estimators developed in Section 2.2 from experimental input-output data:

- Regard $\varsigma_k = \begin{bmatrix} u_k^T & y_{1,k}^T & y_{2,k}^T \end{bmatrix}^T$ as a joint input-output time series, apply standard system identification techniques for estimating the parameters in an appropriately structured model of ς_k (see e.g. Söderström and Stoica, 1989), and finally construct the optimal estimators (2.34) and (2.41).

- Use u_k as input and $y_k = \begin{bmatrix} y_{1,k}^T & y_{2,k}^T \end{bmatrix}^T$ as output, apply standard system identification techniques and finally construct the optimal estimators.

- Use $\begin{bmatrix} u_k^T & y_{2,k}^T \end{bmatrix}^T$ as input an $y_{1,k}$ as output, and apply standard system identification techniques in order to find the optimal estimators directly.

We will use the last of these approaches. There are two reasons for doing so:

- In a typical industrial case there are many secondary y_2 measurements around the plant, and only one or a few primary y_1 outputs. Using only y_1 as output may therefore considerably reduce the difficulties in finding a useful model.

- In many industrial cases it is difficult and therefore costly to perform an experiment with the same high sampling rate for y_1 as for the secondary y_2 outputs. The primary properties are typically product qualities, that may be found only through laboratory analysis of physical samples, and the available sampling equipment and cost of analysis may limit the sampling rate. At the same time a high y_2 sampling rate may be needed in order to capture the plant dynamics. We are therefore aiming at methods that can combine two different sampling rates (and possibly also an irregular y_1 sampling rate), and the solution to this problem given in Chapter 6 requires the use of only y_1 as output.

In this chapter we will assume experimental data with both y_1 and y_2 sampled at the same high rate. For the identification, we will make use of the iterative prediction error method (PEM) presented in Appendix B.

3.2 Identification of optimal OE estimators

3.2.1 Statement of problem

The basic statement of problem is given in Subsection 2.2.1, only that we now must add that

- data records for u_k, $y_{1,k}$ and $y_{2,k}$ for $k = 1, 2, \cdots, N$ are at hand from an informative experiment (e.g. Goodwin and Payne, 1977), i.e. with u_k persistently exciting of appropriate order (e.g. Söderström and Stoica, 1989) and with a sufficiently large number of samples

- the system operates in open loop (may be relaxed as discussed in Chapter 11)

- the problem now is to identify the optimal output error prediction and current (OEP and OEC) estimators developed in Section 2.2.

For clarity of presentation, we assume that the process noise v and measurement noise $w = \begin{bmatrix} w_1^T & w_2^T \end{bmatrix}^T$ are independent. A theoretical discussion of the case with correlated process and measurement noise sequences is given in Subsection 2.2.6.

3.2.2 Identification of ordinary OE estimator

We start the analysis related to the identification of the optimal discrete-time OE prediction (OEP) and current (OEC) estimators (2.34) and (2.41) by the simpler case of the ordinary OE estimator using only u as input. It is well known that we will then obtain unbiased parameter estimates for the deterministic part of the model (see Söderström and Stoica (1989), p. 205, for the case with the direct input-output matrix $D = 0$). In the following we will show this by an approach that is closely related to the optimal solution for use of the y_2 information.

The starting point is now the system

$$\begin{aligned} x_{k+1} &= Ax_k + Bu_k + Gv_k \\ y_k &= Cx_k + Du_k + w_k, \end{aligned} \tag{3.1}$$

where v_k and w_k are white noise sequences with covariance matrices $R_v = Ev_kv_k^T$ and $R_w = Ew_kw_k^T$, and where $Ev_jw_k^T = 0$, $Eu_jv_k^T = 0$ and $Eu_jw_k^T = 0$ for all j and k.

Express the output equation in (3.1) as

$$y_k = z_k + w_k = G\left(q^{-1}, \theta_0\right) u_k + H\left(q^{-1}, \theta_0\right) v_k + w_k, \tag{3.2}$$

where

$$G\left(q^{-1}, \theta_0\right) = C(qI - A)^{-1}B + D \tag{3.3}$$

and

$$H\left(q^{-1}, \theta_0\right) = C\left(qI - A\right)^{-1} G. \tag{3.4}$$

With the assumptions made z_k and w_k are uncorrelated, i.e. $Ez_kw_k^T = 0$.

Further assume an estimator

$$y_k^{\text{pred}} = z_k^{\text{pred}} = G\left(q^{-1}, \theta\right) u_k, \tag{3.5}$$

such that also $Ez_k^{\text{pred}}w_k^T = 0$. The estimation error is then

$$\varepsilon_k(\theta) = y_k - y_k^{\text{pred}} = \left[G\left(q^{-1}, \theta_0\right) - G\left(q^{-1}, \theta\right)\right] u_k + H\left(q^{-1}, \theta_0\right) v_k + w_k, \tag{3.6}$$

where the three terms are uncorrelated. From this we find

$$\begin{aligned} E\varepsilon_k(\theta)\varepsilon_k^T(\theta) &= E\left\{\left[G\left(q^{-1},\theta_0\right)-G\left(q^{-1},\theta\right)\right]u_k\right\}\left\{[\cdot]\,u_k\right\}^T \\ &\quad +E\left[H\left(q^{-1},\theta_0\right)v_k\right]\left[H\left(q^{-1},\theta_0\right)v_k\right]^T+R_w \\ &\geq E\left[H\left(q^{-1},\theta_0\right)v_k\right]\left[H\left(q^{-1},\theta_0\right)v_k\right]^T+R_w \\ &= CP^{\mathrm{OEU}}C^T+R_w, \end{aligned} \tag{3.7}$$

where P^{OEU} is determined by the Lyapunov equation

$$P^{\mathrm{OEU}} = AP^{\mathrm{OEU}}A^T+GR_vG^T. \tag{3.8}$$

Minimization of the scalar criterion function (with $\mathrm{h}(\cdot)=\det(\cdot)$ or $\mathrm{h}(\cdot)=\mathrm{trace}(\cdot)$)

$$V_N(\theta) = \mathrm{h}\left[\frac{1}{N}\sum_{k=1}^{N}\varepsilon_k(\theta)\varepsilon_k^T(\theta)\right], \tag{3.9}$$

and assuming a correct parametrization, will thus asymptotically (for $N\to\infty$) result in $\theta\to\theta_0$, i.e. we will obtain $G\left(q^{-1},\theta\right)\to G\left(q^{-1},\theta_0\right)$. This gives the OE estimator (2.24), i.e. $y_k^{\mathrm{pred}}\to\hat{y}_k^{\mathrm{OE}}$, with the asymptotic prediction covariance matrix given by the equality in (3.7).

Note that we here take it for granted that the parameter estimate will converge so that the minimum in (3.7) is achieved. This is based on a quite general result that states that the estimate will converge to the best possible approximation of the system that is available in the model set (Ljung, 1978,1987,1999).

Initial model

Due to the possible occurrence of undesired local minima in the criterion function (3.9), it may be essential to use good initial parameter values. Such an initial model can be determined as an LS estimate of an ARX (AutoRegressive with eXogenious inputs) model (Ljung, 1995). This is achieved by rewriting the innovation model (2.22) as the ARMAX model

$$A(q^{-1})y_k = B(q^{-1})u_k+C(q^{-1})e_k, \tag{3.10}$$

which approximately gives

$$A(q^{-1})y_k \approx B(q^{-1})u_k+e_k, \tag{3.11}$$

or

$$\begin{aligned} y_k &\approx \left[I-A(q^{-1})\right]y_k+B(q^{-1})u_k+e_k \\ &= \varphi_k^T\theta_0+e_k. \end{aligned} \tag{3.12}$$

From this we find approximate parameter estimates θ^{init} by use of the ordinary LS method.

3.2.3 Identification of optimal OEP estimator

We now turn to the present case with also the secondary y_2 measurements used as inputs, and we thus want to identify the OEP model (2.30) developed in Chapter 2, i.e.

$$\begin{aligned} y_{1,k} &= C_1 \left[qI - A + AK_2^{\mathrm{OE}} C_2\right]^{-1} \\ &\quad \times \left[\left(B - AK_2^{\mathrm{OE}} D_2\right) u_k + AK_2^{\mathrm{OE}} y_{2,k}\right] + D_1 u_k + \vartheta_k, \end{aligned} \tag{3.13}$$

where

$$\vartheta_k = C_1(x_k - \hat{x}_{k|k-1}^{\mathrm{OE}}) + w_{1,k}, \tag{3.14}$$

with $\hat{x}_{k|k-1}^{\mathrm{OE}}$ given by (2.40). In order to do so we use the predictor in Fig. 3.1, where we may choose a canonical representation with $C_1 = \begin{bmatrix} I & 0 \end{bmatrix}$ (Kailath, 1980).

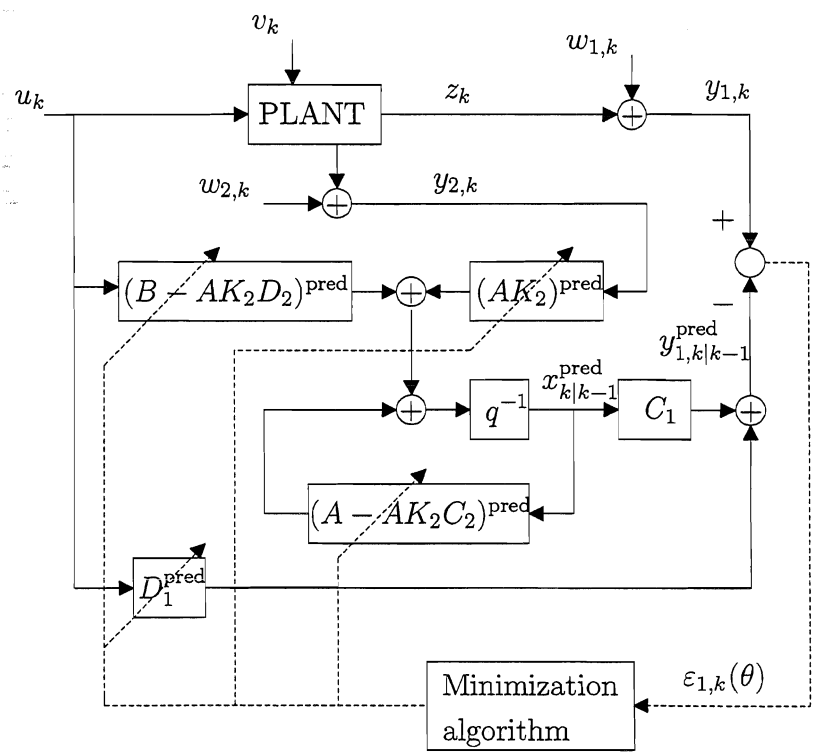

Figure 3.1 Identification of OEP estimator by prediction error minimization.

We thus have

$$\begin{aligned} y_{1,k} &= C_1 x_k + D_1 u_k + w_{1,k} = z_k + w_{1,k} \\ y^{\text{pred}}_{1,k|k-1} &= C_1 x^{\text{pred}}_{k|k-1} + D_1^{\text{pred}} u_k = z^{\text{pred}}_{k|k-1}, \end{aligned} \tag{3.15}$$

with both z_k and $z^{\text{pred}}_{k|k-1}$ uncorrelated with $w_{1,k}$. The estimation error is then

$$\varepsilon_{1,k}(\theta) = \left(z_k - z^{\text{pred}}_{k|k-1}\right) + w_{1,k}, \tag{3.16}$$

with the two terms uncorrelated. From this follows

$$\begin{aligned} E\varepsilon_{1,k}(\theta)\varepsilon^T_{1,k}(\theta) &= E\left(z_k - z^{\text{pred}}_{k|k-1}\right)\left(z_k - z^{\text{pred}}_{k|k-1}\right)^T + Ew_{1,k}w^T_{1,k} \\ &\geq E\left(z_k - \hat{z}^{\text{OE}}_{k|k-1}\right)\left(z_k - \hat{z}^{\text{OE}}_{k|k-1}\right)^T + R_{11} \\ &= C_1 P^{\text{OEP}} C_1^T + R_{11}, \end{aligned} \tag{3.17}$$

where $\hat{z}^{\text{OE}}_{k|k-1}$ and P^{OEP} are given by (2.34) and (2.35). Asymptotically, the equality in (3.17) is obtained when the predictor in Fig. 3.1 is tuned into the Kalman filter in Fig. 2.4. Note that also this is based on the assumption that the parameter estimate will converge to the best possible approximation of the system that is available in the model set (Ljung, 1978). See Chapter 11 for a brief discussion.

From this follows the optimal prediction estimator

$$\begin{aligned} \hat{z}^{\text{OE}}_{k|k-1} &= \hat{y}^{\text{OE}}_{1,k|k-1} = C_1\left[qI - A + AK_2^{\text{OE}}C_2\right]^{-1} \\ &\quad \times \left[\left(B - AK_2^{\text{OE}}D_2\right)u_k + AK_2^{\text{OE}}y_{2,k}\right] + D_1 u_k, \end{aligned} \tag{3.18}$$

earlier found as (2.34).

Covariances for OEP estimator

From (3.14) and (3.15) we obtain the minimized asymptotic covariances

$$\text{Cov}\left(\hat{z}^{\text{OE}}_{k|k-1}\right) = C_1 P^{\text{OEP}} C_1^T \tag{3.19}$$

and

$$\text{Cov}\left(\hat{y}^{\text{OE}}_{1,k|k-1}\right) = E\vartheta_k\vartheta_k^T = C_1 P^{\text{OEP}} C_1^T + R_{11}. \tag{3.20}$$

These are the same as the theoretical covariances (2.37) and (2.38) found earlier.

Remark 5 *In order to determine the covariances (3.19) and (3.20), the model (2.20) must be known, and this is not the case in the present context. We will, however, obtain an estimate of the covariance (3.20) directly from a standard prediction error identification algorithm (Ljung, 1995). Due to overfitting, we will then underestimate the $\hat{z}^{OE}_{k|k-1}$ covariance (see e.g. Ansley and Kohn, 1986). A more reliable covariance estimate is found through validation against independent data (see Example 3.2 to 3.5).*

Special case without y_2 measurements

Without y_2 measurements we would have $C_2 = 0$ and $K_2^{\mathrm{OE}} = 0$. We would then find

$$\mathrm{Cov}\left(\hat{y}_{1,k}^{\mathrm{OE}}\right) = C_1 P^{\mathrm{OEU}} C_1^T + R_{11}, \tag{3.21}$$

where $P^{\mathrm{OEU}} = E(x_k - \hat{x}_k^{\mathrm{OE}})(x_k - \hat{x}_k^{\mathrm{OE}})^T$ is determined by the Lyapunov equation (2.25), i.e.

$$P^{\mathrm{OEU}} = A P^{\mathrm{OEU}} A^T + G R_v G^T. \tag{3.22}$$

This is the same result as found directly in (3.7) and (3.8), and it will be used for simulation comparison purposes in Section 3.5.

3.2.4 Identification of optimal OEC estimator

The optimal OEC estimator utilizing also current y_2 values is given by (2.41), i.e.

$$\begin{aligned} \hat{z}_{k|k}^{OE} &= \hat{y}_{1,k|k}^{\mathrm{OE}} = C_1 \left(I - K_2^{\mathrm{OE}} C_2\right) \left[qI - A + A K_2^{\mathrm{OE}} C_2\right]^{-1} \\ &\quad \times \left[\left(B - A K_2^{\mathrm{OE}} D_2\right) u_k + A K_2^{\mathrm{OE}} y_{2,k}\right] \\ &\quad + C_1 K_2^{\mathrm{OE}} (y_{2,k} - D_2 u_k) + D_1 u_k, \end{aligned} \tag{3.23}$$

and the estimation error was in Chapter 2 found to become

$$\psi_k = C_1 (x_k - \hat{x}_{k|k}^{\mathrm{OE}}) + w_{1,k}, \tag{3.24}$$

with $\hat{x}_{k|k}^{\mathrm{OE}}$ given by (2.39).

For the identification we use the estimator in Fig. 3.2, and also here we may choose a canonical realization with $C_1 (I - K_2 C_2) = \begin{bmatrix} I & 0 \end{bmatrix}$.

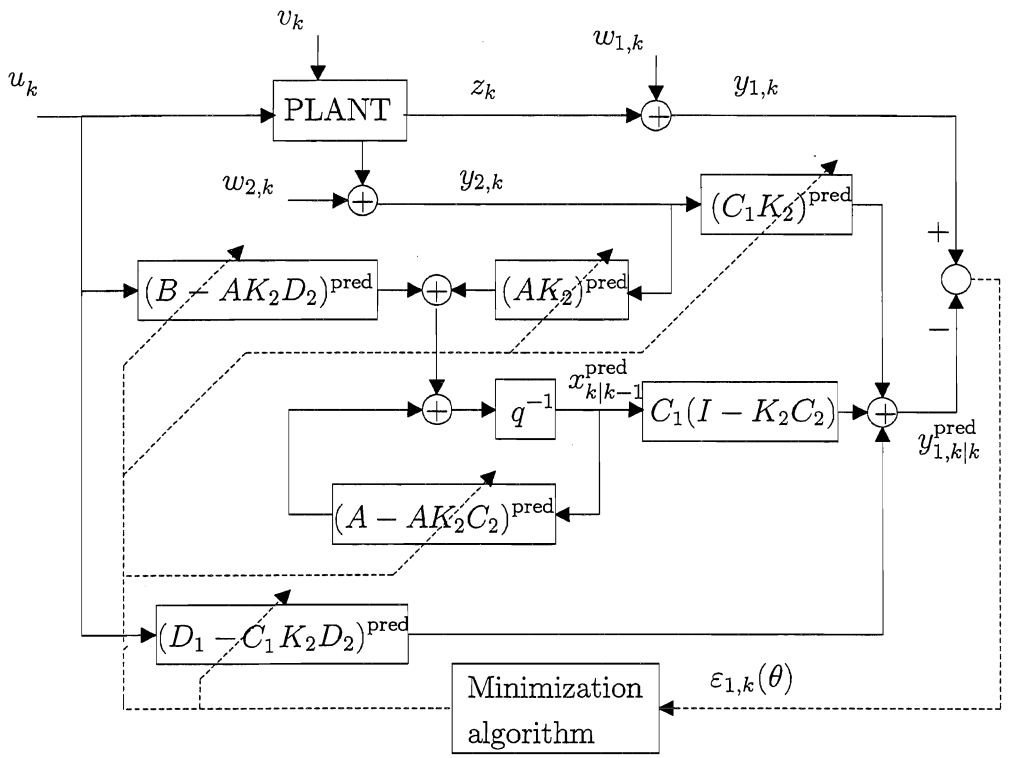

Figure 3.2 Identification of OEC estimator by estimation error minimization.

In this case we have

$$\begin{aligned} y_{1,k} &= C_1x_k + D_1u_k + w_{1,k} = z_k + w_{1,k} \\ y^{\text{pred}}_{1,k|k} &= C_1\left(I - K_2C_2\right)x^{\text{pred}}_{k|k-1} + \left(D_1 - C_1K_2D_2\right)^{\text{pred}}u_k \\ &\quad + \left(C_1K_2\right)^{\text{pred}}y_{2,k} \\ &= z^{\text{pred}}_{k|k}. \end{aligned} \tag{3.25}$$

Since $z^{\text{pred}}_{k|k}$ is correlated with $y_{2,k}$ and thus with $w_{2,k}$, we must now require that $R_{12} = Ew_{1,k}w^T_{2,k} = 0$ in order to get both z_k and $z^{\text{pred}}_{k|k}$ uncorrelated with $w_{1,k}$. The estimation error is then

$$\varepsilon_{1,k}(\theta) = \left(z_k - z^{\text{pred}}_{k|k}\right) + w_{1,k}, \tag{3.26}$$

with the two terms uncorrelated, and from this follows

$$\begin{aligned} E\varepsilon_{1,k}(\theta)\varepsilon_{1,k}^T(\theta) &= E\left(z_k - z_{k|k}^{\text{pred}}\right)\left(z_k - z_{k|k}^{\text{pred}}\right)^T + Ew_{1,k}w_{1,k}^T \\ &\geq E\left(z_k - \hat{z}_{k|k}^{\text{OE}}\right)\left(z_k - \hat{z}_{k|k}^{\text{OE}}\right)^T + R_{11} \\ &= C_1 P^{\text{OEC}} C_1^T + R_{11}, \end{aligned} \tag{3.27}$$

where $\hat{z}_{k|k}^{\text{OE}}$ and P^{OEC} are given by (2.41) and (2.45). Asymptotically, the equality in (3.27) is obtained when the estimator in Fig. 3.2 is tuned into the Kalman filter in Fig. 2.4, modified so that the primary output is taken from $\hat{x}_{k|k}^{\text{OE}}$ instead of $\hat{x}_{k|k-1}^{\text{OE}}$. Note that we again rely on the parameter estimate convergence to the best possible approximation of the system that is available in the model set (Ljung, 1978).

Covariances for OEC estimator

From (3.24) and (3.27) we obtain the minimized asymptotic covariances

$$\text{Cov}\left(\hat{z}_{k|k}^{\text{OE}}\right) = C_1 P^{\text{OEC}} C_1^T \tag{3.28}$$

and

$$\text{Cov}\left(\hat{y}_{1,k|k}^{\text{OE}}\right) = E\psi_k\psi_k^T = C_1 P^{\text{OEC}} C_1^T + R_{11}. \tag{3.29}$$

These are the same as the theoretical covariances (2.43) and (2.44) found earlier.

Remark 6 *When $R_{12} = R_{21}^T \neq 0$, the minimization will result in the minimum mean square error (MSE) for the $y_{1,k}$ estimator. This is not of significant interest, however, since we are basically interested in an estimate of the primary property z_k, related to $y_{1,k}$ through $y_{1,k} = z_k + w_{1,k}$.*

Modification for correlated measurement noise

When $R_{12} = R_{21}^T \neq 0$, we may introduce common noise components v_c and w_c, and augment the system equations (2.20) in the following way:

$$\begin{aligned} \begin{bmatrix} x \\ w_c \end{bmatrix}_{k+1} &= \begin{bmatrix} A & 0 \\ 0 & 0 \end{bmatrix}\begin{bmatrix} x \\ w_c \end{bmatrix}_k + \begin{bmatrix} B \\ 0 \end{bmatrix} u_k + \begin{bmatrix} G & 0 \\ 0 & I \end{bmatrix}\begin{bmatrix} v \\ v_c \end{bmatrix}_k \\ z_k &= C_{11}x_k + D_1 u_k \\ y_{1,k} &= z_k + C_{12}w_{c,k} + w_{11,k} \\ y_{2,k} &= \begin{bmatrix} C_{21} & C_{22} \end{bmatrix}\begin{bmatrix} x \\ w_c \end{bmatrix}_k + D_2 u_k + w_{22,k}. \end{aligned} \tag{3.30}$$

We now have a system of the general type (2.20), but with uncorrelated measurement noise sources $w_{11,k}$ and $w_{22,k}$. This is, however, a problematic solution. Whether it gives an improved OEC estimator depends on the number of samples in the data record, and since z_k is not available the result cannot be validated.

3.3 Identification of ARMAX estimators

In Chapter 2 we have shown that primary property estimators based on ARMAX models are not optimal in the present case, i.e. when no primary measurements are available as basis for the estimation. As pointed out in Chapter 2, there are still some reasons to study this type of estimators:

- With near perfect y_2 measurements it may be advantageous to use y_2 as ordinary known inputs, and identify a parsimonious ARMAX model.
- When a direct measurement of the primary property z is included in the y_2 measurements, we may choose to ignore the y_1 measurements and identify a z estimator using only u and y_2 (see Example 3.5 in Section 3.5).
- Identification of ARMAX models may be convenient means to find initial parameter values for the identification of the optimal OE estimators (see Example 3.2).
- It is of general theoretical interest to study estimators based on ARMAX models, especially since it may be tempting to use the secondary y_2 measurements as ordinary inputs to such an estimator.

Note, however, that identification of an ARMAX model, making use of past primary y_1 measurements, is not possible in the low y_1 sampling rate case discussed in Chapter 6.

Innovations form

A convenient starting point is now the innovations form (2.32), i.e.

$$\begin{aligned} \hat{x}^{\text{ARMAX}}_{k+1|k} &= A\hat{x}^{\text{ARMAX}}_{k|k-1} + Bu_k + AK^{\text{ARMAX}}e^{\text{ARMAX}}_k \\ y_{1,k} &= C_1\hat{x}^{\text{ARMAX}}_{k|k-1} + D_1u_k + e^{\text{ARMAX}}_{1,k} \\ y_{2,k} &= C_2\hat{x}^{\text{ARMAX}}_{k|k-1} + D_2u_k + e^{\text{ARMAX}}_{2,k}, \end{aligned} \tag{3.31}$$

where $K^{\text{ARMAX}} = \begin{bmatrix} K_1^{\text{ARMAX}} & K_2^{\text{ARMAX}} \end{bmatrix}$ and $e^{\text{ARMAX}}_k = \begin{bmatrix} e^{\text{ARMAX}}_{1,k} \\ e^{\text{ARMAX}}_{2,k} \end{bmatrix}$.

Identification with y_2 used as output

Identification with y_2 used as output together with y_1 may be attempted using a standard prediction error or subspace identification method. This might, however, be a difficult task with a large number of secondary measurements.

The PEM criterion to be minimized is then for example the scalar function

$$J_N(\theta) = \mathrm{tr}\left(\frac{1}{N}\sum_{k=1}^{N}\varepsilon_k\varepsilon_k^T\right) = \mathrm{tr}\left(\frac{1}{N}\sum_{k=1}^{N}\varepsilon_{1,k}\varepsilon_{1,k}^T\right) + \mathrm{tr}\left(\frac{1}{N}\sum_{k=1}^{N}\varepsilon_{2,k}\varepsilon_{2,k}^T\right), \quad (3.32)$$

where

$$\varepsilon_k = \begin{bmatrix} \varepsilon_{1,k} \\ \varepsilon_{2,k} \end{bmatrix} = \begin{bmatrix} y_{1,k} - y_{1,k|k-1}^{\mathrm{pred}} \\ y_{2,k} - y_{2,k|k-1}^{\mathrm{pred}} \end{bmatrix}. \quad (3.33)$$

Initial parameter values for the minimization may be found by use of an ordinary least squares method (Ljung, 1995).

Once a model is found, the prediction and current primary output estimators can be constructed according to (2.68) and (2.73).

Identification with y_2 used as input

Another and more appealing choice, especially with only one or a few primary y_1 measurements and many y_2 measurements, is to eliminate $e_{2,k}^{\mathrm{ARMAX}}$ and reorganize (3.31) into the partitioned innovations model

$$\begin{aligned} \hat{x}_{k+1|k}^{ARMAX} &= \left(A - AK_2^{\mathrm{ARMAX}}C_2\right)\hat{x}_{k|k-1}^{\mathrm{ARMAX}} + \left(B - AK_2^{\mathrm{ARMAX}}D_2\right)u_k \\ &\quad + AK_2^{\mathrm{ARMAX}}y_{2,k} + AK_1^{\mathrm{ARMAX}}e_{1,k}^{\mathrm{ARMAX}} \\ y_{1,k} &= C_1\hat{x}_{k|k-1}^{\mathrm{ARMAX}} + D_1u_k + e_{1,k}^{\mathrm{ARMAX}} \end{aligned} \quad (3.34)$$

before the identification.

In (3.31) the innovations process e_k^{ARMAX} can be seen as the error in estimating $y_k = \begin{bmatrix} y_{1,k}^T & y_{2,k}^T \end{bmatrix}^T$ using u_j for $j \leq k$ and y_j for $j < k$., i.e. e_k^{ARMAX} carries the new information in y_k not carried by u_k and y_{k-1} (hence the name innovations). This means that $e_{1,k}^{\mathrm{ARMAX}}$ in (3.34) is uncorrelated with u_j and $y_{2,j}$ for $j < k$, and we thus have $y_{1,k} = \hat{z}_{k|k-1}^{\mathrm{ARMAX}} + e_{1,k}^{\mathrm{ARMAX}}$ with $\hat{z}_{k|k-1}^{\mathrm{ARMAX}}$ and $e_{1,k}^{\mathrm{ARMAX}}$ uncorrelated. From this follows that identification of (3.34) results in the optimal prediction estimator (2.68), just as when (3.31) is identified directly. The difference is only that a simplified criterion function, e.g. $V_N(\theta) = \mathrm{trace}\left(\frac{1}{N}\sum\varepsilon_{1,k}(\theta)\varepsilon_{1,k}^T(\theta)\right)$, is used, and that $A - AK_2^{\mathrm{ARMAX}}C_2$ and $B - AK_2^{\mathrm{ARMAX}}D_2$ are treated as single matrices.

Construction of non-optimal prediction estimator

After the identification of (3.34), we may set $K_1^{\mathrm{ARMAX}} = 0$ and construct the prediction estimator

$$\begin{aligned} \hat{z}_{k|k-1}^{\mathrm{ARMAX}_2} &= \hat{y}_{1,k|k-1}^{\mathrm{ARMAX}_2} = C_1 \left[qI - A + AK_2^{\mathrm{ARMAX}} C_2\right]^{-1} \\ &\quad \times \left[\left(B - AK_2^{\mathrm{ARMAX}} D_2\right) u_k + AK_2^{\mathrm{ARMAX}} y_{2,k}\right] + D_1 u_k, \end{aligned} \tag{3.35}$$

which is not using y_1 information. This estimator is earlier developed as (2.76), and it is simply the deterministic part of (3.34). The resulting asymptotic ($N \to \infty$) estimation covariances are then given by the theoretical covariances (2.79) and (2.80).

Identification of current estimator with y_2 used as input

We may also attempt to identify the optimal current estimator (2.73) using $y_{2,k}$ as an input as in (3.34). In this case we will, however, find $y_{1,k} = \hat{z}_{k|k} + e_{1,k}^{\mathrm{ARMAX}}$ with $\hat{z}_{k|k}$ and $e_{1,k}^{\mathrm{ARMAX}}$ correlated, and minimization of the criterion function will therefore not give the correct result. Since identification of ARMAX models in any case gives non-optimal estimators when the y_1 measurements are not available, this possibility is not further investigated in the thesis, except for some related simulation results in Example 3.2 in Section 3.5.

3.4 Dynamical errors-in-variables problems

Errors-in-variables problems occur when both the system inputs and the system outputs are corrupted by noise. In the following we briefly discuss how such problems are related to the optimal estimator problem.

With u_k not known and with $C_2 = 0$ and $D_2 = I$, the model (2.20) is turned into the dynamic errors-in-variables model

$$\begin{aligned} x_{k+1} &= Ax_k + Bu_k + Gv_k \\ y_{1,k} &= C_1 x_k + D_1 u_k + w_{1,k} \\ y_{2,k} &= u_k + w_{2,k}, \end{aligned} \tag{3.36}$$

see e.g. Anderson (1985) and Chou and Verhaegen (1997). Provided that the unknown inputs u_k can be modeled as filtered white noise, we thus have the model

$$\begin{aligned}
\begin{bmatrix} x_{k+1} \\ u_{k+1} \end{bmatrix} &= \begin{bmatrix} A & B \\ 0 & A_u \end{bmatrix} \begin{bmatrix} x_k \\ u_k \end{bmatrix} + \begin{bmatrix} G & 0 \\ 0 & G_u \end{bmatrix} \begin{bmatrix} v_{1,k} \\ v_{2,k} \end{bmatrix} \\
y_{1,k} &= \begin{bmatrix} C_1 & D_1 \end{bmatrix} \begin{bmatrix} x_k \\ u_k \end{bmatrix} + w_{1,k} \\
y_{2,k} &= \begin{bmatrix} 0 & I \end{bmatrix} \begin{bmatrix} x_k \\ u_k \end{bmatrix} + w_{2,k},
\end{aligned} \tag{3.37}$$

where $v_{1,k} = v_k$ and $v_{2,k}$ are white process noise sequences. This is the same type of system as (2.20), but without known inputs.

It is possible to identify the optimal OEP estimator (2.34) for the system (3.37), i.e. to identify the system

$$\begin{aligned}
\begin{bmatrix} \hat{x}^{\mathrm{OE}}_{k+1|k} \\ \hat{u}^{\mathrm{OE}}_{k+1|k} \end{bmatrix} &= \begin{bmatrix} A & B - AK^{\mathrm{OE}}_{12} - BK^{\mathrm{OE}}_{22} \\ 0 & A_u - A_u K^{\mathrm{OE}}_{22} \end{bmatrix} \begin{bmatrix} x^{\mathrm{OE}}_{k|k-1} \\ \hat{u}^{\mathrm{OE}}_{k|k-1} \end{bmatrix} \\
&\quad + \begin{bmatrix} AK^{\mathrm{OE}}_{12} + BK^{\mathrm{OE}}_{22} \\ A_u K^{\mathrm{OE}}_{22} \end{bmatrix} y_{2,k} \\
y_{1,k} &= \begin{bmatrix} C_1 & D_1 \end{bmatrix} \begin{bmatrix} \hat{x}^{\mathrm{OE}}_{k|k-1} \\ \hat{u}^{\mathrm{OE}}_{k|k-1} \end{bmatrix} + \vartheta_k.
\end{aligned} \tag{3.38}$$

This will give us unbiased estimates of A, B, A_u, C_1, D_1, K^{OE}_{12} and K^{OE}_{22}. It is also possible to identify the ARMAX model (3.34) using $y_{2,k}$ as an input, in which case the full noise model will be found.

Identification of the errors-in variables model (3.36) as indicated above is essentially the same as the joint output approach described in Söderström (1981), in that the information used is contained in the outputs $y_{1,k}$ and $y_{2,k}$. The difference is that the secondary outputs $y_{2,k}$ are turned into inputs in the identification stage, which in cases with many y_2 and few y_1 measurements may considerably reduce the computational burden.

Note that the errors-in-variables problem represented by (3.36) is a simple one, with white noise errors $w_{1,k}$ and $w_{2,k}$. Use of the present approach on more complex problems is left for further research.

3.5 Simulation results

Simulation studies are undertaken, using primarily *dlsim.m* in the Control System Toolbox for use with Matlab (Grace et al., 1992), and the prediction error method implemented in *pem.m* in the System Identification Toolbox for use with Matlab (Ljung, 1995). The *pem.m* function identifies the system matrices and the Kalman

gain, based on the general ARMAX innovation model (3.31), or the partitioned ARMAX innovation model (3.34) when the measurements y_2 are also used as input signals. Provided a proper parametrization, it also identifies the optimal OEP and OEC estimators (2.34) and (2.41).

Example 3.1 - A pure delay second-order system

The pure delay system in Example 2.2 with no $y_{21,k}$ measurements was simulated with u_k as a filtered pseudo random binary sequence (PRBS) with autocovariance $r_{uu}(p) = 0.8^{|p|}$ (Söderström and Stoica (1989), example 5.11 with $\alpha = 0.8$), and with v_k, $w_{1,k}$ and $w_{22,k}$ as normally distributed white noise sequences with zero mean and variances $r_v = 0.04$, $r_{11} = 0.0001$ and $r_{22} = 0.01$. The theoretical estimator (2.57) is then

$$\hat{z}^{\mathrm{OE}}_{k|k} = \hat{z}^{\mathrm{OE}}_{k|k-1} = b_1 u_{k-2} + b_2 y_{2,k-1}, \tag{3.39}$$

with parameters given in Table 3.1.

Identification was performed with u_k and $y_{22,k}$ as input signals and $y_{1,k}$ as output signal, using $N = 10000$ samples and the model (see Appendix B for a definition of nn)

$$nn = [0, [\ 1 \quad 1\ ], 0, 0, [\ 0 \quad 0\ ], [\ 2 \quad 1\ ]]. \tag{3.40}$$

The simulation and identification was repeated in $M = 100$ Monte Carlo runs, resulting in mean values and standard deviations for the two coefficients and their sum as given in Table 3.1.

Table 3.1: Theoretical parameter values and identification results for pure delay system in Example 2.2.

parameter	theoretical value	mean value
$\hat{b}_1$	0.2	0.1999 ± 0.0039
$\hat{b}_2$	0.8	0.8002 ± 0.0037
$\hat{b}_1 + \hat{b}_2$	1.0	1.0001 ± 0.0009

Note that each of the two parameters b_1 and b_2 are identified with greater errors than the error in the sum $b_1 + b_2$. This is natural, since u_{k-2} and $y_{2,k-1}$ carry the same information except for noise. With decreasing noise levels (and the same variance ratio) it will be increasingly difficult to identify the two parameters separately. With $r_v = r_{22} = 0$ we must expect to encounter numerical problems.

■

Example 3.2 - A second-order plant with a first-order noise model

The main aim of this example is to confirm that the developed estimators are consistently identified by use of a prediction error method with both u_k and $y_{2,k}$ as inputs. For this purpose we use a simple system and a large number of samples, and compare the obtained mean-squared validation errors with the theoretical covariances. Note, however, that the theoretical covariances are based on perfect model information, which would not be available in a practical situation.

As a starting point, the following continuous-time second-order model with an additional first-order process noise model was used:

$$\begin{aligned} \dot{x} &= \begin{bmatrix} -1 & 1 & 0 \\ 1 & -2 & 1 \\ 0 & 0 & -1 \end{bmatrix} x + \begin{bmatrix} 0 \\ 1 \\ 0 \end{bmatrix} u + \begin{bmatrix} 0 \\ 0 \\ 1 \end{bmatrix} v \\ y_1 &= \begin{bmatrix} 1 & 0 & 0 \end{bmatrix} x + w_1 \\ y_2 &= \begin{bmatrix} 0 & 1 & 0 \end{bmatrix} x + w_2. \end{aligned} \tag{3.41}$$

This might be a system of interacting mixing tanks or thermal processes, as illustrated by the equivalent electrical circuit in Fig. 3.3.

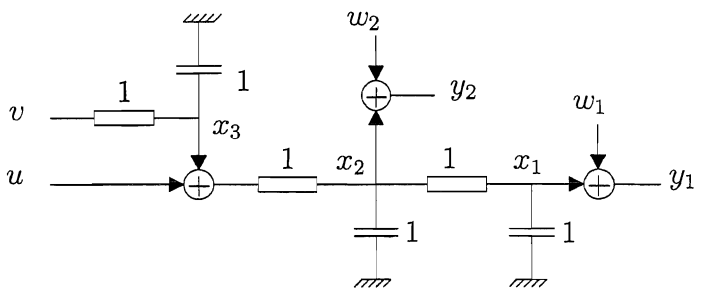

Figure 3.3 Equivalent electrical circuit for second-order system with first-order noise model.

The system was discretized assuming zero-order hold elements on the u and v inputs and a sampling interval $T = 0.1$, resulting in the discrete-time model

$$\begin{aligned} x_{k+1} &= \begin{bmatrix} 0.9092 & 0.0863 & 0.0044 \\ 0.0863 & 0.8230 & 0.0863 \\ 0 & 0 & 0.9048 \end{bmatrix} x_k + \begin{bmatrix} 0.0045 \\ 0.0908 \\ 0 \end{bmatrix} u_k + \begin{bmatrix} 0.0002 \\ 0.0045 \\ 0.0952 \end{bmatrix} v_k \\ y_{1,k} &= \begin{bmatrix} 1 & 0 & 0 \end{bmatrix} x_k + w_{1,k} \\ y_{2,k} &= \begin{bmatrix} 0 & 1 & 0 \end{bmatrix} x_k + w_{2,k}. \end{aligned} \tag{3.42}$$

Remark 7 *Since all state variables have an influence on y_2, (C_2, A^c) for a system as shown in Fig. 3.3 is structurally observable (Appendix A). However, with the specific parameter values chosen it turns out that (C_2, A^c) is not observable, and this is also the case for the discrete-time system (3.42). Since the system in any case is detectable, the Kalman filtering theory can still be applied (Appendix A), and that is the requirement in the present context.*

The system was then simulated with u_k as a filtered pseudo random binary sequence (PRBS) with autocovariance $r_{uu}(p) = 0.95^{|p|}$ (Söderström and Stoica (1989), example 5.11 with $\alpha = 0.95$), i.e. an input that was persistently exciting of sufficient order. The noise sources v_k, $w_{1,k}$ and $w_{2,k}$ were independent and normally distributed white noise sequences with zero mean and fixed variances $r_v = 1$ and $r_{22} = 0.01$, while r_{11} varied as given in Table 3.2 and Table 3.3 below.

Remark 8 *Since the sampling interval is short compared with the time constants in the system, $r_v = 1$ corresponds to an approximate continuous-time process noise variance $r_v^c \approx r_v T = 0.1$ (Franklin et al., 1990). Assuming direct sampling we also have $r_{11}^c = r_{11}$ and $r_{22}^c = r_{22}$.*

Typical input-output-data with $r_{11} = 0.0001$ are shown in Fig. 3.4.

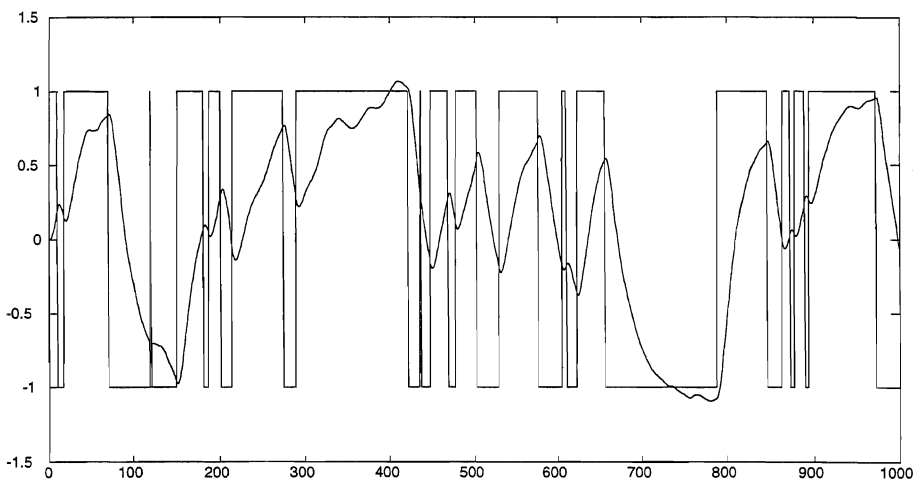

Figure 3.4 Typical PRBS input u_k and response $y_{1,k}$.

Non-optimal ARMAX estimators and the optimal OE estimators were identified from simulated data with u_k and $y_{2,k}$ as input signals and $y_{1,k}$ as output signal, using $N = 10000$ samples.

The ARMAX partitioned innovation model (3.34) was specified as (see Appendix B)

$$nn_{\text{ARMAXP}} = [3, [\ 3 \quad 3\ ], 3, 0, [\ 0 \quad 0\ ], [\ 1 \quad 1\ ]], \tag{3.43}$$

i.e. a model

$$A(q^{-1})y_{1,k} = B_1(q^{-1})u_k + B_2(q^{-1})y_{2,k} + C(q^{-1})e_{1,k} \tag{3.44}$$

with

$$A(q^{-1}) = 1 + a_1q^{-1} + a_2q^{-2} + a_3q^{-3} \tag{3.45}$$

$$B_1(q^{-1}) = b_{11}q^{-1} + b_{12}q^{-2} + b_{13}q^{-3} \tag{3.46}$$

$$B_2(q^{-1}) = b_{21}q^{-1} + b_{22}q^{-2} + b_{23}q^{-3} \tag{3.47}$$

$$C(q^{-1}) = 1 + c_1q^{-1} + c_2q^{-2} + c_3q^{-3}. \tag{3.48}$$

The deterministic part of this model was then used in the non-optimal prediction estimator (3.35).

The state space representation of the ARMAX model (3.44) was also used to find initial values for a third order state space representation of the OEP estimator (2.34), i.e. for a model

$$y_{1,k} = \frac{B_1^{\mathrm{OEP}}(q^{-1})u_k + B_2^{\mathrm{OEP}}(q^{-1})y_{2,k}}{A^{\mathrm{OEP}}(q^{-1})} + \vartheta_k, \tag{3.49}$$

with $A^{\mathrm{OEP}}(q^{-1})$, $B_1^{\mathrm{OEP}}(q^{-1})$ and $B_2^{\mathrm{OEP}}(q^{-1})$ of the same form as in (3.45) to (3.47). This model was then identified.

An attempt was also made to identify an ARMAX model with (3.43) modified into

$$nn_{\mathrm{ARMAXC}} = [3, [\ 3 \quad 4\ ], 3, 0, [\ 0 \quad 0\ ], [\ 1 \quad 0\ ]], \tag{3.50}$$

i.e. a model with

$$B_2(q^{-1}) = b_{20} + b_{21}q^{-1} + b_{22}q^{-2} + b_{23}q^{-3}. \tag{3.51}$$

The deterministic part of this model was then used in a current estimator. As pointed out in Section 3.3, such a current model with $y_{2,k}$ used as input cannot be consistently identified, but the results are nevertheless presented below. However, the main purpose of this current ARMAX model was to use its state space representation as a means for finding initial values for a third-order state space representation of the OEC estimator (2.41), i.e. for a model

$$y_{1,k} = \frac{B_1^{\mathrm{OEC}}(q^{-1})u_k + B_2^{\mathrm{OEC}}(q^{-1})y_{2,k}}{A^{\mathrm{OEC}}(q^{-1})} + \psi_k, \tag{3.52}$$

with $A^{\mathrm{OEC}}(q^{-1})$, $B_1^{\mathrm{OEC}}(q^{-1})$ and $B_2^{\mathrm{OEC}}(q^{-1})$ of the same form as in (3.45), (3.46) and (3.51). This model was then identified.

As the main purpose of the simulations was to support the theory, no attempt was made to find the model order and model structure from the data. The model

order can, however, be found by ordinary use of one of the several available subspace identification methods, e.g. Di Ruscio (1997), and a systematic method for finding the structure will be presented in Chapter 5.

Each identified model was validated against an independent data set with the same number of samples and the same noise variances as used for identification. Validation comparisons between the different identified models were based on the root mean square error criterion

$$RMSE = \sqrt{\frac{1}{N}\sum_{k=1}^{N}(y_{1,k} - \hat{y}_{1,k})^2}, \tag{3.53}$$

where $\hat{y}_{1,k} = \hat{y}^{\mathrm{ARMAX_2}}_{1,k|k-1}$ according to (3.35), $\hat{y}_{1,k} = \hat{y}^{\mathrm{OE}}_{1,k|k-1}$ according to (2.34) or $\hat{y}_{1,k} = \hat{y}^{\mathrm{OE}}_{1,k|k}$ according to (2.41).

As a basis for comparisons given a specific experimental condition, each model was identified and validated in $M = 100$ Monte Carlo runs using independent data sets. The mean RMSE values and RMSE standard deviations for $N = 10000$ samples and varying variances r_{11} are given in Table 3.2 and Table 3.3. The tables also include theoretical RMSE values $\sqrt{Var\left(\hat{y}^{\mathrm{ARMAX_2}}_{1,k|k-1}\right)}$, $\sqrt{Var\left(\hat{y}^{\mathrm{OE}}_{1,k|k-1}\right)}$ and $\sqrt{Var\left(\hat{y}^{\mathrm{OE}}_{1,k|k}\right)}$ computed according to (2.80), (2.38) and (2.44).

Table 3.2 also includes results for the non-optimal current estimator using the deterministic part of the ARMAX model obtained with $y_{2,k}$ as input, as specified in (3.50). Since this model cannot be consistently identified, no theoretical values are given.

Table 3.2: Validation RMSE mean values with standard deviations and theoretical RMSE values for $\mathrm{ARMAX_2}$ estimators. The number of samples was $N = 10000$, and the RMSE values are multiplied by 10^4.

r_{11}	$\mathrm{ARMAX_2P}$	$\mathrm{ARMAX_2P_{theor.}}$	$\mathrm{ARMAX_2C}$
10^{-8}	1013 ± 95	1007	683 ± 25
10^{-7}	888 ± 80	888	597 ± 37
10^{-6}	699 ± 49	694	475 ± 26
10^{-5}	484 ± 29	478	357 ± 18
10^{-4}	330 ± 16	328	280 ± 13
10^{-3}	399 ± 7	394	386 ± 6
10^{-2}	1022 ± 8	1022	1025 ± 8

Table 3.3: Validation RMSE mean values with standard deviations and theoretical RMSE values for OE estimators. The number of samples was $N = 10000$, and the RMSE values are multiplied by 10^4.

r_{11}	OEP	$\text{OEP}_{\text{theor.}}$	OEC	$\text{OEC}_{\text{theor.}}$
10^{-8}	221 ± 7	219	209 ± 7	208
10^{-7}	221 ± 6	219	209 ± 6	208
10^{-6}	220 ± 6	219	208 ± 6	208
10^{-5}	222 ± 5	221	211 ± 5	210
10^{-4}	241 ± 5	241	231 ± 5	230
10^{-3}	387 ± 5	385	381 ± 5	378
10^{-2}	1024 ± 8	1024	1022 ± 8	1021

The tables show an obvious agreement between results based on simulation and theory. In order to visualize this, the RMSE results for the ARMAX_2P and OEP models in Table 3.2 and Table 3.3 are also shown in Fig. 3.5, together with the theoretical results for the OEU predictor (2.24) based only on the independent inputs u_k, and for the optimal ARMAXP predictor (2.68) utilizing also past y_1 values.

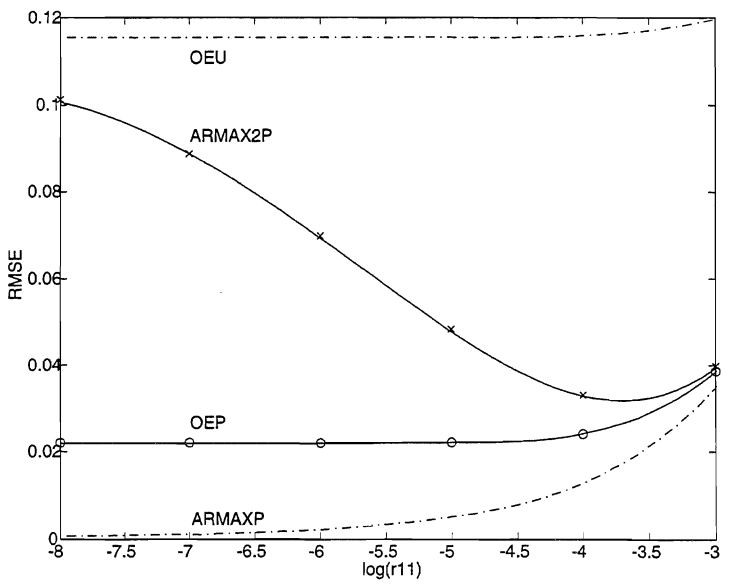

Fig. 3.5 Validation RMSE values for identified ARMAX_2P (x-markings) and OEP (o-markings) estimators as function of $\log(r_{11})$ with $r_v = 1$, $r_{22} = 0.01$ and $N = 10000$. These estimators utilize the information in both u and y_2. Theoretical values are shown as lines, including RMSE values for estimators based only on u (OEU) and on u and past y_1 as well as past y_2 values (ARMAXP).

■

Example 3.3 - Example 3.2 with $D_1 \neq 0$ and $D_2 \neq 0$

As a simple test of the convergence properties with $D_1 \neq 0$ and $D_2 \neq 0$, Example 3.2 was repeated with the output equations altered to

$$\begin{aligned} y_1 &= \begin{bmatrix} 1 & 0 & 0 \end{bmatrix} x + 2u + w_1 \\ y_2 &= \begin{bmatrix} 0 & 1 & 0 \end{bmatrix} x + 3u + w_2. \end{aligned} \tag{3.54}$$

Based on $M = 10$ Monte Carlo runs, the results in Table 3.3 were then altered as shown in Table 3.4.

Table 3.4: Validation RMSE mean values with standard deviations and theoretical RMSE values for OE estimators for a system with $D_1 \neq 0$ and $D_2 \neq 0$. The number of samples was $N = 10000$, and the RMSE values are multiplied by 10^4.

r_{11}	OEP	$\text{OEP}_{\text{theor.}}$	OEC	$\text{OEC}_{\text{theor.}}$
10^{-8}	222 ± 5	219	211 ± 5	208
10^{-7}	221 ± 5	219	209 ± 5	208
10^{-6}	221 ± 5	219	209 ± 4	208
10^{-5}	223 ± 5	221	212 ± 5	210
10^{-4}	242 ± 5	241	232 ± 5	230
10^{-3}	387 ± 4	385	381 ± 5	378
10^{-2}	1019 ± 10	1024	1017 ± 10	1021

The results are very much the same as in Table 3.3.

■

Example 3.4 - Example 3.2 with a reduced number of samples

The results in Example 3.2 were obtained from $N = 10000$ samples in each identification experiment. To indicate expected results for a more realistic number of samples, additional validation results based on $M = 100$ Monte Carlo runs for models based on $N = 1000$ and $N = 200$ samples and with $r_{11} = 0.0001$ are shown in Table 3.5. In order to secure persistent excitation also for $N = 200$, the PRBS filtering parameter α was reduced from 0.95 to 0.8.

In order to limit the influence of local minima problems, each identification based on $N = 200$ samples was repeated $R = 5$ times with randomized initial parameter values in the $B^{\text{OEP}}(q^{-1})$ and $B^{\text{OEC}}(q^{-1})$ polynomials ($b_{ij,r+1} = b_{ij,r}(1 + 0.05e)$, where e is a normal random variable with zero mean and variance 1). The model with the best fit was then validated and kept as the final model.

Table 3.5 also includes results for the OEU predictor (2.24) with only u used as input. The model was then specified as (see Appendix B)

$$nn_{\mathrm{OEU}} = [0, 3, 0, 0, 3, 1], \tag{3.55}$$

i.e.

$$y_{1,k} = \frac{B^{\mathrm{OEU}}(q^{-1})}{A^{\mathrm{OEU}}(q^{-1})} u_k + \eta_k, \tag{3.56}$$

with

$$B^{\mathrm{OEU}}(q^{-1}) = b_1 q^{-1} + b_2 q^{-2} + b_3 q^{-3} \tag{3.57}$$

and

$$A^{\mathrm{OEU}}(q^{-1}) = 1 + a_1 q^{-1} + a_2 q^{-2} + a_3 q^{-3}. \tag{3.58}$$

Table 3.5: Validation RMSE mean values with standard deviations and theoretical RMSE values for OE estimators. The primary output noise variance was $r_{11} = 0.0001$, and the RMSE values are multiplied by 10^4.

N	OEU	$\mathrm{OEU}_{\mathrm{theor.}}$	OEP	$\mathrm{OEP}_{\mathrm{theor.}}$	OEC	$\mathrm{OEC}_{\mathrm{theor.}}$
10000	-	1159	241 ± 5	241	231 ± 5	230
1000	1220 ± 304	1159	250 ± 23	241	238 ± 20	230
200	1343 ± 920	1159	336 ± 188	241	285 ± 77	230

As expected, Table 3.5 shows increased estimation error as the number of samples is reduced from $N = 10000$ (with RMSE values from Table 3.3) to more realistic values.

In order to visualize the degree of model misfit behind the RMSE values in the tables, specific validation responses for models based on $N = 200$ samples are shown in Fig. 3.6. This figure also gives a representative picture of the improvement achieved by including y_2 as an input signal.

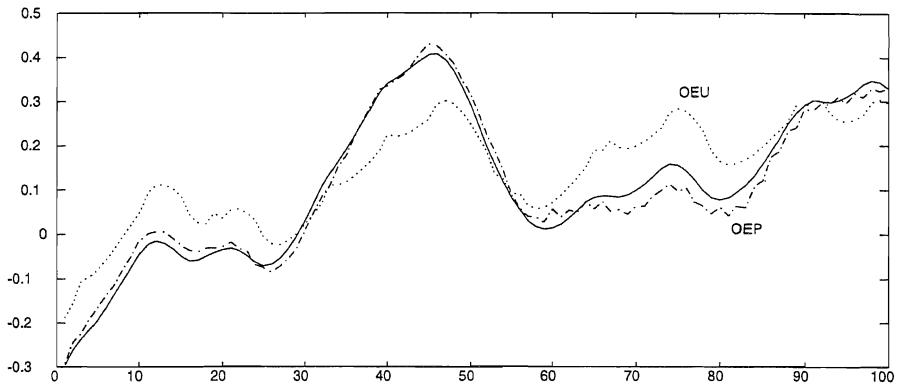

Figure 3.6 Segment of primary output validation responses for the OEP model (3.49) using both u and y_2 as inputs (dash-dotted, $RMSE = 0.0239$) and the OEU model (3.56) using only u as input (dotted, $RMSE = 0.1078$). The experimental conditions are given by $r_v = 1$, $r_{11} = 0.0001$, $r_{22} = 0.01$ and $N = 200$, and the ideal validation response is shown by solid line.

■

Example 3.5 - Estimator based on noisy primary property measurements

In some cases there may exist primary property information at a high measurement noise level and a high sampling rate. It is then possible to use an ARMAX estimator based on these measurements, with a result that obviously very much depends on the noise level. This solution may be useful when it is difficult to obtain a sufficient number of experimental low noise primary output measurements.

In order to test the outcome in such a case, the output equations in the system (3.41) in Example 3.2 were altered into

$$\begin{aligned} y_1 &= \begin{bmatrix} 1 & 0 & 0 \end{bmatrix} x + w_1 \\ y_{21} &= \begin{bmatrix} 1 & 0 & 0 \end{bmatrix} x + w_{21} \\ y_{22} &= \begin{bmatrix} 0 & 1 & 0 \end{bmatrix} x + w_{22}, \end{aligned} \tag{3.59}$$

i.e. an extra output y_{21} was added. The system was then discretized in the same way as in Example 3.2, and noise components were added.

The ARMAX partitioned innovation model (3.34) was specified in the same way as in Example 3.2, and identified using u_k and $y_{22,k}$ as inputs and $y_{21,k}$ as output, and the prediction estimator (3.35) was then constructed. The excitation was the same filtered PRBS as in Example 3.2, with $\alpha = 0.8$, and the noise variances were $r_v = 1$, $r_{11} = 0.0001$ and $r_{22} = 0.01$, while $r_{21} = Ew_{21}^2$ varied as shown in Table 3.6 below. For each experimental condition, the estimator was

determined and validated in $M = 10$ Monte Carlo runs using independent data sets with $N = 1000$ samples. The validations were performed against $y_{1,k}$ data (although considered not available as a basis for estimator identification), with the RMSE results shown in Table 3.6.

For comparison purposes the OEC estimator (2.41) was identified and validated in the same way as in Example 3.2, only that the identification was performed using $y_{21,k}$ as output instead of $y_{1,k}$, while $y_{1,k}$ was still used for validation. The RMSE results for $M = 10$ Monte Carlo runs are included in Table 3.6

Table 3.6 also includes the RMSE values for the simple estimator $\hat{y}_{1,k|k} = y_{21,k}$, and the best result for each value of r_{21} is shown in bold types.

Table 3.6: Validation RMSE mean values with standard deviations, and theoretical RMSE values, for estimators based on more or less noisy primary property measurements. The number of samples was $N = 1000$, and the RMSE values are multiplied by 10^4.

r_{21}	ARMAXP	$\text{ARMAXP}_{\text{theor.}}$	OEC	$\text{OEC}_{\text{theor.}}$	$\hat{y}_{1,k\|k} = y_{21,k}$
10^{-6}	103 ± 2	102	256 ± 36	230	**100**
10^{-5}	109 ± 1	108	247 ± 20	230	**105**
10^{-4}	$\mathbf{137 \pm 11}$	129	239 ± 20	230	141
10^{-3}	$\mathbf{178 \pm 13}$	175	231 ± 14	230	332
10^{-2}	296 ± 131	222	$\mathbf{272 \pm 26}$	230	1005
10^{-1}	629 ± 440	238	$\mathbf{439 \pm 69}$	230	3164

The simulations were finally repeated with the number of samples reduced to $N = 200$. As in Example 3.4, each identification was now repeated $R = 5$ times with randomized initial parameter values in the $A(q^{-1})$ and $B(q^{-1})$ polynomials, and for the ARMAX models also in the $C(q^{-1})$ polynomials ($a_{ij,r+1} = a_{ij,r} + 0.01e$, $b_{ij,r+1} = b_{ij,r} + e$ and $c_{ij,r+1} = c_{ij,r} + 0.1e$, with e as normal random variables with zero mean and variance 1). The best of the models obtained in this way was validated and kept as the final model. The results are shown in Table 3.7.

Table 3.7: Validation RMSE mean values with standard deviations, and theoretical RMSE values, for estimators based on more or less noisy primary output measurements. The number of samples was reduced to $N = 200$, and the RMSE values are multiplied by 10^4.

r_{21}	ARMAXP	$\text{ARMAXP}_{\text{theor.}}$	OEC	$\text{OEC}_{\text{theor.}}$	$\hat{y}_{1,k\|k} = y_{21,k}$
10^{-6}	101 ± 6	102	335 ± 184	230	**100**
10^{-5}	111 ± 5	108	257 ± 44	230	**105**
10^{-4}	$\mathbf{135 \pm 6}$	129	302 ± 99	230	141
10^{-3}	$\mathbf{205 \pm 30}$	175	253 ± 41	230	332
10^{-2}	563 ± 295	222	$\mathbf{404 \pm 39}$	230	1005
10^{-1}	1829±945	238	$\mathbf{1065 \pm 488}$	230	3164

The tables show that the best estimator choice depends on the variance r_{21}. For near perfect y_{21} measurements, the best choice is simply to use $\hat{y}_{1,k|k} = y_{21,k}$, while the ARMAX estimator is the best for medium y_{21} measurement noise levels. For high y_{21} noise levels, the OEC estimator is to prefer, especially when the number of samples is small.

■

Chapter 4

Perfect measurement cases

In this chapter we study special cases that may occur when some or all of the secondary measurements are perfect in the sense that they are noise free. When such measurements are used as inputs in an identification procedure, it may at least theoretically be required that the model order is reduced in order to secure identifiability. An analysis of such cases leads to the discovery of some specific properties of the gain in Kalman filters. A more important consequence from a practical point of view is the possibilities to use parsimonious reduced models, which is further developed in the next chapter. Pure deterministic systems without any form of noise, and systems with colored measurement noise are also discussed in the present chapter.

4.1 The reduced model case

4.1.1 Continuous-time systems

Model structure for analysis

In order to analyze the asymptotic perfect y_2 measurement case for a specific and in the context interesting type of system, we use the model (2.1) partitioned in the following way (using $D_1 = D_2 = 0$ for simplicity and without consequence for the results that follow):

$$\begin{bmatrix} \dot{x}_1 \\ \dot{x}_2 \\ \dot{x}_3 \end{bmatrix} = \begin{bmatrix} A^c_{11} & A^c_{12} & 0 \\ A^c_{21} & A^c_{22} & A^c_{23} \\ A^c_{31} & A^c_{32} & A^c_{33} \end{bmatrix} \begin{bmatrix} x_1 \\ x_2 \\ x_3 \end{bmatrix} + \begin{bmatrix} B^c_1 \\ B^c_2 \\ B^c_3 \end{bmatrix} u + \begin{bmatrix} 0 \\ G^c_2 \\ G^c_3 \end{bmatrix} v$$

$$\begin{bmatrix} y_1 \\ y_2 \end{bmatrix} = \begin{bmatrix} C_{11} & 0 & 0 \\ 0 & I & 0 \end{bmatrix} \begin{bmatrix} x_1 \\ x_2 \\ x_3 \end{bmatrix} + \begin{bmatrix} w_1 \\ w_2 \end{bmatrix}, \tag{4.1}$$

where we for simplicity also assume an asymptotically stable system (may be relaxed to the appropriate detectability requirements). Here x_2 is the part of the state that directly corresponds to the available y_2 measurements, while x_1 is the part that via C_{11} gives the primary output y_1. We assume $A^c_{13} = 0$ and $G^c_1 = 0$, which implies that the process noise v influences x_1 and thus also y_1 only through the state x_2, which is measured by y_2. More specifically we assume in (4.1) that

$$\begin{aligned} \frac{dx_1}{dt} &= A^c_{11}x_1 + A^c_{12}x_2 + B^c_1 u \\ y_1 &= C_{11}x_1 + w_1 \\ y_2 &= x_2 + w_2. \end{aligned} \tag{4.2}$$

From this we see that noise free y_2 measurements make it possible to use u and y_2 as inputs in a reduced model, i.e.

$$\begin{aligned} \frac{dx_1}{dt} &= A^c_{11}x_1 + A^c_{12}y_2 + B^c_1 u \\ y_1 &= C_{11}x_1 + w_1. \end{aligned} \tag{4.3}$$

The consequence of this is that use of both u and y_2 as inputs will result in the reduced model (4.3), while the rest of the system is decoupled. A similar case may also occur if we only assume that some y_2 measurements are noise free.

Kalman gain in estimator based on u and y_2

The innovations model corresponding to (4.2) and assuming an underlying Kalman filter driven by u and y_2 is

$$\begin{aligned} \frac{d\hat{x}_1}{dt} &= A^c_{11}\hat{x}_1 + A^c_{12}\hat{x}_2 + B^c_1 u + K^c_{12}e_2 \\ y_2 &= \hat{x}_2 + e_2, \end{aligned} \tag{4.4}$$

which after elimination of e_2 results in

$$\frac{d\hat{x}_1}{dt} = A^c_{11}\hat{x}_1 + (A^c_{12} - K^c_{12})\hat{x}_2 + B^c_1 u + K^c_{12}(x_2 + w_2). \tag{4.5}$$

Introducing $\tilde{x} = x - \hat{x}$, we find from (4.2) and (4.5)

$$\frac{d\tilde{x}_1}{dt} = A^c_{11}\tilde{x}_1 + (A^c_{12} - K^c_{12})\tilde{x}_2 - K^c_{12}w_2. \tag{4.6}$$

As the system $\left(A^c_{11}, \begin{bmatrix} A^c_{12} & B^c_1 \end{bmatrix}, C_{11}\right)$ is assumed to be asymptotically stable, and also assuming that all state variables in $\tilde{x}_2$ are none-zero, we find that $K^c_{12} \equiv A^c_{12}$ results in $E\tilde{x}_1\tilde{x}_1^T \to 0$ when $R^c_{22} = Ew_2w_2^T \to 0$. All state variables in $\tilde{x}_2$ are non-zero when they are influenced by the process noise either directly via G^c_2 or via the non-measured states x_3 and A^c_{23}, and we have thus proved the following theorem:

Theorem 4.1

Assume the asymptotically stable system (4.1) with

- noise free y_2 measurements, i.e. $R_{22}^c \to 0$
- all state variables in x_2 influenced by the process noise v either through G_2^c or through the state variables x_3, and not only through other x_2 state variables.

The optimal gain in a Kalman filter driven by u and y_2 is then given by

$$K_2^c = \begin{bmatrix} A_{12}^c \\ \times \\ \times \end{bmatrix}. \tag{4.7}$$

■

Kalman gain in estimator based on u, y_1 and y_2

The innovation model corresponding to (4.2) and assuming an underlying Kalman filter driven by u, y_1 and y_2 is (with $\hat{x}$ and e_2 different from the $\hat{x}$ and e_2 used in (4.4))

$$\begin{aligned} \frac{d\hat{x}_1}{dt} &= A_{11}^c\hat{x}_1 + A_{12}^c\hat{x}_2 + B_1^c u + K_{11}^c e_1 + K_{12}^c e_2 \\ y_1 &= C_{11}\hat{x}_1 + e_1 \\ y_2 &= \hat{x}_2 + e_2, \end{aligned} \tag{4.8}$$

which after elimination of e_2 results in

$$\begin{aligned} \frac{d\hat{x}_1}{dt} &= (A_{11}^c - K_{11}^c C_{11})\hat{x}_1 + (A_{12}^c - K_{12}^c)\hat{x}_2 + B_1^c u + K_{11}^c y_1 + K_{12}^c y_2 \\ y_1 &= C_{11}\hat{x}_1 + e_1. \end{aligned} \tag{4.9}$$

With $\tilde{x} = x - \hat{x}$, we find from (4.2) and (4.9)

$$\frac{d\tilde{x}_1}{dt} = (A_{11}^c - K_{11}^c C_{11})\tilde{x}_1 + (A_{12}^c - K_{12}^c)\tilde{x}_2 - K_{11}^c w_1 - K_{12}^c w_2. \tag{4.10}$$

Assume again that all state variables in $\tilde{x}_2$ are non-zero, i.e. that they are influenced by the process noise either directly via G_2^c or via the non-measured states x_3 and A_{23}^c. Also assuming that $R_{22}^c \to 0$, we must now treat two different situations:

- When $R_{11}^c \neq 0$, we will obtain $E\tilde{x}_1\tilde{x}_1^T \to 0$ by choosing $K_{11}^c = 0$ and $K_{12}^c = A_{12}^c$, and these are then optimal Kalman gains.

- When also the y_1 measurements are noise free, i.e. when $R_{11}^c \rightarrow 0$, we will find that $\hat{x}_1 \rightarrow x_1$ and $y_1 \rightarrow C_{11}x_1$. This means that y_1 is eliminated from the state equation in (4.9) , which is therefore simplified to (4.5). Then $K_{12}^c = A_{12}^c$ will still be an optimal gain, while K_{11}^c in this case will be determined by the actual R_{11}^c and R_{22}^c values (though small) on the basis of the following system derived from (4.2):

$$\begin{aligned} \frac{dx_1}{dt} &= A_{11}^c x_1 + A_{12}^c y_2 + B_1^c u - A_{12}^c w_2 \\ y &= C_{11}x_1 + w_1. \end{aligned} \tag{4.11}$$

  Application of the Kalman filter equations (2.3) and (2.4) now results in

$$K_{11}^c = P_{11}^c C_{11}^T \left(R_{11}^c\right)^{-1}, \tag{4.12}$$

  where P_{11}^c is given by

$$0 = A_{11}^c P_{11}^c + \left(A_{11}^c P_{11}^c\right)^T + A_{12}^c R_{22}^c \left(A_{12}^c\right)^T - P_{11}^c C_{11}^T \left(R_{11}^c\right)^{-1} C_{11} P_{11}^c. \tag{4.13}$$

  We summarize this in the following theorem:

Theorem 4.2

Assume the asymptotically stable system (4.1) with

- noise free y_2 measurements, i.e. $R_{22}^c \rightarrow 0$
- y_1 measurements that are not noise free, i.e. $R_{11}^c \neq 0$
- all state variables in x_2 influenced by the process noise v either through G_2^c or through the state variables x_3, and not only through other x_2 state variables.

The optimal gain in a Kalman filter driven by u, y_1 and y_2 is then given by

$$K^c = \begin{bmatrix} 0 & A_{12}^c \\ \times & \times \\ \times & \times \end{bmatrix}. \tag{4.14}$$

When also the y_1 measurements are noise free, i.e. when also $R_{11}^c \rightarrow 0$, the Kalman gain is given by

$$K^c = \begin{bmatrix} K_{11}^c & A_{12}^c \\ \times & \times \\ \times & \times \end{bmatrix}, \tag{4.15}$$

with K_{11}^c determined by (4.12).

■

Comparison with known result

The results in Theorem 4.1 and Theorem 4.2 may be compared with a known perfect measurement Kalman filtering result. For a square plant with the same number of measurements as number of process noise sources and $R_v^c = \sigma I$ it is known (Anderson and Moore, 1989) that

$$\lim_{\sigma \to \infty} \sigma^{-1/2} K^c (R_w^c)^{1/2} = G^c V, \tag{4.16}$$

where V is some orthogonal matrix. From this follows that with $R_v^c = I$ and $R_w^c = \mu R_{w0}^c$ we have

$$\lim_{\mu \to 0} K^c = \mu^{-1/2} G^c V (R_{w0}^c)^{-1/2} + K_0^c, \tag{4.17}$$

where K_0^c is a finite matrix. For systems covered by Theorem 4.1 and Theorem 4.2 above, we will be able to determine certain elements in K_0^c.

Example 4.1

Consider the continuous-time system

$$\begin{bmatrix} \dot{x}_1 \\ \dot{x}_2 \\ \dot{x}_3 \\ \dot{x}_4 \\ \dot{x}_5 \end{bmatrix} = \begin{bmatrix} -2 & 1 & 1 & 0 & 0 \\ 2 & -6 & 2 & 2 & 0 \\ 1 & 1 & -3 & 0 & 1 \\ 0 & 2 & 0 & -4 & 0 \\ 0 & 0 & 1 & 0 & -2 \end{bmatrix} \begin{bmatrix} x_1 \\ x_2 \\ x_3 \\ x_4 \\ x_5 \end{bmatrix} + \begin{bmatrix} 0 & 0 \\ 0 & 0 \\ 0 & 0 \\ 2 & 0 \\ 0 & 1 \end{bmatrix} \begin{bmatrix} u_1 + v_1 \\ u_2 + v_2 \end{bmatrix}$$

$$y_1 = \begin{bmatrix} 1 & 0 & 0 & 0 & 0 \\ 0 & 1 & 0 & 0 & 0 \end{bmatrix} \begin{bmatrix} x_1 \\ x_2 \\ x_3 \\ x_4 \\ x_5 \end{bmatrix} + w_1 = \begin{bmatrix} x_1 \\ x_2 \end{bmatrix} + \begin{bmatrix} w_{11} \\ w_{12} \end{bmatrix} \tag{4.18}$$

$$y_2 = \begin{bmatrix} 0 & 0 & 0 & 1 & 0 \\ 0 & 0 & 0 & 0 & 1 \end{bmatrix} \begin{bmatrix} x_1 \\ x_2 \\ x_3 \\ x_4 \\ x_5 \end{bmatrix} + w_2 = \begin{bmatrix} x_4 \\ x_5 \end{bmatrix} + \begin{bmatrix} w_{21} \\ w_{22} \end{bmatrix}.$$

This might be an interacting stirred-tanks system, as illustrated by the equivalent electrical circuit in Fig. 4.1.

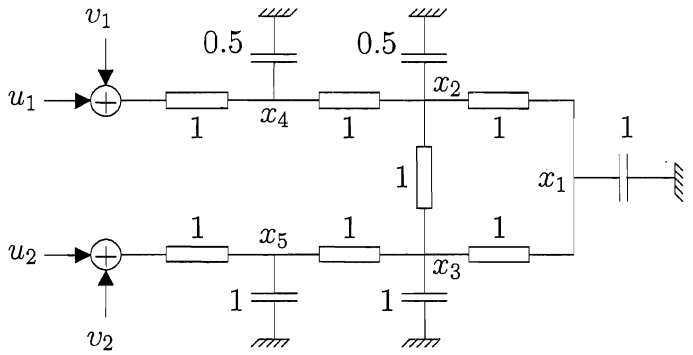

Figure 4.1 Equivalent electrical circuit for interacting stirred-tanks system.

With perfect secondary measurements $y_2 = \begin{bmatrix} x_4 & x_5 \end{bmatrix}^T$, the reduced system according to (4.3) becomes

$$\begin{bmatrix} \dot{x}_1 \\ \dot{x}_2 \\ \dot{x}_3 \end{bmatrix} = \begin{bmatrix} -2 & 1 & 1 \\ 2 & -6 & 2 \\ 1 & 1 & -3 \end{bmatrix} \begin{bmatrix} x_1 \\ x_2 \\ x_3 \end{bmatrix} + \begin{bmatrix} 0 & 0 \\ 2 & 0 \\ 0 & 1 \end{bmatrix} y_2 \tag{4.19}$$

$$y_1 = \begin{bmatrix} 1 & 0 & 0 \\ 0 & 1 & 0 \end{bmatrix} \begin{bmatrix} x_1 \\ x_2 \\ x_3 \end{bmatrix} + w_1.$$

We may now look at some different Kalman filter results:

- When we choose $R_v^c = I$ and $R_{22}^c = \mu I = 10^{-16} I$, we find by use of *lqe.m* in the Control System Toolbox for use with Matlab (Grace et al., 1992) the following gain for a Kalman filter driven by u and y_2 (a square plant):

$$K_2^c = \begin{bmatrix} 0.000000 & 0.000000 \\ 2.000000 & 0.000000 \\ 0.000000 & 1.000000 \\ 199999996 & 0.000000 \\ 0.000000 & 99999998 \end{bmatrix} \approx \mu^{-\frac{1}{2}} G^c + \begin{bmatrix} A_{12}^c \\ \times \end{bmatrix}. \tag{4.20}$$

  This is in accordance with (4.17) and (4.7).

- With $R_w^c = \begin{bmatrix} 10^{-4} I & 0 \\ 0 & 10^{-16} I \end{bmatrix}$ and a Kalman filter driven by u, y_1 and y_2

we find (for a non-square plant)

$$K^c = \begin{bmatrix} 0.000000 & 0.000000 & 0.000000 & 0.000000 \\ 0.000000 & 0.000000 & 2.000000 & 0.000000 \\ 0.000000 & 0.000000 & 0.000000 & 1.000000 \\ 0.000000 & 0.000000 & 199999996 & 0.000000 \\ 0.000000 & 0.000000 & 0.000000 & 99999998 \end{bmatrix} = \begin{bmatrix} 0 & A_{12}^c \\ 0 & \times \end{bmatrix}, \tag{4.21}$$

which is in accordance with (4.14).

- With $R_w^c = \begin{bmatrix} 10^{-16}I & 0 \\ 0 & 10^{-16}I \end{bmatrix}$ and use of (4.12) and (4.13) we find

$$K_{11}^c = \begin{bmatrix} 0.107511 & 0.114069 \\ 0.114069 & 0.399942 \\ 0.113238 & 0.128998 \end{bmatrix}, \tag{4.22}$$

and with a Kalman filter driven by u, y_1 and y_2 we further find (for a non-square plant)

$$K^c = \begin{bmatrix} 0.107511 & 0.114069 & 0.000000 & 0.000000 \\ 0.114069 & 0.399942 & 2.000000 & 0.000000 \\ 0.113238 & 0.128998 & 0.000000 & 1.000000 \\ 0.000000 & 2.000000 & 199999996 & 0.000000 \\ 0.000000 & 0.000000 & 0.000000 & 99999998 \end{bmatrix} = \begin{bmatrix} K_{11}^c & A_{12}^c \\ 0 & \times \end{bmatrix}, \tag{4.23}$$

in accordance with (4.15).

■

4.1.2 Discrete-time systems

Model structure for analysis

We now assume a discrete-time system with the same structure as in (4.1), i.e.

$$\begin{aligned} \begin{bmatrix} x_1 \\ x_2 \\ x_3 \end{bmatrix}_{k+1} &= \begin{bmatrix} A_{11} & A_{12} & 0 \\ A_{21} & A_{22} & A_{23} \\ A_{31} & A_{32} & A_{33} \end{bmatrix} \begin{bmatrix} x_1 \\ x_2 \\ x_3 \end{bmatrix}_k + \begin{bmatrix} B_1 \\ B_2 \\ B_3 \end{bmatrix} u_k + \begin{bmatrix} 0 \\ G_2 \\ G_3 \end{bmatrix} v_k \\ \begin{bmatrix} y_1 \\ y_2 \end{bmatrix}_k &= \begin{bmatrix} C_{11} & 0 & 0 \\ 0 & I & 0 \end{bmatrix} \begin{bmatrix} x_1 \\ x_2 \\ x_3 \end{bmatrix}_k + \begin{bmatrix} w_1 \\ w_2 \end{bmatrix}_k, \end{aligned} \tag{4.24}$$

or more specifically

$$\begin{aligned} x_{1,k+1} &= A_{11}x_{1,k} + A_{12}x_{2,k} + B_1u_k \\ y_{1,k} &= C_{11}x_{1,k} + w_{1,k} \\ y_{2,k} &= x_{2,k} + w_{2,k}. \end{aligned} \tag{4.25}$$

Also here we see that noise free y_2 measurements make it possible to use u and y_2 as inputs in a reduced model, i.e.

$$\begin{aligned} x_{1,k+1} &= A_{11}x_{1,k} + A_{12}y_{2,k} + B_1u_k \\ y_{1,k} &= C_{11}x_{1,k} + w_{1,k}. \end{aligned} \tag{4.26}$$

The consequence of this is that using both u and y_2 as inputs, we can only identify the reduced model (4.26), while the rest of the system is decoupled. A similar case may also occur if we only assume that some y_2 measurements are noise free.

Kalman gain in OE type of estimator

Quite analogously to the continuous-time case we find the results given in Theorem 4.3 below. In addition to that we find a specific result by constructing the optimal y_2 current estimator corresponding to the optimal y_1 estimator (2.41),

$$\begin{aligned} \hat{y}^{\mathrm{OE}}_{2,k|k} &= C_2\left(I - K_2^{\mathrm{OE}}C_2\right)\left[qI - A + AK_2^{\mathrm{OE}}C_2\right]^{-1} \\ &\quad \times \left[Bu_k + AK_2^{\mathrm{OE}}y_{2,k}\right] + C_2K_2^{\mathrm{OE}}y_{2,k}. \end{aligned} \tag{4.27}$$

From this we see that perfect y_2 measurements give the optimal estimate $\hat{y}^{\mathrm{OE}}_{2,k|k} = y_2$ for $C_2K_2^{\mathrm{OE}} = I$, with the consequence given in (4.29) below.

We summarize the results in Theorem 4.3 below. Since it follows that $A_{11}K_{12}^{\mathrm{OE}} + A_{12} = A_{12}$, it also follows that $A_{11}K_{12}^{\mathrm{OE}} = 0$, and we therefore make this a part of the theorem.

Theorem 4.3

Assume the asymptotically stable system (4.24) with

- noise free $y_{2,k}$ measurements, i.e. $R_{22} \to 0$
- all state variables in $x_{2,k}$ influenced by the process noise v_k either through G_2 or through the state variables $x_{k,3}$, and not only through other $x_{2,k}$ state variables.

The optimal gain in a Kalman filter driven by u and y_2 is then given by

$$AK_2^{\mathrm{OE}} = \begin{bmatrix} A_{12} \\ \times \\ \times \end{bmatrix} \tag{4.28}$$

and

$$K_2^{\mathrm{OE}} = \begin{bmatrix} \times \\ I \\ \times \end{bmatrix}. \tag{4.29}$$

From this follows that

$$A_{11}K_{12}^{\mathrm{OE}} = 0. \tag{4.30}$$

■

Remark 9 *As input signals entering the system through B_2, B_3, G_2 or G_3 are not a part of the reduced model in (4.26), these inputs may as well include unknown time delays, non-linearities, non-stationary noise etc.*

Remark 10 *With perfect measurements $y_{2,k} = x_{2,k}$, the reduced model in (4.26) is a deterministic model as far as u and y_2 are concerned. If a measured state variable x_i in x_2 is then determined purely by other measured state variables, and if all y_2 measurements are used as input signals, we will have a similar collinearity problem as treated in Section 4.2 below. The solution to this problem follows from the discussion there.*

Remark 11 *A theoretical consequence of Theorem 4.3 is that given the system (4.24) with $A_{13} = 0$, $G_1 = 0$ and near perfect noise free y_2 measurements, a reduced model not utilizing all u and y_2 signals must be used. Otherwise, numerical problems due to decoupling will theoretically occur when the parameter estimates are sought. Numerical problems may in theory occur as soon as we have two or more near perfect y_2 measurements. A more important consequence in practice is that a parsimonious reduced model may result in less variance in the y_1 estimates. In such a case only part of the model will be identified, and as long as there is some noise in one or several of the y_2 signals used as inputs, the parameter estimates will then be biased (Söderström, 1981). In spite of this, the result might be an overall reduction in the mean squared estimation error, as illustrated in a simulation example in Chapter 5.*

Example 4.2

Discretization of the system in Example 4.1 with a sampling interval T and a zero-order hold on the input, gives an exact deterministic solution with

$$A = e^{A^c T}, \tag{4.31}$$

$$B = \int_0^T e^{A^c \eta} d\eta B^c \tag{4.32}$$

and

$$C = C^c. \tag{4.33}$$

With a short sampling interval T this will approximately give

$$A \approx \begin{bmatrix} 1 & T & T & 0 & 0 \\ 2T & 1 & 2T & 2T & 0 \\ T & T & 1 & 0 & T \\ 0 & 2T & 0 & 1 & 0 \\ 0 & 0 & T & 0 & 1 \end{bmatrix}. \tag{4.34}$$

When we choose C_1 and C_2 as in Example 4.1 and assume $R_v = I$ and $R_{22} = 10^{-10}I$, we find by use of the *dlqe.m* function in the Control System Toolbox for use with Matlab (Grace et al., 1992)

$$AK_2^{\mathrm{OE}} = \begin{bmatrix} 0 & 0 \\ 2T & 0 \\ 0 & T \\ 199796T & 0 \\ 0 & 99948T \end{bmatrix} = T\mu^{-\frac{1}{2}} G^c + T \begin{bmatrix} A_{12}^c \\ \times \end{bmatrix}. \tag{4.35}$$

This is the same as result (4.20) in Example 4.1, only multiplied with T. It should be mentioned, however, that this result was obtained with the sampling interval as short as $T = 10^{-8}$.

With the y_2 measurement noise reduced even more to $R_{22} = 10^{-18}I$, the solution was altered to

$$AK_2^{\mathrm{OE}} = \begin{bmatrix} 0 & 0 \\ 2T & 0 \\ 0 & T \\ 0.9975 & 0 \\ 0 & 0.9902 \end{bmatrix}, \tag{4.36}$$

which follows from (4.30) and the fact that we for this specific system have

$$A_{21}K_{12}^{\mathrm{OE}} + A_{22} = A_{21}A_{11}^{-1}A_{11}K_{12}^{\mathrm{OE}} + A_{22} = A_{22} = I. \tag{4.37}$$

■

Kalman gain in ARMAX type of estimator

We also here find results quite analogously to the continuous-time case (see Theorem 4.4 below). In addition we also now find a specific result by constructing the

optimal y_2 current estimator corresponding to the optimal y_2 estimator (4.27) (see also (2.73))

$$\begin{aligned}\hat{y}_{2,k|k}^{\text{ARMAX}} &= C_2\left(I - K_1^{\text{ARMAX}}C_1 - K_2^{\text{ARMAX}}C_2\right)\\ &\times\left[qI - A + AK_1^{\text{ARMAX}}C_1 + AK_2^{\text{ARMAX}}C_2\right]^{-1}\\ &\times\left[Bu_k + AK_2^{\text{ARMAX}}y_{2,k} + AK_2^{\text{ARMAX}}y_{2,k}\right]\\ &+C_2K_1^{\text{ARMAX}}y_{1,k} + C_2K_2^{\text{ARMAX}}y_{2,k}.\end{aligned} \tag{4.38}$$

From this we see that perfect y_2 measurements give the optimal estimate $\hat{y}_{2,k|k}^{\text{ARMAX}} = y_2$ for $C_2K_1^{\text{ARMAX}} = 0$ and $C_2K_2^{\text{ARMAX}} = I$, with the result given in (4.40) below.

We summarize this in the following theorem:

Theorem 4.4

Assume the asymptotically stable system given in (4.24) with

- noise free $y_{2,k}$ measurements, i.e. $R_{22} \to 0$
- $y_{1,k}$ measurements that are not noise free, i.e. $R_{11} \neq 0$
- all state variables in $x_{2,k}$ influenced by the process noise v_k either through G_2 or through the state variables $x_{3,k}$, and not only through other $x_{2,k}$ state variables.

The optimal gain in a Kalman filter driven by u, y_1 and y_2 is then given by

$$AK^{\text{ARMAX}} = \begin{bmatrix} 0 & A_{12} \\ \times & \times \\ \times & \times \end{bmatrix} \tag{4.39}$$

and

$$K^{\text{ARMAX}} = \begin{bmatrix} \times & \times \\ 0 & I \\ \times & \times \end{bmatrix}. \tag{4.40}$$

From this follows that

$$A_{11}K_{12}^{\text{ARMAX}} = 0. \tag{4.41}$$

When also the y_1 measurements are noise free, i.e. when also $R_{11} \to 0$, the Kalman gain is given by

$$K^{\text{ARMAX}} = \begin{bmatrix} K_{11}^{\text{ARMAX}} & \times \\ 0 & I \\ \times & \times \end{bmatrix}, \tag{4.42}$$

with K_{11}^{ARMAX} given by

$$K_{11}^{\text{ARMAX}} = P_{11}^{\text{ARMAX}} C_{11}^T \left(C_{11} P_{11}^{\text{ARMAX}} C_{11}^T + R_{11} \right)^{-1}, \tag{4.43}$$

where P_{11}^{ARMAX} is determined by the Riccati equation

$$\begin{aligned} P_{11}^{\text{ARMAX}} &= A_{11} P_{11}^{\text{ARMAX}} A_{11}^T + A_{12} R_{22} A_{12}^T \\ &\quad - A_{11} P_{11}^{\text{ARMAX}} C_{11}^T \left(C_{11} P_{11}^{\text{ARMAX}} C_{11}^T + R_{11} \right)^{-1} C_{11} P_{11}^{\text{ARMAX}} A_{11}^T. \end{aligned} \tag{4.44}$$

■

4.2 The deterministic case

4.2.1 General discussion

Although a nearly noise free system is very unlikely in a practical case, it is of theoretical interest to study the identification of deterministic systems. It is well known (e.g. Lewis, 1992), that the Kalman gain cannot be determined in a pure deterministic case, that is when both the process noise v_k and the measurement noise w_k are zero. In the present case, this means that the optimal estimators utilizing the information in both the known inputs u and the secondary measurements y_2 developed in Chapter 2 cannot be identified when $R_v = 0$ and $R_{22} = 0$. This is most easily demonstrated by examples:

Example 4.3

For the continuous-time system in Example 2.1, we found $K^c = f(r_v^c / r_{22}^c)$ as given by (2.14). When $r_v^c \to 0$ and $r_{22}^c \to 0$, this is an indeterminate expression. From Fig. 2.2b we see that $v = 0$ and $w_2 = 0$ result in $y_2 = 0$, and the solution is then obviously to use a first-order model with only u as input.

■

Example 4.4

For the pure delay system in Example 2.2 without y_{21} measurements, we found the estimators (2.57)

$$\hat{z}_{k|k-1}^{\text{OE}} = \hat{z}_{k|k}^{\text{OE}} = \frac{1}{1 + r_v / r_{22}} u_{k-2} + \frac{r_v / r_{22}}{1 + r_v / r_{22}} y_{22,k-1}. \tag{4.45}$$

When $r_v \to 0$ and $r_{22} \to 0$ this is an indeterminate expression. We have two solutions:

- Identify a second-order estimator with only u as input, which gives $\hat{z}^{\mathrm{OE}}_{k|k-1} = u_{k-2}$.

- Identify a first-order estimator with only y_{22} as input, which gives $\hat{z}^{\mathrm{OE}}_{k|k-1} = y_{22,k-1}$.

■

4.2.2 Special case with reduced models

For systems with the structure given in (4.1) and (4.24) we found that with noise free y_2 measurements we can only identify the reduced models (4.3) and (4.26). With more than one y_2 measurement we may have the same type of problem as mentioned above, i.e. we cannot use all of the y_2 measurements as inputs at the same time.

Example 4.5

Assume the system in Example 1.1, but now with $u = 0$. If both y_{22} and y_{23} are perfect, we may use y_{23} as a known input and identify a second-order model. We cannot at the same time utilize the information in y_{22}, because the underlying Kalman filter will then be indeterminate. The best solution in this case is obviously to use only y_{22} as input and identify a first-order model.

■

4.2.3 General solutions in the deterministic case

The Kalman gain will quite generally for both continuous-time and discrete-time systems be determined by ratios between process noise variances r_v and measurement noise variances r_w, and we will therefore always find indeterminate Kalman gains when both $R_v \to 0$ and $R_{22} \to 0$. Examples 4.3 and 4.4 and the discussion in Example 1.1 point to some general solutions to the problem:

- Identify a model with only u as input signal.

- Identify an appropriately reduced model with u and y_2 as input signals.

- Identify an appropriately reduced model with only y_2 as input signal.

A systematic method for finding such models is proposed in Chapter 5.

4.3 The colored measurement noise case

Colored y_2 measurement noise sources must quite generally be modeled as filtered white noise, and incorporated in the following way (assuming independent process and measurement noise):

$$\begin{aligned}
\begin{bmatrix} x_1 \\ x_2 \end{bmatrix}_{k+1} &= \begin{bmatrix} A_1 & 0 \\ 0 & A_2 \end{bmatrix} \begin{bmatrix} x_1 \\ x_2 \end{bmatrix}_k + \begin{bmatrix} B \\ 0 \end{bmatrix} u_k + \begin{bmatrix} G_1 & 0 \\ 0 & G_2 \end{bmatrix} \begin{bmatrix} v_1 \\ v_2 \end{bmatrix}_k \\
y_{1,k} &= \begin{bmatrix} C_1 & 0 \end{bmatrix} \begin{bmatrix} x_1 \\ x_2 \end{bmatrix}_k + D_1 u_k + w_{1,k} \qquad (4.46) \\
y_{2,k} &= \begin{bmatrix} C_{21} & C_{22} \end{bmatrix} \begin{bmatrix} x_1 \\ x_2 \end{bmatrix}_k + D_2 u_k + w_{2,k}.
\end{aligned}$$

Here $C_{22}x_{2,k}$ is the colored y_2 measurement noise, and we may quite realistically have $R_{22} = Ew_{2,k}w_{2,k}^T = 0$, in which case we formally have a perfect measurement case. Since $C_{22}x_{2,k}$ is not influenced by u_k, this will in itself not constitute an identification problem due to use of both u_k and $y_{2,k}$ as inputs.

Chapter 5

Model structure determination

As in other practical system identification cases, there is also in the present case a need to find parsimonious solutions that give good primary output estimators using as few parameters as possible. We thus need a method for finding estimators that give a good compromise between bias and variance, and such a method is presented in this chapter.

5.1 Introduction

The discussion in Chapter 4 has shown that numerical identification problems may occur as a result of perfect noise free y_2 measurements. This is not a very likely problem in a practical situation, especially not in an industrial process environment. If it turns out to be a problem, the solution is to leave some known inputs or some perfect measurements out, and use the most parsimonious model.

A more important task seen from a practical point of view is to settle for a good set of independent inputs and secondary measurements to be used as inputs in the identification procedure. This is similar to the problem of finding regressor variables in ordinary least-squares estimation (Ljung, 1987,1999), only that it is complicated by the fact that also other aspects of the model structure (model order, time delays etc.) must be chosen. The inclusion of noisy measurements will in any case give only a limited contribution to the estimation of the primary properties, and at the same time the number of unknown parameters to be identified will increase.

As briefly discussed in Chapter 1, the model structure determination aims at finding the primary output estimator with the lowest possible mean-squared estimation error (MSE) when used on an independent validation data set. Several aspects of the model structure must then be determined:

- Which model order should be used? If possible, prior knowledge of the system (physical insight etc.) should be used in order to determine the range

of model orders to be considered. Note, however, that high noise levels and limited data records often make it quite unrealistic to identify anything else than very low order models.

- Which of the known u inputs and secondary y_2 measurements should be used? In ordinary system identification, this is normally an issue related to known inputs that are only measured without being manipulated. In the present case, however, some manipulated as well as only measured inputs may be effectively replaced by secondary measurements, while some other secondary measurements may carry very little useful information.

- How should the model be parametrized? In the thesis we use standard difference equation input-output models and the corresponding observability canonical form state-space representations. This follows from the use of the standard prediction error identification methods in the System Identification Toolbox for use with Matlab (Ljung, 1995), but this may not be the best choice seen from a numerical point of view (Moore, 1981).

Finally it must be noted that the optimal choice of model structure can only be found through proper validation.

5.2 Systematic method

5.2.1 OE model selection

The following method for identification of the optimal OE primary output estimators (2.34) and (2.41) is proposed:

1. Perform an informative identification experiment with only u as input signal and y_1 and y_2 as output signals (e.g. Goodwin and Payne, 1977). Separate the data in one part for identification/calibration and one part for validation.

2. Identify the system with u as input and y_1 as output, using different model orders n. This may be done by use of the ordinary OE model (2.23) or the ordinary ARMAX model (2.27) and a standard prediction error method as described in Chapter 3, or possibly by use of a subspace system identification method (e.g. Di Ruscio, 1997). Validate the models, using for example the scalar case root mean square error $RMSE = \sqrt{\frac{1}{N}\sum_{k=1}^{N}(y_{1,k} - \hat{y}_{1,k})^2}$ as a validation criterion. Visual inspection of the validation response is also recommended. Choose the lowest possible model order that gives a good validation result (see Example 5.1).

3. Use one of the y_2 measurements at a time as input together with u, identify the optimal OEC estimator (2.41) (or the optimal OEP estimator (2.34)) by

use of a prediction error method as described in Chapter 3, and note the validation improvements for all y_2 signals as expressed by for example the RMSE value.

4. Include the most informative y_2 signals as inputs together with u. Choose the number of y_2 signals to use through validation.

5. Explore the possibilities to omit some or all of the manipulated u inputs, using validation as selection tool.

6. Explore the possibilities for using a reduced order model, relying on some or all of the dependent y_2 signals and some of the independent u inputs, and possibly direct coupling from some other independent inputs to y_1.

7. Use all available data and the best validated model structure found, and identify the final estimator.

5.2.2 ARMAX models

For models without dependent y_2 outputs, including reduced models using y_2 measurements as independent inputs, the best solution is to identify an ARMAX model and use the deterministic part of that as a basis for the primary property estimator. This will give a reduced estimator covariance compared with identification of an OE estimator (Söderström and Stoica, 1989). Note, however, that ARMAX models cannot be identified in the low y_1 sampling rate case that will be discussed in Chapter 6.

5.2.3 Discussion on validation

It is in order to point to an inherent difficulty in this and similar procedures that use the same validation data set for comparison of different models. Due to the fact that both the modeling and the validation data sets are randomly sampled, local minima problems and random initial parameter values, some models may give better validation results than others in a way that is not generally justified. Extensively repeated use of the same validation set may therefore lead to a model that is specifically adjusted to fit that particular data set, which then gradually becomes a part of the total modeling set, and we must therefore look for validation differences that can be considered as significant (see also Sjöberg and Ljung, 1995). The only totally safe way out of this risk of circular reasoning is to use extra independent validation sets for each new model. The phenomenon is demonstrated in Example 5.1 below, and a preliminary discussion of the general problem is given in Chapter 11.

5.3 Simulation results

Simulation studies are undertaken, using the prediction error method implemented in *pem.m* in the System Identification Toolbox for use with Matlab (Ljung, 1995) and *dlsim.m* in the Control System Toolbox for use with Matlab (Grace et al., 1992).

Example 5.1 - Primary output estimator for a fifth-order system

The systematic method in Section 5.2 was tested by simulations based on a continuous-time system

$$\begin{bmatrix} \dot{x}_1 \\ \dot{x}_2 \\ \dot{x}_3 \\ \dot{x}_4 \\ \dot{x}_5 \end{bmatrix} = \begin{bmatrix} -2 & 1 & 1 & 0 & 0 \\ 2 & -6 & 2 & 2 & 0 \\ 1 & 1 & -3 & 0 & 1 \\ 0 & 2 & 0 & -4 & 0 \\ 0 & 0 & 1 & 0 & -2 \end{bmatrix} \begin{bmatrix} x_1 \\ x_2 \\ x_3 \\ x_4 \\ x_5 \end{bmatrix} + \begin{bmatrix} 0 & 0 \\ 0 & 0 \\ 0 & 0 \\ 2 & 0 \\ 0 & 1 \end{bmatrix} \begin{bmatrix} u_1 \\ u_2 \end{bmatrix}$$

$$\begin{bmatrix} y_1 \\ y_{22} \\ y_{23} \\ y_{24} \end{bmatrix} = \begin{bmatrix} \begin{bmatrix} 1 & 0 & 0 & 0 & 0 \end{bmatrix} \\ \begin{bmatrix} 0 & 1 & 0 & 0 & 0 \\ 0 & 0 & 1 & 0 & 0 \\ 0 & 0 & 0 & 1 & 0 \end{bmatrix} \end{bmatrix} x. \tag{5.1}$$

This is the system used in Example 4.1. It might be an interacting stirred-tanks system, as illustrated by the equivalent electrical circuit in Fig. 5.1.

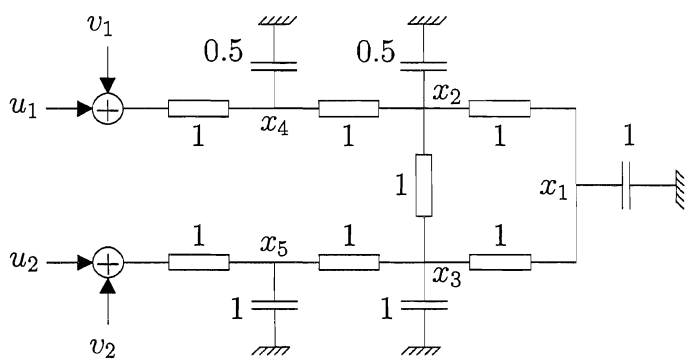

Figure 5.1 Equivalent electrical circuit for interacting stirred-tanks system.

The system was converted to discrete-time assuming zero-order hold elements on the inputs, with a sampling interval $T = 0.1$, and discrete process and measurement noise was added. The process noise sources $v_{1,k}$ and $v_{2,k}$ were independent and normally distributed zero mean white sequences with variances $r_{v_1} = 1$ and

$r_{v_2} = 0.1$ directly added to the inputs. The measurements y_1, y_{22}, y_{23} and y_{24} were independent and normally distributed zero mean white sequences with variances $r_{11} = 10^{-4}$ and $r_{22} = r_{23} = r_{24} = 0.01$.

The procedure in Section 5.2 was followed, except that each identification and validation was repeated in $M = 10$ Monte Carlo runs with independent data sets. The identification experiment in step 1 was simulated with the controlled inputs u_1 and u_2 as independent filtered PRBS with autocovariance $r_{uu}(p) = 0.8^{|p|}$ (see Söderström and Stoica (1989), example 5.11 with $\alpha = 0.8$). A modeling data set and a validation data set were recorded, each with $N = 1000$ samples.

In steps 2 to 6, the optimal OEC estimator (2.41) was specified as

$$nn = [0, [n, \cdots, n, n+1, \cdots n+1], 0, 0, [n, \cdots, n], [1, \cdots, 1, 0, \cdots 0]], \qquad (5.2)$$

adjusted to the number of u and y_2 inputs used (see Appendix B for definition of nn). The results are summarized in Table 5.1, with theoretical RMSE values for model order $n = 5$ included.

Table 5.1: Use of systematic model determination method based on $N = 1000$ samples and $M = 10$ Monte Carlo runs for each model alternative (RMSE values multiplied by 10^4).

step	n	u_1	u_2	y_{22}	y_{23}	y_{24}	$RMSE$	$RMSE_{\text{theor.}}$
2	1	x	x				990 ± 158	638
2	2	x	x				690 ± 88	638
2	3	x	x				767 ± 125	638
2	4	x	x				726 ± 179	638
2	5	x	x				753 ± 276	638
3	2	x	x	x			242 ± 7	226
3	2	x	x		x		368 ± 39	353
3	2	x	x			x	228 ± 17	204
4	2	x	x	x		x	200 ± 13	180
4	2	x	x	x	x	x	175 ± 10	158
5	2	x		x	x	x	224 ± 15	–
5	2		x	x	x	x	174 ± 10	–
5	2			x	x	x	211 ± 6	–
6	1		x	x	x	x	220 ± 10	–

The conclusion from this is that we should use u_2, y_{22}, y_{23} and y_{24} as inputs and system order $n = 2$. That would very likely be the result also when using only one specific data set, bearing in mind that we would look for a parsimonious model.

The results in Table 5.1 also illustrate the validation problem discussed in Section 5.2. The two best models gave very similar validation results, with one being better than the other in approximately 50% of the Monte Carlo runs. The same is also the case when the model order is increased to $n = 3$, and with a single data set we might thus end up with any one of four different models as the best choice. The aim for a parsimonious model would still make the choice indicated above most likely.

The simulations presented above were repeated with use of only one specific data set with $N = 200$ samples, and the results are given in Table 5.2.

Table 5.2: Use of systematic model determination method on a single data set with $N = 200$ samples (RMSE values multiplied by 10^4).

step	n	u_1	u_2	y_{22}	y_{23}	y_{24}	$RMSE$	$RMSE_{\text{theor.}}$
2	1	x	x				830	638
2	2	x	x				799	638
2	3	x	x				1180	638
2	4	x	x				1205	638
2	5	x	x				1235	638
3	2	x	x	x			269	226
3	2	x	x		x		447	353
3	2	x	x			x	242	204
4	2	x	x	x		x	320	180
4	2	x	x	x	x	x	220	158
4	2	x	x		x	x	228	168
5	2	x		x	x	x	274*)	–
5	2		x	x	x	x	251*)	–

*)best of five identifications with different initial values (when both manipulated inputs u_1 and u_2 were used, different initial values had no effect on the result)

With these results, the final choice would be to use model order $n = 2$ and all the available information in u_1, u_2, y_{22}, y_{23} and y_{24}. This was also one of the two best and equally good results based on $N = 1000$ samples, although we then found it natural to choose the more parsimonious solution without use of the u_1 information.

With a short sampling interval, the system in this example will be of the type considered in Theorem 4.3, and numerical problems should therefore be expected with near perfect measurements. However, in order to encounter such problems with $N = 1000$, all secondary measurement noise levels had to be decreased to $r_{22} = r_{23} = r_{24} = 10^{-15}$ at the same time as the sampling interval was reduced to $T = 0.001$.

■

Example 5.2 - Example 5.1 with reduced measurement noise

The Monte Carlo simulations based on $N = 1000$ samples in Example 5.1 was repeated with the y_{22} and y_{23} noise levels reduced to $r_{22} = r_{23} = 0.0001$. Some results are shown in Table 5.3.

Table 5.3: Use of systematic model determination method in $M = 10$ Monte Carlo runs using $N = 1000$ samples and reduced y_{22} and y_{23} noise levels (RMSE values multiplied by 10^4).

n	u_1	u_2	y_{22}	y_{23}	y_{24}	$RMSE$	$RMSE_{\text{theor.}}$
2	x	x	x	x	x	102 ± 4	102
1	x	x	x	x	x	104 ± 2	102
1			x	x		102 ± 3	–

From the table we see that there is no reason to use anything else than a first-order model with only y_{22} and y_{23} as inputs. We might then also identify an ARMAX estimator or use a subspace method.

■

Chapter 6

The low primary output sampling rate case

In many practical cases it is not feasible to perform an experiment with high rate sampling of the primary system outputs, and it is therefore a need for methods based on low and possibly also irregular sampling rate y_1 data. A simple and general prediction error method that handles this type of situation is described in the present chapter, as an extension of the methods presented in Chapter 3. This is made possible by the fact that the optimal primary output estimators developed in Chapter 2 are of the OE type, with the secondary y_2 outputs used as estimator inputs. It turns out that the real difficulty of the problem is to find the initial parameter values for the optimization that are necessary in order to find the globally optimal prediction and current estimators, and solutions to that problem are therefore also outlined.

6.1 Statement of problem

The basic statement of problem is given in Subsection 2.2.1, only that we now must add that

- data records for u_k and $y_{2,k}$ for $k = 1, 2, \cdots, N_2$ are at hand from an informative experiment (e.g. Goodwin and Payne, 1977), i.e. with u_k persistently exciting of appropriate order (e.g. Söderström and Stoica, 1989) and with a sufficiently large number of samples

- a data record for $y_{1,j}$ from the same experiment is also available, with $j = 1, 2, \cdots, N_1$, where $N_1 \leq N_2$ is a sufficiently large number and where each sampling of $y_{1,j}$ coincides in time with one of the u_k and $y_{2,k}$ samplings

- the system operates in open loop (may be relaxed as discussed in Chapter 11)
- the primary property measurement noise $w_{1,j}$ is white in the outset, i.e. there is no need to model the noise at the high sampling rate (which would not be possible from the low sampling rate $y_{1,j}$ data)
- the $y_{1,j}$ samples that are available at a low and possibly irregular sampling rate are representative measurements of the primary property z_k, i.e. the underlying primary property $z_j = C_1 x_j + D_1 u_j$ has the same statistical distribution as $z_k = C_1 x_k + D_1 u_k$
- the problem now is to identify the optimal output error prediction and current (OEP and OEC) estimators developed in Section 2.2.

For clarity of presentation, we assume that the process noise v_k and measurement noise $w_{2,k}$ are independent. A theoretical discussion of the case with correlated process and measurement noise sequences is given in Subsection 2.2.6.

6.2 Modified criterion function

In the prediction error method used in Chapter 3 for identification of the optimal primary property OE estimators, we minimize the scalar criterion function

$$V_N(\theta) = \mathrm{h}\left[\frac{1}{N}\sum_{k=1}^{N}\varepsilon_{1,k}(\theta)\varepsilon_{1,k}^T(\theta)\right], \tag{6.1}$$

where the scalar function may be $\mathrm{h}[\cdot] = \det[\cdot]$ or $\mathrm{h}[\cdot] = \mathrm{trace}[\cdot]$. When $y_{1,k}$ is not generally available due to a low and possibly also irregular sampling rate, we must give the prediction errors zero weight when $y_{1,k}$ does not exist. We therefore minimize

$$V_{N_1}(\theta) = \mathrm{h}\left[\frac{1}{N_1}\sum_{k=1}^{N_2}\alpha_k\varepsilon_{1,k}(\theta)\varepsilon_{1,k}^T(\theta)\right] = \mathrm{h}\left[\frac{1}{N_1}\sum_{j=1}^{N_1}\varepsilon_{1,j}(\theta)\varepsilon_{1,j}^T(\theta)\right], \tag{6.2}$$

where

$$\alpha_k = \begin{cases} 1, & \text{at the time instants } k \text{ where } y_1 \text{ is sampled} \\ 0, & \text{at the time instants } k \text{ where } y_1 \text{ is not sampled.} \end{cases} \tag{6.3}$$

Asymptotically (for $N_1 \to \infty$) minimization of (6.2) will then give the same result as minimization of (6.1), provided that the $y_{1,j}$ samples are representative, i.e. that they have the same statistical distribution as ordinary $y_{1,k}$ samples would have had.

The modified criterion function (6.2) may in principle be used also when ARMAX models are identified, although that would make little sense since we for such models anyhow will need all $y_{1,k}$ samples. For the prediction and current estimators (2.34) and (2.41), however, $\varepsilon_{1,j}(\theta)$ is based on only the present $y_{1,j}$ value (in addition to past and present u and y_2 values), and minimization of (6.2) is then a feasible option.

As in the ordinary case, minimization of (6.2) normally requires good initial values in order to avoid local minima problems. In this case we cannot, however, use an ARX model obtained by least squares modeling for this purpose, which is otherwise a part of the recommended solution (Ljung, 1987,1999).

Ordinary OE models

Identification of ordinary OE models may also be based on low and irregular sample rate y data, since $\varepsilon_j(\theta)$ in that case is based on only present y_j values, in addition to past and present u values. The initial value problem will then be essentially the same as mentioned above.

6.3 Determination of initial parameters

6.3.1 Initial parameters for ordinary OE model

Identification of ordinary OE model

We start the discussion on methods for initial parameter determination with the ordinary OE case. We then have a model

$$\begin{aligned} x_{k+1} &= Ax_k + Bu_k + Gv_k \\ y_k &= Cx_k + Du_k + w_k, \end{aligned} \tag{6.4}$$

where v_k and w_k are independent white noise sequences with covariance matrices $R_v = Ev_kv_k^T$ and $R_w = Ew_kw_k^T$.

Assuming that a true parameter vector θ_0 exists, the corresponding input-output OE model is

$$y_k = G(q^{-1}, \theta_0)u_k + \eta_k, \tag{6.5}$$

where

$$G(q^{-1}, \theta_0) = C(qI - A)^{-1}B + D, \tag{6.6}$$

and where

$$\eta_k = C(qI - A)^{-1}Gv_k + w_k \tag{6.7}$$

is colored noise.

A prediction error identification method will then result in the prediction error

$$\varepsilon_k(\theta) = y_k - y_k^{\text{pred}}(\theta) = \left[G(q^{-1},\theta_0) - G(q^{-1},\theta)\right] u_k + \eta_k, \tag{6.8}$$

which after minimization of the scalar criterion function (6.1) (with ε_1 replaced by ε) asymptotically (for $N \to \infty$) results in $\theta \to \hat{\theta} \equiv \theta_0$ (see Subsection 3.2.2. for details). We here assume a correct parametrization and an initial parameter vector of sufficient quality.

When y_k does not exist for all k, we may still identify the model by minimization of (6.2) (with ε_1 replaced by ε). As mentioned above, however, we cannot then find an initial model by least squares estimation. In order to find a solution to that problem, we make use of some basic system realization theory.

Realization theory

Assuming that the system (6.4) is of order n, the so-called Hankel matrix of the system is defined by

$$H_n = \begin{bmatrix} h_1 & h_2 & \cdots & h_n \\ h_2 & h_3 & & \vdots \\ \vdots & & \ddots & \vdots \\ h_n & \cdots & \cdots & h_{2n-1} \end{bmatrix}. \tag{6.9}$$

Here, h_i are the Markov parameters in the impulse response, which we find by series expansion of (6.5) as

$$\begin{aligned} y_k &= \left[C(qI - A)^{-1}B + D\right] u_k + \eta_k \\ &= \left[D + CBq^{-1} + CABq^{-2} + CA^2Bq^{-3} + \cdots\right] u_k + \eta_k \\ &= \sum_{i=0}^{\infty} h_i u_{k-i} + \eta_k, \end{aligned} \tag{6.10}$$

i.e.

$$h_i = \begin{cases} 0 & , \text{ for } i < 0 \\ D & , \text{ for } i = 0 \\ CA^{i-1}B & , \text{ for } i > 0. \end{cases} \tag{6.11}$$

The dimension of h_i is $m \times r$, where r is the number of inputs in the u vector and m is the number of outputs in the y vector.

Using (6.11) it is straightforward to show that H_n can be factored as

$$H_n = \Gamma_n \Omega_n, \tag{6.12}$$

where

$$\Gamma_n = \begin{bmatrix} C \\ CA \\ \vdots \\ CA^{n-1} \end{bmatrix} \tag{6.13}$$

is the observability matrix of the system, while

$$\Omega_n = \begin{bmatrix} B & AB & \cdots & A^{n-1}B \end{bmatrix} \tag{6.14}$$

is the reachability matrix. For a minimal realization, these two matrices have full rank (Kailath, 1980).

Initial values by identification of FIR model

The series expansion (6.10) gives us a way of finding initial parameter values in the low output sampling rate case. Assuming that the system is asymptotically stable, we will find that $h_i \to 0$ when $i \to \infty$, and we may therefore use the finite impulse response (FIR) model

$$y_k \approx \sum_{i=0}^{L} h_i u_{k-i} + \eta_k = \begin{bmatrix} h_0 & h_1 & \cdots & h_L \end{bmatrix} \begin{bmatrix} u_k \\ u_{k-1} \\ \vdots \\ u_{k-L} \end{bmatrix} + \eta_k, \tag{6.15}$$

where L is chosen sufficiently large. We can then determine a Markov matrix estimate $\begin{bmatrix} \hat{h}_0 & \hat{h}_1 & \cdots & \hat{h}_L \end{bmatrix}$ by a least squares solution of (6.15). This is possible also when most of the y_k values are missing, in which case we use only the y_j samples that are available, together with the corresponding past and present u_k values. The model found in this way will be biased due to both the truncation and the lack of noise modeling. Note, however, that with a low y_j sampling rate, the noise terms η_j will not be consecutive, which means that the correlation from one sample to the next is reduced, with reduced bias in the LS parameter estimate as a consequence.

Once the Markov parameters are determined, we are in a position to recover the system matrices from $\hat{h}_0$ and the Hankel matrix (6.9). In order to reduce the effect of errors we use the extended Hankel matrix

$$\hat{H}_{\frac{L+1}{2}} = \begin{bmatrix} \hat{h}_1 & \hat{h}_2 & \cdots & \hat{h}_{\frac{L+1}{2}} \\ \hat{h}_2 & \hat{h}_3 & & \vdots \\ \vdots & & \ddots & \vdots \\ \hat{h}_{\frac{L+1}{2}} & \cdots & \cdots & \hat{h}_L \end{bmatrix}, \tag{6.16}$$

where we assume that L is an odd number. Using an algorithm of Ho and Kalman (1966) with modifications by Kung (1978), we may do that in the following way:

1. Find $\hat{D} = \hat{h}_0$.
2. Perform a singular value decomposition (SVD) of $\hat{H}_{\frac{L+1}{2}}$ and decide on the number of significant singular values (see details below). In the ideal noise-free case only the n first singular values are nonzero, where n is the model order (Kailath, 1980).
3. Compute the factorization $\hat{H}_{\frac{L+1}{2}} = \hat{\Gamma}_{\frac{L+1}{2}}\hat{\Omega}_{\frac{L+1}{2}}$, where $\Gamma_{\frac{L+1}{2}}$ and $\Omega_{\frac{L+1}{2}}$ are extended observability and reachability matrices of dimensions $m\frac{L+1}{2} \times n$ and $n \times r\frac{L+1}{2}$.
4. Read $\hat{C}$ from the first block row of $\hat{\Gamma}_{\frac{L+1}{2}}$.
5. Read $\hat{B}$ from the first block column of $\hat{\Omega}_{\frac{L+1}{2}}$.
6. Define the submatrix $\hat{\Gamma}_{1:\frac{L+1}{2}-1}$ by deleting the last block row in $\hat{\Gamma}_{\frac{L+1}{2}}$, and the submatrix $\hat{\Gamma}_{2:\frac{L+1}{2}}$ by deleting the first block row. Note from (6.13) that

$$\Gamma_{2:\frac{L+1}{2}} = \Gamma_{1:\frac{L+1}{2}-1}A, \tag{6.17}$$

   and find $\hat{A}$ from the overdetermined equations (6.17) as the least squares solution

$$\hat{A} = \left(\hat{\Gamma}^T_{1:\frac{L+1}{2}-1}\hat{\Gamma}_{1:\frac{L+1}{2}-1}\right)^{-1}\hat{\Gamma}^T_{1:\frac{L+1}{2}-1}\hat{\Gamma}_{2:\frac{L+1}{2}}. \tag{6.18}$$

7. Finally transform the result into the canonical form utilized in the prediction error method used.

Step 2 - Model order determination An SVD of the matrix $\hat{H}_{\frac{L+1}{2}}$ in (6.16) results in

$$\begin{aligned}\hat{H}_{\frac{L+1}{2}} &= \begin{bmatrix} \hat{U}_s & \hat{U}_{\text{noise}} \end{bmatrix}\begin{bmatrix} \hat{S}_s & 0 \\ 0 & \hat{S}_{\text{noise}} \end{bmatrix}\begin{bmatrix} \hat{V}^T_s \\ \hat{V}^T_{\text{noise}} \end{bmatrix} \\ &= \hat{U}_s\hat{S}_s\hat{V}^T_s + \text{noise},\end{aligned} \tag{6.19}$$

where $\hat{S}_s$ is a diagonal matrix with the significant singular values in descending order, and where the number of singular values used in $\hat{S}_s$ determines the model order n. The decision on the number of significant singular values is a non-trivial task, that in the end can only be made through proper validation. This means that we must make a preliminary decision on the model order to use, and possibly revise this choice after validation of the final result.

Step 3 - Factorization of $\hat{H}_{\frac{L+1}{2}}$ When a preliminary decision on the model order n is made, the factorization of (6.16) results in

$$\hat{H}_{\frac{L+1}{2}} \approx \hat{\Gamma}_{\frac{L+1}{2}} \hat{\Omega}_{\frac{L+1}{2}} = \hat{U}_s \hat{S}_s \hat{V}_s^T. \tag{6.20}$$

Following the definitions by Moore (1981), we may now choose $\hat{\Gamma}_{\frac{L+1}{2}}$ and $\hat{\Omega}_{\frac{L+1}{2}}$ in three different ways:

$$\begin{array}{lll} \hat{\Gamma}_{\frac{L+1}{2}} = \hat{U}_s \hat{S}_s^{1/2} & \text{and} \quad \hat{\Omega}_{\frac{L+1}{2}} = \hat{S}_s^{1/2} \hat{V}_s^T & \text{, internally balanced form} \\ \hat{\Gamma}_{\frac{L+1}{2}} = \hat{U}_s & \text{and} \quad \hat{\Omega}_{\frac{L+1}{2}} = \hat{S}_s \hat{V}_s^T & \text{, output normal form} \\ \hat{\Gamma}_{\frac{L+1}{2}} = \hat{U}_s \hat{S}_s & \text{and} \quad \hat{\Omega}_{\frac{L+1}{2}} = \hat{V}_s^T & \text{, input normal form.} \end{array} \tag{6.21}$$

After choosing the model form, we proceed in order to find the C, B and A matrices as described in the steps 4 to 6 above.

6.3.2 Initial parameters for OEP and OEC estimators

Initial parameters for identification of the optimal OEP and OEC estimators (2.34) and (2.41) may be found in different ways, dependent on the observability of the system.

Systems with directly observable output state

Consider the system

$$\begin{aligned} x_{k+1} &= Ax_k + Bu_k + Gv_k \\ y_{1,j} &= \begin{bmatrix} C_{11} & 0 \end{bmatrix} x_j + D_1 u_j + w_{1,j} = C_{11} x_{1,j} + D_1 u_j + w_{1,j} \\ y_{2,k} &= \begin{bmatrix} C_{21} & 0 \end{bmatrix} x_k + D_2 u_k + w_{2,k} = C_{21} x_{1,k} + D_2 u_k + w_{2,k}, \end{aligned} \tag{6.22}$$

where x_1 is the part of the state x that directly via C_{11} determines $y_{1,j}$, and where $x_{1,k}$ is also directly observable through the $y_{2,k}$ measurements via the invertible matrix C_{21}.

In this case we may identify the system (A, B, C_{21}, D_2) using $y_{2,k}$ as output signal, and then find C_{11} and D_1 as a least squares solution of the set of equations given by

$$y_{1,j} = C_{11} C_{21}^{-1} y_{2,j} + (D_1 - C_{11} C_{21}^{-1} D_2) u_j + w_{1,j} - C_{11} C_{21}^{-1} w_{2,j}. \tag{6.23}$$

In this way we will obtain all the necessary initial values in the optimal OEP and OEC estimators (2.34) and (2.41).

The model found may also be used as the final solution, although minimization of the criterion function (6.2) must be expected to give improved primary property

estimation results when y_1 has a much lower noise level than y_2 (compare with the results in Example 6.2 in Section 6.4 below). If necessary, the solution of (6.23) may also be regularized by use of for example principal component regression (PCR) or partial least squares regression (PLSR). We will return to that subject in the following chapters.

Systems structurally observable from the y_2 outputs

Consider the system

$$\begin{aligned} x_{k+1} &= Ax_k + Bu_k + Gv_k \\ y_{1,j} &= C_1 x_j + D_1 u_j + w_{1,j} \\ y_{2,k} &= C_2 x_k + D_2 u_k + w_{2,k}, \end{aligned} \tag{6.24}$$

where (C_2, A) is structurally observable (Appendix A). The innovations model using u_k as input and $y_{2,k}$ as output is then

$$\begin{aligned} \hat{x}^{\mathrm{OE}}_{k+1|k} &= A\hat{x}^{\mathrm{OE}}_{k|k-1} + Bu_k + AK_2^{\mathrm{OE}} e^{\mathrm{OE}}_{2,k} \\ y_{2,k} &= C_2 \hat{x}^{\mathrm{OE}}_{k|k-1} + D_2 u_k + e^{\mathrm{OE}}_{2,k}, \end{aligned} \tag{6.25}$$

which may be identified by use of an ordinary prediction error or subspace method. When this is done we can reconstruct the innovation model state vector $\hat{x}^{\mathrm{OE}}_{k|k-1}$ by use of

$$\hat{x}^{\mathrm{OE}}_{k+1|k} = \left(A - AK_2^{\mathrm{OE}} C_2\right) \hat{x}^{\mathrm{OE}}_{k|k-1} + \left(B - AK_2^{\mathrm{OE}} D_2\right) u_k + AK_2^{\mathrm{OE}} y_{2,k}. \tag{6.26}$$

The remaining matrices in the optimal OE estimators (2.34) and (2.41) will then be C_1 and D_1, and they can be approximately found as a least squares solution of the set of equations given by

$$y_{1,j} = C_1 \hat{x}^{\mathrm{OE}}_j + D_1 u_j + \vartheta_j. \tag{6.27}$$

Note that ϑ_j here is a non-white sequence, although the dependence from one sample to the next may be small with a low $y_{1,k}$ sampling rate. The system matrices found in this manner may then be used to construct initial parameter values in the optimal estimators, as a starting point for minimization of the criterion function (6.2).

The model found may also be used as the final solution, although minimization of the criterion function (6.2) must also here be expected to give improved primary property estimation results (see simulation results in Example 6.2 in Section 6.4 below).

Systems only detectable from the y_2 outputs

In this case we have a system of the type

$$\begin{aligned}\begin{bmatrix} x_1 \\ x_2 \end{bmatrix}_{k+1} &= \begin{bmatrix} A_{11} & A_{12} \\ 0 & A_{22} \end{bmatrix} \begin{bmatrix} x_1 \\ x_2 \end{bmatrix}_k + \begin{bmatrix} B_1 \\ B_2 \end{bmatrix} u_k + \begin{bmatrix} G_1 \\ G_2 \end{bmatrix} v_k \\ y_{1,j} &= \begin{bmatrix} C_{11} & C_{12} \end{bmatrix} \begin{bmatrix} x_1 \\ x_2 \end{bmatrix}_j + D_1 u_j + w_{1,j} \\ y_{2,k} &= \begin{bmatrix} 0 & C_{22} \end{bmatrix} \begin{bmatrix} x_1 \\ x_2 \end{bmatrix}_k + D_2 u_k + w_{2,k}, \end{aligned} \tag{6.28}$$

and the innovations model

$$\begin{aligned}\begin{bmatrix} \hat{x}_1^{\mathrm{OE}} \\ \hat{x}_2^{\mathrm{OE}} \end{bmatrix}_{k+1|k} &= \begin{bmatrix} A_{11} & A_{12} \\ 0 & A_{22} \end{bmatrix} \begin{bmatrix} \hat{x}_1^{\mathrm{OE}} \\ \hat{x}_2^{\mathrm{OE}} \end{bmatrix}_{k|k-1} + \begin{bmatrix} B_1 \\ B_2 \end{bmatrix} u_k \\ &\quad + \begin{bmatrix} A_{11}K_{12}^{\mathrm{OE}} + A_{12}K_{22}^{\mathrm{OE}} \\ A_{22}K_{22}^{\mathrm{OE}} \end{bmatrix} e_{2,k}^{\mathrm{OE}} \\ y_{2,k} &= \begin{bmatrix} 0 & C_{22} \end{bmatrix} \begin{bmatrix} \hat{x}_1^{\mathrm{OE}} \\ \hat{x}_2^{\mathrm{OE}} \end{bmatrix}_{k|k-1} + D_2 u_k + e_{2,k}^{\mathrm{OE}}. \end{aligned} \tag{6.29}$$

It is then possible to identify the system $(A_{22}, B_2, C_{22}, D_2, A_{22}K_{22}^{\mathrm{OE}})$ by an ordinary prediction error or subspace method, and reconstruct the innovation model state vector $\hat{x}_{2,k|k-1}^{\mathrm{OE}}$ by use of

$$\hat{x}_{2,k+1|k}^{\mathrm{OE}} = \left(A_{22} - A_{22}K_{22}^{\mathrm{OE}}C_{22}\right)\hat{x}_{2,k|k-1}^{\mathrm{OE}} + \left(B_2 - AK_{22}^{\mathrm{OE}}D_2\right)u_k + A_{22}K_{22}^{\mathrm{OE}}y_{2,k}. \tag{6.30}$$

When this is done, it remains to find initial values for the dynamic primary output model (for a moment assuming that all $y_{1,k}$ samples exist)

$$\begin{aligned}\hat{x}_{1,k+1|k}^{\mathrm{OE}} &= A_{11}\hat{x}_{1,k|k-1}^{\mathrm{OE}} + \tilde{B}\tilde{u}_k \\ y_{1,k} &= C_{11}\hat{x}_{1,k|k-1}^{\mathrm{OE}} + \tilde{D}\tilde{u}_k + \vartheta_k, \end{aligned} \tag{6.31}$$

or

$$y_{1,k} = \left[C_{11}\left(qI - A_{11}\right)^{-1}\tilde{B} + \tilde{D}\right]\tilde{u}_k + \vartheta_k, \tag{6.32}$$

where $\tilde{B} = \begin{bmatrix} B_1 - \tilde{K}D_2 & A_{12} - \tilde{K}C_{22} & \tilde{K} \end{bmatrix}$, $\tilde{D} = \begin{bmatrix} D_1 & C_{12} & 0 \end{bmatrix}$ and $\tilde{u}_k = \begin{bmatrix} u_k \\ \hat{x}_{2,k|k-1}^{\mathrm{OE}} \\ y_{2,k} \end{bmatrix}$, with $\tilde{K} = A_{11}K_{12}^{\mathrm{OE}} + A_{12}K_{22}^{\mathrm{OE}}$. This is the same type of system as the ordinary OE model (6.5), and since $y_{1,k}$ is not generally available, we may

find the initial values by use of the FIR modeling method presented in Subsection 6.3.1.

In this way we find initial values for $(A_{11}, \tilde{B}, C_{11}, \tilde{D})$, and with the initial values $(A_{22}, B_2, C_{22}, D_2, A_{22}K_{22}^{\mathrm{OE}})$ found above, we have all the initial values needed for identification of the optimal OEP and OEC estimators (2.34) and (2.41). It must be emphasized that this solution requires a substantial number of primary output samples. We need a large dimension of the extended Hankel matrix (6.16) in order to reduce the effect of errors in the estimation of the A matrix, and each Markov parameter h_i will be a matrix with a column dimension determined by the dimension of the $\tilde{u}$ vector above. We may, however, use simplified solutions as indicated in Example 6.3 below.

6.3.3 Initial parameters by resampling of low sample rate estimator

With a sufficiently high $y_{1,j}$ sampling rate, it may be possible to identify an approximate discrete-time OE estimator using only the corresponding samples u_j and $y_{2,j}$. From this it is straightforward to find an approximate continuous-time estimator, and finally initial estimator parameter values by resampling at the u_k and $y_{2,k}$ sampling rate. We will see an industrial data example of that in Chapter 10.

6.3.4 Initial parameters from filtered data

With a low y_1 sampling rate, the primary property z_k may vary a lot in the inter-sample periods. We must then expect a narrow global minimum of the criterion function (6.2), and a difficult task to find the optimal estimator without very good initial values. A solution to the problem may be to filter all signals used in the identification procedure by equal low-pass filters before the attempt to find an estimator. This is a well known method in general system identification, where it may be used in order to enhance the low-frequency fit of the model (e.g. Ljung, 1987,1999). In the present context the aim of the prefiltering is only to facilitate initial values for an identification without prefiltering. A preliminary test on acoustic data presented in Chapter 10 indicates that this method may work satisfactory.

6.3.5 Iterative search with randomized initial values

Difficult initial value problems with a low primary output sampling rate may be solved by an iterative search with randomized initial parameter values. This is demonstrated in the acoustic data example in Chapter 10.

6.4 Simulation examples

Simulation studies are undertaken, using a modified version of the prediction error method implemented in *pem.m* in the System Identification Toolbox for use with Matlab (Ljung, 1995). The modifications consist of setting both the primary output $y_{1,k} = 0$ and the prediction error $e_k = 0$ for all sampling instants k where a measurement $y_{1,k}$ does not exist. In order to compensate for the reduced information content in the data due to lack of y_1 measurements, the number of iterations in the optimization procedure was in the examples increased from the default value 10 to 25, while the tolerance limit was reduced from 0.01 to 0.001. In all examples the systems were simulated with the known input u_k as a filtered PRBS with autocovariance $r_{uu}(p) = \alpha^{|p|}$, where $0 \leq \alpha < 1$ (Söderström and Stoica, 1989, example 5.11), i.e. inputs that were persistently exciting of sufficient order.

Example 6.1 Identification of ordinary OE estimator

In this example we use a modified version of the system in Example 3.2, with the following continuous-time second-order process model with an additional first-order process noise model used as a starting point:

$$\begin{aligned} \dot{x} &= \begin{bmatrix} -1 & 1 & 0 \\ 0 & -1 & 1 \\ 0 & 0 & -1 \end{bmatrix} x + \begin{bmatrix} 0 \\ 1 \\ 0 \end{bmatrix} u + \begin{bmatrix} 0 \\ 0 \\ 1 \end{bmatrix} v \\ y &= \begin{bmatrix} 1 & 0 & 0 \end{bmatrix} x + w. \end{aligned} \tag{6.33}$$

The system was discretized assuming zero-order hold elements on the u and v inputs and a sampling interval $T = 0.1$, and the PRBS input autocovariance was $r_{uu}(p) = 0.5^{|p|}$. The scalar noise sources v_k and w_k were independent and normally distributed white noise sequences with zero mean, variance r_v as given in Table 6.1 below, and $r_w = 0.0001$.

The number of samples were chosen to $N_2 = 2000$ for the input u_k and $N_1 = 200$ for the output y_j, with equally spaced y_j measurements ($y_j = y_k$, for $j = 1, 2, 3, \cdots$ and $k = 10, 20, 30, \cdots$).

Initial parameter values for the OEU model (2.23) were found by use of the FIR method in Section 6.3 with the impulse response truncated at $L = 99$. Typical singular values in the FIR method were for $r_v = 1$ in descending order $\sigma = 0.68$, 0.50, 0.21, 0.20, 0.19, ..., from which a model order $n = 2$ was a natural choice. The extended observability and reachability matrices found from SVD factorization of the extended Hankel matrix (6.16) were defined in the output normal form in (6.21). The initial state-space model was transformed to the controllability canonical form using the function *canon.m* in the Control System Toolbox for use with Matlab (Grace et al., 1992), and further to the observability canonical form

by use of duality relations (Kailath, 1980). A state space representation of the second-order model

$$y_k = \frac{B(q^{-1})}{A(q^{-1})}u_k + \eta_k = \frac{b_1 q^{-1} + b_2^{-2}}{1 + a_1 q^{-1} + a_2 q^{-2}}u_k + \eta_k \tag{6.34}$$

was then identified using the modified prediction error method.

Simulations and identifications were repeated in $M = 10$ Monte Carlo runs, where each identified model was validated against an independent data set with the same number of samples and the same noise variances as used for identification. Validation comparisons between the different identified models were based on the root mean square error criterion

$$RMSE = \sqrt{\frac{1}{N_2}\sum_{k=1}^{N_2}\left(y_k - \hat{y}_k^{\mathrm{OE}}\right)^2}, \tag{6.35}$$

where all the known values of y_k were used (although assumed sampled at a reduced rate).

In order to limit the influence of local minima problems, each identification given specific data sets was repeated $R = 5$ times with randomized initial $B(q^{-1})$ parameters ($b_{ij,r+1} = b_{ij,r} \cdot (1 + 0.05e)$, with e as a zero mean and normal random variable with variance 1). The best of the five models was then validated and kept as the final model.

The mean RMSE values and RMSE standard deviations for different numbers of samples are given in Table 6.1. The table also includes theoretical RMSE values $\sqrt{Cov(\hat{y}_k^{\mathrm{OE}})} = \sqrt{CP^{\mathrm{OEU}}C^T + r_w}$, where P^{OEU} is given by (2.25).

Table 6.1: Validation results for ordinary OE estimator based on $M = 10$ Monte Carlo runs. The table shows RMSE mean values and standard deviations and theoretical RMSE mean values for different process noise variances and measurement noise variance $r_w = 0.0001$. The RMSE values are multiplied by 10^4.

r_v	N_2	N_1	Initial FIR estimator	OEU	$\mathrm{OEU}_{\mathrm{theor.}}$
0.01	2000	200	4027 ± 198	192 ± 37	170
0.1	2000	200	1662 ± 1251	565 ± 210	444
1	2000	200	1655 ± 89	1400 ± 191	1373

The large RMSE value for the initial FIR model with reduced process noise level is due to oscillatory behavior caused by a pole close to the unit circle. It is not further investigated why this is improved with increased noise level. At all noise levels the final RMSE results are close to the theoretical values.

■

Example 6.2 Identification of optimal OEC estimator with (C_2, A) structurally observable

This example is basically the same as Example 3.2, only modified with respect to the y_1 sampling rate. The intention is now primarily to verify that the optimal estimators will be found also in the low y_1 sampling rate case, and we choose to limit the simulations to the OEC estimator (2.41). As a starting point, the following continuous-time second-order process model with an additional first-order process noise model was used (e.g. interacting mixing tanks or thermal processes):

$$\begin{aligned} \dot{x} &= \begin{bmatrix} -1 & 1 & 0 \\ 1 & -2 & 1 \\ 0 & 0 & -1 \end{bmatrix} x + \begin{bmatrix} 0 \\ 1 \\ 0 \end{bmatrix} u + \begin{bmatrix} 0 \\ 0 \\ 1 \end{bmatrix} v \\ y_1 &= \begin{bmatrix} 1 & 0 & 0 \end{bmatrix} x + w_1 \\ y_2 &= \begin{bmatrix} 0 & 1 & 0 \end{bmatrix} x + w_2. \end{aligned} \tag{6.36}$$

Remark 12 *As pointed out in Example 3.2, (C_2, A^c) is here structurally observable, although the specific parameter values chosen make (C_2, A^c) non-observable.*

The system was discretized assuming zero-order hold elements on the u and v inputs and a sampling interval $T = 0.1$ (see Example 3.2), and the PRBS input autocovariance was $r_{uu}(p) = 0.8^{|p|}$. The scalar noise sources v_k, $w_{1,k}$ and $w_{2,k}$ were independent and normally distributed white noise sequences with zero mean and variances $r_v = 1$, $r_{11} = 0.0001$ and $r_{22} = 0.01$. As in Example 6.1, it was assumed that $y_{1,j}$ was recorded at every tenth u_k and $y_{2,k}$ sampling, resulting in $N_1 = N_2/10$ samples.

The initial parameter values for the OEC estimator (2.41) were found by first identifying an ARMAX model using N_2 samples with u_k as input and $y_{2,k}$ as output (see Subsection 6.3.2). The static relation from the state vector $\hat{x}_k^{\mathrm{OE}}$ to $y_{1,k}$ was then found as a least squares solution based on the available $y_{1,j}$ measurements and the corresponding $\hat{x}_j^{\mathrm{OE}}$ values, i.e. by use of (6.27) with $D_1 = 0$. The ARMAX model was here specified as

$$A(q^{-1})y_{2,k} = B(q^{-1})u_k + C(q^{-1})e_k, \tag{6.37}$$

with

$$A(q^{-1}) = 1 + a_1 q^{-1} + a_2 q^{-2} + a_3 q^{-3}, \tag{6.38}$$

$$B(q^{-1}) = b_1 q^{-1} + b_2 q^{-2} + b_3 q^{-3} \tag{6.39}$$

and

$$C(q^{-1}) = 1 + c_1 q^{-1} + c_2 q^{-2} + c_3 q^{-3}. \tag{6.40}$$

After an appropriate similarity transformation of the initial estimator, the OEC estimator (2.41) was identified with u_k and $y_{2,k}$ as input signals and $y_{1,j}$ as output signal. The OEC model was specified as an observer canonical form (Kailath, 1980) state space representation of

$$y_{1,k} = \frac{B_1^{\mathrm{OEC}}(q^{-1})u_k + B_2^{\mathrm{OEC}}(q^{-1})y_{2,k}}{A^{\mathrm{OEC}}(q^{-1})} + \vartheta_k, \tag{6.41}$$

with

$$B_1^{\mathrm{OEC}}(q^{-1}) = b_{11}q^{-1} + b_{12}q^{-2} + b_{13}q^{-3}, \tag{6.42}$$

$$B_2^{\mathrm{OEC}}(q^{-1}) = b_{20} + b_{21}q^{-1} + b_{22}q^{-2} + b_{23}q^{-3} \tag{6.43}$$

and

$$A^{\mathrm{OEC}}(q^{-1}) = 1 + a_1q^{-1} + a_2q^{-2} + a_3q^{-3}. \tag{6.44}$$

As the main purpose of the simulations was to show the feasibility of the low sampling rate solution, no attempt was made to find the model order and model structure from the data. The model order can, however, be found by ordinary use of one of the several available subspace identification methods, e.g. Di Ruscio (1997), and a systematic method for finding the structure was presented in Chapter 5.

Each identified model was validated against an independent data set with the same number of samples and the same noise variances as used for identification. Validation comparisons between the different identified models were based on the root mean square error criterion

$$RMSE = \sqrt{\frac{1}{N_2}\sum_{k=1}^{N_2}\left(y_{1,k} - \hat{y}_{2,k|k}^{\mathrm{OE}}\right)^2}, \tag{6.45}$$

where all the known values of $y_{1,k}$ were used (although $y_{1,j}$ data sampled at a reduced rate was used in the identification stage).

As a basis for comparisons given specific numbers of samples N_1 and N_2, each model was identified and validated in $M = 10$ Monte Carlo runs using independent data sets. In order to limit the influence of local minima problems, each identification given a specific data set was repeated $R = 5$ times with randomized initial $B_1(q^{-1})$ and $B_2(q^{-1})$ parameters ($b_{ij,r+1} = b_{ij,r} \cdot (1 + 0.05e)$, with e as a zero mean and normal random variable with variance 1). The best of the five models was validated and kept as the final model.

The mean RMSE values and RMSE standard deviations for different numbers of samples are given in Table 6.2. The table also includes theoretical RMSE values $\sqrt{Cov(\hat{y}_{1,k|k}^{\mathrm{OE}})}$ computed according to (2.44).

Table 6.2: Validation results for $M = 10$ Monte Carlo runs for estimator for system with (C_2, A) structurally observable. The table shows RMSE mean values and standard deviations and theoretical RMSE mean values for different numbers of samples and $r_v = 1$, $r_{11} = 0.0001$ and $r_{22} = 0.01$. The RMSE values are multiplied by 10^4.

N_2	N_1	Initial ARMAX+LS estimator	OEC	$\text{OEC}_{\text{theor.}}$
400	40	1211 ± 343	333 ± 48	230
2000	200	969 ± 94	245 ± 12	230
10000	1000	972 ± 37	238 ± 7	230

As expected, Table 6.2 shows reduced estimation error when the number of samples is increased from realistically small values to $N_2 = 10000$. In all cases, however, the OEC estimator is considerably better than the initial ARMAX+LSE estimator. For a large number of samples, the OEC estimation variance approaches the theoretical value. For $N_1 = 200$, the results are clearly better than the corresponding results in the high y_1 sampling rate case with $N_2 = N_1$ given in Example 3.4. It is verified that this is not due to the increased number of iterations or the reduced tolerance limit, and judged from the RMSE value the initial model in Example 3.4 is considerably better ($RMSE = 313 \pm 88$). It is not further investigated whether the initial model in Example 3.4 is inferior in other respects, or if it is the large number of input and secondary measurement samples in the present example that is beneficial.

In order to visualize the degree of model misfit behind the RMSE values in Table 6.2, specific validation responses for models based on $N_2 = 400$ samples, are shown in Fig. 6.1. The figure also gives a representative picture of the improvement from the initial ARMAX+LS to the final OEC solution. Note that the number of y_1 measurements behind the estimators is only $N_1 = 40$.

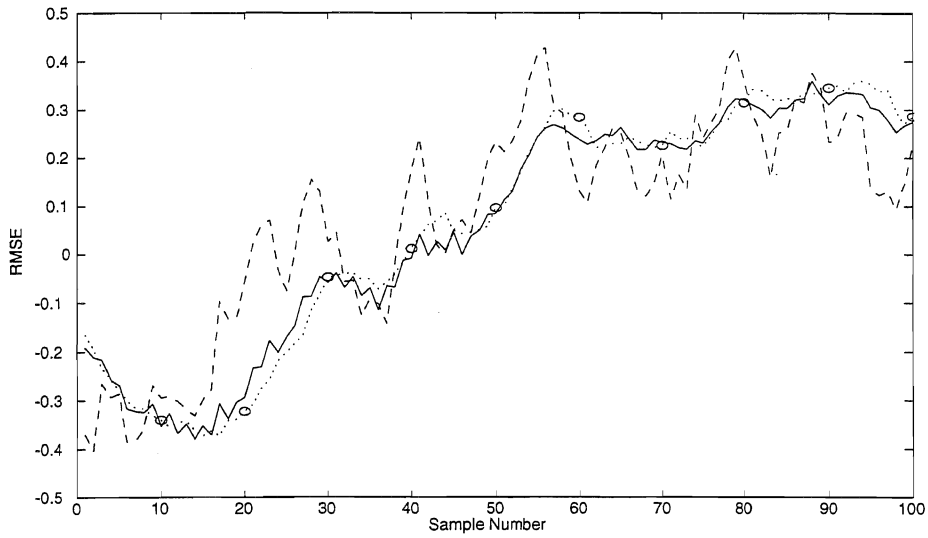

Figure 6.1. Segment of validation responses for an initial ARMAX+LS estimator (dashed, $RMSE = 0.1295$) and the OEC estimator (2.41) (solid, $RMSE = 0.0380$). The experimental conditions are given by $r_v = 1$, $r_{11} = 0.0001$, $r_{22} = 0.01$, $N_2 = 400$ and $N_1 = 40$, and the ideal validation response is shown by dotted line with o-markings at the j sampling instants.

■

Example 6.3 Identification of optimal OEC estimator with (C_2, A) only detectable

In this example we use a modified version of the system in Example 3.2, with the following continuous-time second-order process model with an additional first-order process noise model used as a starting point:

$$\dot{x} = \begin{bmatrix} -1 & 1 & 0 \\ 0 & -1 & 1 \\ 0 & 0 & -1 \end{bmatrix} x + \begin{bmatrix} 0 \\ 1 \\ 0 \end{bmatrix} u + \begin{bmatrix} 0 \\ 0 \\ 1 \end{bmatrix} v \tag{6.46}$$

$$y_1 = \begin{bmatrix} 1 & 0 & 0 \end{bmatrix} x + w_1$$

$$y_2 = \begin{bmatrix} 0 & 1 & 0 \end{bmatrix} x + w_2. \tag{6.47}$$

This is also the same system as in Example 6.1, only that the y_2 measurement is added.

The system was discretized assuming zero-order hold elements on the u and v inputs and a sampling interval $T = 0.1$ (see Example 3.2). The PRBS input autocovariance was $r_{uu}(p) = 0.5^{|p|}$. The scalar noise sources v_k, $w_{1,k}$ and $w_{2,k}$

were independent and normally distributed white noise sequences with zero mean, and variances $r_v = 1$, $r_{11} = 0.0001$ and r_{22} as shown in Table 6.3 below.

The number of samples were chosen to $N_2 = 2000$ for the input u_k and the secondary output $y_{2,k}$, and $N_1 = 200$ for the primary output $y_{1,j}$, with equally spaced $y_{1,j}$ measurements ($y_{1,j} = y_{1,k}$, for $j = 1, 2, 3, \cdots$ and $k = 10, 20, 30, \cdots$).

Initial parameter values for the OEC estimator (2.41) can in theory be found by use of the FIR method in Section 6.3. With the impulse response truncated at $L = 99$ and use of a second-order model with y_2 as input, we would then have 594 parameters in the extended Hankel matrix (6.16). Since we would have only 191 equations of the type given in (6.15), and since a considerable reduction of L was found unacceptable, we were forced to use a simplified approach:

- Identify the second-order system (6.29), i.e. find $(A_{22}, B_2, C_{22}, A_{22}K_{22}^{\mathrm{OE}})$ with $C_{22} = \begin{bmatrix} 1 & 0 \end{bmatrix}$.
- Identify a first-order system with $y_{2,k}$ as input and $y_{1,j}$ as output by use of the FIR method in Section 6.3, resulting in the parameters a^{FIR}, b^{FIR} and c^{FIR}.
- Assume the following deterministic part of the total model:

$$\begin{aligned} \hat{x}_{k+1|k} &= \begin{bmatrix} a^{\mathrm{FIR}} & b^{\mathrm{FIR}} & 0 \\ 0 & A_{22} - A_{22}K_{22}^{\mathrm{OE}}C_{22} \end{bmatrix} \hat{x}_{k|k-1} \\ &\quad + \begin{bmatrix} 0 & b^{\mathrm{FIR}} \\ B_2 & A_{22}K_{22}^{\mathrm{OE}} \end{bmatrix} \begin{bmatrix} u_k \\ y_{2,k} \end{bmatrix} \\ y_{1,j} &= \begin{bmatrix} c^{\mathrm{FIR}} & 0 & 0 \end{bmatrix}. \end{aligned} \tag{6.48}$$

- Transform the model to the observer form (Kailath, 1980) and use the result as initial model for the modified prediction error method.

A state space representation of the model

$$y_{1,k} = \frac{B_1^{\mathrm{OEC}}(q^{-1})u_k + B_2^{\mathrm{OEC}}(q^{-1})y_{2,k}}{A^{\mathrm{OEC}}(q^{-1})} + \vartheta_k \tag{6.49}$$

with the polynomials given by (6.42) to (6.44) was then identified. The simulations and identifications were repeated in $M = 10$ Monte Carlo runs, where each identified model was validated against an independent data set with the same number of samples and the same noise variances as used for identification. Validation comparisons between the different identified models were based on the root mean

square error criterion

$$RMSE = \sqrt{\frac{1}{N_2}\sum_{k=1}^{N_2}\left(y_{1,k} - \hat{y}^{\mathrm{OE}}_{1,k|k}\right)^2}, \tag{6.50}$$

where all the known values of $y_{1,k}$ were used (although $y_{1,j}$ data sampled at a reduced rate was used in the identification stage).

In order to limit the influence of local minima problems, each identification given specific data sets was repeated $R = 5$ times with randomized initial $B_1(q^{-1})$ and $B_2(q^{-1})$ parameters ($b_{ij,r+1} = b_{ij,r} \cdot (1 + 0.05e)$, with e as a zero mean and normal random variable with variance 1). The best of the five models was then validated and used as the final model.

The mean RMSE values and RMSE standard deviations for different variances r_{22} are given in Table 6.3. The table also includes theoretical RMSE values $\sqrt{Cov(\hat{y}^{\mathrm{OE}}_{1,k|k})}$ computed according to (2.44).

Table 6.3: Validation results from $M = 10$ Monte Carlo runs for estimator for system with (C_2, A) only detectable. The table shows RMSE mean values and standard deviations and theoretical RMSE mean values for different r_{22} variances with $r_v = 1$ and $r_{11} = 0.0001$. The RMSE values are multiplied by 10^4.

r_{22}	N_2	N_1	Initial ARMAX+FIR estimator	OEC	$\mathrm{OEC}_{\mathrm{theor.}}$
0.01	2000	200	2362 ± 150	276 ± 44	233
0.1	2000	200	1931 ± 474	621 ± 34	590

The final results are reasonably close to the theoretical values, and very much better than the initial estimator results. One may, however, raise the question if not a reduced estimator with only $y_{2,k}$ as input would give comparably good results. This is investigated in the next example.

■

Example 6.4 Identification of optimal OEC estimator with (C_2, A) only detectable by use of reduced model

Example 6.3 above was repeated, but now using a first-order model with only $y_{2,k}$ as input. The initial estimator was found by use of the FIR method in Section 6.3, and the validation results are given in Table 6.4.

In order to verify the need for a dynamic output model, a static estimator $\hat{y}_{1,k} = cy_{2,k}$ was also established through a least squares solution based on the available $y_{1,j}$ measurements and the corresponding $y_{2,j}$ values. The RMSE values for this estimator are also shown in Table 6.4, and results for the OEC estimator in Table 6.3 are included for comparison purposes.

Table 6.4: Validation results from $M = 10$ Monte Carlo runs for reduced estimator for a system with (C_2, A) only detectable. A first-order model with only $y_{2,k}$ as input was used. The table shows RMSE mean values and standard deviations and theoretical RMSE mean values for different r_{22} variances with $r_v = 1$ and $r_{11} = 0.0001$. The RMSE values are multiplied by 10^4.

r_{22}	N_2	N_1	$\hat{y}_1 = cy_2$	Init. est.	Red. OEC	OEC	$\text{OEC}_{\text{th.}}$
0.01	2000	200	2098 ± 59	485 ± 79	245 ± 10	276 ± 44	233
0.1	2000	200	2478 ± 107	905 ± 298	685 ± 45	621 ± 34	590

From Table 6.4 we see that the reduced first-order estimator is to be preferred when $r_{22} = 0.01$, while the effort to find a third-order model with also u_k as input is somewhat rewarded at the $r_{22} = 0.1$ noise level. However, note that a dynamic output model in any case is needed.

■

Example 6.5 Identification of OEC estimator with (C_2, A) structurally observable by use of reduced model

In a final example in this chapter we repeat Example 6.2, but now using a first-order model with only $y_{2,k}$ as input. As in Example 6.4 the initial estimator was found by use of the FIR method in Section 6.3, and the validation results are given in Table 6.5. The table also includes results for the full OEC model used in Example 6.2. In all cases we chose the excitation parameter $\alpha = 0.5$.

In order to verify the need for a dynamic output model also for this system, a static estimator $\hat{y}_{1,k} = cy_{2,k}$ was established through a least squares solution based on the available $y_{1,j}$ measurements and the corresponding $y_{2,j}$ values. The RMSE values for this estimator are also shown in Table 6.5.

Table 6.5: Validation results from $M = 10$ Monte Carlo runs for a reduced estimator for a system with (C_2, A) structurally observable. A first-order model with only $y_{2,k}$ as input was used. The table shows RMSE mean values and standard deviations and theoretical RMSE mean values for different r_{22} variances with $r_v = 1$ and $r_{11} = 0.0001$. The RMSE values are multiplied by 10^4.

r_{22}	N_2	N_1	$\hat{y}_1 = cy_2$	Init. est.	Red. OEC	OEC	$\text{OEC}_{\text{th.}}$
0.01	2000	200	1650 ± 66	414 ± 54	252 ± 21	245 ± 12	230
0.1	2000	200	2106 ± 157	845 ± 163	682 ± 34	587 ± 38	555

From Table 6.5 we see that the reduced first-order model is almost as good as the full model for $r_{22} = 0.01$, while the effort to find a third-order model with also u_k as input is more rewarded at the $r_{22} = 0.1$ noise level. As in Example 6.4 we note that a dynamic output model is in any case needed.

■

Chapter 7

Least squares estimation as special case

A static least squares estimator may in theory and practice be seen as a special case of the dynamic and Kalman filter based optimal current (a posteriori) estimator discussed in Chapter 2 and Chapter 3. The theoretical link between Kalman filtering and linear regression is further developed in the present chapter, which also forms a link to the principal component and partial least squares regression (PCR and PLSR) methods treated in the next chapter.

7.1 Introduction

The linear regression model arises in different settings, as described in e.g. Johnson and Wichern (1992).

Classical model with independent regressor variables

The classical model is concerned with the association between an $m \times 1$ vector of response variables influenced by noise, and a collection of known and independent regressor variables. Assuming centered data and in the notation used in the thesis, this model can be expressed as

$$Y_1 = UB_1 + E_1, \tag{7.1}$$

where Y_1 is the $N \times m$ matrix of primary response variables, U is the $N \times r$ matrix of manipulated and independent regressor variables, B_1 is the $r \times m$ matrix of unknown parameters and E_1 is the $N \times m$ matrix of independent observation errors. If the data is not centered, this is altered to

$$Y_1 - Y_{10} = (U - U_0)B_1 + E_1, \tag{7.2}$$

where Y_{10} and U_0 are matrices of mean values.

The well known least square estimate of B_1 and its statistical properties are presented in Section 7.4, as a special case of a more general estimator developed below.

Model with independent regressor variables

In the other linear regression setting, all variables are dependent and affected by noise. Assuming centered data and in the notation used in the thesis, this model can be expressed as

$$Y_1 = Y_2 B_2 + E_2, \tag{7.3}$$

where Y_2 is an $N \times p$ matrix of secondary response variables and B_2 is the $p \times m$ matrix of unknown parameters. If the data is not centered, this is altered to

$$Y_1 - Y_{10} = (Y_2 - Y_{20})B_2 + E_2, \tag{7.4}$$

where Y_{10} and Y_{20} are matrices of mean values.

The least squares estimate of B_2 and the corresponding statistical results are also presented in Section 7.4.

General model

In the case of both independent and dependent regressor variables, and assuming centered data, the model becomes a combination of (7.1) and (7.3) above, i.e.

$$Y_1 = \begin{bmatrix} U & Y_2 \end{bmatrix} \begin{bmatrix} B_1 \\ B_2 \end{bmatrix} + E, \tag{7.5}$$

or with data that is not centered

$$Y_1 - Y_{10} = \begin{bmatrix} U - U_0 & Y_2 - Y_{20} \end{bmatrix} \begin{bmatrix} B_1 \\ B_2 \end{bmatrix} + E. \tag{7.6}$$

7.2 Optimal estimator for dynamic systems

In the following we will show that the least squares estimators B_1 and B_2 introduced above are special cases of the optimal output error current (OEC) estimator developed in Chapter 2. For clarity of presentation, we summarize this development below. Consider the general discrete-time system

$$\begin{aligned} x_{k+1} &= Ax_k + Bu_k + Gv_k \\ y_{1,k} &= C_1 x_k + D_1 u_k + w_{1,k} \\ y_{2,k} &= C_2 x_k + D_2 u_k + w_{2,k}, \end{aligned} \tag{7.7}$$

with primary measurements $y_{1,k}$ and secondary measurements $y_{2,k}$, and assuming centered data. Here, x_k is the state vector, while v_k, $w_{1,k}$ and $w_{2,k}$ are white, independent and normally distributed process and measurement noise vectors with covariance matrices $R_v = Ev_kv_k^T$, $R_{11} = Ew_{1,k}w_{1,k}^T$ and $R_{22} = Ew_{2,k}w_{2,k}^T$. As will be shown below, we must in this context assume independent measurement noise sources, i.e. $R_{12} = R_{21}^T = Ew_{1,k}w_{2,k}^T = 0$. Also assume that (C_2, A) is detectable and that $(A, G\sqrt{R_v})$ is stabilizable.

Next consider a Kalman filter utilizing only the secondary y_2 measurements. The optimal prediction (a priori) state estimate will then be governed by

$$\begin{aligned}\hat{x}_{k+1|k}^{\mathrm{OE}} &= \left(A - AK_2^{\mathrm{OE}}C_2\right)\hat{x}_{k|k-1}^{\mathrm{OE}} + \left(B - AK_2^{\mathrm{OE}}D_2\right)u_k \\ &\quad + AK_2^{\mathrm{OE}}y_{2,k},\end{aligned} \tag{7.8}$$

where K_2^{OE} is the gain in a Kalman filter driven by u_k and $y_{2,k}$ (see Appendix A for Kalman filtering background). The optimal current (a posteriori) state estimate will become

$$\hat{x}_{k|k}^{\mathrm{OE}} = \left(I - K_2^{\mathrm{OE}}C_2\right)\hat{x}_{k|k-1}^{\mathrm{OE}} + K_2^{\mathrm{OE}}\left(y_{2,k} - D_2u_k\right). \tag{7.9}$$

From (7.7), (7.8) and (7.9) we find the OEC model

$$\begin{aligned}y_{1,k} &= C_1(I - K_2^{\mathrm{OE}}C_2)\left[qI - A + AK_2^{\mathrm{OE}}C_2\right]^{-1} \\ &\quad \times \left[\left(B - AK_2^{\mathrm{OE}}D_2\right)u_k + AK_2^{\mathrm{OE}}y_{2,k}\right] \\ &\quad + C_1K_2^{\mathrm{OE}}(y_{2,k} - D_2u_k) + D_1u_k + \psi_k,\end{aligned} \tag{7.10}$$

or

$$y_{1,k} = G_1(q^{-1}, \theta_0)u_k + G_2(q^{-1}, \theta_0)y_{2,k} + \psi_k, \tag{7.11}$$

where q^{-1} is the unit time delay operator and θ_0 is the exact parameter vector assumed to exist, while ψ_k is colored noise given by

$$\psi_k = C_1(x_k - \hat{x}_{k|k}^{\mathrm{OE}}) + w_{1,k}. \tag{7.12}$$

Here the Kalman gain is determined by

$$K_2^{\mathrm{OE}} = P^{\mathrm{OEP}}C_2^T\left(C_2P^{\mathrm{OEP}}C_2^T + R_{22}\right)^{-1}, \tag{7.13}$$

where $P^{\mathrm{OEP}} = E(x_k - \hat{x}_{k|k-1}^{\mathrm{OE}})(x_k - \hat{x}_{k|k-1}^{\mathrm{OE}})^T$ is given by the algebraic Riccati equation

$$\begin{aligned}P^{\mathrm{OEP}} &= AP^{\mathrm{OEP}}A^T + GR_vG \\ &\quad - AP^{\mathrm{OEP}}C_2^T\left(C_2P^{\mathrm{OEP}}C_2^T + R_{22}\right)^{-1}C_2P^{\mathrm{OEP}}A^T.\end{aligned} \tag{7.14}$$

The OEC model (7.10) can be identified by use of a prediction error method (Appendix B). We would then utilize an estimator

$$y^{\text{pred}}_{1,k|k}(\theta) = G_1(q^{-1},\theta)u_k + G_2(q^{-1},\theta)y_{2,k}, \tag{7.15}$$

resulting in an estimation error

$$\begin{aligned}\varepsilon_{1,k}(\theta) &= y_{1,k} - y^{\text{pred}}_{1,k|k}(\theta) = \left[G_1(q^{-1},\theta_0) - G_1(q^{-1},\theta)\right]u_k \\ &\quad + \left[G_2(q^{-1},\theta_0) - G_2(q^{-1},\theta)\right]y_{2,k} + \psi_k.\end{aligned} \tag{7.16}$$

Minimization of the scalar loss function

$$V_N(\theta) = \det\left(\frac{1}{N}\sum_{k=0}^{N}\varepsilon_{1,k}(\theta)\varepsilon^T_{1,k}(\theta)\right) \tag{7.17}$$

will then asymptotically ($N \to \infty$) result in $\theta = \hat{\theta} \equiv \theta_0$, i.e. $G_1(q^{-1},\theta) \equiv G_1(q^{-1},\theta_0)$ and $G_2(q^{-1},\theta) \equiv G_2(q^{-1},\theta_0)$, when and only when $E\psi_k\psi^T_k$ is simultaneously minimized. To find conditions for this to occur, we assume $\hat{\theta} \equiv \theta_0$ and develop from (7.12) and (7.9)

$$\begin{aligned}\psi_k &= C_1\left[x_k - \left(I - K^{\text{OE}}_2 C_2\right)\hat{x}^{\text{OE}}_{k|k-1}\right] \\ &\quad -C_1K^{\text{OE}}_2\left(C_2x_k + w_{2,k}\right) + w_{1,k} \\ &= C_1\left(I - K^{\text{OE}}_2C_2\right)\left(x_k - \hat{x}^{\text{OE}}_{k|k-1}\right) - C_1K^{\text{OE}}_2w_{2,k} + w_{1,k}\end{aligned} \tag{7.18}$$

and

$$\begin{aligned}E\psi_k\psi^T_k &= C_1\left(I - K^{\text{OE}}_2C_2\right)P^{\text{OEP}}\left(I - K^{\text{OE}}_2C_2\right)^T C^T_1 \\ &\quad +C_1K^{\text{OE}}_2R^T_{22}\left(C_1K^{\text{OE}}_2\right)^T + R_{11} \\ &\quad -C_1K^{\text{OE}}_2R_{21} - R_{12}\left(C_1K^{\text{OE}}_2\right)^T \\ &= C_1P^{\text{OEC}}C^T_1 + R_{11} - C_1K^{\text{OE}}_2R_{21} - R_{12}\left(C_1K^{\text{OE}}_2\right)^T.\end{aligned} \tag{7.19}$$

Here,

$$\begin{aligned}P^{\text{OEC}} &= E(x_k - \hat{x}_{k|k})(x_k - \hat{x}_{k|k})^T \\ &= \left(I - K^{\text{OE}}_2C_2\right)P^{\text{OEP}}\left(I - K^{\text{OE}}_2C_2\right)^T + K^{\text{OE}}_2R_{22}\left(K^{\text{OE}}_2\right)^T\end{aligned} \tag{7.20}$$

is the minimized covariance matrix related to the current state estimate. From this we see that $E\psi_k\psi^T_k|_{\hat{\theta}\equiv\theta_0}$ represent a true minimum only when $R_{12} = R^T_{21} = 0$, i.e. the $w_{1,k}$ and $w_{2,k}$ noise sources must be independent (see Section 3.2 for an alternative argument).

From (7.16) and (7.19) with $R_{12} = R^T_{21} = 0$ it follows that the asymptotic ($N \to \infty$) estimation covariance is

$$Cov\left(\hat{y}_{1,k|k}\right) = E\varepsilon_k(\theta_0)\varepsilon^T_k(\theta_0) = E\psi_k\psi^T_k = C_1P^{\text{OEC}}C^T_1 + R_{11}. \tag{7.21}$$

7.3 General static linear regression model

Theoretical static estimator

Consider next the special pure delay discrete-time system

$$\begin{aligned} x_{k+1} &= v_k \\ y_{1,k} &= C_1 x_k + D_1 u_k + w_{1,k} \\ y_{2,k} &= C_2 x_k + D_2 u_k + w_{2,k}, \end{aligned} \tag{7.22}$$

i.e. the model (7.7) with $A = 0$, $B = 0$ and $G = I$. The assumption that $R_{12} = R_{21}^T = 0$ is in this case no limitation, since common measurement noise components may be included in x_k.

Remark 13 *In the chemometrical terminology (e.g. Martens and Næs, 1989) we would call the state variables x for latent variables. We will elaborate on that in the next chapter.*

The general input-output-model (7.10) is in this case simplified to

$$y_{1,k} = C_1 K_2^{\mathrm{OE}}(y_{2,k} - D_2 u_k) + D_1 u_k + \psi_k, \tag{7.23}$$

where the Kalman gain according to (7.13) and (7.14) is determined by

$$K_2^{\mathrm{OE}} = R_v C_2^T \left(C_2 R_v C_2^T + R_{22}\right)^{-1}. \tag{7.24}$$

From (7.8) we also find that $\hat{x}_{k|k-1} = 0$, and then from (7.12), (7.9) and (7.22)

$$\psi_k = C_1 v_{k-1} - C_1 K_2^{\mathrm{OE}} C_2 v_{k-1} - C_1 K_2^{\mathrm{OE}} w_{2,k} + w_{1,k}, \tag{7.25}$$

which shows that $\psi_k = e_k$ is a white noise sequence independent of u_k and $y_{2,k}$. Since (7.23) describes a pure static system, it is valid also when the u and y_2 information is available only at a slow and possibly irregular sampling rate, and even when the variables are spatial rather than temporal. The input-output model can therefore be reformulated as

$$y_{1,j} = C_1 K_2^{\mathrm{OE}}(y_{2,j} - D_2 u_j) + D_1 u_j + e_j. \tag{7.26}$$

Collecting u_j^T, $y_{1,j}^T$, $y_{2,j}^T$ and e_j^T for $j = 1, 2, \ldots, N$ in data matrices, we find from (7.26)

$$Y_1 = Y_2 \left(C_1 K_2^{\mathrm{OE}}\right)^T + U \left(D_1 - C_1 K_2^{\mathrm{OE}} D_2\right)^T + E, \tag{7.27}$$

or

$$\begin{aligned} Y_1 &= \begin{bmatrix} U & Y_2 \end{bmatrix} \begin{bmatrix} B_1 \\ B_2 \end{bmatrix} + E \\ &= \begin{bmatrix} U & Y_2 \end{bmatrix} \begin{bmatrix} (D_1 - C_1 K_2^{\mathrm{OE}} D_2)^T \\ (C_1 K_2^{\mathrm{OE}})^T \end{bmatrix} + E. \end{aligned} \tag{7.28}$$

This is a general linear regression model, with independent regressors collected in U and dependent regressors collected in Y_2. The theoretical estimator follows as

$$\begin{bmatrix} B_1^{\mathrm{KF}} \\ B_2^{\mathrm{KF}} \end{bmatrix} = \begin{bmatrix} (D_1 - C_1 K_2^{\mathrm{OE}} D_2)^T \\ (C_1 K_2^{\mathrm{OE}})^T \end{bmatrix}, \tag{7.29}$$

where the B^{KF} notation is introduced in order to indicate the relation to the Kalman filtering theory.

Data based static estimator

When the theoretical model (7.22) is not known, we may still find estimates $\hat{B}_1^{\mathrm{LS}}$ and $\hat{B}_2^{\mathrm{LS}}$ from experimental data. Since e_j is a white noise sequence, we can find consistent parameter estimates by linear regression, i.e. from (7.28)

$$\begin{aligned} \begin{bmatrix} \hat{B}_1^{\mathrm{LS}} \\ \hat{B}_2^{\mathrm{LS}} \end{bmatrix} &= \left(\begin{bmatrix} U^T \\ Y_2^T \end{bmatrix} \begin{bmatrix} U & Y_2 \end{bmatrix} \right)^{-1} \begin{bmatrix} U^T \\ Y_2^T \end{bmatrix} Y_1 \\ &= \begin{bmatrix} U^T U & U^T Y_2 \\ Y_2^T U & Y_2^T Y_2 \end{bmatrix}^{-1} \begin{bmatrix} U^T \\ Y_2^T \end{bmatrix} Y_1. \end{aligned} \tag{7.30}$$

In order to verify that this asymptotically results in the theoretical estimator (7.29), we assume that u_k is a stochastic process and introduce the expectation

$$E u_j u_j^T = R_u. \tag{7.31}$$

We further construct Y_1 and Y_2 from (7.22) as

$$Y_1 = X C_1^T + U D_1^T + W_1 \tag{7.32}$$

$$Y_2 = X C_2^T + U D_2^T + W_2. \tag{7.33}$$

Utilizing that x_j, $w_{1,j}$ and $w_{2,j}$ are independent white noise sequences with $E x_j x_j^T = R_v$ and $E w_{2,j} w_{2,j}^T = R_{22}$, we now find

$$\begin{aligned} & E \frac{1}{N} \begin{bmatrix} U^T \\ Y_2^T \end{bmatrix} \begin{bmatrix} U & Y_2 \end{bmatrix} \\ &= \begin{bmatrix} R_u & R_u D_2^T \\ D_2 R_u & C_2 R_v C_2^T + D_2 R_u D_2^T + R_{22} \end{bmatrix}, \end{aligned} \tag{7.34}$$

and

$$E\frac{1}{N}\begin{bmatrix} U^T \\ Y_2^T \end{bmatrix} Y_1 = \begin{bmatrix} R_u D_1^T \\ C_2 R_v C_1^T + D_2 R_u D_1^T \end{bmatrix}. \tag{7.35}$$

By use of the matrix inversion lemma (e.g. Kailath, 1980) and inserting (7.34) and (7.35) into (7.30) we now readily find

$$E\begin{bmatrix} \hat{B}_1^{\mathrm{LS}} \\ \hat{B}_2^{\mathrm{LS}} \end{bmatrix} = \begin{bmatrix} B_1^{\mathrm{KF}} \\ B_2^{\mathrm{KF}} \end{bmatrix} = \begin{bmatrix} \left(D_1 - C_1 K_2^{\mathrm{OE}} D_2\right)^T \\ \left(C_1 K_2^{\mathrm{OE}}\right)^T \end{bmatrix}, \tag{7.36}$$

with K_2^{OE} according to (7.24). Note that R_u is eliminated from the final expression, which makes the expectation (7.36) equal to the theoretical estimator (7.29).

Estimator covariance

In this static case, the asymptotic ($N \to \infty$) estimation covariance is found from (7.14), (7.20), (7.21) and (7.24) as

$$\begin{aligned} Cov\left(\hat{y}_{1,j|j}\right) &= C_1\left(I - K_2^{\mathrm{OE}} C_2\right) R_v \left(I - K_2^{\mathrm{OE}} C_2\right)^T C_1^T \\ &\quad + C_1 K_2^{\mathrm{OE}} R_{22} \left(C_1 K_2^{\mathrm{OE}}\right)^T + R_{11} \\ &= C_1\left(I - K_2^{\mathrm{OE}} C_2\right) R_v C_1^T + R_{11}. \end{aligned} \tag{7.37}$$

7.4 Standard statistical results

The general results obtained above, may be compared with standard statistical results for some special cases.

Special case 1: Classical regression

With only independent regressor variables, i.e. $Y_2 = 0$, $R_v = 0$ and $K_2 = 0$, we obtain from (7.28) the linear regression model (7.1), i.e.

$$Y_1 = UB_1 + E = UD_1^T + E_1. \tag{7.38}$$

With data that is not centered, this is altered to

$$Y_1 - Y_{10} = (U - U_0)B_1 + E_1 = (U - U_0)D_1^T + E_1. \tag{7.39}$$

This can be reformulated as

$$Y_1 = Y_{10} - U_0 B_1 + UB_1 + E_1 = \begin{bmatrix} \mathbf{1}_N & U \end{bmatrix} \begin{bmatrix} b_0^T \\ B_1 \end{bmatrix} + E_1, \tag{7.40}$$

where $\mathbf{1}_N$ is an $N \times 1$ vector of ones. We will thus be able to determine unbiased estimates of both b_0^T and B_1 by the least squares method.

The asymptotic estimation covariance in this case follows from (7.37) as

$$Cov\left(\hat{y}_{1,j|j}\right) = R_{11}.$$

This is in accordance with the general statistical forecasting result (Johnson and Wichern, 1992)

$$\begin{aligned} Cov\left(\hat{y}_{1,j|j}\right) &= R_{11}\left(1+\begin{bmatrix} 1 & u_j^T \end{bmatrix}\left(\begin{bmatrix} \mathbf{1}_N^T \\ U^T \end{bmatrix}\begin{bmatrix} \mathbf{1}_N & U \end{bmatrix}\right)^{-1}\begin{bmatrix} 1 \\ u_j \end{bmatrix}\right) \\ &= R_{11}\left(1+\frac{1}{N}\begin{bmatrix} 1 & u_j^T \end{bmatrix}\begin{bmatrix} 1 & \frac{1}{N}\mathbf{1}_N^T U \\ \frac{1}{N}U^T\mathbf{1}_N & \frac{1}{N}U^T U \end{bmatrix}^{-1}\begin{bmatrix} 1 \\ u_j \end{bmatrix}\right) \\ &\to R_{11};\ N \to \infty, \end{aligned} \tag{7.41}$$

which follows from the fact that $[\cdot]^{-1}$ is a constant covariance matrix for large N.

Special case 2: Regression with only dependent variables

With constant independent variables $u_j = u_0$, i.e. $U = U_0$, we obtain from (7.28) the theoretical model

$$\begin{aligned} Y_1 &= U_0 B_1 + Y_2 B_2 + E = B_0 + Y_2 B_2 + E \\ &= U_0\left(D_1 - C_1 K_2^{\mathrm{OE}} D_2\right)^T + Y_2\left(C_1 K_2^{\mathrm{OE}}\right)^T + E, \end{aligned} \tag{7.42}$$

where K_2^{OE} is given by (7.24).

In order to compare this with theoretical results from a statistical analysis, we introduce the mean values (see Johnson and Wichern (1992) for notation)

$$\mu_1 = Ey_{1,j} = D_1 u_0 \tag{7.43}$$

$$\mu_2 = Ey_{2,j} = D_2 u_0. \tag{7.44}$$

From (7.26) we then find the optimal prediction

$$\hat{y}_{1,j|j} = \beta_0 + \beta y_{2,j}, \tag{7.45}$$

where

$$\beta = C_1 K_2^{\mathrm{OE}} \tag{7.46}$$

and

$$\beta_0 = \mu_1 - \beta\mu_2. \tag{7.47}$$

From (7.22) we find (with $R_{12} = R_{21}^T = 0$)

$$\Sigma_{12} = E(y_{1,j} - \mu_1)(y_{2,j} - \mu_2)^T = C_1 R_v C_2^T \tag{7.48}$$

and

$$\Sigma_{22} = E(y_{2,j} - \mu_2)(y_{2,j} - \mu_2)^T = C_2 R_v C_2^T + R_{22}. \tag{7.49}$$

From (7.46) and (7.24) we also find

$$\beta = C_1 K_2^{\mathrm{OE}} = C_1 R_v C_2^T \left(C_2 R_v C_2^T + R_{22} \right)^{-1} = \Sigma_{12} \Sigma_{22}^{-1}. \tag{7.50}$$

The asymptotic estimation covariance in (7.37) will in this case become

$$Cov\left(\hat{y}_{1,j|j}\right) = \Sigma_{11} - \Sigma_{12}\Sigma_{22}^{-1}\Sigma_{21}, \tag{7.51}$$

where Σ_{12} and Σ_{22} are found form (7.48) and (7.49), while Σ_{11} and Σ_{21} are found from (7.22) as

$$\Sigma_{11} = E(y_{1,j} - \mu_1)(y_{1,j} - \mu_1)^T = C_1 R_v C_1^T + R_{11} \tag{7.52}$$

and

$$\Sigma_{21} = E(y_{2,j} - \mu_2)(y_{1,j} - \mu_1)^T = C_2 R_v C_1^T. \tag{7.53}$$

The results in (7.45), (7.47), (7.50) and (7.51) can also be found by a straightforward statistical analysis (Johnson and Wichern, 1992).

In order to find data based parameter estimates for the model (7.42) by use of linear regression, we first note from (7.43) and (7.44) that

$$\hat{U}_0 D_1^T = \mathbf{1}_N \frac{1}{N} \sum_{j=1}^{N} y_{1,j}^T = Y_{10} \tag{7.54}$$

and

$$\hat{U}_0 D_2^T = \mathbf{1}_N \frac{1}{N} \sum_{j=1}^{N} y_{2,j}^T = Y_{20}. \tag{7.55}$$

Inserted into (7.42), this results in

$$Y_1 - Y_{10} = (Y_2 - Y_{20}) B_2 + E_2, \tag{7.56}$$

where $B_2^{\mathrm{KF}} = \left(C_1 K_2^{\mathrm{OE}}\right)^T$. From this relation between centered y_1 and y_2 data, we find an unbiased estimate $\hat{B}_2^{\mathrm{LS}}$ by use of the ordinary least squares method.

From the data it is also possible to find an unbiased estimate of the covariance theoretically given by (7.51) (Johnson and Wichern, 1992).

The connection between Kalman filtering and least squares regression for this special case was discussed in Berntsen (1988), but then without basis in the general dynamic OEC estimator (2.41) or the OEC model (7.10). It was also limited to the case with $C_1 = I$ (or at least an invertible matrix) and $w_{1,k} = 0$, i.e. the case with $y_{1,k}$ as noise free measurements of all state variables in the system (possibly after a similarity transformation).

7.5 A static experimental setup for dynamic systems

The static LS method may also be used in stationary analyses of dynamic systems. Consider again the system (7.7) with the optimal y_1 current estimator model (7.10), and let the input u_k be piecewise constant over periods that are much longer than both the time constants in the underlying continuous-time system and the discretization sampling time. Also split u_k into two parts as $u = \begin{bmatrix} d_k^T & u_{m,k}^T \end{bmatrix}$, where d_k is a vector of unknown offsets or disturbances and where $u_{m,k}$ is a known vector of manipulated or measured inputs. Assume collinear observations $y_j = \begin{bmatrix} y_{1,j}^T & y_{2,j}^T \end{bmatrix}^T$ with a data sampling interval that also is much longer than both the time constants in the underlying continuous-time system and the discretization sampling interval, and samples taken at time instants where the system has settled after the last change of u_k. The experimental setup is illustrated in Fig. 7.1, where also the samples u_j at the y_j sampling instants are indicated.

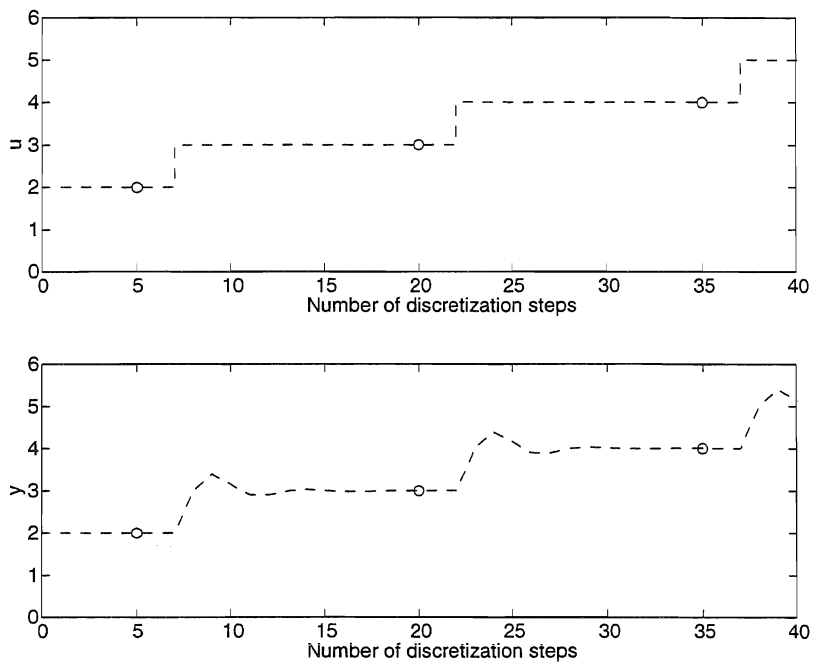

Figure 7.1 Input and output signals with piecewise constant inputs and settling outputs. The o-markings indicate the samples used in a least squares solution.

Also assume that d_j is a white noise sequence, i.e. that the unknown offsets and disturbances are independent from one observation to the next. With a piecewise static input vector u_k and enough time for settlement, it follows from (7.7) that

the observations will be given by

$$\begin{aligned} y_{1,j} &= \left[C_1(I-A)^{-1}B + D_1\right]\begin{bmatrix} d \\ u_m \end{bmatrix}_j \\ &\quad + \sum_{k=-\infty}^{i} v_k g_{1,i-k} + w_{1,j} \\ y_{2,j} &= \left[C_2(I-A)^{-1}B + D_2\right]\begin{bmatrix} d \\ u_m \end{bmatrix}_j \\ &\quad + \sum_{k=-\infty}^{i} v_k g_{2,i-k} + w_{2,j}, \end{aligned} \tag{7.57}$$

where i is the value of k at the j sampling instants, and where g_1 and g_2 are the impulse responses from v to y_1 and y_2. All measurements are thus linear combinations of d and u_m plus noise, and since we assume a stable system with piecewise constant inputs and a settling time shorter than the data sampling interval, this noise will be approximately white. Since the noise is partly determined by the common process noise v_k, the noise components in $y_{1,j}$ and $y_{2,j}$ will not be independent, as required for the optimal estimator model (7.10). For calibration purposes it is also a normal procedure to use mean values of the measurements over a certain period of time in order to reduce the noise, but this does not affect the theoretical analysis.

If both d and u_m are completely known, there is no need to utilize the information in the y_2 measurements, we can simply solve the first equation in (7.57) as an ordinary least squares problem. In the present case, however, we consider d as unknown, and the y_2 measurements may then give valuable information about d and indirectly also about y_1.

Assume now that $u_{m,j}$ is a persistently exciting stochastic signal, and that all data are centered, i.e. that d_j, $u_{m,j}$, $y_{1,j}$ and $y_{2,j}$ are stochastic variables with zero mean. Further, model d_j as generated by white noise through a pure delay system, and model also the common noise part $e_{c,j}$ in $y_{1,j}$ and $y_{2,j}$ as generated by a delayed white noise sequence. Expressing y_1 and y_2 as linear combinations of $x = \begin{bmatrix} d^T & e_c^T \end{bmatrix}^T$ and u_m, we then arrive at the dynamic system

$$\begin{aligned} x_{j+1} &= \begin{bmatrix} d \\ e_c \end{bmatrix}_{j+1} = e_j \\ y_{1,,j} &= C_1 x_j + D_1 u_{m,j} + e_{1,j} \\ y_{2,j} &= C_2 x_j + D_2 u_{m,j} + e_{2,j}, \end{aligned} \tag{7.58}$$

i.e. a system as given in (7.22). Note that all plant dynamics are lost in this setup.

7.6 Static errors-in-variables problems

The pure delay system (7.22) with $D_1 = D_2 = 0$ gives

$$\begin{aligned} x_{k+1} &= v_k \\ y_{1,k} &= C_1 x_k + w_{1,k} \\ y_{2,k} &= C_2 x_k + w_k. \end{aligned} \tag{7.59}$$

With $C_2 = I$ the output equations will represent a static errors-in-variables problem.

In order to apply the ordinary LS method on this problem, we collect the data in matrices $Y_1$and Y_2, and obtain the estimator

$$\hat{y}_1^T = y_2^T \left(Y_2^T Y_2\right)^{-1} Y_2^T Y_1 = y_2^T \hat{B}^{\mathrm{LS}}. \tag{7.60}$$

The theoretical and asymptotic estimator (7.29) is then

$$E\hat{B}^{\mathrm{LS}} = \left(C_1 K_2^{\mathrm{OE}}\right)^T = \left(R_v + R_{22}\right)^{-1} R_v C_1^T. \tag{7.61}$$

Note that this is the optimal solution when the problem is to find $\hat{y}_{1,k}$ estimates from known $y_{2,k}$ values. If the goal is to find an estimate of C_1, other methods should be used. We illustrate this by an example borrowed from Roorda and Heij (1995):

Example 7.1

Assume a system

$$\begin{aligned} y_{1,k} &= a x_k + w_{1,k} \\ y_{2,k} &= x_k + w_{2,k}, \end{aligned} \tag{7.62}$$

where x_k, $w_{1,k}$ and $w_{2,k}$ are white and uncorrelated sequences with $Ex_k^2 = r_v = 1$, $Ew_{1,k}^2 = r_{11} = 0.5$ and $Ew_{2,k}^2 = r_{22} = 0.5$. From (7.61) we find the optimal estimate

$$\hat{y}_{1,k} = \frac{1}{1 + 0.5} a y_{2,k} = 0.6667 a y_{2,k}. \tag{7.63}$$

Based on $N = 20$ observations Roorda and Heij (1995) found the least squares estimator $\hat{a}^{\mathrm{LS}} = 0.69a$, i.e. fairly close to the optimal result. As a good estimate of a they found the total least squares solution $\hat{a}^{\mathrm{TLS}} = 0.96a$.

■

7.7 Simulation example

Example 7.2

For an application of the least squares estimation above, assume a process stream with varying but known concentrations $u_{m,1}$, $u_{m,2}$ and $u_{m,3}$ of three substances A, B and C, and varying unknown concentrations d_1, d_2 and d_3 of three other substances D, E and F. Also assume a scalar primary property z measured by y_1 and $p = 3$ secondary noisy y_2 measurements that all are linear combinations of the six concentrations. Assuming that the y_1 measurements can be obtained only through delayed laboratory analyses of physical samples, it is of interest find the relation between the estimator variables u_m and y_2 and the z property. A calibration experiment is therefore performed on the system, with a data sampling interval such that the unknown concentrations are independent white noise sequences. We thus have a system as given in (7.58) with $e_c = 0$.

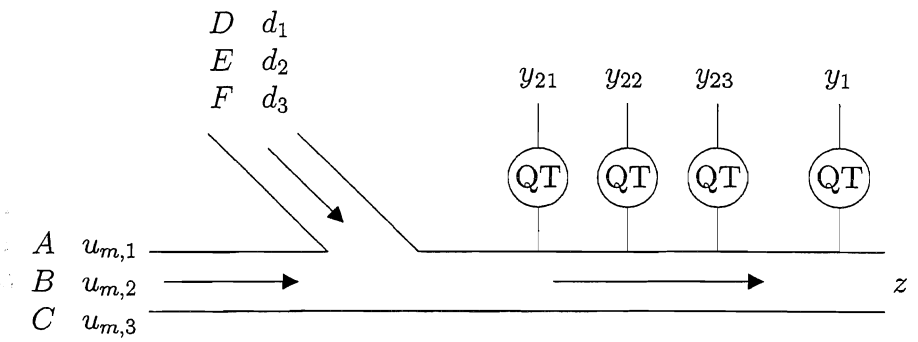

Figure 7.2 Process streams with known and unknown input concentrations u and d, a concentration dependent primary property z, primary property measurement y_1 and secondary measurements y_2.

Calibration experiments were performed in $M = 100$ Monte Carlo simulations with $Ee_1^2 = r_{11} = 0.0001$. In each experiment, d, u_m and e_2 were generated as normally distributed random numbers with diagonal covariance matrices R_d, R_u and R_{22}. The parameters in R_d, R_u, C_1, D_1, C_2 and D_2 were uniformly distributed random numbers in the interval $(0, 1)$, while the parameters in R_{22} were uniformly distributed random numbers in the interval $(0, 0.01)$ The resulting mean parameter values for the theoretical estimator (7.29) were

$$b^{\mathrm{KF}} = 10^{-4} \cdot \begin{bmatrix} 1675 & 3048 & -1347 & -4712 & 13191 & 1021 \end{bmatrix}^T. \tag{7.64}$$

Least squares estimation according to (7.30) with $N = 10000$ samples gave the corresponding mean parameter values

$$\hat{b}^{\mathrm{LS}}_{N=10000} = 10^{-4} \cdot \begin{bmatrix} 1692 & 3049 & -1350 & -4720 & 13186 & 1030 \end{bmatrix}^T, \tag{7.65}$$

while $N = 200$ samples gave the mean parameter values

$$\hat{b}^{\mathrm{LS}}_{N=200} = 10^{-4} \cdot \begin{bmatrix} 1863 & 2658 & -880 & -4035 & 12346 & 840 \end{bmatrix}^T. \tag{7.66}$$

The mean theoretical RMSE value $RMSE_{\mathrm{theor.}} = \sqrt{Cov(\hat{y}_{1,j|j})}$ with $Cov(\hat{y}_{1,j|j})$ determined according to (7.37) was

$$RMSE^{\mathrm{KF}} = \sqrt{Cov(\hat{y}_{1,k|k})} = 0.1136. \tag{7.67}$$

Least squares estimation according to (7.30) with $N = 10000$ samples and validation against an independent data set of the same length gave the mean value

$$RMSE^{\mathrm{LS}}_{N=10000} = 0.1134, \tag{7.68}$$

while estimation and validation with $N = 200$ samples gave the mean value

$$RMSE^{\mathrm{LS}}_{N=200} = 0.1182. \tag{7.69}$$

We notice here that the reduction from $N = 10000$ to $N = 200$ gave a 7% to 53% impairment in all entries of the estimated parameter vector, while the overall RMSE value is increased by only 4%. This shows that the optimum represented by the theoretical solution is not a very distinct one, which explains why regularization methods like principal component regression (PCR) and partial least squares regression (PLSR) can give good y_1 estimates even though the estimated parameters might have significant errors. We will study such methods in the next chapter.

■

Chapter 8

Multivariate calibration as special case

With a large number of secondary output variables and a limited number of observations, a static least squares (LS) estimator may give very large estimation covariance due to overfitting. In the common case with highly collinear regressor variables, we can then make use of the chemometrical regularization methods principal component regression (PCR) and partial least squares regression (PLSR). These methods make use of estimated latent variables that are linear combinations of all regressor variables, defined by a weighting matrix W. The present chapter develops theoretical and data based PCR and PLSR estimators as extensions of the least squares estimators in Chapter 7. In this way a theoretical link back to Kalman filtering is established, and it is shown that with the assumed latent variable structure the theoretical optimal weighting matrix is a transposed Kalman gain $W = (K_2^{\mathrm{OE}})^T$. Seen from a practical point of view, a more interesting result is that a small number of known input variables u should not necessarily be included in the PCR/PLSR solution together with the secondary measurements y_2, but treated separately in a two-step PCA/PLSR +LS solution.

The present chapter is also a link between the optimal OE estimators discussed in Chapter 2 and Chapter 3, and the dynamical latent variables methods presented in the next chapter.

8.1 Latent variable regression models

When the number of regressor variables y_2 is large and the number of observations is limited, the ordinary solution to the LS problem as presented in Chapter 7 may have very large variance due to overfitting, and some form of regularization is

then called for. In many such cases, fortunately, the estimator variables are highly collinear, and most of the information can then be compressed into a few estimated latent variables within a subspace of the variable space. Basic tools for this data compression are singular value decomposition (SVD) and principal component analysis (PCA), and the regression method directly based on this is principal component regression (PCR), while partial least squares regression (PLSR) combines data compression and regression. Detailed presentations of the PCR and PLSR methods are given in Martens and Næs (1989) and Høskuldsson (1996) (see also Appendix C for an introduction and further references). The PCA, PCR and PLSR tools for multivariate data analysis are used in many cases of great practical interest, also when the estimator variables far outnumber the observations at hand. An example is product quality characterization by use of near-infrared spectroscopy, with several thousand estimator variables (frequencies) and often less than one hundred observations.

The PCR and PLSR methods are based on latent variable modeling. In the pure delay model (7.22) the latent variables are the state variables x_k. If we for simplicity set $u_k = 0$, and collect the x_k, $y_{1,k}$ and $y_{2,k}$ variables in matrices $T = \begin{bmatrix} x_1 & x_2 & \cdots & x_N \end{bmatrix}^T$, $Y_1 = \begin{bmatrix} y_{1,1} & y_{1,2} & \cdots & y_{1,N} \end{bmatrix}^T$ and $Y_2 = \begin{bmatrix} y_{2,1} & y_{2,2} & \cdots & y_{2,N} \end{bmatrix}^T$, the output equations in (7.22) can be written as

$$\begin{aligned} Y_1 &= TC_1^T + W_1 \\ Y_2 &= TC_2^T + W_2. \end{aligned} \tag{8.1}$$

In the chemometrical terminology this is called a latent variable regression model, and it is found useful in multivariate calibration (MC), chemical process modeling (CPM) and chemical analysis of quantitative structure activity/property relationships (QSAR/QSPR) (Wold, 1993).

In the following we will take a closer look at the PCR and PLSR methods with the linear regression analysis in Chapter 7 as a starting point. A preliminary work in this direction was also presented by Berntsen (1988).

8.2 The pure dependent regressor variables case

8.2.1 Introduction

In this section we will assume the data structure in (8.1), i.e. $u_k = 0$. More general cases with $u_k \neq 0$ are treated in the following sections.

Regularized latent variables estimator without known inputs

In the PCR and PLSR methods we compress the data matrix Y_2 into a matrix $\hat{T} = \begin{bmatrix} \hat{\tau}_1 & \hat{\tau}_2 & \cdots & \hat{\tau}_N \end{bmatrix}^T$ of estimated latent variables $\hat{\tau}$ by use of the factorization

$$Y_2 = T\hat{W}^T + E, \tag{8.2}$$

with E as a residual matrix. Here $\hat{W}$ is an $m \times a_2$ weighting matrix $\hat{W} = \hat{W}_{\text{PCR}} = \hat{P}$ or $\hat{W} = \hat{W}_{\text{PLS}}$, where m is the number of y_2 variables and a_2 is the number of components used. Since $\hat{W}^T\hat{W} = I$, we thus have the LS solution

$$\hat{T} = Y_2\hat{W} \tag{8.3}$$

(see Appendix C for details).

With the matrix Y_1 of response variables recorded in an experiment, and with the $\hat{\tau}$ variables as regressor variables, the ordinary least squares method gives the estimator

$$\hat{B}_{\text{T}}^{\text{LV}} = \left(\hat{T}^T\hat{T}\right)^{-1}\hat{T}^TY = \left(\hat{W}^TX^TX\hat{W}\right)^{-1}\hat{W}^TX^TY. \tag{8.4}$$

Since $\hat{\tau}^T = y_2^T\hat{W}$ and thus $\hat{y}_1^T = \tau^T\hat{B}_{\text{T}}^{\text{LV}} = y_2^T\hat{W}\hat{B}_{\text{T}}^{\text{LV}}$, the regularized latent variables estimator related to the y_2 variables becomes

$$\hat{B}^{\text{LV}} = \hat{W}\left(\hat{W}^TX^TX\hat{W}\right)^{-1}\hat{W}^TX^TY. \tag{8.5}$$

In the following we will return to this expression in connection with an optimal estimator using $\hat{W} = \left(K_2^{\text{OE}}\right)^T$, and in connection with PCR and PLSR estimators using $\hat{W} = \hat{P}$ and $\hat{W} = \hat{W}_{\text{PLS}}$.

Pure delay dynamic model

We will in the following apply the PCR and PLSR methods to the pure delay model used in Chapter 7, and we start with the pure dependent regressor variables case. With $u_k = 0$ the pure delay dynamic system (7.22) is simplified to

$$\begin{aligned} \tau_{k+1} &= v_k \\ y_{1,k} &= C_1\tau_k + w_{1,k} \\ y_{2,k} &= C_2\tau_k + w_{2,k}, \end{aligned} \tag{8.6}$$

where we choose to adopt the chemometrical notation τ_k for the latent state variables. This model is the starting point for the analysis of Kalman filter based estimators and PCR/PLSR estimators.

8.2.2 Kalman filter based estimators

As a basis for comparison, we first develop optimal representations of the theoretical and data based least squares estimators (7.29) and (7.30). In the present static case with $A = B = 0$, we find from (7.8) that the prediction state estimate is

$$\hat{\tau}_{k|k-1} = 0, \tag{8.7}$$

while (7.9) with $u_k = 0$ gives the current state estimate

$$\hat{\tau}_{k|k} = K_2^{\mathrm{OE}} y_{2,k}, \tag{8.8}$$

i.e. $\hat{W}$ in (8.3) is replaced by $\left(K_2^{\mathrm{OE}}\right)^T$. Assuming that K_2^{OE} is known and that samples are collected at a possibly irregular sampling rate, we can thus reformulate the model (8.6) into the estimator

$$\begin{aligned} \tau_{k+1} &= v_k \\ \hat{\tau}_j &= K_2^{\mathrm{OE}} C_2 \tau_j + K_2^{\mathrm{OE}} w_{2,j} \\ \hat{y}_{1,j} &= C_1 \hat{\tau}_j. \end{aligned} \tag{8.9}$$

Theoretical Kalman filter estimator

With $u = 0$ the theoretical estimator (7.29) is modified into

$$B^{\mathrm{KF}} = \left(C_1 K_2^{\mathrm{OE}}\right)^T = \left(C_2 R_v C_2^T + R_{22}\right)^{-1} C_2 R_v C_1^T, \tag{8.10}$$

where K_2^{OE} is found from (7.24). With $\hat{\tau}$ as regressor instead of y_2, we find from (8.9) and (8.10)

$$B_{\mathrm{T}}^{\mathrm{KF}} = \left(K_2^{\mathrm{OE}} C_2 R_v \left(K_2^{\mathrm{OE}} C_2\right)^T + K_2^{\mathrm{OE}} R_{22} \left(K_2^{\mathrm{OE}}\right)^T\right)^{-1} K_2^{\mathrm{OE}} C_2 R_v C_1^T, \tag{8.11}$$

which with $\hat{y}_{1,j}^T = \hat{\tau}_j^T B_{\mathrm{T}}^{\mathrm{KF}} = y_{2,j}^T \left(K_2^{\mathrm{OE}}\right)^T B_{\mathrm{T}}^{\mathrm{KF}} = y_{2,j}^T B^{\mathrm{KF}}$ results in

$$\begin{aligned} B^{\mathrm{KF}} &= B^{\mathrm{KF+KF}} \\ &= \left(K_2^{\mathrm{OE}}\right)^T \left(K_2^{\mathrm{OE}} C_2 R_v \left(K_2^{\mathrm{OE}} C_2\right)^T + K_2^{\mathrm{OE}} R_{22} \left(K_2^{\mathrm{OE}}\right)^T\right)^{-1} K_2^{\mathrm{OE}} C_2 R_v C_1^T. \end{aligned} \tag{8.12}$$

Remark 14 *We use the B^{KF+KF} notation because the Kalman filtering formalism is used twice, first to find $\hat{\tau}$ according to (8.8) and then to find the estimator.*

We thus find two alternative expressions for B^{KF}, and we will find (8.12) to be more in line with the data based estimators (8.5) above and (8.14) below. The expression (8.12), with K_2^{OE} replaced by $W_{\mathrm{PCA}}^T = P^T$ or W_{PLS}^T, will in the following be used to find asymptotic ($N \to \infty$) PCR and PLSR estimators. However, note that the expression (8.12) in itself is of purely theoretical interest. Based on theoretical matrix values, the inversion involved will be very poorly conditioned.

Data based Kalman filter estimator assuming K_2^{OE} known

With K_2^{OE} assumed known, only C_1 in (8.10) is unknown. We may, however, choose to order the state variables in (8.6) such that $C_1 = \begin{bmatrix} I & 0 \end{bmatrix}$, and a known K_2^{OE} thus implies a completely known estimator B^{KF}. From a theoretical point of view it is still of interest to find the data based estimator when K_2^{OE} is known, and we therefore pursue this a little further. From (8.3) and (8.8) we find

$$\hat{T}_{\mathrm{KF}} = Y_2 \left(K_2^{\mathrm{OE}}\right)^T, \tag{8.13}$$

and the ordinary least squares method thus gives

$$\hat{B}^{\mathrm{KF+LS}} = \left(K_2^{\mathrm{OE}}\right)^T \left(K_2^{\mathrm{OE}} Y_2^T Y_2 \left(K_2^{\mathrm{OE}}\right)^T\right)^{-1} K_2^{\mathrm{OE}} Y_2^T Y_1. \tag{8.14}$$

This is the latent variable estimator (8.5) with $\hat{W} = \left(K_2^{\mathrm{OE}}\right)^T$. Since it is based on an underlying Kalman filter, it is the optimal unbiased estimator with minimized covariance according to (7.37). This is considered to be an interesting result seen from a theoretical point of view, and it is therefore summarized in the following theorem:

Theorem 8.1

Assuming data generated by the latent variable system (8.6), the optimal weighting matrix in the regularized estimator (8.5) is $\hat{W} = \left(K_2^{\mathrm{OE}}\right)^T$, with K_2^{OE} given by (7.24). The resulting estimator (8.14) is the optimal unbiased estimator, with $E\hat{B}^{\mathrm{KF+LS}} = B^{\mathrm{KF}}$ given by (8.10) and the estimation covariance given by (7.37).

Remark 15 *This theoretical connection between the regularized least squares solution and Kalman filtering, is a parallel to the connection between a regularized solution of a convolution integral and Wiener filtering presented by Tikhonov and Arsenin (1977).*

8.2.3 Principal component regression

With principal components as defined in Appendix C, equation (8.13) is replaced by

$$\hat{T}_{\mathrm{PCA}} = Y_2 \hat{P}, \tag{8.15}$$

where $\hat{P}$ is the loading matrix, and where $\hat{T}_{\mathrm{PCA}}^T \hat{T}_{\mathrm{PCA}}$ is diagonal. From this follows

$$\hat{\tau}_j = \hat{P}^T y_{2,j}. \tag{8.16}$$

Theoretical PCR estimator

Assuming P exactly known and with K_2^{OE} replaced by P^T, the theoretical estimator (8.12) is modified into

$$B^{\mathrm{PCR}} = B^{\mathrm{PCA+KF}} = P\left(P^T C_2 R_v C_2^T P + P^T R_{22} P\right)^{-1} P^T C_2 R_v C_1^T. \tag{8.17}$$

Data based PCR estimator

With K_2^{OE} replaced by $\hat{P}^T$, the data based estimator (8.14) is modified into

$$\hat{B}^{\mathrm{PCR}} = \hat{B}^{\mathrm{PCA+LS}} = \hat{P}\left(\hat{P}^T Y_2^T Y_2 \hat{P}\right)^{-1} \hat{P}^T Y_2^T Y_1. \tag{8.18}$$

This is the general estimator (8.5) with $\hat{W} = \hat{W}_{\mathrm{PCR}} = \hat{P}$. As noted above, this is a biased estimator, i.e. $E\hat{B}^{\mathrm{PCR}} \neq B^{\mathrm{KF}}$ given by (8.10).

Also note that (8.6) asymptotically ($N \to \infty$) results in $\frac{1}{N} Y_2^T Y_2 \to C_2 R_v C_2^T + R_{22}$ and $\frac{1}{N} Y_2^T Y_1 \to C_2 R_v C_1^T$, i.e. $\hat{B}^{\mathrm{PCR}} \to B^{\mathrm{PCR}}$ given by (8.17).

Remark 16 *The estimator (8.18) is found by a PCA compression of the Y_2 data into $\hat{T}_{PCA} = Y_2\hat{P}$, followed by a LS solution. We therefore introduce the notation $\hat{B}^{PCR} = \hat{B}^{PCA+LS}$.*

8.2.4 Partial least squares regression - the Martens algorithm

The aim of partial least squares regression (PLSR) is to improve PCR by finding latent variable estimates $\hat{\tau}$ that explain both the Y_2 and the Y_1 data, and there exist at least two slightly different PLSR algorithms (Appendix C). It is convenient to start with the $\mathrm{PLSR_M}$ method of Martens (1987) that makes use of linear combinations

$$\hat{\tau}_{\mathrm{M},k} = \hat{W}_{\mathrm{PLS}}^T y_{2,k}. \tag{8.19}$$

This gives the same solution as in the PCR case above, only that the loading matrix $\hat{P}$ is replaced by $\hat{W}_{\mathrm{PLS}}$. The loading weight matrix $\hat{W}_{\mathrm{PLS}}$ is traditionally found iteratively (Appendix C), but it can also be found directly by QR decomposition of a certain Krylov matrix (Di Ruscio, 1998). The matrix $\hat{T}_{\mathrm{M}}^T \hat{T}_{\mathrm{M}} = \begin{bmatrix} \hat{\tau}_{\mathrm{M},1} & \hat{\tau}_{\mathrm{M},2} & \cdots & \hat{\tau}_{\mathrm{M},N} \end{bmatrix} \begin{bmatrix} \hat{\tau}_{\mathrm{M},1} & \hat{\tau}_{\mathrm{M},2} & \cdots & \hat{\tau}_{\mathrm{M},N} \end{bmatrix}^T$ will in this case be non-diagonal, and the $\mathrm{PLSR_M}$ method of Martens is therefore called non-orthogonal PLSR.

Theoretical PLSR$_M$ estimator

Assuming W_{PLS} exactly known, the result of replacing P with W_{PLS} is that (8.17) is replaced by the theoretical PLSR$_{\text{M}}$ estimator

$$\begin{aligned} B^{\text{PLSR}} &= B^{\text{PLSR+KF}} \\ &= W_{\text{PLS}} \left(W_{\text{PLS}}^T C_2 R_v C_2^T W_{\text{PLS}} + W_{\text{PLS}}^T R_{22} W_{\text{PLS}} \right)^{-1} W_{\text{PLS}}^T C_2 R_v C_1^T. \end{aligned} \tag{8.20}$$

Data based PLSR$_M$ estimator

The data based PCR estimator (8.18) is replaced by the PLSR$_M$ estimator

$$\hat{B}^{\text{PLSR}} = \hat{B}^{\text{PLSR+LS}} = \hat{W}_{\text{PLS}} \left(\hat{W}_{\text{PLS}}^T Y_2^T Y_2 \hat{W}_{\text{PLS}} \right)^{-1} \hat{W}_{\text{PLS}}^T Y_2^T Y_1. \tag{8.21}$$

This is also a biased estimator, i.e. $E\hat{B}^{\text{PLSR}} \neq B^{\text{KF}}$ given by (8.10), and as for the PCR estimator we find that $\hat{B}^{\text{PLSR}} \to B^{\text{PLSR}}$ when $N \to \infty$.

Remark 17 *The estimator (8.21) is found by a PLSR compression of the Y_2 data into $\hat{T}_M = Y_2 \hat{W}_{PLS}$, followed by a LS solution. We therefore introduce the notation $\hat{B}^{PLSR} = \hat{B}^{PLSR+LS}$.*

8.2.5 Partial least squares regression - the Wold algorithm

The PLSR method of Wold et al. (1983) makes use of linear combinations

$$\hat{\tau}_{\text{W},k} = \left(\hat{W}_{\text{PLS}}^T \hat{P}_{\text{W}} \right)^{-1} \hat{W}_{\text{PLS}}^T y_{2,k}, \tag{8.22}$$

with the same $\hat{W}_{\text{PLS}}$ matrix as in the Martens algorithm, and with a special loading matrix $\hat{P}_{\text{W}}$ as defined in Appendix C. The result of this is a diagonal matrix $\hat{T}_{\text{W}}^T \hat{T}_{\text{W}} = \begin{bmatrix} \hat{\tau}_{\text{W},1} & \hat{\tau}_{\text{W},1} & \cdots & \hat{\tau}_{\text{W},N} \end{bmatrix} \begin{bmatrix} \hat{\tau}_{\text{W},1} & \hat{\tau}_{\text{W},2} & \cdots & \hat{\tau}_{\text{W},N} \end{bmatrix}^T$, and the Wold algorithm is therefore called orthogonal PLSR.

Theoretical PLSR$_W$ estimator

It is straightforward to show that a factor $\left(W_{\text{PLS}}^T P_{\text{W}} \right)^{-1}$ or any other invertible factor has no effect on the final estimator, which is therefore identical with (8.20).

Data based PLSR$_W$ estimator

Since the loading weight matrix $\hat{W}_{\text{PLS}}$ is the same as in the Martens algorithm, the data based PLSR$_{\text{W}}$ estimator will be identical to the estimator (8.21) above.

8.2.6 Discussion

Equivalence of the Wold and Martens algorithms

The equivalence of the Wold and Martens algorithms in the sense that they use the same weighting matrix W_{PLS} is of course well known (e.g. Martens and Næs, 1989), although the present treatment by use of Kalman filtering formalism appears to be new.

The regularized LS solution

The general regularized estimator (8.5) can be found in two equivalent though conceptually different ways:

1. Start with the theoretically optimal estimator $\hat{B}^{\text{KF}}$ according to (8.14), and end up with (8.5) by replacing $\left(K_2^{\text{OE}}\right)^T$ with the weighting matrix $\hat{P}$ or $\hat{W}_{\text{PLS}}$ that may be found from the data. We may thus see $\hat{P}$ and $\hat{W}_{\text{PLS}}$ as approximations of $\left(K_2^{\text{OE}}\right)^T$.

2. Compress the data into $\hat{T}_{\text{PCR}} = Y_2\hat{P}$ or e.g. $\hat{T}_{\text{M}} = Y_2\hat{W}_{\text{PLS}}$. Then find $\hat{B}_{\text{T}}^{\text{PCR}} = \left(\hat{T}_{\text{PCA}}^T\hat{T}_{\text{PCA}}\right)^{-1}\hat{T}_{\text{PCA}}^T Y_1$ or $\hat{B}_{\text{T}}^{\text{PLSR}} = \left(\hat{T}_{\text{M}}^T\hat{T}_{\text{M}}\right)^{-1}\hat{T}_{\text{M}}^T Y_1$ and end up with (8.5) by use of $\hat{B}^{\text{PCA}} = \hat{P}\hat{B}_{\text{T}}^{\text{PCA}}$ or $\hat{B}^{\text{PLSR}} = \hat{W}_{\text{PLS}}\hat{B}_{\text{T}}^{\text{PLSR}}$. This might be seen as a PCA/PLSR+LS solution, and we will return to this concept in Subsection 8.3 below.

Bias

The PCR and PLSR methods are often referred to as biased regression (e.g. Martens and Næs, 1989). Although this is certainly true, it is still important to notice the meaning of bias related to latent variable modeling. The ordinary least squares estimator $\hat{B}^{\text{LS}} = \left(Y_2^T Y_2\right)^{-1} Y_2 Y_1$ is unbiased in the sense that it leads to unbiased estimates of y_1, but the variance tend to be large when the number of observations is limited compared to the number of Y_2 variables. A solution to this problem is to use the regularized estimator (8.5), and with the optimal weighting matrix $\hat{W} = \hat{W}_{\text{KF}} = \left(K_2^{\text{OE}}\right)^T$ as in (8.14) the estimator $\hat{B}_{KF}$ is still unbiased at the same time as the variance is minimized. When K_2^{OE} is replaced by $\hat{W}_{\text{PCR}}^T = \hat{P}^T$ or $\hat{W}_{\text{PLS}}^T$, the resulting estimators will be biased, and that is the price we pay for a reduction of the variance as compared to the LS solution.

8.3 The general case with y_2 independent of u

In the general case, we have known and independent input variables u as well as dependent y_2 variables. With the appropriate prior information available, we may

know that the y_2 measurements are independent of the known inputs u, i.e. that $D_2 = 0$, and the theoretical Kalman filter based y_1 estimate is then from (7.29) found to be

$$\hat{y}_{1,j}^{\mathrm{KF}} = D_1 u_j + C_1 K_2^{\mathrm{OE}} y_{2,j}. \tag{8.23}$$

Assuming that the need for regularization is due to a large number of y_2 variables, we now have the choice between two approaches:

1. We may use a standard PCR or PLSR algorithm (Appendix C) with both u and y_2 data included in the X matrix, i.e. $X = \begin{bmatrix} U & Y_2 \end{bmatrix}$. In that way we find both $\hat{D}_1$ and $\widehat{C_1 K_2^{\mathrm{OE}}}$ as parts of the regularized solution.

2. With a limited total number of y_2 PCA or PLSR components and known input variables, i.e. $a_2 + \dim(u) << N$, the PCR and PLSR regularization methods can be applied to the y_2 variables separately, while $\hat{D}_1$ is found by a LS solution. Since this will give a better estimate of D_1, it is reasonable to expect better results with this approach (see Example 8.2 and 8.3 in Section 8.5 below for simulation results).

8.3.1 Kalman filter based estimators

As a basis for comparison, we also now develop optimal representations of the least squares estimators (7.29) and (7.30).

Theoretical Kalman filter estimator

With $\hat{\tau} = K_2^{\mathrm{OE}} y_2$ as regressor instead of y_2 and with $D_2 = 0$, and using $B_{1,T}^{\mathrm{KF}}$ from (8.11), the theoretical estimator (7.29) is modified into

$$\begin{aligned} \begin{bmatrix} B_{1,\mathrm{T}}^{\mathrm{KF}} \\ B_{2,\mathrm{T}}^{\mathrm{KF}} \end{bmatrix} &= \begin{bmatrix} B_{1,\mathrm{T}}^{\mathrm{KF+KF}} \\ B_{2,\mathrm{T}}^{\mathrm{KF+KF}} \end{bmatrix} \\ &= \begin{bmatrix} D_1^T \\ \left(K_2^{\mathrm{OE}} C_2 R_v \left(K_2^{\mathrm{OE}} C_2\right)^T + K_2 R_{22} \left(K_2^{\mathrm{OE}}\right)^T\right)^{-1} K_2^{\mathrm{OE}} C_2 R_v C_1^T \end{bmatrix}. \end{aligned} \tag{8.24}$$

Since

$$\begin{aligned} \hat{y}_{1,j}^T &= \begin{bmatrix} u_j^T & \hat{\tau}_j^T \end{bmatrix} \begin{bmatrix} B_{1,\mathrm{T}}^{\mathrm{KF}} \\ B_{2,\mathrm{T}}^{\mathrm{KF}} \end{bmatrix} \\ &= \begin{bmatrix} u_j^T & y_{2,j}^T \end{bmatrix} \begin{bmatrix} B_{1,\mathrm{T}}^{\mathrm{KF}} \\ \left(K_2^{\mathrm{OE}}\right)^T B_{2,\mathrm{T}}^{\mathrm{KF}} \end{bmatrix} = \begin{bmatrix} u_j^T & y_{2,j}^T \end{bmatrix} \begin{bmatrix} B_1^{\mathrm{KF}} \\ B_2^{\mathrm{KF}} \end{bmatrix}, \end{aligned} \tag{8.25}$$

this results in

$$\begin{bmatrix} B_1^{\mathrm{KF}} \\ B_2^{\mathrm{KF}} \end{bmatrix} = \begin{bmatrix} B_1^{\mathrm{KF+KF}} \\ B_2^{\mathrm{KF+KF}} \end{bmatrix} \tag{8.26}$$
$$= \begin{bmatrix} D_1^T \\ (K_2^{\mathrm{OE}})^T \left(\begin{array}{c} K_2^{\mathrm{OE}} C_2 R_v \left(K_2^{\mathrm{OE}} C_2\right)^T \\ +K_2^{\mathrm{OE}} R_{22} \left(K_2^{\mathrm{OE}}\right)^T \end{array} \right)^{-1} K_2^{\mathrm{OE}} C_2 R_v C_1^T \end{bmatrix}.$$

Just as for (8.12) in relation to (8.10), this can be simplified to

$$\begin{bmatrix} B_1^{\mathrm{KF}} \\ B_2^{\mathrm{KF}} \end{bmatrix} = \begin{bmatrix} D_1^T \\ (C_1 K_2^{\mathrm{OE}})^T \end{bmatrix}. \tag{8.27}$$

We will, however, need (8.26) as it is in the development below.

Data based Kalman filter estimator

Defining $\hat{T}_{\mathrm{KF}} = \begin{bmatrix} \hat{\tau}_1 & \hat{\tau}_2 & \cdots & \hat{\tau}_N \end{bmatrix}^T$ we find from (8.8)

$$\hat{T}_{\mathrm{KF}} = Y_2 \left(K_2^{\mathrm{OE}}\right)^T, \tag{8.28}$$

and the ordinary least squares method assuming K_2^{OE} known thus gives

$$\begin{bmatrix} \hat{B}_{1,\mathrm{T}}^{\mathrm{KF}} \\ \hat{B}_{2,\mathrm{T}}^{\mathrm{KF}} \end{bmatrix} = \begin{bmatrix} U^T U & U^T \hat{T}_{\mathrm{KF}} \\ \hat{T}_{\mathrm{KF}}^T U & \hat{T}_{\mathrm{KF}}^T \hat{T}_{\mathrm{KF}} \end{bmatrix}^{-1} \begin{bmatrix} U^T \\ \hat{T}_{\mathrm{KF}}^T \end{bmatrix} Y_1 \tag{8.29}$$
$$= \begin{bmatrix} U^T U & U^T Y_2 \left(K_2^{\mathrm{OE}}\right)^T \\ K_2^{\mathrm{OE}} Y_2^T U & K_2^{\mathrm{OE}} Y_2^T Y_2 \left(K_2^{\mathrm{OE}}\right)^T \end{bmatrix}^{-1} \begin{bmatrix} U^T \\ K_2^{\mathrm{OE}} Y_2^T \end{bmatrix} Y_1.$$

From the relation between $B_{\mathrm{T}}^{\mathrm{KF}}$ and B^{KF} in (8.25), we find the unbiased estimator

$$\begin{bmatrix} \hat{B}_1^{\mathrm{KF}} \\ \hat{B}_2^{\mathrm{KF}} \end{bmatrix} = \begin{bmatrix} \hat{B}_{1,\mathrm{T}}^{\mathrm{KF}} \\ \left(K_2^{\mathrm{OE}}\right)^T \hat{B}_{2,\mathrm{T}}^{\mathrm{KF}} \end{bmatrix}. \tag{8.30}$$

Since it is based on an underlying Kalman filter, this is the optimal unbiased estimator. Note, however, that we cannot find K_2^{OE} from the data, and we use (8.30) only as a starting point for the development of PCR and PLSR solutions below.

8.3.2 Principal component regression

Theoretical PCA+KF estimator

With principal components as defined in Appendix C, the Kalman gain K_2^{OE} is replaced by P^T defined by (8.15) (although assumed exactly known). The theoretical estimator (8.26) is thus replaced by

$$B^{\mathrm{PCA+KF}} = \begin{bmatrix} B_1^{\mathrm{PCA+KF}} \\ B_2^{\mathrm{PCA+KF}} \end{bmatrix} = \begin{bmatrix} D_1^T \\ P\left(P^T C_2 R_v C_2^T P + P^T R_{22} P\right)^{-1} P^T C_2 R_v C_1^T \end{bmatrix}. \tag{8.31}$$

A two-step PCA+LS solution

Ordinary PCR is a two-step PCA+LS method (Appendix C), but then with all data used in the first step. We will now introduce a method which uses only part of the data in the first PCA step, and includes the rest in the LS step. First find

$$\hat{T}_{1,\mathrm{PCA}} = Y_2 \hat{P}_1, \tag{8.32}$$

i.e.

$$\hat{\tau}_{1,j}^T = y_{2,j}^T \hat{P}_1, \tag{8.33}$$

with $\dim(\hat{P}_1) = m \times a_2$, where m is the number of y_2 measurements and a_2 the number of y_2 components used. Assuming a limited total number of components and known variables u, i.e. $a_2 + \dim(u) << N$, we may include the U data first in the second step and use the LS solution

$$\hat{B}^{\mathrm{PCA+LS}} = \begin{bmatrix} \hat{B}_{1,\mathrm{T}}^{\mathrm{PCA+LS}} \\ \hat{P}_1 \hat{B}_{2,\mathrm{T}}^{\mathrm{PCA+LS}} \end{bmatrix}, \tag{8.34}$$

where

$$\begin{bmatrix} \hat{B}_{1,\mathrm{T}}^{\mathrm{PCA+LS}} \\ \hat{B}_{2,\mathrm{T}}^{\mathrm{PCA+LS}} \end{bmatrix} = \left(\begin{bmatrix} U^T \\ \hat{T}_{1,\mathrm{PCA}}^T \end{bmatrix} \begin{bmatrix} U & \hat{T}_{1,\mathrm{PCA}} \end{bmatrix} \right)^{-1} \begin{bmatrix} U^T \\ \hat{T}_{1,\mathrm{PCA}}^T \end{bmatrix} Y_1. \tag{8.35}$$

This is (8.30) and (8.29) with K_2^{OE} replaced by $\hat{P}_1^T$, and a comparison with (8.31) shows that $\hat{B}_{1,T}^{\mathrm{PCA+LS}} = \hat{D}_1^T$.

Note that we asymptotically ($N \to \infty$) with $D_2 = 0$ in (7.22) obtain $\frac{1}{N} U^T U \to R_u$, $\frac{1}{N} U^T Y_2 \to 0$, $\frac{1}{N} Y_2^T Y_2 \to C_2 R_v C_2^T + R_{22}$, $\frac{1}{N} U^T Y_1 \to R_u D_1$ and $\frac{1}{N} Y_2^T Y_1 \to C_2 R_v C_1^T$. Insertion of this in (8.35) results in $\hat{B}^{\mathrm{PCA+LS}} \to B^{\mathrm{PCA+KF}}$ given by (8.31).

A two-step PCA+PCR solution

With a large total number of components and known variables, the LS solution (8.35) will give large variance due to overfitting, and assuming collinear u variables the second step above may be replaced by the PCR solution

$$\hat{B}^{\text{PCA+PCR}} = \begin{bmatrix} \hat{B}_{1,\text{T}}^{\text{PCA+PCR}} \\ \hat{P}_1 \hat{B}_{2,\text{T}}^{\text{PCA+PCR}} \end{bmatrix}, \tag{8.36}$$

where

$$\begin{bmatrix} \hat{B}_{1,\text{T}}^{\text{PCA+PCR}} \\ \hat{B}_{2,\text{T}}^{\text{PCA+PCR}} \end{bmatrix} = P_2 \left[P_2^T \begin{bmatrix} U^T \\ \hat{T}_{1,\text{PCA}}^T \end{bmatrix} \begin{bmatrix} U & \hat{T}_{1,\text{PCA}} \end{bmatrix} P_2 \right]^{-1} P_2^T \begin{bmatrix} U^T \\ \hat{T}_{1,\text{PCA}}^T \end{bmatrix} Y_1, \tag{8.37}$$

with $\hat{P}_2 = \begin{bmatrix} \hat{P}_{21}^T & \hat{P}_{22}^T \end{bmatrix}^T$ defined by

$$\begin{bmatrix} U & \hat{T}_{1,\text{PCA}} \end{bmatrix} \begin{bmatrix} \hat{P}_{21} \\ \hat{P}_{22} \end{bmatrix} = \hat{T}_{2,\text{PCA}}. \tag{8.38}$$

With the number of components used in the second step $a = a_2 + \dim(u)$, where a_2 is the number of components in y_2 from the first step, the PCA+PCR =PCA+PCA+LS method will give the same result as the PCA+LS method above. The reason for this is that the second step uses all available variables, i.e. there is no data compression in the second PCA step.

A one-step PCR solution

The result of an ordinary PCR as compared with the two-step methods above, will depend on the number of u variables and the scaling of the u and y_2 variables. With a small number of u variables, the result must be expected to be poorer than with the PCA+LS solution above. The reason for this is that $\hat{D}_1$ is determined after an unnecessary regularization (see Example 8.2 and 8.3 in Section 8.5 below).

8.3.3 Partial least squares regression

Theoretical PLSR+KF estimator

With loading weights as defined in Appendix C, the Kalman gain K_2^{OE} is replaced by W_{PLS}^T. The theoretical estimator (8.26) is thus replaced by

$$\begin{bmatrix} B_1^{\text{PLSR+KF}} \\ B_2^{\text{PLSR+KF}} \end{bmatrix} = \begin{bmatrix} D_1^T \\ W_{\text{PLS}} \begin{pmatrix} W_{\text{PLS}}^T C_2 R_v C_2^T W_{\text{PLS}} \\ + W_{\text{PLS}}^T R_{22} W_{\text{PLS}} \end{pmatrix}^{-1} W_{\text{PLS}}^T C_2 R_v C_1^T \end{bmatrix}. \tag{8.39}$$

A two-step PLSR+LS solution

We may find also a PLSR solution in two steps. First use the response variables Y_1 and find

$$\hat{T}_{1,\text{PLS}} = Y_2 \hat{W}_1, \tag{8.40}$$

i.e.

$$\hat{\tau}_{1,j}^T = y_{2,j}^T \hat{W}_1, \tag{8.41}$$

with $\dim \hat{W}_1 = m \times a_2$, where m is the number of y_2 measurements and a_2 the number of y_2 components used. Assuming a limited total number of components and known variables u, i.e. $a_2 + \dim(u) << N$, we may in the second step use the LS solution

$$\hat{B}^{\text{PLSR+LS}} = \begin{bmatrix} \hat{B}_{1,\text{T}}^{\text{PLSR+LS}} \\ \hat{W}_1 \hat{B}_{2,\text{T}}^{\text{PLSR+LS}} \end{bmatrix}, \tag{8.42}$$

where

$$\begin{bmatrix} \hat{B}_{1,\text{T}}^{\text{PLSR+LS}} \\ \hat{B}_{2,\text{T}}^{\text{PLSR+LS}} \end{bmatrix} = \left(\begin{bmatrix} U^T \\ \hat{T}_{1,\text{PLS}}^T \end{bmatrix} \begin{bmatrix} U & \hat{T}_{1,\text{PLS}} \end{bmatrix} \right)^{-1} \begin{bmatrix} U^T \\ \hat{T}_{1,\text{PLS}}^T \end{bmatrix} Y_1. \tag{8.43}$$

A comparison with (8.39) shows that $\hat{B}_{1,\text{T}}^{\text{PLSR+LS}} = \hat{D}_1^T$.

Note that $N \to \infty$ results in $\hat{B}^{\text{PLSR+LS}} \to B^{\text{PLSR+KF}}$ given by (8.39), just as $\hat{B}^{\text{PCA+LS}} \to B^{\text{PCA+KF}}$.

A two-step PLSR+PLSR solution

With a large total number of components and known variables and assuming collinear u variables, the second step above may be replaced by the PLSR solution

$$\hat{B}^{\text{PLSR+PLSR}} = \begin{bmatrix} \hat{B}_{1,\text{T}}^{\text{PLSR+PLSR}} \\ \hat{W}_1 \hat{B}_{2,\text{T}}^{\text{PLSR+PLSR}} \end{bmatrix}, \tag{8.44}$$

where

$$\begin{bmatrix} \hat{B}_{1,T}^{\text{PLSR+PLSR}} \\ \hat{B}_{2,T}^{\text{PLSR+PLSR}} \end{bmatrix} = \hat{W}_2 \left[\hat{W}_2^T \begin{bmatrix} U^T \\ \hat{T}_{1,\text{PLS}}^T \end{bmatrix} \begin{bmatrix} U & \hat{T}_{1,\text{PLS}} \end{bmatrix} \hat{W}_2 \right]^{-1} \hat{W}_2^T \begin{bmatrix} U^T \\ \hat{T}_{1,\text{PLS}}^T \end{bmatrix} Y_1, \tag{8.45}$$

with $\hat{W}_2 = \begin{bmatrix} \hat{W}_{21}^T & \hat{W}_{22}^T \end{bmatrix}^T$ defined by

$$\begin{bmatrix} U & \hat{T}_{1,\text{PLS}} \end{bmatrix} \begin{bmatrix} \hat{W}_{21} \\ \hat{W}_{22} \end{bmatrix} = \hat{T}_{2,\text{PLS}}. \tag{8.46}$$

With the number of components used in the second step $a = a_2 + \dim(u)$, where a_2 is the number of components in y_2 from the first step, the PLSR+PLSR

method will give the same result as the PLSR+LS method above. The reason is the same as for the two-step PCA+PCR method, i.e. there is no data compression in the second step.

A one-step PLSR solution

As for an ordinary PCR, the result of an ordinary PLSR as compared with the two-step methods above, will depend on the number of u variables and the scaling of the u and y_2 variables. With a small number of u variables, the result must also here be expected to be poorer than with the PLSR+LS solution above (since $\hat{D}_1$ is determined after an unnecessary regularization).

8.4 The general case with correlated u and y_2 data

With the appropriate prior knowledge we may know that y_2 and u are correlated (see Example 8.2), and without prior knowledge we must assume that they may be correlated. The model (8.6) is then modified into

$$\begin{aligned} \tau_{k+1} &= v_k \\ y_{1,j} &= C_1\tau_j + D_1u_j + w_{1,j} \\ y_{2,j} &= C_2\tau_j + D_2u_j + w_{2,j}. \end{aligned} \tag{8.47}$$

8.4.1 Kalman filter based estimators

With a known model, the optimal current state estimate would in this case be

$$\hat{\tau}_j = K_2^{\mathrm{OE}}\,(y_{2,j} - D_2u_j) = \begin{bmatrix} -K_2^{\mathrm{OE}}D_2 & K_2^{\mathrm{OE}} \end{bmatrix} \begin{bmatrix} u_j \\ y_{2,j} \end{bmatrix}, \tag{8.48}$$

while the optimal y_1 estimate is

$$\hat{y}_{1,j} = (D_1 - C_1K_2^{\mathrm{OE}}D_2)u_j + C_1K_2^{\mathrm{OE}}y_{2,j}. \tag{8.49}$$

8.4.2 Regularized solutions

Assuming that the problem is a large number of y_2 variables, we may also in this case choose between

- a total PCR or PLSR based on $X = \begin{bmatrix} U & Y_2 \end{bmatrix}$
- a PCA or PLSR based on $X = Y_2$, followed by a LS solution.

In the case with $D_2 = 0$ discussed above, we argued that the PCA/PLSR+LS approach must be expected to give the best result assuming $a_2 + \dim(u) << N$. The same argument can be used here. However, the relation to the theoretical Kalman filter solutions is in this case not straightforward, and two approaches may be argued for and used in practice:

1. From (8.48) follows that $\hat{\tau}$ could be found as $\hat{\tau} = \hat{P}_1^T \begin{bmatrix} u^T & y_2^T \end{bmatrix}^T$ or $\hat{\tau} = \hat{W}_{1,\mathrm{PLS}}^T \begin{bmatrix} u^T & y_2^T \end{bmatrix}^T$, i.e. that $\begin{bmatrix} -K_2^{\mathrm{OE}} D_2 & K_2^{\mathrm{OE}} \end{bmatrix}$ could be approximated by $\hat{P}_1^T$ or $\hat{W}_{1,\mathrm{PLS}}^T$. This means that the first PCA/PLSR step could be based on $X = \begin{bmatrix} U & Y_2 \end{bmatrix}$, while D_1 and e.g. $C_1 \begin{bmatrix} -K_2^{\mathrm{OE}} D_2 & K_2^{\mathrm{OE}} \end{bmatrix} \hat{W}_{1,\mathrm{PLS}}$ would remain to be estimated in the second LS step (where we may choose $C_1 = \begin{bmatrix} I & 0 \end{bmatrix}$).

2. From (8.49) follows that the problem could be solved by a compression of only the y_2 data, leaving $D_1 - C_1 K_2^{\mathrm{OE}} D_2$ and e.g. $C_1 K_2^{\mathrm{OE}} \hat{W}_{2,\mathrm{PLS}}$ to be found in the second LS step (where we may choose $C_1 = \begin{bmatrix} I & 0 \end{bmatrix}$).

Since the LS step asymptotically will give the optimal estimator given the result from the first step, and assuming a sufficient number of observations, the two approaches must be expected to give very similar results, provided the assumptions given. This is confirmed by the simulations in Example 8.3, although a more thorough analysis and more practical testing are needed before final conclusions can be drawn.

8.5 Simulation examples

Example 8.1

Tests on the pure dependent regressor ($D_1 = D_2 = 0$) system (8.6) were performed in $M = 100$ Monte Carlo simulations with model order $n = 3$. Each element in the R_v matrix was a uniformly distributed random number in the interval $(0, 1)$. C_1 was a 1×3 matrix while C_2 was a 100×3 matrix, both with elements as normal random variables with variance 1. The primary output measurement noise was normal with variance $r_{11} = 0.0001$, while the secondary output measurement noise was normal with R_{22} as a diagonal matrix with uniformly distributed random parameters in the interval $(0, 0.01)$.

Validation RMSE values using independent data sets were determined for the following cases:

- Theoretical RMSE according to (7.37).
- Theoretical Kalman filter based estimator $B^{\mathrm{KF}} = \left(C_1 K_2^{\mathrm{OE}}\right)^T$ according to (8.10).
- Data based Kalman filter based estimator $\hat{B}^{\mathrm{KF+LS}} = \left(K_2^{\mathrm{OE}}\right)^T \left(K_2^{\mathrm{OE}} Y_2^T Y_2 \left(K_2^{\mathrm{OE}}\right)^T\right)^{-1} K_2^{\mathrm{OE}} Y_2^T Y_1$ according to (8.14).
- Ordinary LS estimator $\hat{B}^{\mathrm{LS}} = \left(Y_2^T Y_2\right)^{-1} Y_2^T Y_1$.
- PCR estimator $\hat{B}^{\mathrm{PCR}} = \hat{P}\left(\hat{P}^T Y_2^T Y_2 \hat{P}\right)^{-1} \hat{P}^T Y_2^T Y_1$ according to (8.18).
- PLSR estimator $\hat{B}^{\mathrm{PLSR}} = \hat{W}_{\mathrm{PLS}} \left(\hat{W}_{\mathrm{PLS}}^T Y_2^T Y_2 \hat{W}_{\mathrm{PLS}}\right)^{-1} \hat{W}_{\mathrm{PLS}}^T Y_2^T Y_1$ according to (8.21).

For different numbers of observations the results were as given in Table 8.1.

Table 8.1: Validation RMSE values for different estimators and different number of samples N, based on $M = 100$ Monte Carlo simulations.

	$N = 5$	$N = 10$	$N = 100$	$N = 1000$
Theoretical	116	103	118	115
B^{KF}	124	120	128	125
$\hat{B}^{\mathrm{KF}}$	206	145	126	125
$\hat{B}^{\mathrm{LS}}$	708	482	4198	132
$\hat{B}^{\mathrm{PCR}}$	334	194	153	154
$\hat{B}^{\mathrm{PLSR}}$	331	194	153	153

We see from this that

- the B^{KF} results are close to the theoretical value also for very few observations
- the $\hat{B}^{\mathrm{KF+LS}}$ results are poorer than the PCR and PLSR results for $N = 5$ but otherwise better, and they are approaching the theoretical result for $N \to \infty$
- The $\hat{B}^{\mathrm{LS}}$ results show large variance for few observations, and approach the theoretical result for $N \to \infty$
- PCR and PLSR give better results than LS for few observations, and poorer results for many observations

- PCR and PLSR give very similar results, which is as expected with the randomly generated data used.

These results are all in line with the theory discussed.

Example 8.2

Assume the same system as in Example 7.2, but with two modifications such that the y_2 measurement

- are moved to the disturbance stream with unknown concentrations
- has $p = 100$ variables (e.g. spectrum frequencies).

The system is shown in Fig. 8.1.

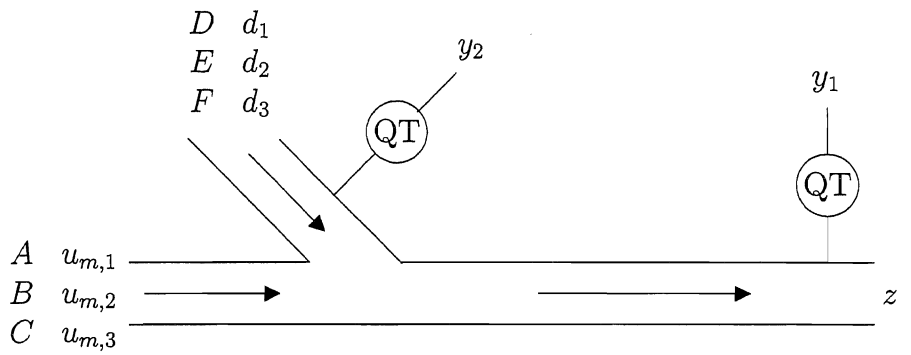

Figure 8.1 Main process stream with known concentrations u and disturbance stream with unknown concentrations d, a concentration dependent primary property z, primary property measurement y_1 and a secondary multivariate measurement y_2 in the disturbance stream.

The mean validation RMSE results and standard deviations from $M = 100$ Monte Carlo runs were determined using the data based least squares estimator (7.30), and the various regularized estimators developed in the present chapter. In the first step in the PCA+LS, PLSR+LS, PCA+PCR and PLSR+PLSR methods, only Y_2 data was used, with the number of components $a_2 = 3$, which was easily found from the eigenvalues of the $Y_2^T Y_2$ data matrix (for a typical simulation with $N = 100$ observations, these were in descending order $\lambda_i = 4906$, 521, 304, 2, 2, 2, 2, $\cdots$). In the second step, and in the one-step PCR and PLSR methods the number of components were $a = 6$. The validation RMSE results for the different methods at different numbers of observations are shown in Table 8.2.

Table 8.2: Validation RMSE mean values and standard deviations for the system in Fig. 8.1 for different number of samples and different methods. The results are based on $M = 100$ Monte Carlo runs, and the RMSE values are multiplied by 10^4.

Method	$N = 50$	$N = 100$	$N = 1000$
LS estimator (7.30)	719 ± 323	1175 ± 660	135 ± 17
PCA+LS estimator (8.34)	167 ± 34	164 ± 32	159 ± 26
PLSR+LS estimator (8.42)	261 ± 216	204 ± 104	162 ± 27
PCA+PCR estimator (8.36)	167 ± 34	164 ± 32	159 ± 26
PLSR+PLSR estimator (8.44)	261 ± 216	204 ± 104	162 ± 27
One-step PCR estimator	365 ± 180	259 ± 150	182 ± 88
One-step PLSR estimator	319 ± 123	226 ± 77	163 ± 27

From Table 8.2 we see the following:

- The LS method gives very poor results for $N = 50$ and $N = 100$, which is as expected since 103 estimator parameters are to be determined.
- The one-step PCR and PLSR methods give far better results for $N = 50$ and $N = 100$, but show less improvement for an increased number of samples.
- The two-step methods are clearly better than the one-step methods, which is as expected since $a_2 + \dim(u) = 6 << N$.
- The PCA+LS and PCA+PCR methods give the same results, and the so do the PLSR+LS and PLSR+PLSR methods. The reason for this is that no data compression is performed in the second step.
- With a small number of samples, the PCA+LS estimator is significantly better than the PLSR+LS estimator. The reason is that the first PLSR step involves Y_1 data, which also depends on the U data.

■

Example 8.3

The system in Example 8.2 was modified such that the multivariate y_2 measurement was applied to the total process stream at the outlet (see Fig. 8.2).

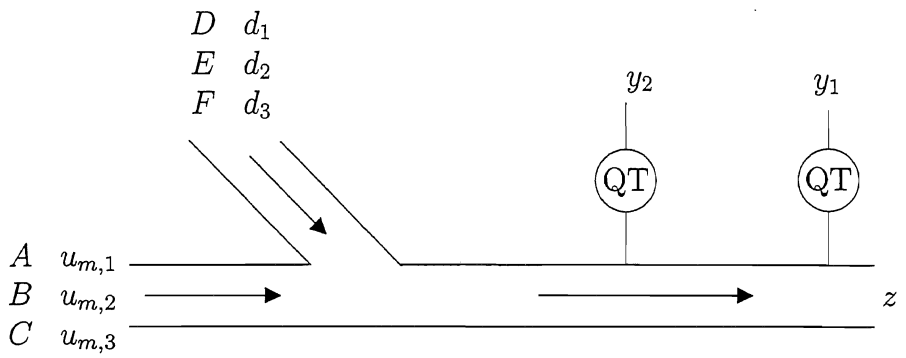

Figure 8.2 Main process stream with known concentrations u and disturbance stream with unknown concentrations d, a concentration dependent primary property z, primary property measurement y_1 and a secondary multivariate measurement y_2 in the mixed stream.

The mean validation RMSE results and standard deviations from $M = 100$ Monte Carlo runs were determined using the data based least squares estimator (7.30), and the various regularized estimators. For the first step in the PCA+LS, PLSR+LS, PCA+PCR and PLSR+PLSR methods, only Y_2 data was used. The number of components used in the two-step methods as well as in the ordinary PCR and PLSR algorithms were $a_2 = 6$, which was easily found from the eigenvalues of the $Y_2^T Y_2$ data matrix (for a typical simulation with $N = 100$ observations, these were in descending order λ_i = 8780, 997, 819, 451, 212, 18, 2, 2, 2, 2, $\cdots\cdots$) and the $\begin{bmatrix} U & Y_2 \end{bmatrix}^T \begin{bmatrix} U & Y_2 \end{bmatrix}$ data matrix (typically λ_i = 8742, 916, 786, 423, 192, 17, 2, 2, 2, 2, $\cdots\cdots$). The validation RMSE results for different numbers of observations and different methods are given in Table 8.3.

Table 8.3: Validation RMSE mean values and standard deviations for the system in Fig. 8.2 for different number of samples and different methods. The results are based on $M = 100$ Monte Carlo runs, and the RMSE values are multiplied by 10^4.

Method	$N = 50$	$N = 100$	$N = 1000$
LS estimator (7.30)	810 ± 303	1268 ± 992	133 ± 19
PCA+LS estimator	170 ± 36	168 ± 28	156 ± 29
PLSR+LS estimator	177 ± 39	173 ± 28	156 ± 28
PCA+PCR estimator	205 ± 37	201 ± 27	194 ± 30
PLSR+PLSR estimator	207 ± 38	202 ± 28	194 ± 30
One-step PCR estimator	205 ± 37	201 ± 27	194 ± 30
One-step PLSR estimator	204 ± 36	201 ± 27	193 ± 29

From the table we see the following:

- As in Table 8.2, the LS method gives very poor results for $N = 50$ and $N = 100$.
- The PCR and PLSR methods give far better results for $N = 50$ and $N = 100$, but show little improvement for an increased number of samples.
- There are no obvious differences between the one-step PCR and PLSR methods, which is as expected with the data used, and the two-step PCA+PCR and PLSR+PLSR methods give very similar results.
- The two-step PCA+LS and PLSR+LS methods give clearly improved results, which is as expected since $a_2 + \dim(u) = 9 << N$. The PCA+LS estimator is somewhat better than the PLSR+LS estimator.

When the number of components used in the second step of the PCA+PCR and PLSR+PLSR methods was increased to $a = 9$, the same results as for the PCA+LS and PLSR+LS were obtained. The reason for this is the same as in Example 8.2, i.e. that no data compression is then performed in the second step. ■

Example 8.4

Example 8.3 was repeated, but now with the parameters in the diagonal R_{22} covariance matrix as uniformly distributed random numbers in the interval $(0, 1)$ instead of $(0, 0.01)$, i.e. a significant increase in the y_2 measurements noise values. It was still relatively simple to decide on $a_2 = 6$ components (typical values for the $Y_2^T Y_2$ eigenvalues were [770,73,60,49,37,18,12,12,11,11, ...] 10^4). The results are given in Table 8.4, showing very much the same type of differences as in Table 8.3 (for $N = 1000$ the three estimators involving PLSR are somewhat better than the

corresponding PCA/PCR estimators, but then the pure LS estimator is anyhow the best).

Table 8.4: Validation RMSE mean values and standard deviations for the system in Fig. 8.2 for different number of samples and different methods. The y_2 measurement noise variances has increased 100 times compared with Example 8.3. The results are based on $M = 100$ Monte Carlo runs, and the RMSE values are multiplied by 10^4.

Method	$N = 50$	$N = 100$	$N = 1000$
LS estimator (7.30)	7490 ± 2934	7981 ± 5405	780 ± 279
PCA+LS estimator	1558 ± 531	1229 ± 418	1179 ± 378
PLSR+LS estimator	1944 ± 509	1424 ± 404	1091 ± 331
PCA+PCR estimator	2182 ± 582	1824 ± 499	1638 ± 352
PLSR+PLSR estimator	2039 ± 485	1607 ± 380	1214 ± 286
One-step PCR estimator	2175 ± 580	1808 ± 483	1625 ± 338
One-step PLSR estimator	1995 ± 476	1616 ± 388	1266 ± 282

As shown in Fig. 8.3, the estimators were still reasonably good, also with the very considerable noise on the secondary measurements.

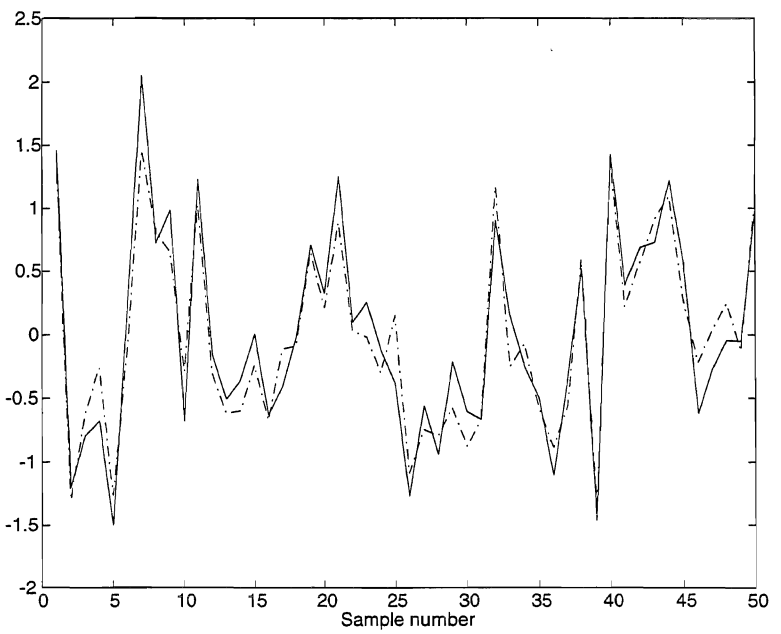

Figure 8.3 Validation response for PCA+LS estimator based on $N = 50$ samples and $p = 100$ very noise corrupted y_2 measurements. The ideal validation response is shown by solid line, while the estimator response is dash-dotted.

■

Example 8.5

Example 8.3 was repeated, but now with both U and Y_2 data used in the first step in the PCA+LS, PLSR+LS, PCA+PCR and PLSR+PLSR methods. For the PCA+LS method, the mean difference in RMSE value using only Y_2 and both U and Y_2 data and based on $M = 100$ Monte Carlo runs was $6 \cdot 10^{-8}$, while the corresponding difference for the PLSR+LS method was $7 \cdot 10^{-5}$. These differences are negligible.

■

Example 8.6

Example 8.2 was also repeated without known input variables, i.e. with $D_1 = D_2 = 0$, and the number of components $a_2 = 3$. The results are given in Table 8.5.

Table 8.5: Validation RMSE mean values and standard deviations for the system in Fig. 8.2 without known inputs, and for different number of samples and different methods. The RMSE values are multiplied by 10^4.

Method	$N = 50$	$N = 100$	$N = 1000$
LS estimator (7.30)	630 ± 41	4228 ± 9376	136 ± 19
PCA+LS estimator	160 ± 32	153 ± 25	162 ± 26
PLSR+LS estimator	160 ± 31	153 ± 25	162 ± 26
PCA+PCR estimator	160 ± 32	153 ± 25	162 ± 26
PLSR+PLSR estimator	160 ± 31	153 ± 25	162 ± 26
One-step PCR estimator	160 ± 32	153 ± 25	162 ± 26
One-step PLSR estimator	160 ± 31	153 ± 25	162 ± 26

Note that without known u_k inputs there are no D_1 parameters to estimate in the second step of the two-step methods, and given N the results are therefore the same for all the regularized estimators.

■

Chapter 9

Dynamical latent variables methods

The optimal OE estimators discussed in Chapter 2, 3 and 6 may be combined with the latent variable regression methods discussed in Chapter 8, resulting in PCA+OE and PLSR+OE methods. This is of special interest in the low primary output sampling rate case discussed in Chapter 6, where we often have a very limited number of primary output observations. It is then especially important to use a parsimonious model with a minimum of unknown parameters, and methods utilizing a small number of estimated latent variables instead of a high number of secondary measurements may then be helpful. Dynamical latent variables solutions are also of interest in chemometrical frequency spectrum applications with response variables as time series.

9.1 Introduction

Many industrial plants have a considerable number of secondary y_2 measurements available as a basis for primary output estimates. At the same time the dynamic models found by system identification tend to be of a low order, which implies that the y_2 measurements are more or less collinear. In addition to that, and due to the experimental cost, the data series will often be fairly short. This situation calls for some form of regularization, and it is therefore natural to study the use of the multivariate calibration PCA, PCR and PLSR methods also in the dynamical case.

Special cases occur in chemometrical frequency spectrum applications, where the calibration of the spectrum against the response variables may be done in a static environment, although the response variables to be predicted actually form time series. In such cases an altogether dynamical calibration may be advanta-

geous, and ARMAX as well as OE models may be appropriate, dependent on the data structure.

9.2 Discussion

9.2.1 FIR models

Some authors have discussed the use of PCR and PLSR in order to determine finite impulse response (FIR) models for dynamic systems. Ricker (1988) discussed identification of FIR models using PLSR and singular value decomposition (SVD), and applied this to an anaerobic wastewater treatment plant. Wise and Ricker (1992) discussed identification of FIR models by use of PCR, and looked especially at frequency response properties.

As shown in Chapter 6, a FIR model is a truncated form of an impulse response model, i.e.

$$y_k = \sum_{i=0}^{\infty} h_i u_{k-i} + \eta_k \approx \sum_{i=0}^{L} h_i u_{k-i} + \eta_k, \tag{9.1}$$

where h_i are the Markov parameters, and where the integer L is chosen so that LT is large in comparison with the dominating time constants of the system (the system is assumed to be asymptotically stable, and T is the sampling interval). The noise term η_k is generally a non-white sequence. The corresponding model for primary outputs $y_{1,k}$ with also secondary outputs used as inputs is

$$y_{1,k} \approx \sum_{i=0}^{L} h_i \begin{bmatrix} u_{k-i} \\ y_{2,k-i} \end{bmatrix} + \eta_k. \tag{9.2}$$

Due to both the truncation and the lack of noise modeling, use of FIR models will result in biased primary output estimates, and compression of the u_k and $y_{2,k}$ information into latent variables adds to this bias. However, some bias is not necessarily a serious drawback in a practical case. A more important disadvantage with FIR estimators may be the large number of parameters that often have to be identified.

Finally note that the FIR model (9.2) may be identified also in the low y_1 sampling rate case discussed in Chapter 6, although the problem with a large number of parameters to estimate might then be even more pronounced.

9.2.2 ARX models

Several authors have discussed the use of PCR and PLSR in order to determine ARX (AutoRegressive with eXogenous inputs) models for dynamic systems. Wise (1991) studied the relations between ARX models and PCA based on lagged values of both the system inputs and the system outputs. Qin and McAvoy (1992) used

PLSR in a similar way to find an ARX model for a catalytic reforming system. Wise et al. (1995) compared neural networks, PLSR and a genetic algorithm used for identification of nonlinear FIR and ARX models. Dayal and McGregor (1997) presented a recursive PLSR algorithm, and used it to identify an ARX model used for adaptive control of a simulated stirred-tank reactor. Wikström et al. (1998) used PLSR for time series modeling related to an electrolysis process (they had no known inputs, and were thus identifying an AR model). Harnett et al. (1998) extended the work of Wise (1991) in order to facilitate the development of a predictive model of the overheads condensor and reflux drum system for a distillation column.

ARX models are generally equivalent to LS models applied to lagged input-output data, and due to the lack of noise modeling they will give biased results also without data compression (with all PCR/PLSR components used). In addition we must in the present context consider the fact that an ARX estimator makes use of past y_1 values that are not available as the present problem is formulated in Section 3.1. Just as for the ARMAX estimator (2.76), an ARX estimator would therefore not utilize secondary y_2 information in an optimal way. One obvious effect of this would be that noisy y_2 measurements collinear with y_1 would be effectively ignored when the identification experiment gives low noise y_1 information (compare with Example 2.4).

Finally note that ARX models cannot be identified in the low primary output sampling rate case discussed in Chapter 6.

9.3 Dynamic system PCA+OE solutions

The fact that FIR and ARX least squares solutions are not asymptotically optimal does not mean, of course, that the PCR and PLSR solutions referred to above may not give useful results in some realistic cases with a limited number of observations. In the following we will, however, study latent variables solutions based on the optimal OE estimators presented in Chapter 2, 3 and 6. As mentioned above, though, also ARMAX models using estimated latent variables may be used (see an acoustic chemometry example in Chapter 10).

The most generally useful dynamic system application of the multivariate calibration methods is to use dynamical equivalents to the two-step PCA+LS methods presented in Chapter 8, for example a two-step PCA+OE method. We will then in the first step perform a PCA on the secondary y_2 measurements, just as in the static case. In the second stage we identify the dynamic OE estimator (OEP or OEC) using the estimated latent variables $\hat{\tau}_k$ from the first step as inputs together with the known inputs u_k. Note that this PCA+OE method can be applied also in the low y_1 sampling rate case.

PCA

The principal components of y_2 are found by factorizing the Y_2 matrix as

$$Y_2 = \begin{bmatrix} y_{2,1} & y_{2,2} & \cdots & y_{2,N} \end{bmatrix}^T = T\hat{P}^T + E, \tag{9.3}$$

where E is a matrix of residuals (see Appendix C). Since $\hat{P}^T\hat{P} = I$, the estimated latent variables then become

$$\hat{\tau}_k = \hat{P}^T y_{2,k}. \tag{9.4}$$

The equation for the secondary outputs from the dynamic system is thus altered from

$$y_2 = C_2 x_k + D_2 u_k + w_{2,k}, \tag{9.5}$$

to

$$\hat{\tau}_k = \hat{P}^T C_2 x_k + \hat{P}^T D_2 u_k + \hat{P}^T w_{2,k}. \tag{9.6}$$

Theoretical PCA+OEC estimator

The estimated latent variables may be used directly in e.g. the OEC estimator (2.41), resulting in the primary output estimator

$$\begin{aligned} \hat{y}_{1,k|k} &= C_1 \left(I - K_P^{\mathrm{OE}} \hat{P}^T C_2\right) \left(qI - A + AK_P^{\mathrm{OE}} \hat{P}^T C_2\right)^{-1} \cdot \\ &\quad \left[\left(B - AK_P^{\mathrm{OE}} \hat{P}^T D_2\right) u_k + AK_P^{\mathrm{OE}} \hat{\tau}_k\right] + C_1 K_P^{\mathrm{OE}} (\hat{\tau}_k - \hat{P}^T D_2 u_k) + D_1 u_k, \end{aligned} \tag{9.7}$$

where the Kalman gain is given by appropriately modified versions of (2.35) and (2.36), i.e.

$$K_P^{\mathrm{OE}} = P_P^{\mathrm{OEP}} C_2^T \hat{P} \left(\hat{P}^T C_2 \hat{P}_P^{\mathrm{OEP}} C_2^T \hat{P} + \hat{P}^T R_{22} \hat{P}\right)^{-1}, \tag{9.8}$$

with P_P^{OEP} determined by the algebraic Riccati equation

$$\begin{aligned} P_P^{\mathrm{OEP}} &= AP_P^{\mathrm{OEP}} A^T + GR_v G^T \\ &\quad - AP_P^{\mathrm{OEP}} C_2^T \hat{P} \left(\hat{P}^T C_2 P_P^{\mathrm{OEP}} C_2^T \hat{P} + \hat{P}^T R_{22} \hat{P}\right)^{-1} \hat{P}^T C_2 P_P^{\mathrm{OEP}} A^T. \end{aligned} \tag{9.9}$$

In (9.7) we assume that the total number of estimated latent variables $\hat{\tau}$ and known inputs u is small compared to the number N of observations available (the same assumption as for the PCA+LS method in Chapter 8). With many collinear known inputs from for example measured plant disturbances, we may compress also this information into principal components.

With $u_k = 0$, the estimator (9.7) is simplified to

$$\begin{aligned} \hat{y}_{1,k|k} &= C_1 \left(I - K_P^{\mathrm{OE}} \hat{P}^T C_2\right) \left(qI - A + AK_P^{\mathrm{OE}} \hat{P}^T C_2\right)^{-1} AK_P^{\mathrm{OE}} \hat{\tau}_k \\ &\quad + C_1 K_P^{\mathrm{OE}} \hat{\tau}_k, \end{aligned} \tag{9.10}$$

showing the dynamical relation between the collinear time series $y_{2,k}$ represented by $\hat{\tau}_k$ and the time series $y_{1,k}$.

Data based PCA+OEC estimator

The estimators (9.7) and (9.10) may be identified by specification of an OEC model in a standard prediction error method, as described in Chapter 3, using u_k and $\hat{\tau}_k$ as inputs. In the low primary output sampling rate case, it can also be identified by use of a modified prediction error method as described in Chapter 6.

9.4 Dynamic system PLSR+OE solutions

In cases where there exist a pure static (although normally noise corrupted) relation between the secondary y_2 and the primary y_1 measurements, it is possible to apply a two-step PLSR+OE method (PLSR+OEP or PLSR+OEC).

Consider for example the system

$$\begin{aligned} x_{k+1} &= Ax_k + Bu_k + Gv_k \\ y_{1,k} &= \begin{bmatrix} C_1 & 0 \end{bmatrix} x_k + D_1 u_k + w_{1,k} = C_1 x_{1,k} + D_1 u_k + w_{1,k} \\ y_{2,k} &= \begin{bmatrix} C_2 & 0 \end{bmatrix} x_k + D_2 u_k + w_{2,k}, = C_2 x_{1,k} + D_2 u_k + w_{2,k}, \end{aligned} \tag{9.11}$$

where all state variables in $x_{1,k}$ that directly influences $y_{1,k}$ via C_1, also directly influences $y_{2,k}$ via C_2.

PLSR

The PLSR method with y_1 as response variables and y_2 as collinear regressor variables, will in the first step result in e.g.

$$\hat{\tau}_k = \hat{W}_{\text{PLS}}^T y_{2,k} \tag{9.12}$$

(choosing the Martens algorithm, see Appendix C). This may be done also in the low y_1 sampling rate case, although the quality of the model may be poor with a limited number of y_1 samples.

Theoretical PLSR+OEC estimator

In the second step we use the dynamic estimator (9.7) with the loading matrix $\hat{P}$ replaced by the loading weight matrix $\hat{W}_{\text{PLS}}$, i.e.

$$\begin{aligned} \hat{y}_{1,k|k} &= C_1 \left(I - K_W^{\text{OE}} \hat{W}_{\text{PLS}}^T C_2\right) \left(qI - A + AK_W^{\text{OE}} \hat{W}_{\text{PLS}}^T C_2\right)^{-1} \\ &\quad \times \left[\left(B - AK_W^{\text{OE}} \hat{W}_{\text{PLS}}^T D_2\right) u_k + AK_W^{\text{OE}} \hat{\tau}_k\right] \\ &\quad + C_1 K_W^{\text{OE}} (\hat{\tau}_k - \hat{W}_{\text{PLS}}^T D_2 u_k) + D_1 u_k, \end{aligned} \tag{9.13}$$

with the Kalman gain given by

$$K_W^{\mathrm{OE}} = P_W^{\mathrm{OEP}} C_2^T \hat{W}_{\mathrm{PLS}} \left(\hat{W}_{PLS}^T C_2 P_W^{\mathrm{OEP}} C_2^T \hat{W}_{\mathrm{PLS}} + \hat{W}_{\mathrm{PLS}}^T R_{22} \hat{W}_{\mathrm{PLS}} \right)^{-1}, \quad (9.14)$$

where P_W^{OEP} is determined by the algebraic Riccati equation

$$\begin{aligned} P_W^{\mathrm{OEP}} &= A P_W^{\mathrm{OEP}} A^T + G R_v G^T \quad (9.15) \\ &\quad - A P_W^{\mathrm{OEP}} C_2^T \hat{W}_{\mathrm{PLS}} \left(\begin{array}{c} \hat{W}_{\mathrm{PLS}}^T C_2 P_W^{\mathrm{OEP}} C_2^T \hat{W}_{\mathrm{PLS}} \\ + \hat{W}_{PLS}^T R_{22} \hat{W}_{\mathrm{PLS}} \end{array} \right)^{-1} \hat{W}_{\mathrm{PLS}}^T C_2 P_W^{\mathrm{OEP}} A^T. \end{aligned}$$

Data based PLSR+OEC estimator

The estimator (9.13) may be identified by specifying an OEC model with u_k and $\hat{\tau}_k$ as inputs in a prediction error method. If necessary the known input data may also here be compressed into principal components by use of PCA.

9.5 Combined PCA+PLSR+OE solution

In some cases there may exist a pure static relation between some secondary measurements y_{21} and the primary y_1 measurements, while there is a dynamical relation between other secondary measurements y_{22} and y_1. It is then possible to combine the PCA+OE and PLSR+OE methods above, i.e. the y_{21} data is compressed into $\hat{\tau}_1$ by use of PLSR, while the y_{22} data is compressed into $\hat{\tau}_2$ by use of PCA, and u, $\hat{\tau}_1$ and $\hat{\tau}_2$ are then used as inputs when the OE estimator is identified. We may also use some additional measurements y_{23} as inputs.

9.6 Simulation example

Monte Carlo simulation studies are undertaken by use of the *dlsim.m* function in the Control System Toolbox for use with Matlab (Grace et al., 1992), and the prediction error method implemented in the *pem.m* function in the System Identification Toolbox for use with Matlab (Ljung, 1995). With an appropriate OE model specified, the *pem.m* function identifies the dynamic PCA+OE estimator (9.7) or (9.10), or the dynamic PLSR+OE estimator (9.13), where u_k and the estimated latent variables $\hat{\tau}_k$ are used as input signals.

Example 9.1

For an application of the dynamical PCA+OE and PLSR+OE solutions, three independent filtered white noise sequences were generated. The following continuous-time system consisting of three independent second-order systems was used as a

starting point:

$$\dot{x} = \begin{bmatrix} -1 & 0 & 0 & 1 & 0 & 0 \\ 0 & -1 & 0 & 0 & 1 & 0 \\ 0 & 0 & -1 & 0 & 0 & 1 \\ 0 & 0 & 0 & -1 & 0 & 0 \\ 0 & 0 & 0 & 0 & -1 & 0 \\ 0 & 0 & 0 & 0 & 0 & -1 \end{bmatrix} x + \begin{bmatrix} 0 & 0 & 0 \\ 0 & 0 & 0 \\ 0 & 0 & 0 \\ 1 & 0 & 0 \\ 0 & 1 & 0 \\ 0 & 0 & 1 \end{bmatrix} v \qquad (9.16)$$

$$y_1 = \begin{bmatrix} 1 & 1 & 1 & 0 & 0 & 0 \end{bmatrix} x + w_1$$

$$y_2 = \begin{bmatrix} C_{21} & 0 \end{bmatrix} x + w_2.$$

The system is shown in Fig. 9.1.

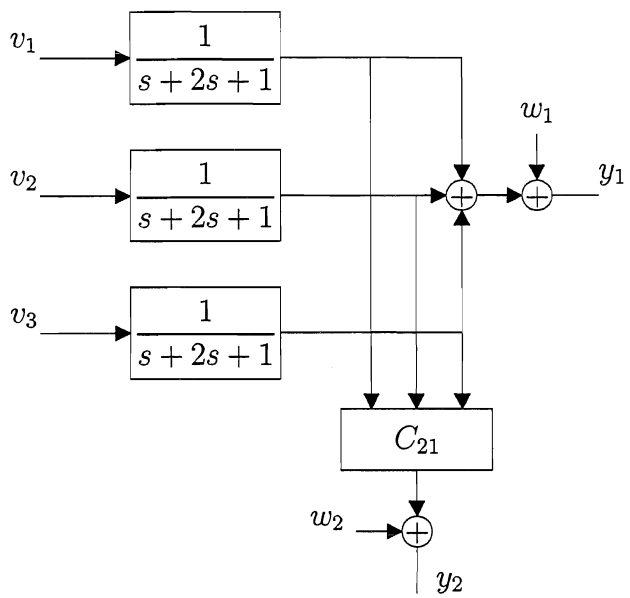

Figure 9.1 Three second-order latent variable generating systems, with scalar primary output and multivariate secondary output.

Here, C_{21} was a 200×3 matrix with uniformly distributed random parameters in the interval $(0, 1)$. The system was discretized assuming zero-order hold elements on the inputs and a sampling interval $T = 0.1$. The system was then simulated with v, w_1 and w_2 as independent and normally distributed zero mean white noise sequences. The R_v and R_{22} covariance matrices were diagonal, with uniformly distributed random parameters in the intervals $(0, 1)$ and $(0, r_{22})$ respectively, while the y_1 variance was $r_{11} = 0.0001$. Different values of r_{22} were used as described below.

The simulations started with $r_{22} = 0.01$, and the ordinary static PCR and PLSR estimators (8.18) and (8.21) based on $N = 200$ samples were first determined for different numbers of y_2 components a_2. In addition the dynamic PCA+OE and PLSR+OE estimators according to (9.7) and (9.13) were identified using the OEC model (see Appendix B for the definition of nn)

$$nn = [0, [2, \ldots, 2], 0, 0, [2, \ldots, 2], [0, \ldots, 0]] . \tag{9.17}$$

Each estimator was determined in $M = 10$ Monte Carlo runs using $N = 200$, with validation against independent data sets with the same number of samples. The resulting mean validation RMSE values are plotted in Fig. 9.2.

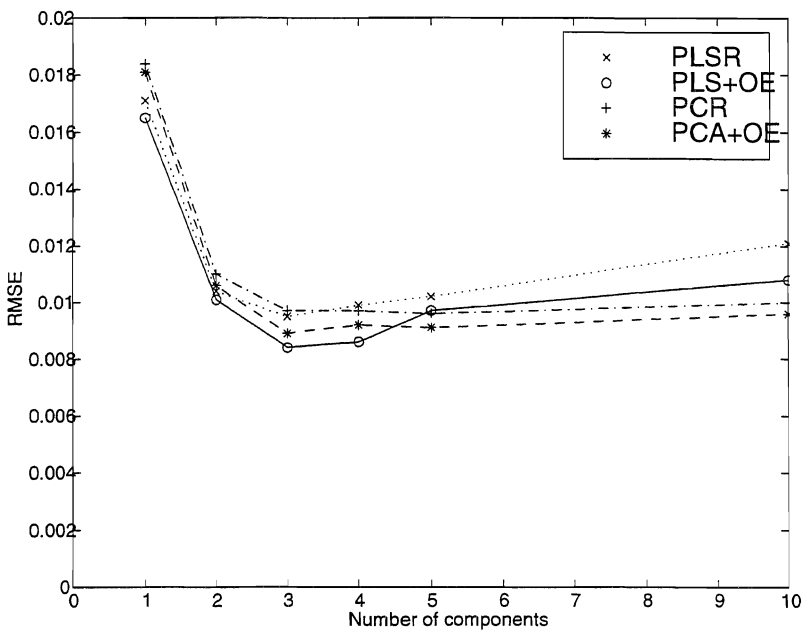

Figure 9.2 Validation RMSE mean values as function of number of components used in PCR, PLSR, PCA+OE and PLSR+OE estimators for $r_{22} = 0.01$, based on 10 Monte Carlo runs with $N = 200$ samples.

From Fig. 9.2 we find the optimal number of components $a_2 = 3$, which is not surprising since the system has three independent noise sources. The figure also indicates that PLSR is slightly better than PCR, and that the dynamical PCA+OE and PLSR+OE solutions are better than the static ones.

The models for $a_2 = 2$, 3 and 4 were also determined using $M = 100$ Monte Carlo runs, with mean validation results and standard deviations as shown in Table 9.1. The results clearly indicate the improvement obtained by use of the

dynamical solutions. Table 9.1 also includes the proportion of the y_2 sample variance explained by the PCR components used. This proportion is a function of the sample eigenvalues $\widehat{\lambda}_1 \geq \widehat{\lambda}_2 \geq \cdots \geq \widehat{\lambda}_p$ in a principal component analysis (see e.g. Johnson and Wichern, 1992), defined as

$$\text{explained proportion of sample variance} = \frac{\sum_{i=1}^{a_2} \widehat{\lambda}_i}{\sum_{i=1}^{p} \widehat{\lambda}_i}, \tag{9.18}$$

where p is the number of y_2 variables and a_2 the number of components used.

Table 9.1: Validation RMSE mean values and standard deviations for data based PCR, PCA+OEC, PLSR and PLSR+OEC estimators with $r_{22} = 0.01$, based on $N = 200$ samples and with different numbers of components. The explained proportions of y_2 sample variance are included. The RMSE values are multiplied by 10^4.

a	PCR	PCA+OEC	PLSR	PLSR+OEC	expl. var. (%)
2	124 ± 44	121 ± 59	103 ± 15	95 ± 20	67
3	100 ± 9	91 ± 17	97 ± 6	86 ± 7	69
4	100 ± 9	91 ± 11	99 ± 8	89 ± 8	70

The PLSR and PLSR+OEC simulations were finally repeated using also $r_{22} = 0.001$ and $r_{22} = 0.1$. Mean validation RMSE results based on $M = 100$ Monte Carlo runs with $a_2 = 3$ are given in Table 9.2, indicating that the improvement obtained by use of the dynamic estimator increases with increasing y_2 noise level. At the same time the explained proportion of sample variance related to the corresponding PCR components decreases. For $r_{22} = 0.1$ the optimal number of components is in fact $a_2 = 2$, with slightly reduced validation RMSE values as compared with use of $a_2 = 3$.

Table 9.2: Validation RMSE mean values and standard deviations for data based PCR, PCA+OE, PLSR and PLSR+OE estimators with various r_{22} values, based on $N = 200$ samples and with $a_2 = 3$ components. The explained proportions of y_2 sample variance are included. The RMSE values are multiplied by 10^4.

r_{22}	PLSR	PLSR+OE	$\frac{RMSE^{\text{PLSR+OE}}}{RMSE^{\text{PLSR}}}$	expl. var. (%)
0.001	30 ± 3	31 ± 2	0.99	95
0.01	97 ± 6	86 ± 7	0.89	69
0.1	318 ± 35	257 ± 54	0.81	19

■

Chapter 10

Real data examples

The methods for identification of primary output estimators developed in the thesis are tested on data from laboratory experiments and industrial plants. These cases make use of data from an experimental extruder at the Borealis polyolefine plant in Bamble, Norway, a civil engineering polyethylene pipe extruder at the Icopal plant in Drangedal, Norway, a complex industrial plant run by Norsk Hydro, Norway, and an acoustic chemometrics experimental setup at Telemark Institute of Technology, Porsgrunn, Norway.

10.1 Introduction

The intention with the following examples is to show that the estimator identification methods developed and discussed in the theoretical part of the thesis work also on data sampled from physical plants. The main theoretical points to be supported are the following:

- With the main data structure assumed in the thesis, OE estimators should theoretically perform better than ARMAX estimators, assuming that past primary $y_{1,k}$ measurements are not available as a basis for present $y_{1,k}$ estimates. As pointed out in Chapter 2, this is due to the fact that the OE estimators will then be based on an underlying Kalman filter, while the ARMAX estimators will be non-optimal. However, note that the theoretical difference may be small when the $y_{1,k}$ noise level is high (see Fig. 3.5).

- The OE estimators can be identified also when the primary $y_{1,k}$ data is sampled at a low and irregular rate. As pointed out in Chapter 6, this is so because the criterion function used in a prediction error identification method is then basically the same as in the high $y_{1,k}$ sampling rate case. This possibility does not exist for ARMAX estimators.

- Dynamic PCA+OE and PLSR+OE estimators may perform better than static PCR=PCA+LS and PLSR=PLSR+LS estimators in cases where the predicted primary $y_{1,k}$ output is a time series that can be modeled as a response to known inputs u_k and/or white process noise v_k. With a latent variable data structure, the OE estimators will also here theoretically perform better than the ARMAX estimators.

Since the emphasis is on the system identification and multivariate calibration principles and methods involved, the physical plants are given only very brief descriptions. To some extent the full background for the data is in fact confidential. In some of the data sets the manipulated inputs have a low degree of excitation, and the data sets are in some cases rather short. Better results may thus be obtained with more careful experimental designs.

All estimator identifications were performed by use of the *pem.m* function in the System Identification Toolbox for use with Matlab (Ljung, 1995), when necessary modified to handle low sampling rate y_1 data.

10.2 Experimental extruder

Fig. 10.1 shows an experimental twin-screw extruder at the Borealis polyolefine plant in Bamble, Norway. In a student project, this extruder was used to produce hard polypropylene foam, with the foam density as the primary quality output $y_{1,k}$ (Faanes, Gjermundbo, Gundersen and Tvedt, 1997). The manipulated u_k inputs were the common temperature setpoint for some of the heating zones along the extruder and the gas injection pressure, while the secondary $y_{2,k}$ outputs were four temperature measurements along the extruder and the outlet pressure.

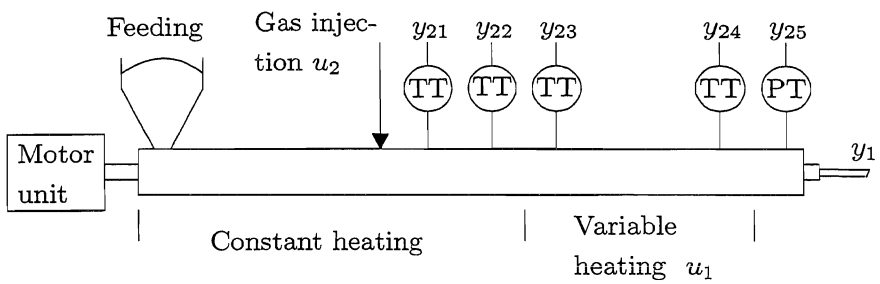

Figure 10.1. Experimental extruder with variable heating setpoint u_1 [°C], gas injection pressure u_2 [bar], temperature measurements y_{21} to y_{24} [°C], outlet pressure y_{25} [bar] and foam density y_1 [g/cm^3]. The total length of the extruder without motor unit is 120 cm.

The manipulated inputs for the entire experiment with a total of 230 samples with a sampling interval $T = 30\,\text{sec}.$ is shown in Fig. 10.2. As indicated in the

figure, the data is divided into two parts, the first 115 samples used for modeling and the remaining 115 samples used for validation. Note that the gas pressure was constant in the modeling set.

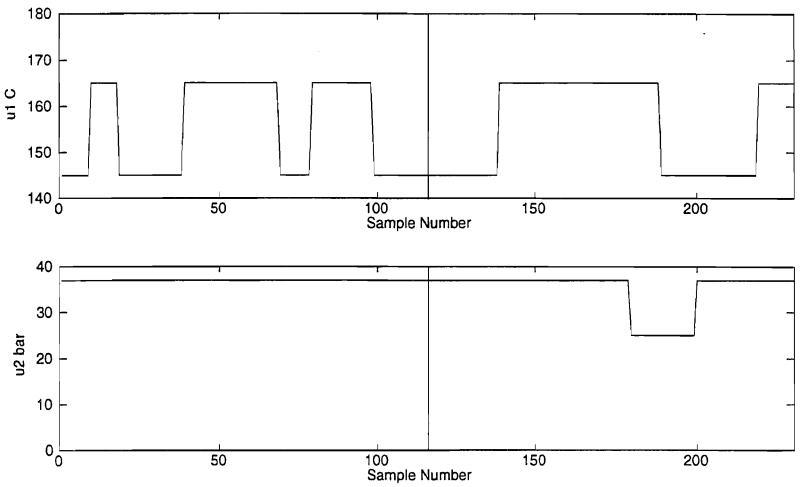

Figure 10.2 Manipulated inputs for experimental extruder, the first part of the data used for modeling and the last part used for validation.

The corresponding secondary outputs are shown in Fig. 10.3.

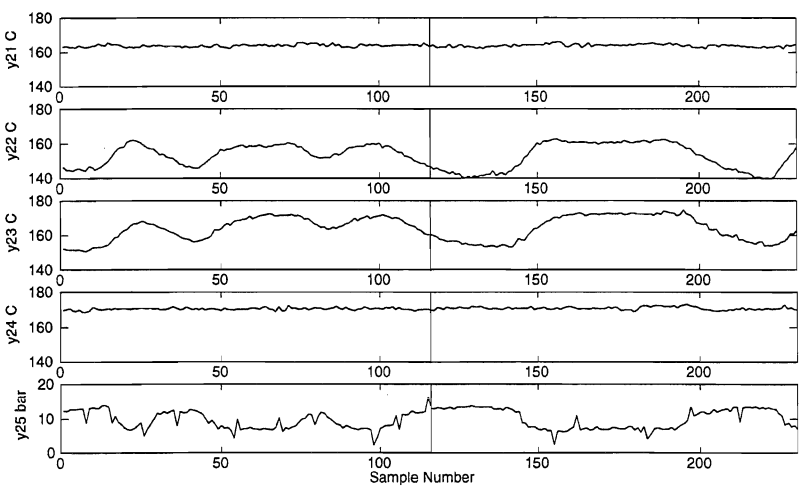

Figure 10.3 Secondary outputs for experimental extruder, the first part of the data used for modeling and the last part used for validation.

The primary $y_{1,k}$ outputs were determined by laboratory density measurements of physical samples of the product, with a considerable variance in the obtained

values. The y_1 sampling rate was the same as for u and y_2. The result is shown in Fig. 10.4 below, together with estimated primary output values.

Both ARMAX and OE estimators were identified, and mean-centered data from the first 115 samples were used as the modeling set. The last 115 samples were used for validation, and the best results were obtained with all u_k and $y_{2,k}$ variables used as inputs. Since the gas injection pressure was constant in the modeling set, nothing but zero-order and first-order estimators could be identified. The estimators were specified as general polynomial models, in which different delays of the input signals are easily tested. Initial values were found by the LS and instrumental variable algorithm that is a part of the *pem.m* Matlab function. Repeated identifications using randomized initial values gave no improvement.

The best ARMAX estimator was found with the specification (see Appendix B)

$$nn = [1, [1,1,1,1,1,1,2], 1, 0, [0,0,0,0,0,0,0], [1,1,2,2,1,1,0]], \tag{10.1}$$

corresponding to the estimator structure

$$\hat{y}_{1,k}^{\mathrm{ARMAX}} = \frac{1}{1+\hat{a}q^{-1}} \begin{bmatrix} \hat{b}_{11}q^{-1}u_{1,k} + \hat{b}_{12}q^{-1}u_{2,k} + \hat{b}_{21}q^{-2}y_{21,k} + \hat{b}_{22}q^{-2}y_{22,k} \\ +\hat{b}_{23}q^{-1}y_{23,k} + \hat{b}_{24}q^{-1}y_{24,k} + \left(\hat{b}_0 + \hat{b}_{25}q^{-1}\right) y_{25,k} \end{bmatrix}. \tag{10.2}$$

The RMSE validation result was then

$$RMSE^{\mathrm{ARMAX}} = \sqrt{\frac{1}{115}\sum_{k=116}^{230}\left(y_{1,k} - \hat{y}_{1,k}^{\mathrm{ARMAX}}\right)^2} = 0.0144. \tag{10.3}$$

The best OE estimator was found with the specification (see Appendix B)

$$nn = [0, [1,1,1,1,1,1,2], 0, 0, [1,1,1,1,1,1,1], [1,1,2,2,1,1,0]], \tag{10.4}$$

corresponding to the estimator structure

$$\begin{aligned} \hat{y}_{1,k}^{\mathrm{OE}} \;=\; & \frac{\hat{b}_{11}q^{-1}u_{1,k}}{1+\hat{f}_{11}q^{-1}} + \frac{\hat{b}_{12}q^{-1}u_{2,k}}{1+\hat{f}_{12}q^{-1}} + \frac{\hat{b}_{21}q^{-2}y_{21,k}}{1+\hat{f}_{21}q^{-1}} + \frac{\hat{b}_{22}q^{-2}y_{22,k}}{1+\hat{f}_{22}q^{-1}} \\ & + \frac{\hat{b}_{23}q^{-1}y_{23,k}}{1+\hat{f}_{23}q^{-1}} + \frac{\hat{b}_{24}q^{-1}y_{24,k}}{1+\hat{f}_{24}q^{-1}} + \frac{\left(\hat{b}_0 + \hat{b}_{25}q^{-1}\right) y_{25,k}}{1+\hat{f}_{25}q^{-1}}. \end{aligned} \tag{10.5}$$

The RMSE validation result was then

$$RMSE^{\mathrm{OE}} = \sqrt{\frac{1}{115}\sum_{k=116}^{230}\left(y_{1,k} - \hat{y}_{1,k}^{\mathrm{OE}}\right)^2} = 0.0130, \tag{10.6}$$

i.e. clearly better than the ARMAX result.

The results from the laboratory determination of the $y_{1,k}$ values are shown in Fig. 10.4 as rather noisy signals, while the estimated $\hat{y}_{1,k}^{\mathrm{ARMAX}}$ and $\hat{y}_{1,k}^{\mathrm{OE}}$ values give the less noisy signals. The validation RMSE values may also be used as estimated standard deviation limits, resulting in the dotted curves in Fig. 10.4.

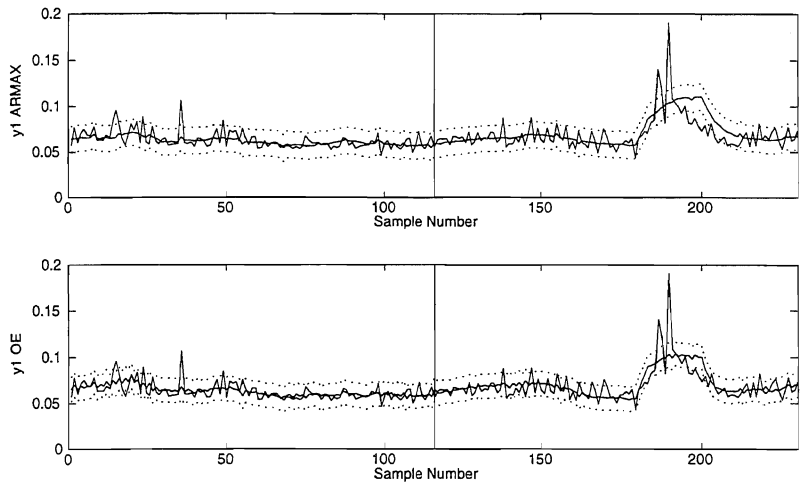

Figure 10.4 Measured primary output (noisy signals) and estimated primary output (less noisy signals) using ARMAX and OE estimators. The first part of the measured data was used for modeling and the last part for validation, resulting in $RMSE^{\mathrm{ARMAX}} = 0.0144$ and $RMSE^{\mathrm{OE}} = 0.0130$. The validation standard deviation limits (RMSE limits) are shown as dotted lines.

In the RMSE values obtained and illustrated as standard deviation limits in Fig. 10.4 are also included the y_1 measurement error. This means that the error in the estimated product quality (foam density) is smaller than given by the RMSE value, and the figure indicates that for the major part of the samples the estimation error may be quite overestimated. On the other hand it appears to be underestimated for the samples between $k = 180$ and $k = 200$, when there is a drop in the gas injection pressure.

In order to check if the estimation residual (prediction error) ε_k is a white noise sequence, the autocorrelation function of ε_k for the OE estimator is computed by use of the *resid.m* function in the System Identification Toolbox for use with Matlab (Ljung, 1995). The result is shown in Fig. 10.5, together with the 99% confidence intervals plotted as dotted lines, under the assumption that ε_k is white and independent of u_k and $y_{2,k}$.

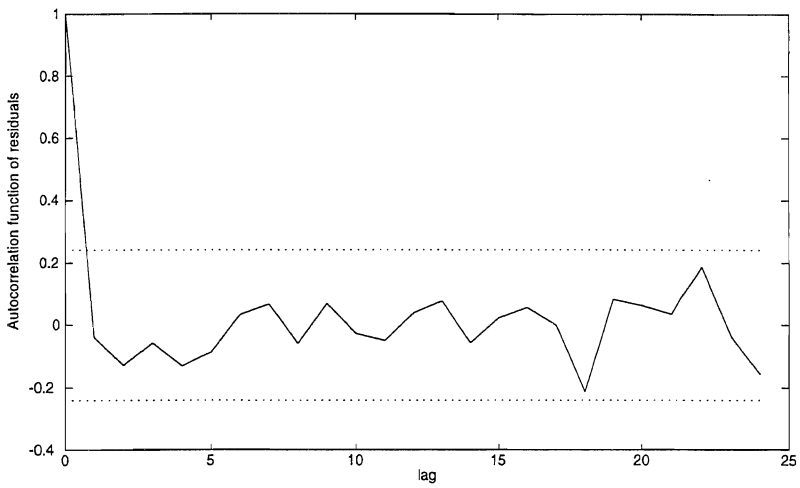

Figure 10.5 Autocorrelation function for the OE estimator residuals.

Fig. 10.5 clearly indicates that ε_k for the OE estimator is white noise, although it theoretically and according to (2.31) and (2.42) should be colored. This also indicates that the estimation error to a large extent is due to a white y_1 measurement error.

In order to compare the results in Fig. 10.4 with other alternatives, the validation results with only u_1 and u_2 used as inputs, and the results with only the y_2 measurements used as inputs are given in Table 10.1.

Table 10.1: Validation RMSE results for estimators using different inputs.

Inputs	$RMSE^{\text{ARMAX}}$	$RMSE^{\text{OE}}$
u_1 and u_2	0.0159	0.0182
y_{21} to y_{25}	0.0201	0.0185
u_1, u_2 and y_{21} to y_{25} (see Fig. 10.4)	0.0144	0.0130

From the table we see that both the known u inputs and the secondary y_2 measurements play significant roles for the result in Fig. 10.4.

10.3 Industrial extruder

Fig. 10.6 shows a production line for civil engineering polyethylene pipe extruding at the Icopal plant in Drangedal, Norway. The pipe diameter y_1 is essentially determined by a calibration die, and the pipe is radially pulled towards this die by an external vacuum force. From the extruder outlet to the pipe diameter measurement at the pipe cut-up position, there is a time delay of approximately 5

min ., and an estimate of y_1 without this delay is thus of interest for an improved control system design.

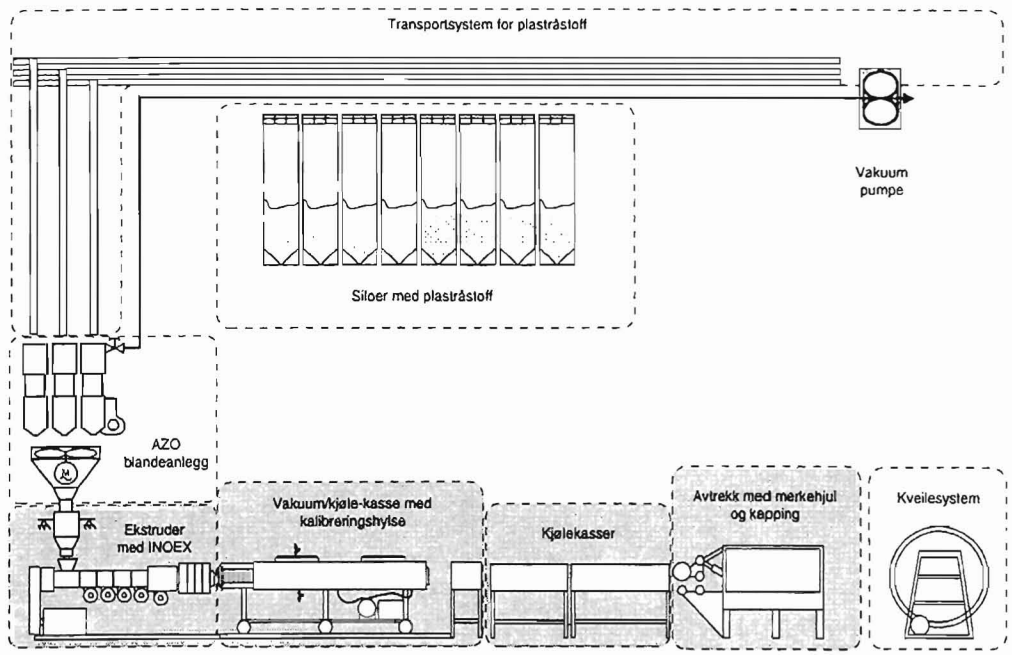

Figure 10.6 Production line for civil engineering polyethylene pipe extruding at Icopal plant, with silos, transport system, mixing unit, extruder with INOEX control system, vacuum/cooling/calibration unit, additional cooling unit, and haul-off and cut-up/coiling units (from Wilhelmsen, 1998).

The available known inputs, secondary measurement and primary measurement are

- the pipe haul-off speed u_1
- the extruder rotational speed u_2
- the external vacuum pressure u_3
- the internal extruder pressure y_2
- the resulting outer pipe diameter y_1 at the extruder outlet, determined after correction for the known time delay from the outlet to the physical measurement at the pipe cut-up position.

An identification experiment on the extruder was part of the M.Sc. thesis work of Wilhelmsen (1998). The sampling interval for u_k and $y_{2,k}$ was then $T_2 = 2$ sec,

while the sampling interval for the diameter $y_{1,j}$ for practical reasons was $T_1 = 12$ sec. Wilhelmsen found that a first-order model gave a good result, and since T_1 is short compared with the time constant in the system, a fairly good estimator can then be identified by use of the low sampling rate data only, although use of all sampled u_k and $y_{2,k}$ data gives a significant improvement. A further search for a good estimator reveals that a second-order estimator gives poorer results when only the low sampling rate data is used, while the results with use also of the high sampling rate data are improved. The results are summarized in Table 10.2.

Since the low sampling rate used for the primary y_1 output is constant and sufficiently high, the initial values for the high u_k and $y_{2,k}$ sampling rate estimators were obtained by identification of the corresponding low sampling rate estimators, followed by a recomputation of the high sampling rate initial estimator from the underlying continuous-time model.

Table 10.2: Validation RMSE values for different y_1 estimators for industrial extruder.

n	u_1	u_2	u_3	y_2	$RMSE^{\text{ARMAX}}_{\text{low rate}}$	$RMSE^{\text{OEC}}_{\text{low rate}}$	$RMSE^{\text{OEC}}_{\text{high rate}}$
1	x				-	-	0.280
1		x			-	-	0.228
1			x		-	-	0.094
1				x	-	-	0.211
1	x	x	x		-	-	0.063
1	x	x	x	x	0.065	0.070	0.062
1	x		x	x	-	-	-
1		x	x	x	-	-	-
1			x	x	-	-	0.081
2	x				-	-	0.288
2		x			-	-	0.207
2			x		-	-	0.092
2				x	-	-	0.208
2	x	x	x		-	-	0.059
2	x	x	x	x	0.093	0.089	0.059
2	x		x	x	-	-	0.059
2		x	x	x	-	-	0.072
2			x	x	-	-	0.070

The results for second-order ARMAX and OEC estimators obtained by use of only the low sampling rate data are visualized in Fig. 10.7, where the first part of the data set from $j = 1$ to 83 was used for modeling and the last part from $j = 84$ to 155 for validation. Note that first-order estimators gave somewhat better results.

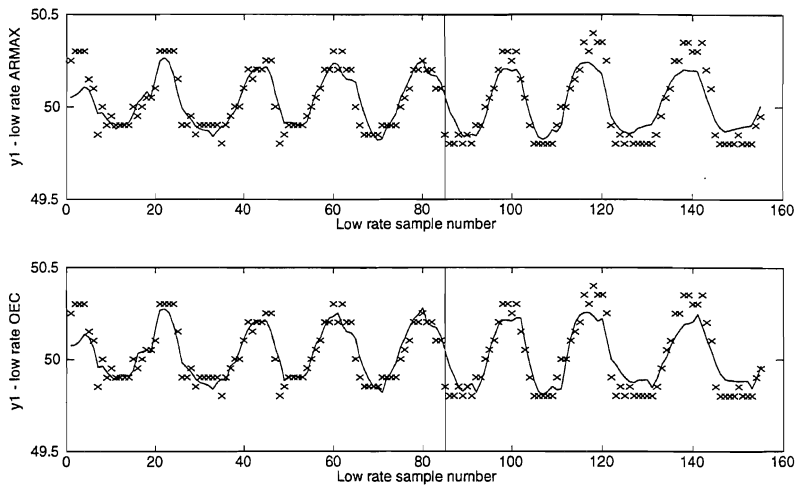

Figure 10.7 Measured primary output (diameter in mm) marked by × and estimated primary output as solid lines, using ARMAX ($RMSE^{\mathrm{ARMAX}} = 0.093$) and OE ($RMSE^{\mathrm{OE}} = 0.089$) second-order estimators based only on low sampling rate data. The first part of the data was used for modeling and the last part for validation.

The results for second-order OEC estimators obtained by use of also the high sampling rate data are visualized in Fig. 10.8, where the first part of the data set from $k = 1$ to 504 was used for modeling and the last part from $k = 505$ to 930 for validation. Note that a first-order estimator in this case gave poorer results.

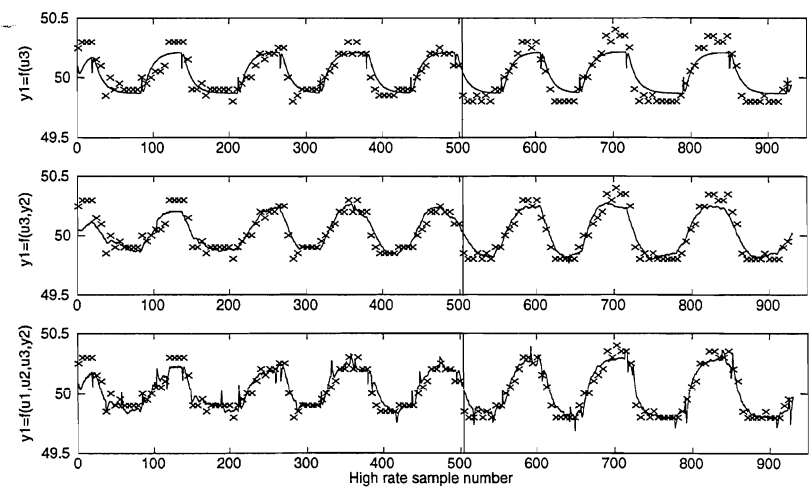

Figure 10.8 Measured primary output (diameter in mm) marked by × and estimated primary output as solid lines, using OEC second-order estimators based also on high sampling rate data. The first part of the data was used for modeling and the last part for validation. The validation RMSE values were $RMSE = 0.092$ (u_3 as input), $RMSE = 0.070$ (u_3 and y_2 as input) and $RMSE = 0.059$ (u_1, u_2, u_2 and y_2 as input).

10.4 Complex industrial plant

Product quality measurements from a complex industrial plant were obtained in two separate periods of ordinary production (Karstang, 1997). Each data set consists of around 1000 samples of altogether 14 manipulated inputs, measured disturbances and secondary outputs, with a sampling interval of 10 minutes. Four primary quality variables were sampled and measured at a low and irregular rate, 38 samples in the first data set used for modeling and 26 samples in the second data set used for validation.

Karstang (1997) identified static estimators for the primary outputs, using four of the secondary outputs as regressor variables, and this was found to be a useful set of inputs also in the dynamical case. These variables in the modeling set are shown in Fig. 10.9, while the corresponding primary outputs are shown in Fig. 10.10.

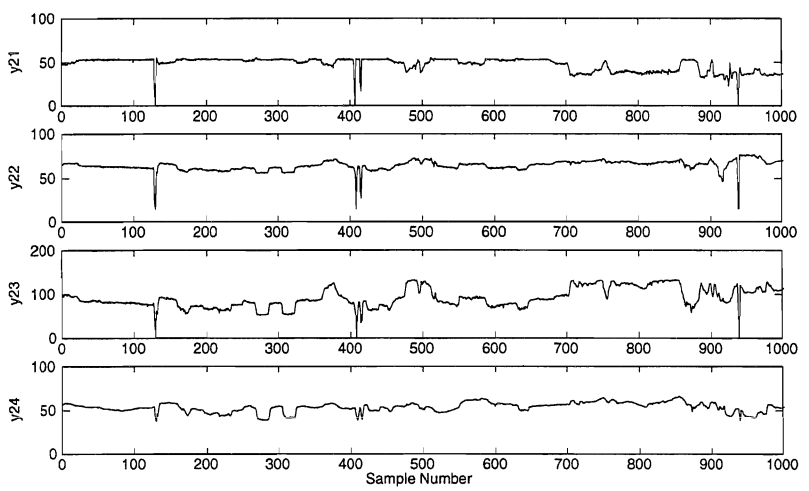

Figure 10.9 Secondary measurements used as estimator modeling inputs.

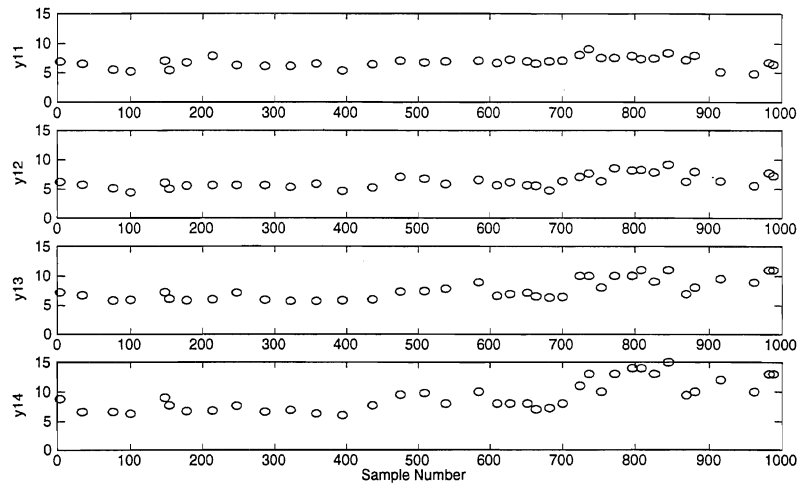

Figure 10.10 Primary measurements used as estimator modeling outputs.

As evident from the figures, the modeling data is characterized by

- a fairly low degree of dynamic excitation, especially for y_{21} and y_{22}
- trends in the primary output data, especially for y_{13} and y_{14}
- some outliers.

Remark 18 *It is not obvious how to handle the apparent outliers in the input data in Fig. 10.9. Since we intend to identify a dynamic system, the outlier data cannot simply be removed from the time series. If the outliers were due to measurement or data handling errors, a simple solution would be to use interpolated values. In this case we know, however, that the outliers correspond to actual physical conditions in the plant (Karstang, 1999), and that therefore also the system outputs must be affected. In lack of detailed plant information, and since the present aim is only to demonstrate the feasibility of the methods developed in the thesis, the input data is used without any form for outlier correction.*

The validation data set has the same low degree of excitation and some outliers, but no apparent trends.

The y_2 data was standardized, i.e.

$$y_{2i,k} \leftarrow \frac{y_{2i,k} - \bar{y}_{2i}}{\sqrt{var(y_{2i})}},\ i = 1, 2, 3 \text{ and } 4, \tag{10.7}$$

where

$$\bar{y}_{2i} = \frac{1}{N_2} \sum_{k=1}^{N_2} y_{2i,k} \tag{10.8}$$

and

$$var(y_{2i}) = \frac{1}{N_2 - 1} \sum_{k=1}^{N_2} (y_{2i,k} - \bar{y}_{2i})^2 . \tag{10.9}$$

The y_1 data was only mean-centered, i.e.

$$y_{1m,j} \leftarrow y_{1m,j} - \bar{y}_{1m}, \; m = 1, 2, 3 \text{ and } 4. \tag{10.10}$$

The four primary outputs were modeled separately. Ordinary static LS estimators $\hat{b}_m^{\mathrm{LS}}$ corresponding to the models

$$y_{1m} = \begin{bmatrix} y_{21} & y_{22} & y_{23} & y_{24} \end{bmatrix} b_m^{\mathrm{LS}} + \varepsilon_m \tag{10.11}$$

were obtained as a basis for comparison.

First-order state space representations of OEC estimators

$$\begin{aligned} \hat{y}_{1m,k} &= \hat{a}_m \hat{y}_{1m,k-1} + \hat{b}_{1m} y_{21,k-1} + \hat{b}_{2m} y_{22,k-1} + \hat{b}_{3m} y_{23,k-1} + \hat{b}_{4m} y_{24,k-1} \\ &\quad + \hat{d}_{1m} y_{21,k} + \hat{d}_{2m} y_{22,k} + \hat{d}_{3m} y_{23,k} + \hat{d}_{4m} y_{24,k} \end{aligned} \tag{10.12}$$

were also identified, using the method described in Chapter 6. Due to the very limited number of primary output samples, initial values were found in an ad hoc manner using

$$\hat{a}_m = 0.9, \tag{10.13}$$

$$\begin{bmatrix} \hat{b}_{1m} & \hat{b}_{2m} & \hat{b}_{3m} & \hat{b}_{4m} \end{bmatrix} = 0.01 e_b^T \tag{10.14}$$

and

$$\begin{bmatrix} \hat{d}_{1m} & \hat{d}_{2m} & \hat{d}_{3m} & \hat{d}_{4m} \end{bmatrix} = \left(\hat{b}_m^{\mathrm{LS}} \right)^T + 0.1 e_d^T \tag{10.15}$$

as a first try, with e_b and e_d as random vectors with independent and normal zero mean elements with variance 1. The identification of each model was repeated in several runs with the b and d parameters modified from one run to the next by adding zero mean random and normal noise with variance 0.0004, while the a parameter from one run was used as initial value in the next run. When a "best possible" estimator was found using only the modeling set, it was validated against the validation set.

In the validations it was assumed that the mean values of the y_1 variables are known. In practice the mean values may be estimated separately from the mean values of the u and y_2 variables, although this gives a substantial error in the present case. They may also be found and updated by sampling of y_1 at time instants and intervals found necessary. This problem is, however, the same for the LS and the OEC estimators, and it is therefore not further considered in the present estimator comparison.

The validation results for the primary output y_{11} is shown in Fig. 10.11, which shows a significant improvement from the LS to the OEC estimator.

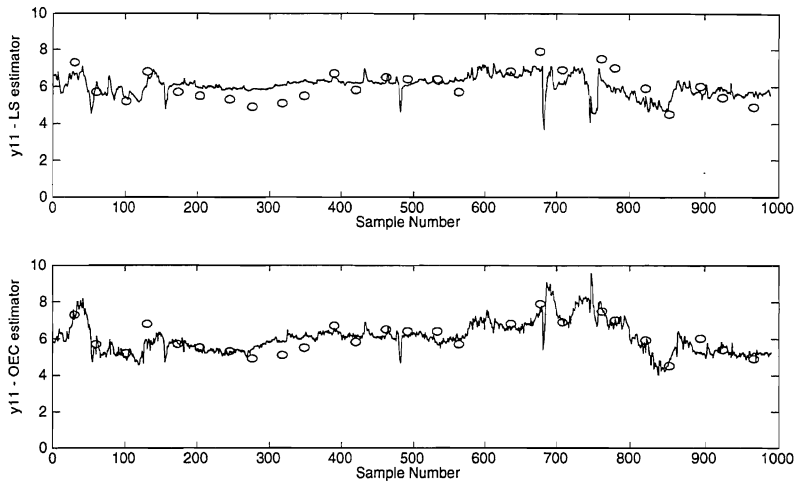

Figure 10.11 Validation $\hat{y}_{11}$ responses with LS ($RMSE = 0.66$) and OEC ($RMSE = 0.48$) estimators shown by solid lines. The o-markings show the ideal validation values.

The validation results for the primary outputs y_{12}, y_{13} and y_{14} are shown in Fig. 10.12, 10.13 and 10.14 below.

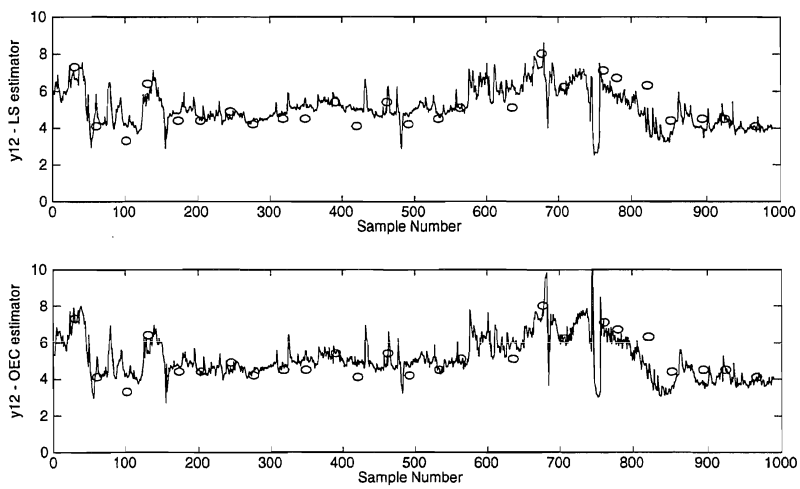

Figure 10.12 Validation $\hat{y}_{12}$ responses with LS ($RMSE = 0.78$) and OEC ($RMSE = 0.68$) estimators shown by solid lines. The o-markings show the ideal validation values.

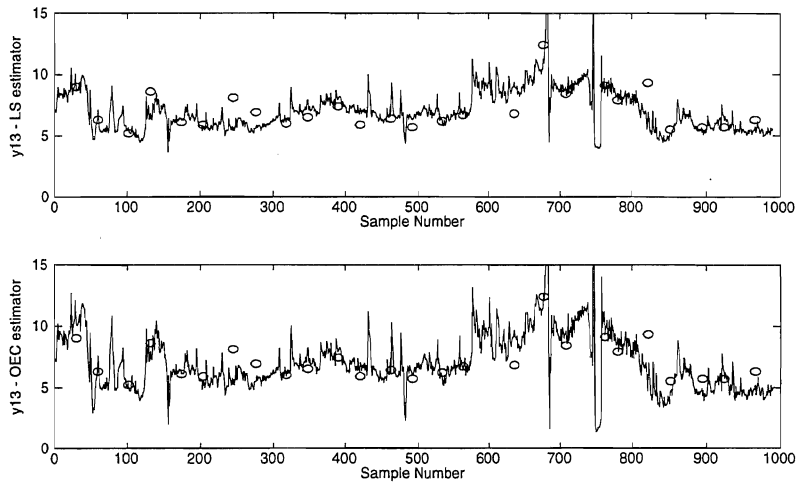

Figure 10.13 Validation $\hat{y}_{13}$ responses with LS ($RMSE = 1.15$) and OEC ($RMSE = 1.27$) estimators shown by solid lines. The o-markings show the ideal validation values.

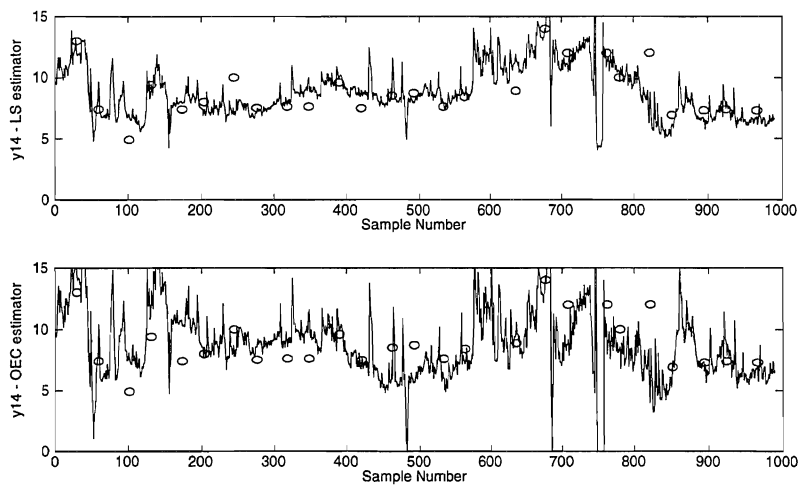

Figure 10.14 Validation $\hat{y}_{14}$ responses for LS ($RMSE = 1.50$) and OEC ($RMSE = 2.33$) estimators shown by solid lines. The o-markings show the ideal validation values.

The validation root mean square errors are summarized in Table 10.3. The RMSE values are computed as

$$RMSE = \sqrt{\frac{1}{N_1}\sum_{j=1}^{N_1}(y_{1m,j} - \hat{y}_{1m,j})^2}, \tag{10.16}$$

where $N_1 = 26$ is the number of y_1 samples in the validation set. As a basis for comparison with earlier results (Karstang, 1997), the mean absolute error

$$MAE = \frac{1}{N_1} \sum_{j=1}^{N_1} |y_{1m,j} - \hat{y}_{1m,j}| \tag{10.17}$$

is also given.

Table 10.3: Validation root mean square and mean absolute errors for static LS and dynamic OEC estimators for a complex industrial plant (best results in bold).

	MAE^{LS}	$RMSE^{\mathrm{LS}}$	MAE^{OEC}	$RMSE^{\mathrm{OEC}}$
y_{11}	0.59	0.66	**0.39**	**0.48**
y_{12}	0.62	0.78	**0.53**	**0.68**
y_{13}	**0.83**	**1.15**	0.94	1.27
y_{14}	**1.06**	**1.50**	1.88	2.32

The table shows a clear improvement from the LS to the OEC estimator for the y_{11} estimator and some improvement for the y_{12} estimator, while the LS estimators give the best results for y_{13} and y_{14}. It is possible that the failure of the OEC estimator for y_{13} and y_{14} is due to the trend in the modeling data shown in Fig. 10.10. However, a simple removal of these trends gave no improvements. The general solution in such cases is to obtain modeling data from a production period without general trends, although with dynamic excitation.

10.5 Acoustic flow meter

Acoustic chemometrics is based on signals from an acoustic sensor (accelerometer) placed for example on, or slightly downstream of, a standard orifice plate. Observations of the power spectrum of the sensor signal is collected in the $X = Y_2$ matrix, and calibrated against physical y_1 primary quantities like multi-component mixture concentrations, density etc., using for example a standard PLSR method (Esbensen et al., 1999).

In an experiment on a test rig at Telemark Institute of Technology, Porsgrunn, Norway, the flow rate of ordinary drinking water was measured by use of an orifice plate. More precisely, the differential pressure across the orifice was measured and used as the response variable y_1, while the acoustic power spectral density at 1024 frequencies were used as y_2 variables. The sampling interval was 5.3 sec.

The response variable had a considerable content of high frequency components, as shown in Fig. 10.15.

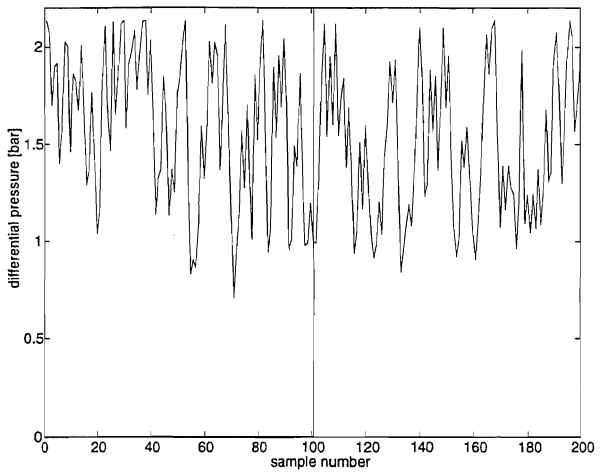

Figure 10.15 Differential pressure across orifice plate.

10.5.1 High primary output sampling rate case

The observations were separated into one part for modeling and one part for validation, as indicated in Fig. 10.15. Six outliers in the acoustic power spectrum results were corrected by use of interpolated values (in a time series analysis, outliers cannot simply be removed). Ordinary static PLSR using mean centered data consisting of all y_1 and y_2 samples and the optimal six components then gave the validation results shown in Fig. 10.16, i.e. rather small differences between y_1 and $\hat{y}_1$.

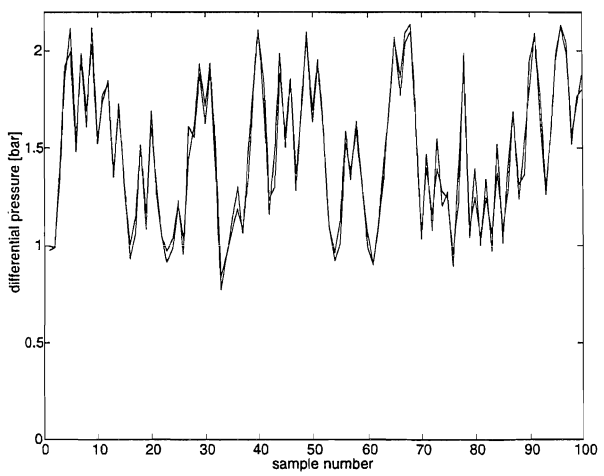

Figure 10.16 Validation result for standard static PLSR estimator.

As can be seen from Fig. 10.15, the measured responses give a time series, with clearly autocorrelated observations. According to the theory in Chapter 9, a dynamic PLSR+OEC estimator must then be expected to give improved performance. A dynamic estimator according to (9.13) was therefore identified, and the results for different numbers of PLSR components were compared with the corresponding results for a static PLSR estimator. The best results were obtained by use of a state-space first-order model. Initial parameter values were chosen at random, with occasional difficulties to obtain a stable predictor. However, when a minimum was found it was always the same minimum for a given number of PLSR components used. As can be seen in Fig. 10.17, the first-order dynamic estimator gave an approximate 30% reduction of the validation RMSE value at the optimal number of PLSR components for the two methods. Corresponding first-order PLSR+ARMAX estimators were also identified, with very much the same results as for the PLSR+OEC estimators. The optimal dynamic alternatives also used only four PLSR components, as compared to six components in the static estimator. A static PLSR estimator with the six outliers completely removed from the data (instead of using interpolated values) gave results that were almost identical with the PLSR results in the figure. Full standardization gave slightly inferior results. Note that the improvement obtained by use of the dynamic estimator is quite comparable with the improvements found by the simulations in Example 9.1, as illustrated in Fig. 9.2.

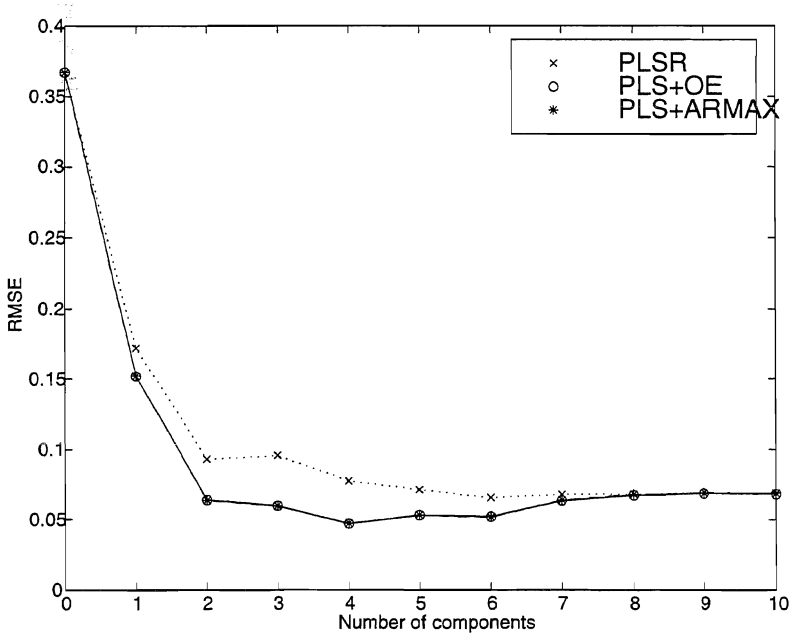

Figure 10.17 Validation RMSE values for different methods as functions of the number of components. The estimators are based on high primary output sampling rate data.

The results in Fig. 10.17 clearly indicate the benefits that may be obtained by the use of dynamic modeling of multivariate time series data, as compared to use of purely static chemometrical methods. A further discussion of the PLSR+OE estimator versus the PLSR+ARMAX estimator requires a detailed analysis of the vibration generating phenomena, which is beyond the scope of the present thesis.

The PLSR+OE estimator obtained with $a = 4$ components was

$$\hat{y}_1 = \frac{\left(\begin{array}{l} (0.98 + 0.42q^{-1})\,\hat{\tau}_1 + (2.1 + 0.8q^{-1})\,\hat{\tau}_2 \\ + (2.5 + 1.2q^{-1})\,\hat{\tau}_3 + (2.3 + 0.9q^{-1})\,\hat{\tau}_4 \end{array} \right)}{1 + 0.26q^{-1}} \cdot 10^{-3}. \tag{10.18}$$

Note that the estimator has its pole at $z = -0.26$ in the z-plane, which means an oscillatory step response with a relative damping coefficient $\zeta = 0.5$ and a natural frequency $\omega_n = \frac{1}{2T} = 0.0943$ sec. (see e.g. Franklin et al., 1990).

For the corresponding static estimator derived from (8.21) we find

$$\hat{b}_T^{\text{PLSR}} = \left(W_{\text{PLS}}^T Y_2^T Y_2 W_{\text{PLS}}\right)^{-1} W_{\text{PLS}}^T Y_2^T Y_1 = \begin{bmatrix} 1.3 \\ 2.8 \\ 5.4 \\ 2.5 \end{bmatrix} \cdot 10^{-3}. \tag{10.19}$$

Note that the $\hat{b}_T^{\text{PLSR}}$ parameters most naturally should be compared with the sum of the corresponding numerator coefficients in the dynamic estimator.

10.5.2 Low primary output sampling rate case

In order to test a combination of the methods developed in Chapter 6 and 9, static PLSR=PLSR+LS and dynamic PCA+OEC estimators were identified using only every 5th of the primary outputs in the modeling data (20 samples). These estimators were validated against the complete validation set, using all 100 primary output samples. Note that the PLSR+OEC estimator (9.13) identified above, now had to be replaced by the PCA+OEC estimator (9.7), with the result that $a = 6$ components was found to be the optimal choice for both the static and dynamical solutions.

Remark 19 *The use of every 5th sampling from high sampling rate data is of course not optimal. However, if the primary property had been for example a concentration of a certain component in a multi-component mixture, and the measurements had to be done through laboratory analyses, the primary property sampling rate would very likely for practical end economical reasons have been lower than the obtainable acoustic data sampling rate. Also the validation would in such a case have to be done against low sampling rate data.*

As must be expected with the significant high frequency content in the primary output signal, it turned out to be difficult to find useful initial values for the PCA+OEC estimators, and use of random values did not work. Instead, the initial parameters in a state space realization corresponding to (10.18) were chosen as $A = 0.5$, $B = \frac{1}{3}\left(\hat{b}_T^{\text{PLSR}}\right)^T$, $C = 1$ (canonical representation) and $D = \frac{2}{3}\left(\hat{b}_T^{\text{PLSR}}\right)^T$, where $\hat{b}_T^{\text{PLSR}}$ was determined as given as in (10.19) from a low sampling rate PLSR. This gave a first minimization result that was useful as a starting point for an iterative search for an optimal solution. In each of the iteration steps for $i = 2$, 3, $\cdots$ with separate minimizations, the initial parameters were then chosen as $A_i = A_{i-1} + 0.0002c_i e_A$, $B_i = B_{i-1} + 0.0001c_i e_B$ and $D_i = D_{i-1} + 0.0002c_i e_D$, with e_A, e_B and e_D as normal zero mean random variables with variance 1. The coefficient c_i was chosen as

$$
\begin{aligned}
c_i &= 1 \text{ for } RMSE^{\text{PLSR}} < RMSE^{\text{PCA+OEC}}(i-1) \\
c_i &= 0.5 \text{ for } 0.9 \cdot RMSE^{\text{PLSR}} < RMSE^{\text{PCA+OEC}}(i-1) < RMSE^{\text{PLSR}} \\
c_i &= 0.25 \text{ for } 0.8 \cdot RMSE^{\text{PLSR}} < RMSE^{\text{PCA+OEC}}(i-1) < 0.9 \cdot RMSE^{\text{PLSR}} \\
c_i &= 0.125 \text{ for } 0.7 \cdot RMSE^{\text{PLSR}} < RMSE^{\text{PCA+OEC}}(i-1) < 0.8 \cdot RMSE^{\text{PLSR}} \\
c_i &= 0.0625 \text{ for } RMSE^{\text{PCA+OEC}}(i-1) < 0.7 \cdot RMSE^{\text{PLSR}}.
\end{aligned}
$$

A typical iteration result for the optimal $a = 6$ number of components is shown in Fig. 10.18, together with the low sampling rate $RMSE^{\text{PLSR}}$ result.

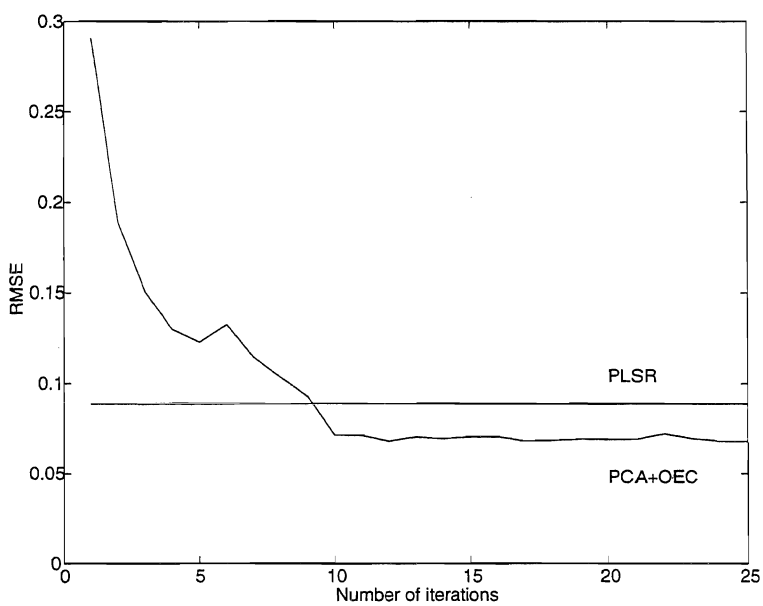

Figure 10.18 Result of low sampling rate PLSR and of iterative search for optimal PCA+OEC estimator, both solutions using $a = 6$ components.

The best dynamical solution obtained in several repeated simulations gave in this case 33% reduction of the validation RMSE value. This result demonstrates the feasibility of the dynamical PCA+OE approach also in the low primary output sampling rate case.

Remark 20 *As mentioned in Chapter 5 and further discussed in Chapter 11, the repeated use of the same validation set opens for the possibility that the validation set gradually becomes a part of the modeling set. In this case good validation results were always accompanied by good results for tests against the modeling set, and we would thus have selected a very similar model by testing only against the modeling set.*

A typical validation result is shown in Fig. 10.19. Note that the estimated output follows the (in this case) measured output well also between the sampled values. This is also the case for the low sampling rate PLSR estimator, although the dynamic estimator gave a lower validation RMSE value.

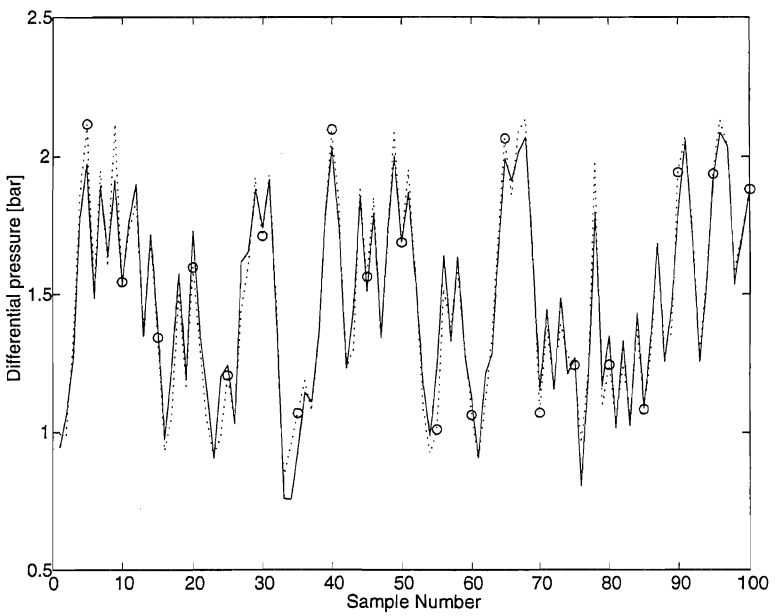

Fig. 10.19 Validation result for dynamic PCA+OEC estimator based on low sampling rate data. The low sampling rate validation data is o-marked, while the (in this case) known intermediate validation values are shown by dotted curve. The estimated values are shown by solid line.

Chapter 11

Further research topics

The theory and methods presented in the thesis raise questions about further methodological developments and possible application areas. Such questions are briefly discussed and to some extent clarified in the present chapter, but are otherwise left for further research.

11.1 Convergence

The prediction error identification method used throughout the thesis rely on the convergence of the estimated parameter vector to the best possible approximation of the theoretical estimator that is available in the model set. This is quite generally true (Ljung, 1978, 1987, 1999), but a specific analysis of the present case with y_2 used as estimator input is not performed. There are, however, no indications in the simulations or in the real data examples that this in itself represents a problem. The problems encountered are related to short data records, which in many cases makes it difficult to find good initial values for the numerical minimization. This is a well known general problem, especially for OE models (Ljung, 1999).

11.2 Multiple-output systems with low primary output sampling rate

Theoretically, the low y_1 sampling rate identification method for OE estimators presented in Chapter 6 will work also for multiple-output systems, although it is tested only for single-output simulation and real data cases. Some work has been done also on prediction error minimization algorithms for the multiple-output case, but so far without entirely satisfactory results, and more work in that direction is thus needed.

11.3 Estimator covariance with low primary output sampling rate

The covariance results in Example 6.2 as compared with results in Example 3.4 indicate that the acceptable number of y_1 samples may be lower in the low sampling rate case than in the ordinary case. Whether the extra u and y_2 samples at a high rate in fact are beneficial, is a question for further investigation.

11.4 Closed loop estimator identification

In Chapter 3 we assumed that identification of the optimal OE estimators was performed with the plant operating in open loop. Due to safety and other plant operation requirements this is often not feasible, and one is then left with the opportunity to use data from the plant operating in closed loop. The basic block diagram is then given by Fig. 11.1, where the controller may be realized by use of more or less sophisticated algorithms. The input r is the vector of setpoint values for all or some of the measured y_2 outputs, while we assume that the y_1 output is not generally available.

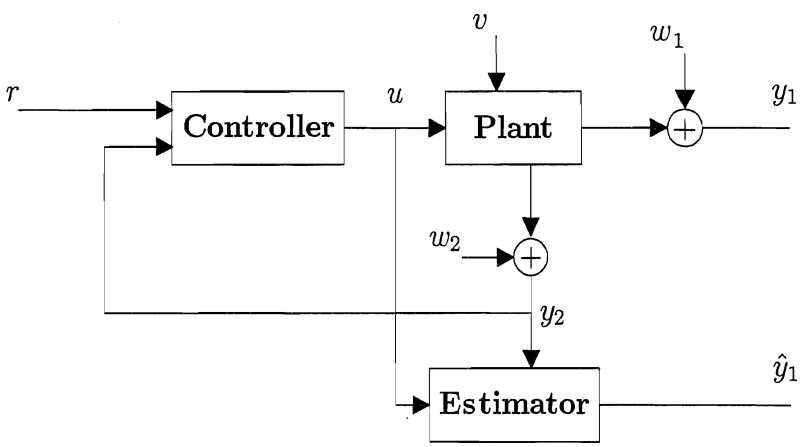

Figure 11.1 General structure for estimator identification with plant operating in a closed feedback loop.

Ordinary identification of systems operating in closed loop by use of prediction error methods is possible, although some difficulties must be circumvented, see e.g. Söderström and Stoica (1989). In general identifiability will be obtained by use of external excitation, such as a time-varying setpoint r_k with sufficient order of persistent excitation.

As illustrated in Fig. 3.1 and Fig. 3.2, identification of one of the optimal OE estimators is obtained by minimization of the prediction/estimation errors with $K_1 = 0$, where K_1 is the gain related to the y_1 measurements. It appears that this should not imply any identifiability problems in the closed loop case, although this ought to be verified by a more detailed theoretical study and appropriate simulations.

11.5 Use of prior knowledge

In system identification of state-space models by use of a prediction error method, it is quite straightforward to make use of prior knowledge based on physical laws etc. (Ljung, 1995). The least known parts of the model are often the noise covariances R_v and R_w, and the corresponding covariance $\Lambda = Ee_k e_k^T$ of the innovation form, and a common solution is therefore to use a directly parametrized innovation form with all entries in the Kalman gain considered as unknown. Since the optimal OEP and OEC estimators developed in Chapter 2 make use of $A - AK_2^{\mathrm{OE}}C_2$ instead of only A, direct parametrization of K_2^{OE} complicates the use of prior knowledge concerning A and C_2. It is, however, generally possible also to make use of known links between the parameters, in this case between K_2^{OE} and $A - AK_2^{\mathrm{OE}}C_2$. The details of this are left for further work.

11.6 Validation

In Chapter 5 we pointed to the inherent difficulty in the proposed procedure for model selection based on validation and comparison of different models. Due to the fact that both the modeling and the validation data sets are realizations of random processes, some models may give better validation results than others in a way that is not generally justified. Extensively repeated use of the same validation set may therefore lead to a model that is specifically adjusted to fit that particular data set, which then gradually becomes a part of the total modeling set (see also Sjöberg and Ljung, 1995). We must therefore look for validation differences that can be considered as significant, alternatively use extra validation sets. The phenomenon was demonstrated in Example 5.1.

It is interesting to compare this validation difficulty to the corresponding problem related to validation of static models:

- In ordinary least squares (LS) regression, inclusion of extra regressor variables will reduce the criterion function also when they explain nothing in the predicted variable y_k. The improved fit is then spurious and can be seen as an overfit to the particular realization of the modeling set. Whether the inclusion of an extra regressor variable is useful or not can in this case be decided by statistical methods (Ljung, 1987,1999).

- When the regressors are chosen through validation, there is always a risk that some regressor variables are included because the specific realizations used give some explanation of the specific validation realization of y_k, also if this is not generally true. If we use a validation set actively in order to find the best set of regressor variables, we will therefore gradually make the validation set a part of the modeling set, and in the end we may not validate at all.

- In principal component regression (PCR) and partial least squares regression (PLSR) the essential choice is the number of principal components to use (see Appendix C). We then have the inherent validation problem that we have to choose the number of components that fits the specific realization in the validation set the best, and the validation set may thus influence the choice. This is, however, done only once, and the problem is therefore limited to an unavoidable low level.

- In PCR and PLSR we may also make a choice of variables to use as a basis for the principal component determination. In such cases we will experience the above mentioned problem of making the validation set a part of the modeling set.

- In the dynamical case, we do not only choose which estimator variables to use, but we also have to choose model order and other details of the model structure. The tendency to make the validation set a part of the modeling set is then an issue of importance.

A tentative conclusion to the problem appears to be the following:

- At each level of model complexity (model order, number of variables, number of principal components etc.), choose the model that fits the modeling set the best.

- Find the level of complexity to use through validation against independent data.

However, this must be studied more carefully before final conclusions can be drawn.

11.7 Estimator robustification

There may be a need for estimators that are robust with respect to unforeseen process noise and disturbances as well as modeling errors. This may be accomplished

by use of increased process noise variances and covariances in the R_v matrix, assuming that R_v is known. We will then "cover" the uncertainties in noise, as sometimes practiced in control system design (Friedland, 1986).

When the estimator is identified by use of the secondary y_2 measurements as inputs, the same effect might be accomplished by manipulation of the K_2^{OE} matrix. With increased elements in some or all of the K_2^{OE} columns, the estimator will rely more on the corresponding y_2 measurements, and thus become less sensitive to increased process noise (assuming that the process noise is well reflected in the y_2 measurements). This is illustrated in Fig. 11.2.

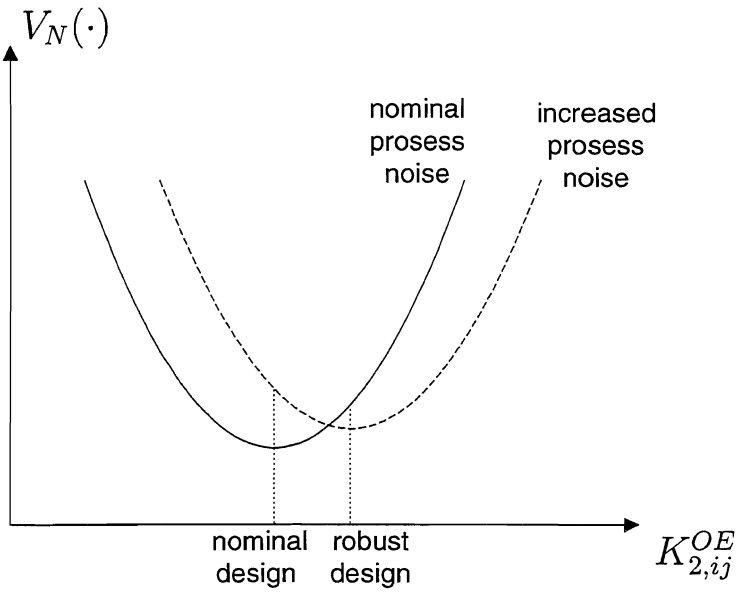

Figure 11.2 Estimator robustification by gain adjustment.

In order to find appropriate K_2^{OE} gain changes to make, we could in theory decrease the y_2 measurement noise levels, which of course is not possible in practice. It may, however, be possible to find the gain sensitivity to the y_2 noise levels by use of added artificial noise, and it may then be possible to find the effect of decreased noise levels by extrapolation. However, it remains to verify that this robustification approach is feasible, and to develop a practical implementation.

11.8 Estimator updating

In practical applications it is very likely that the identified estimators lose some of their validity over time, and estimator updating based on new plant data may then be necessary. This may also be the first step in a fault detection and isolation (FDI) scheme, detecting unacceptable estimator parameter variations.

Updating of static part of estimator

In cases with drift of primary property mean values it may be sufficient to recalibrate those values by use of a small number of y_1 measurements. The number of y_1 samples to use will depend on the variances of the y_1 measurements and the mean value accuracy needed.

Dynamic estimator updating

In cases with parameter drift the entire estimator may have to be updated. A straightforward solution is then to use samples of u, y_1 and y_2 in a moving window with a sufficient although not too long horizon into the past, and identify new estimator parameters as often as necessary. Both high and low y_1 sampling rate data may then be used, and the window may have rectangular, saw-tooth or approximately exponential form. The past prediction errors in the criterion function may thus be weighted, i.e.

$$V_N(\theta) = h\left[\frac{1}{N}\sum_{i=k-N}^{k}\alpha_i\beta_{k-i}\varepsilon_{1,i}(\theta)\varepsilon_{1,i}^T(\theta)\right], \tag{11.1}$$

where

$$\alpha_i = \begin{cases} 1, & \text{at the time instants } i \text{ where } y_{1,i} \text{ is sampled} \\ 0, & \text{at the time instants } i \text{ where } y_{1,i} \text{ is not sampled,} \end{cases} \tag{11.2}$$

and where β_{k-i} defines the form of the window. Since the estimator is identified off-line at each y_1 sampling instant, this is a computer demanding approach. However, in the most interesting industrial case with low y_1 sampling rate, the computation time is likely to be sufficient.

A more elegant and less computer demanding solution would be to use recursive updating of the estimator parameters. Recursive identification methods for the high y_1 sampling rate case are discussed in e.g. Söderström and Stoica (1989), while the details in methods for the low and irregular y_1 sampling rate cases remain to be worked out.

11.9 Identification by use of subspace methods

Since the optimal primary property OE estimators developed in Chapter 2 rely on past primary output estimates, they must be found by iterative methods as for example the prediction error method used in Chapter 3 and Chapter 6. This means that the direct and non-iterative subspace identification methods cannot be directly used for this purpose.

A possibility might be to use direct subspace methods iteratively, such that initial estimates of past outputs are successively refined. That would be similar to a known iterative LS method for OE model identification (Johansson, 1993), and a similar bootstrap method was used by Isaksen (1993) in order to reconstruct missing data. This possibility is left for further research.

11.10 Operator modeling and support

The basic principle for primary property estimation is illustrated in Fig. 1.1. By simply replacing the estimator model block with an operator block we arrive at the basic though limited operator functioning illustration in Fig. 11.3. In words, the operator uses all available information from known inputs and measured secondary outputs in order to estimate the primary output. This estimate may be a binary decision "process in control" or "process out of control", or a more qualified estimate.

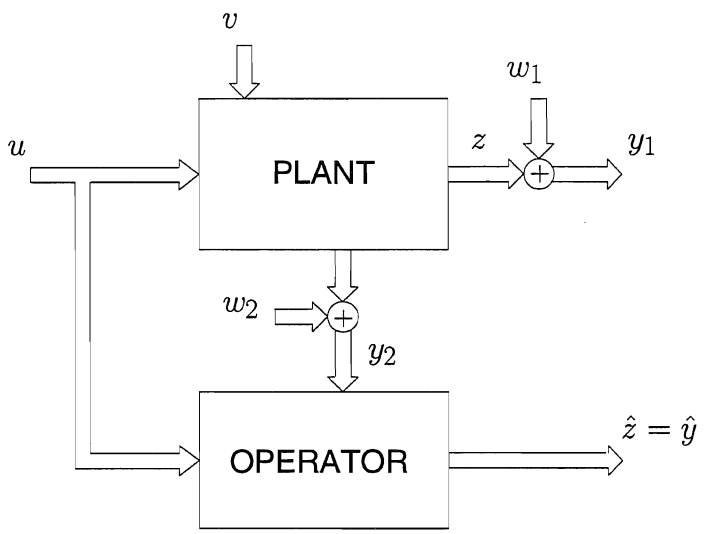

Figure 11.3 Basic principle for part of the operator function.

Fig. 11.3 could possibly be used as a starting point in an attempt to identify and model human skills in this specific situation, in line with the ideas in Rouse et al., (1988). Parts of the developments in the thesis could then form a theoretical basis.

It should be emphasized that the figure depicts only a minor part of the operator function, at what Rasmussen (1983) defines as the skill- and rule-based levels. This part of the operator function may be automated by use of the estimators discussed in the thesis, and there are basically two reasons for doing so:

- In a typical industrial situation with a large number of manipulated inputs, measured disturbances and secondary measurements, the task of primary output estimation may be quite demanding. A compression of the multivariate and dynamic information into primary output estimates may thus give valuable operator support.

- A primary output estimation system will relieve the operator from the tedious low-level task of monitoring a number of process values, and give room for more focus on higher level knowledge-based tasks related to primary output trend evaluation, product quality optimization and plant control functions.

11.11 Fault detection and isolation

Fault detection and isolation (FDI) methods using Kalman filters or non-optimal observers are reported by a number of authors, e.g. Tylee (1983), Patton et al. (1989) and Frank (1990). Such methods are based on use of analytical or functional redundancy contained in the relationships between system inputs and measured outputs, and they thus require a mathematical model of the actual dynamic system. This model may be found through mechanistic modeling or by system identification.

A closer look at some of the FDI methods reveals that it is not quite necessary to use complete system models, it is in many cases sufficient to have good estimators for the different system outputs, and the optimal OE estimators discussed in the thesis may then come to use. The advantage of this approach is that it is easier to identify such estimators using all other system outputs as estimator inputs, than it would be first to identify the system model as such and then construct the different estimators. We illustrate this by a straightforward example, and leave the important question concerning obtainable performance in practice for further research.

Example 11.1

Assume the system in Example 3.2 with an extra output measurement and some offset actuator and instrument errors Δu, Δy_1, Δy_2 and Δy_3 added:

$$\begin{aligned} x_{k+1} &= \begin{bmatrix} 0.9092 & 0.0863 & 0.0044 \\ 0.0863 & 0.8230 & 0.0863 \\ 0 & 0 & 0.9048 \end{bmatrix} x_k \\ &+ \begin{bmatrix} 0.0045 \\ 0.0908 \\ 0 \end{bmatrix} (u_k + \Delta u) + \begin{bmatrix} 0.0002 \\ 0.0045 \\ 0.0952 \end{bmatrix} v_k \end{aligned} \tag{11.3}$$

$$
\begin{aligned}
y_1 &= \begin{bmatrix} 1 & 0 & 0 \end{bmatrix} x + w_{1,k} + \Delta y_1 \\
y_2 &= \begin{bmatrix} 2 & 0 & 0 \end{bmatrix} x + w_{2,k} + \Delta y_2 \\
y_3 &= \begin{bmatrix} 0 & 1 & 0 \end{bmatrix} x + w_{3,k} + \Delta y_3.
\end{aligned}
$$

As Δu etc. may have both positive and negative sign, there are eight possible faults to consider (see Table 11.1). Note that the actuator offset Δu might also be a drift in a plant disturbance that is modeled as constant.

The system was simulated with u_k as a filtered pseudo random binary sequence (PRBS) with aotocovariance $r_{uu}(p) = 0.8^{|p|}$ (Söderström and Stoica, 1989, example 5.11). and independent and normal white noise sources with variances $r_v = 1$, $r_{11} = 0.01, r_{22} = 0.02$ and $r_{33} = 0.01$.

Optimal OEC estimators for each of the three outputs were identified as described in Example 3.2 with u_k and the other two system outputs as estimator inputs, and using $N = 1000$ samples of input-output data without offset errors. The three estimators were then used in a generalized observer scheme (Frank, 1990) as shown in Fig. 11.4.

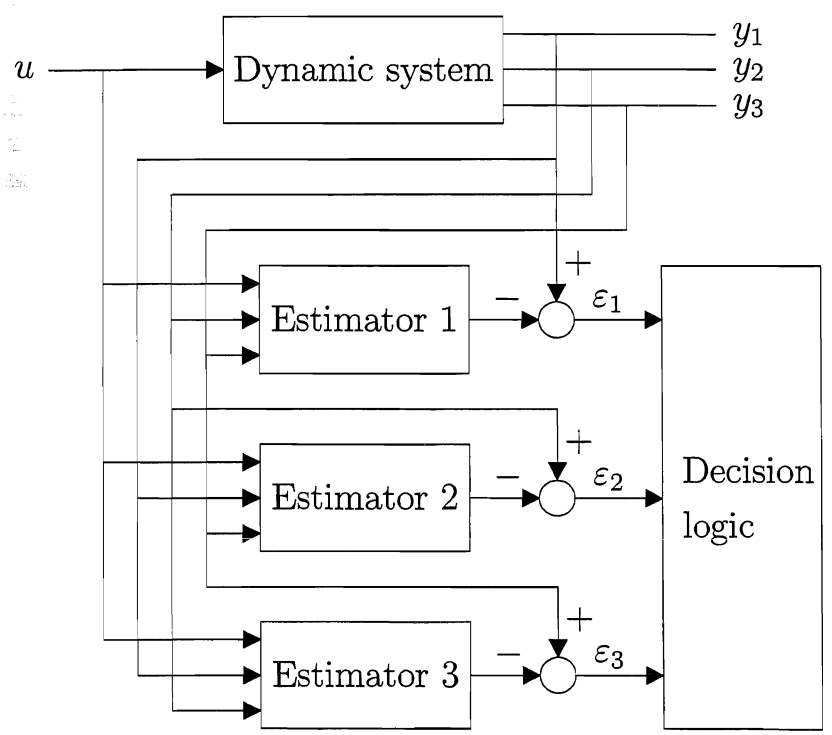

Figure 11.4 Estimator fault detection and isolation (FDI) scheme.

Assuming only one offset error at a time, the expected relations between the errors and the estimator residuals are shown in Table 11.1.

Table 11.1: Expected residual responses for different added static errors.

Δu	Δy_1	Δy_2	Δy_3	ε_1	ε_2	ε_3
+	0	0	0	−	−	−
0	0	0	+	−	−	+
0	0	+	0	−	+	−
0	−	0	0	−	+	+
0	+	0	0	+	−	−
0	0	−	0	+	−	+
0	0	0	−	+	+	−
−	0	0	0	+	+	+

We notice that the residual responses in the table form a standard truth table for three binary variables, and the eight different faults may thus be isolated by use of a simple decision logic.

The truth table in Table 11.1 is verified by the simulation results shown in Fig. 11.5 to 11.8, where $\Delta u = 1$, $\Delta y_1 = 1$, $\Delta y_2 = 1$ and $\Delta y_3 = 1$ for samples number 201 to 400 and $\Delta u = -1$, $\Delta y_1 = -1$, $\Delta y_2 = -1$ and $\Delta y_3 = -1$ for samples number 601 to 800 (with only one offset error at a time).

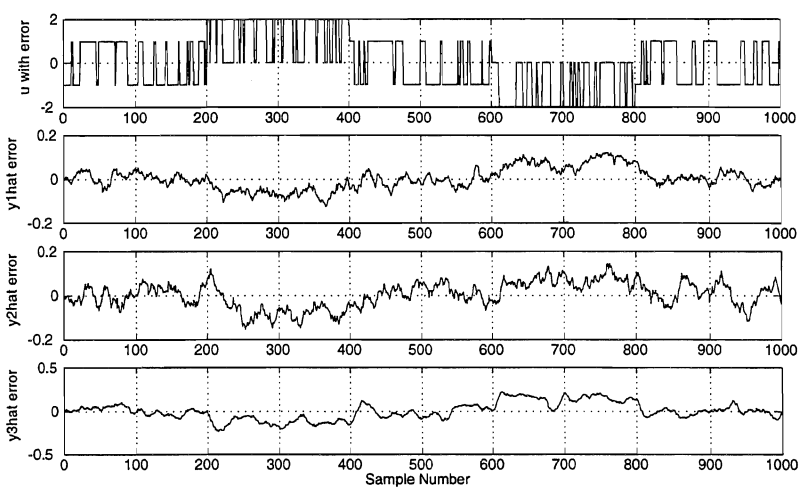

Fig. 11.5 Residuals with added offset error $\Delta u = 1$ for samples number 201-400 and $\Delta u = -1$ for samples number 601-800.

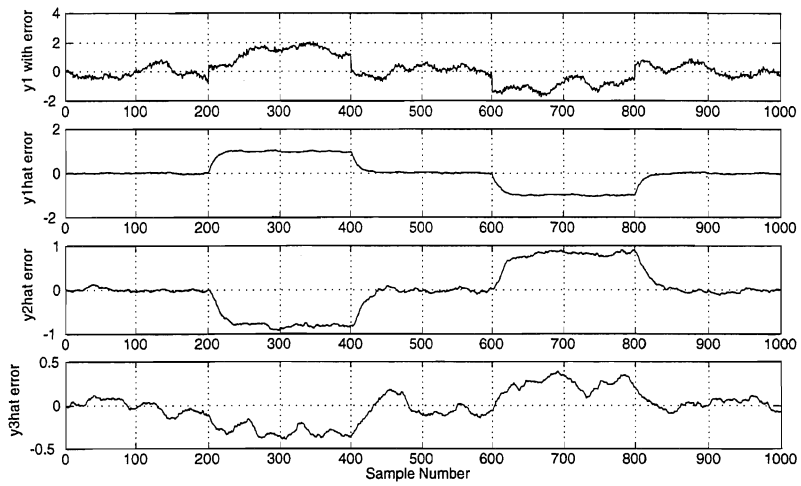

Fig. 11.6 Residuals with added offset error $\Delta y_1 = 1$ for samples number 201-400 and $\Delta y_1 = -1$ for samples number 601-800.

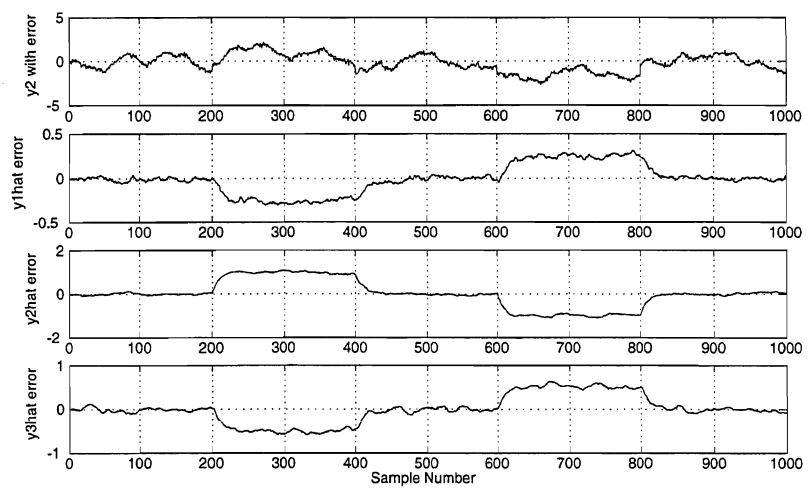

Fig. 11.7 Residuals with added offset error $\Delta y_2 = 1$ for samples number 201-400 and $\Delta y_2 = -1$ for samples number 601-800.

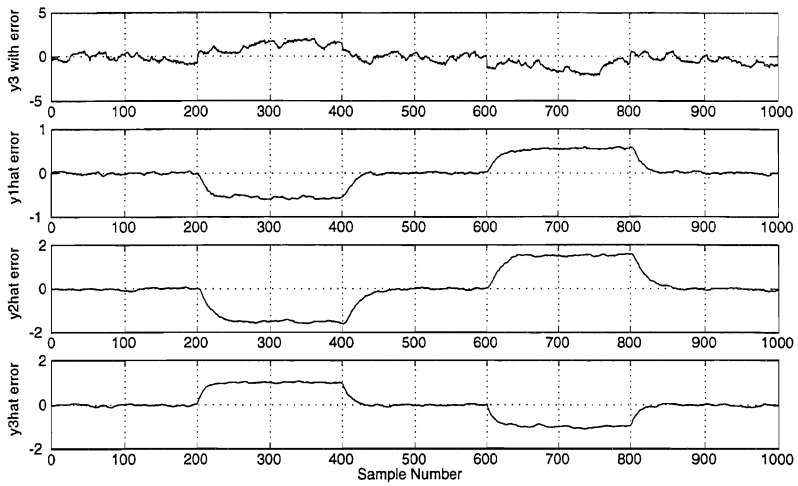

Fig. 11.8 Residuals with added offset error $\Delta y_3 = 1$ for samples number 201-400 and $\Delta y_3 = -1$ for samples number 601-800.

Note that with only two outputs we would not have sufficient information to isolate the different faults (6 faults and only 4 combinations in the truth table), while four or more outputs would give us extra degrees of freedom which might be used in order to isolate simultaneous faults (10 faults and 16 combinations for 4 outputs).

■

11.12 Feedback control

It is natural to consider use of estimated primary outputs $\hat{y}^{\mathrm{OE}}_{1,k|k-1}$ or $\hat{y}^{\mathrm{OE}}_{1,k|k}$ and estimated states $\hat{x}^{\mathrm{OE}}_{k|k-1}$ or $\hat{x}^{\mathrm{OE}}_{k|k}$ for feedback control purposes. In the following we briefly discuss the fundamental reachability question and possible control structures.

11.12.1 Reachability

Assume that the plant defined by (2.20) is state reachable, i.e. that

$$\Omega = \begin{bmatrix} B & AB & \cdots & A^{n-1}B \end{bmatrix} \tag{11.4}$$

has $\mathrm{Rank}(\Omega) = n$, where n is the model order. Also assume that the primary property z_k in Fig. 2.4 is output reachable, i.e. that the C_1 output matrix has linearly independent rows or that $D_1 \neq 0$ (see Appendix A for definitions). Since the estimator in Fig. 2.4 is assumed to be a true model of the plant, the estimator will then be state reachable and the estimates $\hat{z}^{\mathrm{OE}}_{k|k-1}$ and $\hat{z}^{\mathrm{OE}}_{k|k}$ output reachable as well.

11.12.2 General feedback control structure

It follows from the discussion above that both the state and output reachability of the estimator in Fig. 11.1 are determined by the state and output reachability of the plant. The same is true for the observability that is a necessary requirement for feedback control, i.e. if control through feedback from $y_{1,k}$ is possible then also control through feedback from $\hat{y}^{\mathrm{OE}}_{k|k-1}$ or $\hat{y}^{\mathrm{OE}}_{k|k}$ is possible. We may thus make use of all available controller designs for the general feedback structure in Fig. 11.9, where we again assume that the primary y_1 output is not generally available.

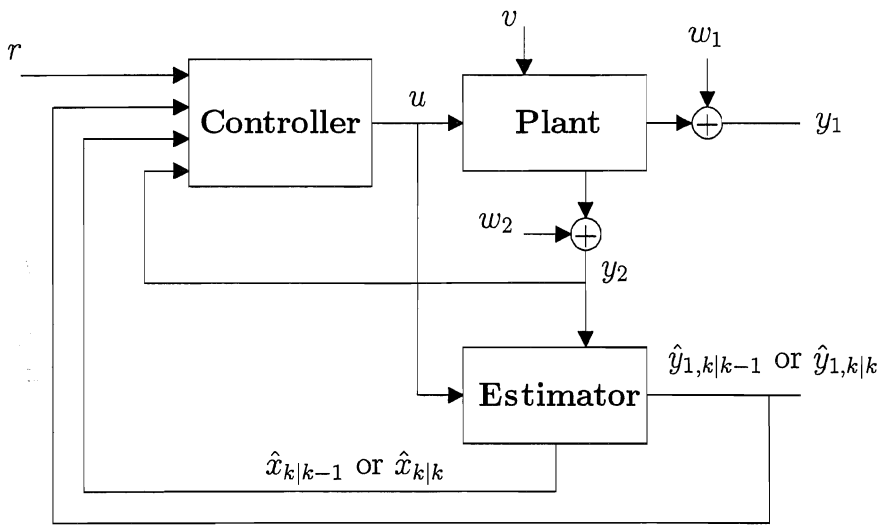

Fig. 11.9 General feedback structure for plant with state and primary output estimator.

The quality of the state and primary output estimates is certainly poorer than with y_1 measurements available, but the estimates may still be useful for feedback control. However, the questions of detailed designs and expected performances for different controller realizations are left for further research.

11.12.3 Modified Smith predictor

An interesting option utilizing secondary measurement information in a modified Smith predictor may be the control structure outlined in Fig. 11.10. It is here assumed that the dead-time in the system is located at the output, only affecting the primary y_1 measurements, and that the primary output is sampled at the same rate as u and y_2. This is basically an ordinary Smith predictor (e.g. Seborg et al., 1989), modified by use of the secondary y_2 information in the inner loop.

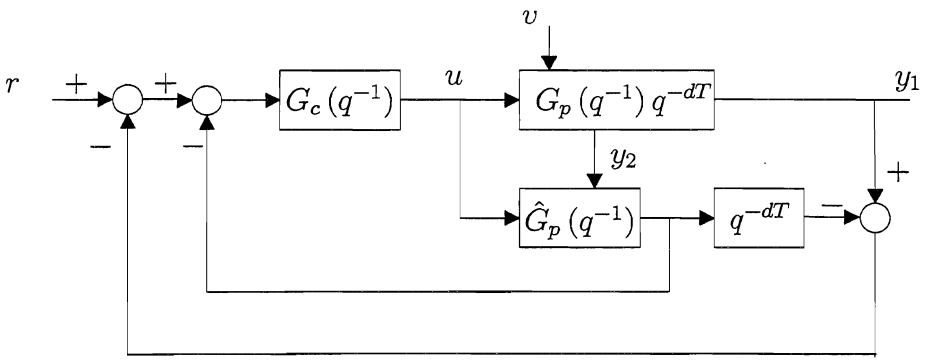

Fig. 11.10 Modified Smith predictor control structure with high primary output sampling rate.

When the primary output is measured at a low sampling rate, the outer feedback loop may be altered as shown in Fig. 11.11, where I is an extra regulator with integral action.

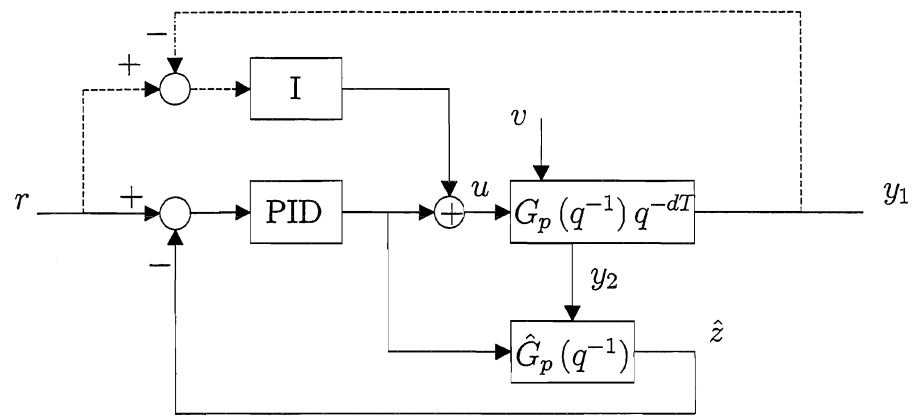

Fig. 11.11 Modified Smith predictor control structure with low primary output sampling rate.

11.13 Dynamical errors-in-variables problems

A simple dynamical errors-in-variables problem was discussed in Section 3.4. The possibilities to use the methods developed in the theses on more complicated problems of this type is left for further research.

11.14 Non-linear applications

The basic concepts and methods of the thesis might be applied also in non-linear cases, both industrial and e.g. biological/ecological/environmental. This represents interesting though demanding challenges for future research.

Chapter 12

Conclusions

The conclusions are presented in form of

- a block diagram showing the structure of the thesis and the interrelations between the issues discussed
- a list of the major conclusions
- a list of real data examples
- a list of further research issues.

Structure

Fig. 12.1 shows the structure of the thesis and the interrelations between the issues discussed. The conclusions concerning the different aspects of the primary output estimation problem are supported by simulations and other examples throughout the thesis. Real data examples are presented separately in Chapter 10.

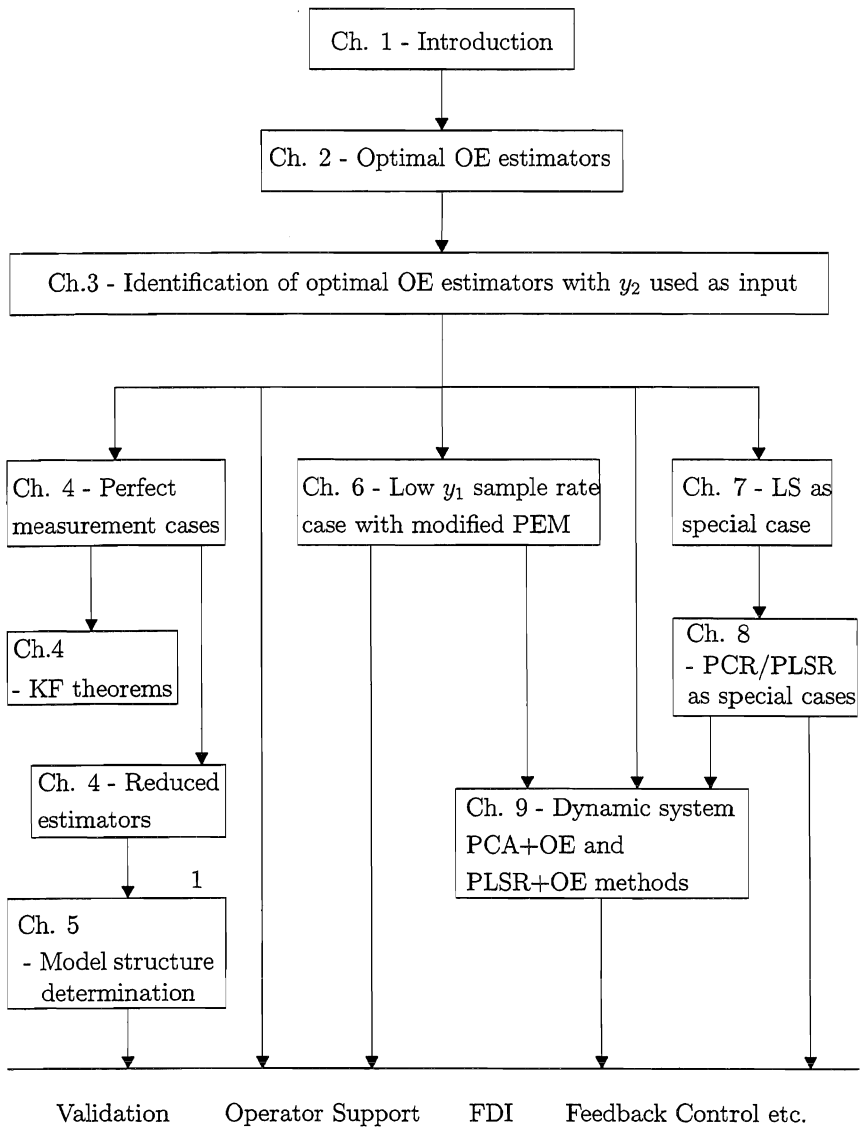

Figure 12.1 Structure of thesis (real data examples come in addition).

Conclusions

The conclusions drawn in the thesis are the following:

1. Primary output estimators for linear systems utilizing the information in known inputs and secondary outputs in an optimal way, are to be based on Kalman filters (Chapter 2).

2. When past as well as present primary outputs are not measured, the optimal estimators are based on output error (OE) models, in the sense that the Kalman gain related to the primary outputs is set to $K_1 = 0$ (Chapter 2).

3. The optimal primary output estimators can be identified from experimental data by use of both the known system inputs and the secondary measurements as estimator inputs (Chapter 3).

4. When perfect noise free secondary measurements are used as estimator inputs, it may theoretically be necessary to use reduced models, where some of the known inputs or some other secondary measurements are decoupled from influencing the estimator output (Chapters 3 and 4).

5. Reduced models may be the best practical choice also when the secondary measurements are not perfect, especially in cases with short experimental data series (Chapter 3).

6. When reduced estimators are identified, the best choice may be to use ARMAX models (Chapter 3).

7. The best estimator to use in a practical case can be found by a systematic search using different combinations of model order and sets of estimator inputs (Chapter 5). The model structure determination is then based on validation, with the inherent problem that the validation set gradually becomes a part of the total modeling set.

8. The fact that the optimal estimators are based on OE models with secondary measurements used as inputs, makes it possible to find them from experimental data with low or even irregular primary output sampling rate (Chapter 6). In industrial applications this may be of considerable practical and economical importance.

9. Ordinary linear regression with a combination of deterministic and random regressor variables, using a least squares (LS) solution, can be seen as a special case of the identification of dynamic optimal output error current (OEC) estimators (Chapter 7).

10. Principal component regression based on principal component analysis (PCA) and a least squares solution (PCR=PCA+LS), and partial least squares regression (PLSR=PLSR+LS), are regularized solutions of the ordinary linear regression problem with random regressor variables. Also these methods can thus be seen as special cases of the dynamical OEC solution (Chapter 8).

11. PCR uses a weighting matrix $W = P$ found by principal component analysis and validation, while PLSR uses $W = W_{\text{PLS}}$ normally found by an iterative procedure. Assuming a latent variable data structure, the theoretically optimal weighting matrix is in fact a Kalman gain related to the secondary measurements, i.e. $W_{\text{opt.}} = (K_2^{\text{OE}})^T$ (Chapter 8).

12. It is common chemometrical practice to collect both independent and dependent regressor variables in the X matrix, and use a one-step PCR or PLSR solution. However, with a combination of a large number of dependent and random regressor variables (secondary measurements) and a few independent and deterministic regressor variables (known inputs), it may well be that the best solution is obtained by a two-step PCA+LS or PLSR+LS solution, where the known inputs are used only in the second step (Chapter 8).

13. The optimal OE estimators for dynamic systems may be combined with the static PCA/PLSR methods. This will result in PCA+OE and PLSR+OE estimators that are optimal except for the error introduced by the PCA/PLSR data compression. This is contrary to known methods based on ARX (AutoRegressive with eXtra input) or FIR (Finite Impulse Response) models, that are biased already before the data compression (Chapter 9).

14. The PCA/PLSR+OE methods are more parsimonious (fewer parameters) than the FIR method, and thus require less experimental data (Chapter 9).

15. The PCA/PLSR+OE methods can be used in the low primary output sampling rate case, as contrary to the ARX method (Chapter 9).

16. For time series data generated by a latent variables structure, the dynamical PCA+OE and PLS+OE methods must be expected to give improved performance as compared to static PCR and PLSR solutions (Chapter 9).

The above conclusions are supported by a number of simulation experiments throughout the thesis. They are also substantiated by the real data applications presented in Chapter 10.

Real data examples

The real data examples presented in Chapter 10 are the following:

1. An experimental extruder at the Borealis polyolefine plant in Bamble, Norway. This example shows that the product quality from the extruder (polypropylene foam density) may be estimated from known inputs (gas injection pressure and heating temperature setpoint) and secondary measurements (temperatures along the extruder and outlet pressure). A dynamic first order estimator is in this example identified from high sampling rate product quality data. The practical usefulness of the estimator is in this case due to the complexity and time delay of the primary output measurement/analysis.

2. An industrial extruder for civil engineering polyethylene pipe production at the Icopal plant in Drangedal, Norway. The product quality in form of pipe diameter is in this example estimated from three known inputs (haul-off speed, rotational speed and external vacuum pressure) an one secondary measurement (internal extruder pressure). A dynamic second order estimator was here identified from low sampling rate product quality data. Although the pipe diameter measurement is easy to perform the way it is now done, the estimator is still useful due to the fact that physical measurements for practical reasons are delayed.

3. A complex industrial plant, where four product qualities are estimated on the basis of four secondary measurements. Four dynamic first order estimators (each with four inputs) were here identified from 38 low sampling rate observations of each product quality, while each secondary measurement in the modeling set had ca. 1000 samples. One of the dynamic estimators gave clearly improved performance compared with a static least squares estimator, for two other product qualities the dynamic and static estimators had approximately the same performance, while a static estimator gave the best result for the fourth product quality. Static quality estimators for this plant are now in use, and possibilities for improvements by use of dynamic estimators ought to be interesting.

4. Acoustic flow measurements on an acoustic chemometrics test rig at Telemark Institute of Technology in Porsgrunn, Norway, where the flow was a rather rapidly varying time series and where the secondary measurements were the acoustic power spectrum at 1024 frequencies. A dynamic estimator based on high sampling rate flow data, gave in this example a significant improvement as compared with static PCR and PLSR estimators. This demonstrates the feasibility of the proposed methods also for highly collinear time series data.

5. Acoustic flow measurements as described above, but now with use of only low sampling rate flow data. The improvement compared with static PCR and PLSR estimators was similar to that in the experiment described above, although the initial value problem turned out to be somewhat difficult. This demonstrates the feasibility of the proposed methods for problems where ARX models cannot be used, and where FIR solutions may be far from satisfactory.

Further research issues

The following additional issues concerning the optimal dynamic and static primary output estimators are raised in the thesis:

1. Convergence properties with secondary measurements used as estimator inputs
2. Multiple-output systems with low primary output sampling rate
3. Estimator covariance with low primary output sampling rate
4. Closed loop optimal identification
5. Use of prior knowledge
6. Validation and choice of input variables and complexity for dynamic systems
7. Estimator robustification
8. Estimator updating in the case of time-variant systems
9. Identification by use of subspace methods
10. Operator modeling and support
11. Estimators in fault detection and isolation
12. Estimators in feedback control
13. Applications on general errors-in-variables problems
14. Non-linear applications.

These issues are briefly discussed in Chapter 11, but are otherwise left for further investigation and research.

Appendix A

Kalman filtering

The optimal primary output estimators discussed in the thesis are based on Kalman filtering theory. A summary of the essential parts of this theory used in the thesis is given in the present appendix. The intention is that readers that are not familiar with Kalman filtering shall be given some basic knowledge, and find suggestions for further reading.

A.1 Statement of problem

Consider the known discrete-time plant model

$$\begin{aligned} x_{k+1} &= Ax_k + Bu_k + Gv_k \\ y_k &= Cx_k + Du_k + w_k, \end{aligned} \tag{A.1}$$

where

- x_k is the $n \times 1$ state vector, where n is the model order
- u_k is the vector of known inputs
- v_k is a stationary zero mean white noise vector sequence, with a covariance matrix determined by the expectation $R_v = Ev_k v_k^T$
- $w_k = \left[\begin{array}{cc} w_{1,k}^T & w_{2,k}^T \end{array} \right]^T$ is a stationary zero mean white noise vector sequence, with a covariance matrix determined by the expectation $R_w = Ew_k w_k^T$
- R_w is positive definite (results for the difficult perfect measurement cases are given in Doyle and Stein (1979), Shaked (1983), Shaked (1985) and Anderson and Moore (1989), and a special case is also discussed in Chapter 4)
- v_k and w_k are uncorrelated, i.e. $Ev_j w_k^T = 0$ for all j and k (may be relaxed, see e.g. Åström and Wittenmark (1990) and Grewal and Andrews (1993))

- both v_k and w_k are uncorrelated with the input u_k, i.e. $Eu_j v_k^T = 0$ and $Eu_j w_k^T = 0$ for all j and k
- (C_2, A) is detectable, which implies that the unobservable part of the system is asymptotically stable (see explanation of observability and detectability below)
- $(A, G\sqrt{R_v})$ is stabilizable, which implies that the unreachable part of the system is asymptotically stable (see explanation of reachability and stabilizability below).

For simplicity and without consequences for the result we will in the following set $D = 0$.

A.2 Detectability and stabilizability

It is possible to design a Kalman filter for the system (A.1) only if (C, A) is detectable and $(A, G\sqrt{R_v})$ is stabilizable.

A.2.1 Observability and detectability

The system (A.1) is observable if and only if the observability matrix

$$\Gamma = \begin{bmatrix} C \\ CA \\ \vdots \\ CA^{n-1} \end{bmatrix} \tag{A.2}$$

has full rank, i.e. if and only if

$$\text{rank}\,(\Gamma) = n. \tag{A.3}$$

This implies that assuming both $u_k = 0$ and $v_k = 0$ for $k \geq j$, it is possible to determine the state x_j of the system by observing y_k for $k = j, j+1, \cdots, j+n-1$.

Detectability is a weaker condition than observability, essentially equivalent to the observability of all unstable modes of the system (Lewis, 1992).

A.2.2 Reachability and stabilizability

The system (A.1) is state reachable if and only if it with $v_k = 0$ is possible to find a sequence of inputs u_k to drive the system from $x_k = 0$ to any desired state in n time steps. The requirement is that

$$\text{rank}\,(\Omega) = n, \tag{A.4}$$

where Ω is the reachability matrix

$$\Omega = \begin{bmatrix} B & AB & \cdots & A^{n-1}B \end{bmatrix}. \tag{A.5}$$

The system (A.1) is output reachable if the C matrix has linearly independent rows or if $D \neq 0$ (Ogata, 1987).

Stabilizability is a weaker condition than state reachability, essentially equivalent to the reachability of all unstable modes of the system (Lewis, 1992).

Structural reachability and observability

Systems may be non-reachable (or non-observable) due to some specific parameter values chosen, although they with other parameter values are reachable (or observable). They are then called structurally reachable (or structurally observable), see e.g. Lunze (1992) for details.

A.2.3 Kalman filter requirements

The assumptions of detectability of (C, A) and stabilizability of $(A, G\sqrt{R_v})$ make it possible to apply the Kalman filtering theory. This means that all the unstable state variables must be corrupted by the process noise v_k, and that all unstable state variables must be influencing the measurements. In addition we normally assume that R_w is positive definite, i.e. that all measurements are corrupted by noise. Also note that process and measurement noise components that are not white must be modeled as filtered white noise, with the filter model included in the system model (A.1).

A.3 State observer

Fig. A.1 shows the system (A.1) with a state observer (assuming $D = 0$ for simplicity). The observer makes it possible to find prediction (a priori) estimates $\hat{x}_{k|k-1}$ and current (a posteriori) estimates $\hat{x}_{k|k}$ of the system state. We will later see how to find an optimal value of the observer gain K, which will turn the observer into a steady-state Kalman filter (optimal observer).

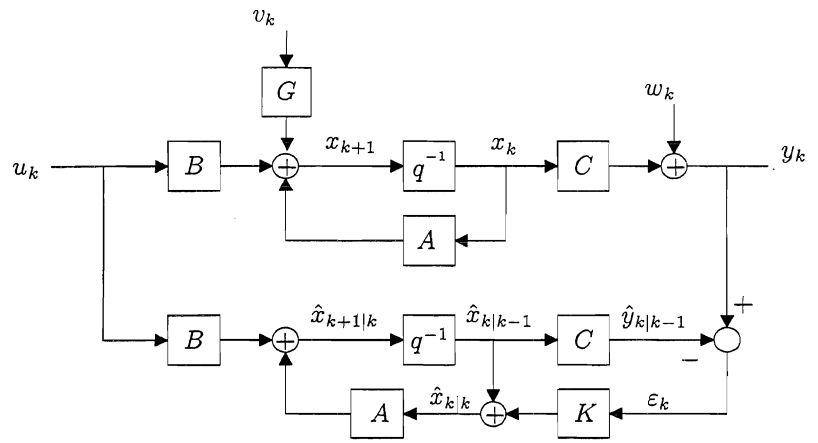

Figure A.1 Discrete-time system with in general non-optimal observer.

The observer is governed by

$$\begin{aligned}\hat{x}_{k+1|k} &= A\hat{x}_{k|k-1} + Bu_k + AK\left(y_k - \hat{y}_{k|k-1}\right) \\ &= A\hat{x}_{k|k-1} + Bu_k + AKCx_k + AKw_k - AKC\hat{x}_{k|k-1}, \end{aligned} \tag{A.6}$$

and defining the prediction (a priori) state estimation error $\tilde{x}_{k|k-1} = x_k - \hat{x}_{k|k-1}$ we find from (A.1) and (A.6)

$$\tilde{x}_{k+1|k} = (A - AKC)\tilde{x}_{k|k-1} + Gv_k - AKw_k. \tag{A.7}$$

From this we see that

- the state estimation error is not affected by the known input u_k
- an initial error will decay if the estimator is asymptotically stable (and the stability is in fact always obtained, also if the system (A.1) is unstable)
- after the decay of the initial error, the state estimation error is driven by the process noise v_k and the measurement noise w_k.

Somewhat loosely we can now make the following observations:

- With a large estimator gain K the initial state estimation error will decay rapidly. At the same time the error due to v_k will be small, while the error due to w_k will be large.
- With a small estimator gain K the errors due to v_k will be more prominent, while the errors due to w_k will be small.

This indicates that there exists an optimal value of K, in some way dependent on the ratio between process and measurement noise covariances.

A.4 Optimal state observer - Kalman filter

Definition of optimal gain

We will now assume a variable gain K_k and determine the optimal gain to use in the state observer in Fig. A.1. In order to define an optimization criterion function we introduce also the current (a posteriori) state estimation error $\tilde{x}_{k|k} = x_k - \hat{x}_{k|k}$ and the state estimation covariances expectations

$$P_k^{\mathrm{P}} = E\tilde{x}_{k|k-1}\tilde{x}_{k|k-1}^T \tag{A.8}$$

and

$$P_k^{\mathrm{C}} = E\tilde{x}_{k|k}\tilde{x}_{k|k}^T. \tag{A.9}$$

The optimal gain K_k is now defined as the gain that minimizes P_k^{P} and P_k^{C}.

Relation between P_k^P and P_k^C

From Fig. A.1 we find that

$$\hat{x}_{k|k} = (I - K_kC)\hat{x}_{k|k-1} + K_kCx_k + K_kw_k, \tag{A.10}$$

and thus

$$\tilde{x}_{k|k} = x_k - \hat{x}_{k|k} = (I - K_kC)\tilde{x}_{k|k-1} - K_kw_k. \tag{A.11}$$

Since $\tilde{x}_{k|k-1}$ and w_k according to (A.7) are uncorrelated, this results in

$$P_k^{\mathrm{C}} = (I - K_kC)P_k^{\mathrm{P}}(I - K_kC)^T + K_kR_wK_k^T. \tag{A.12}$$

Optimal choice of K_k

Assume now that P_k^{P} is minimized by an optimal choice of K_j for all $j < k$, and determine the value of K_k that minimizes the criterion function

$$J_k = \mathrm{trace}\left(P_k^{\mathrm{C}}\right). \tag{A.13}$$

In order to find the value of K_k which provides a minimum, we take the partial derivatives of J_k with respect to K_k and equate the result to zero. We may then use the following relation, valid when H is symmetric (Gelb, 1974):

$$\frac{\partial}{\partial A}\left[\mathrm{trace}\left(FHF^T\right)\right] = 2FH. \tag{A.14}$$

The result is

$$\frac{\partial}{\partial A}\left[\mathrm{trace}\left(P_k^{\mathrm{C}}\right)\right] = -2(I - K_kC)P_k^{\mathrm{P}}C^T + 2K_kR_w \tag{A.15}$$

and thus

$$K_k = P_k^{\mathrm{P}}C^T\left(CP_k^{\mathrm{P}}C^T + R_w\right)^{-1}. \tag{A.16}$$

Riccati equation

With the optimal K_k in (A.16) inserted into (A.12) we find

$$P_k^{\mathrm{C}} = P_k^{\mathrm{P}} - P_k^{\mathrm{P}} C^T \left(C P_k^{\mathrm{P}} C^T + R_w \right)^{-1} C P_k^{\mathrm{P}}. \tag{A.17}$$

From Fig. A.1 we further find

$$\hat{x}_{k+1|k} = A\hat{x}_{k|k} + Bu_k, \tag{A.18}$$

which combined with (A.1) results in

$$\tilde{x}_{k+1|k} = A\tilde{x}_{k|k} + Gv_k, \tag{A.19}$$

and thus

$$P_{k+1}^{\mathrm{P}} = A P_k^{\mathrm{C}} A^T + G R_v G^T. \tag{A.20}$$

Inserting (A.17) into (A.20) we finally find the Riccati equation

$$P_{k+1}^{\mathrm{P}} = A P_k^{\mathrm{P}} A^T + G R_v G^T - A P_k^{\mathrm{P}} C^T \left(C P_k^{\mathrm{P}} C^T + R_w \right)^{-1} C P_k^{\mathrm{P}} A^T. \tag{A.21}$$

When P_0^{P} is known from assumption or prior knowledge, (A.21) makes it possible to compute P_k^{P} as far into the future as found necessary, and the sequence of optimal Kalman gains (A.16) can then also be computed.

Steady-state Kalman filter

Assuming that the system (A.1) including the noise covariances is time-invariant, the Kalman gain K_k will stabilize into a constant gain K_∞. This gain can be determined by solving the algebraic Riccati equation

$$P_\infty^{\mathrm{P}} = A P_\infty^{\mathrm{P}} A^T + G R_v G^T - A P_\infty^{\mathrm{P}} C^T \left(C P_\infty^{\mathrm{P}} C^T + R_w \right)^{-1} C P_\infty^{\mathrm{P}} A^T, \tag{A.22}$$

which results in

$$K_\infty = P_\infty^{\mathrm{P}} C^T \left(C P_\infty^{\mathrm{P}} C^T + R_w \right)^{-1}. \tag{A.23}$$

This is the gain that turns the state observer in Fig. A.1 into an optimal steady-state Kalman filter.

Innovations

It is an essential part of the Kalman filter theory that the prediction error ε_k in Fig. A.1 becomes is a white noise sequence, i.e. $\varepsilon_k \to e_k$ when $K \to K_\infty$, with $E e_j e_k^T = 0$ for all $j \neq k$. This signal thus carries the new information in y_k that is not carried in y_{k-1}, and it is therefore called the innovations process.

A.5 Innovations form

From Fig. A.1 with $K \to K_\infty$ follows

$$\begin{aligned} \hat{x}_{k+1|k} &= A\hat{x}_{k|k-1} + Bu_k + AKe_k \\ y_k &= C\hat{x}_{k|k-1} + e_k, \end{aligned} \tag{A.24}$$

where e_k is a white noise sequence. This is an innovations form of the state-space description, and it may be used as a model of the plant itself. The advantage will then be that the two white noise sources v_k and w_k in (A.1) are replaced by the single white noise source e_k.

A.6 Continuous-time Kalman filter

Dynamical continuous-time solution

For a continuous-time system corresponding to (A.1) the Riccati equation (A.21) is altered into

$$\dot{P}^c(t) = A^c P^c(t) + P^c(t)\,(A^c)^T + G^c R_v^c\,(G^c)^T - P^c(t) C^T\,(R_w^c)^{-1}\,C P^c(t), \tag{A.25}$$

while the Kalman gain (A.16) is altered into

$$K^c(t) = P^c(t) C^T\,(R_w^c)^{-1}. \tag{A.26}$$

Steady-state solution

At statistical steady-state the algebraic Riccati equation becomes

$$0 = A^c P^c(\infty) + P^c(\infty)\,(A^c)^T + G^c R_v^c\,(G^c)^T - P^c(\infty) C^T\,(R_w^c)^{-1}\,C P^c(\infty), \tag{A.27}$$

while the Kalman gain becomes

$$K^c(\infty) = P^c(\infty) C^T\,(R_w^c)^{-1}. \tag{A.28}$$

Appendix B

Prediction error identification method

The optimal primary property estimators discussed in the thesis are identified by use of a prediction error method. The essential features of this method are presented below, and some suggestions for further reading are given.

B.1 Basic principle

The prediction error method used is based on the Kalman filtering theory presented in Appendix A. A predictor with the structure of a Kalman filter is used, as illustrated in Fig. B.1. With a given parameter vector θ, the prediction $y^{\text{pred}}_{k|k-1}$ results in a prediction error $\varepsilon_k(\theta)$. A scalar criterion function

$$V_N(\theta) = h\left[\frac{1}{N}\sum_{k=1}^{N}\varepsilon_k(\theta)\varepsilon_k^T(\theta)\right] \tag{B.1}$$

is computed, with $h[\cdot] = \det[\cdot]$ or $h[\cdot] = \text{trace}[\cdot]$, and based on the N experimental u_k and y_k data assumed available.

The parameter vector is then successively modified by an iterative numerical minimization algorithm, and asymptotically ($N \to \infty$) it is possible to tune the predictor into a Kalman filter by minimization of $V_N(\theta)$. We will then obtain $\theta \to \theta_0$, where θ_0 is the exact parameter vector assumed to exist. We will also obtain that $\varepsilon_k(\theta) \to \varepsilon_k(\theta_0) = e_k$, where e_k is the innovations process in the Kalman filter.

In Fig. B.1 the output matrix C is not tuned. This is because we choose a canonical model representation with $C = \begin{bmatrix} I & 0 \end{bmatrix}$ (e.g. Kailath, 1980).

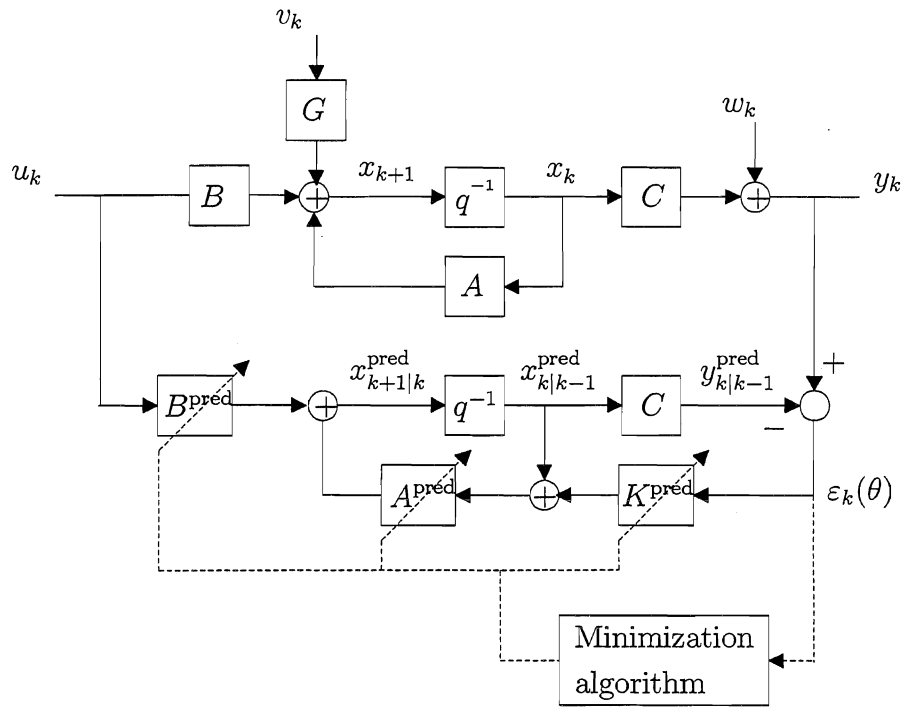

Figure B.1 Basic principle for prediction error identification method.

See e.g. Ljung (1987,1999) and Söderström and Stoica (1989) for more detailed theoretical treatments of this prediction error method.

B.2 Model specification

In the thesis we make use of the *pem.m* function in the System Identification Toolbox for use with Matlab, and in the following we give some information on the model specification. For details see Ljung (1995).

Innovation form

The system is assumed to be represented by the innovations form (A.24), i.e.

$$\begin{aligned} \hat{x}_{k+1|k} &= A\hat{x}_{k|k-1} + Bu_k + AKe_k \\ y_k &= C\hat{x}_{k|k-1} + e_k, \end{aligned} \tag{B.2}$$

where K is the steady-state Kalman gain.

State-space models

The model can be specified by the structure of the matrices A, B and K in Fig. B.1, together with the initial state x_0. Some of the parameters may be fixed, based on prior knowledge, and coupled parameters may be specified. Also the direct input-output matrix D can be specified. With $K = 0$ we obtain output error (OE) models.

Specification of state-space models is the main method used in the thesis. Time delays in the inputs or outputs can be handled by data vector shifting.

Polynomial black-box models

The model can also be specified by use of the general input-output form

$$A(q^{-1})y_k = \frac{B(q^{-1})}{F(q^{-1})}u_{k-nk} + \frac{C(q^{-1})}{D(q^{-1})}e_k, \tag{B.3}$$

where in the single input single output (SISO) case

$$\begin{aligned} A(q^{-1}) &= 1 + a_1q^{-1} + a_2q^{-2} + \cdots + a_{na}q^{-na} \\ B(q^{-1}) &= b_0 + b_1q^{-1} + b_2q^{-2} + \cdots + b_{nb}q^{-nb} \\ F(q^{-1}) &= 1 + f_1q^{-1} + f_2q^{-2} + \cdots + f_{nf}q^{-nf} \\ C(q^{-1}) &= 1 + c_1q^{-1} + c_2q^{-2} + \cdots + c_{nc}q^{-nc} \\ D(q^{-1}) &= 1 + d_1q^{-1} + d_2q^{-2} + \cdots + d_{nd}q^{-nd}, \end{aligned} \tag{B.4}$$

and where nk is the number of extra unit time delays.

With multiple inputs (MISO) we must specify different $B(q^{-1})$ and $F(q^{-1})$ polynomials for each input, and this will lead to a model order that is higher than theoretically necessary. On the other hand it is quite simple to test out different delays for the different inputs by use of nk.

For a SISO system we specify the number of parameters to identify by

$$nn = [na, nb, nc, nd, nf, nk], \tag{B.5}$$

while a MISO system with for example three inputs is specified by

$$nn = [na, [nb_1, nb_2, nb_3], nc, nd, [nf_1, nf_2, nf_3], [nk_1, nk_2, nk_3]]. \tag{B.6}$$

In order to specify an OE model we set $na = nc = nd = 0$.

See Ljung (1995) for details of this, and for the general multiple input multiple output (MIMO) case.

Appendix C

Static multivariate calibration

As shown in Chapter 8 and Chapter 9, the optimal primary property estimators may utilize the data compression techniques used in static multivariate calibration, as it is known from the field of chemometrics. The basic features of these methods are summarized in this appendix, and basic references are given.

C.1 Principal component analysis

Principal components

Principal component analysis (PCA) is concerned with the problem of summarizing the variation in N measurements on p variables with a few judiciously chosen linear combinations (Johnson and Wichern, 1992).

Assume the data matrix

$$X = \begin{bmatrix} x_{11} & x_{12} & \cdots & x_{1p} \\ x_{21} & x_{22} & & x_{2p} \\ \vdots & & \ddots & \\ x_{N1} & x_{N2} & & x_{Np} \end{bmatrix} = \begin{bmatrix} x_1 & x_2 & \cdots & x_p \end{bmatrix} = \begin{bmatrix} \xi_1^T \\ \xi_2^T \\ \vdots \\ \xi_N^T \end{bmatrix}. \qquad \text{(C.1)}$$

The sample principal components are now defined in the following way:

- The first component is the linear combinations $\hat{p}_1^T \xi_j$ which maximizes the variance of $\hat{p}_1^T \xi_j = \xi_j^T \hat{p}_1$ for $j = 1, 2, \ldots, N$, subject to $\hat{p}_1^T \hat{p}_1 = 1$.

- The second component is the linear combinations $\hat{p}_2^T \xi_j$ which maximizes the variance of $\hat{p}_2^T \xi_j = \xi_j^T \hat{p}_2$ for $j = 1, 2, \ldots, N$, subject to $\hat{p}_2^T \hat{p}_2 = 1$ and $\hat{p}_1^T \hat{p}_2 = 0$.

- The ith component is the linear combinations $\hat{p}_i^T \xi_j$ which maximizes the variance of $\hat{p}_i^T \xi_j = \xi_j^T \hat{p}_i$ for $j = 1, 2, \ldots, N$, subject to $\hat{p}_i^T \hat{p}_i = 1$ and $\hat{p}_k^T \hat{p}_i = 0$ for all $k < i$.

The matrix of loadings

The $\hat{p}_i$ loading vectors defined above may be collected in the matrix of loadings

$$\hat{P} = \left[\begin{array}{cccc} \hat{p}_1 & \hat{p}_2 & \cdots & \hat{p}_a \end{array} \right], \tag{C.2}$$

where a is the number of components that one decides to use. It follows from the definition above that

$$\hat{P}^T \hat{P} = I. \tag{C.3}$$

The matrix of scores

The maximum variance of $\hat{p}_i^T \xi_j$ referred to above, and assuming centered X data, implies the maximizing of $\hat{p}_i^T X^T X \hat{p}_i = \hat{t}_i^T \hat{t}_i$, where $\hat{t}_i$ is the general score vector. From $X\hat{p}_i = \hat{t}_i$ follows

$$X\hat{P} = \hat{T}_{\text{PCA}}, \tag{C.4}$$

where

$$\hat{T}_{PCA} = \left[\begin{array}{cccc} \hat{t}_1 & \hat{t}_2 & \cdots & \hat{t}_a \end{array} \right] = \left[\begin{array}{c} \hat{t}_1^T \\ \hat{t}_2^T \\ \vdots \\ \hat{t}_n^T \end{array} \right]. \tag{C.5}$$

In order to find an expression for $\hat{T}_{\text{PCA}}^T \hat{T}_{\text{PCA}}$ we apply a spectral decomposition (e.g. Johnson and Wichern, 1992) of the symmetric sample covariance matrix $\frac{1}{N-1} X^T X$, resulting in

$$\begin{aligned} \frac{1}{N-1} X^T X &= \hat{\lambda}_1 \hat{p}_1 \hat{p}_1^T + \hat{\lambda}_2 \hat{p}_2 \hat{p}_2^T + \cdots + \hat{\lambda}_p \hat{p}_p \hat{p}_p^T \qquad \text{(C.6)} \\ &= \left[\begin{array}{cccc} \hat{p}_1 & \hat{p}_2 & \cdots & \hat{p}_p \end{array} \right] \left[\begin{array}{cccc} \hat{\lambda}_1 & 0 & \cdots & 0 \\ 0 & \hat{\lambda}_2 & \cdots & 0 \\ \vdots & \vdots & \ddots & \vdots \\ 0 & 0 & \cdots & \hat{\lambda}_p \end{array} \right] \left[\begin{array}{c} \hat{p}_1^T \\ \hat{p}_2^T \\ \vdots \\ \hat{p}_p^T \end{array} \right] = \hat{P}_p \hat{\Lambda}_p \hat{P}_p^T, \end{aligned}$$

where $\hat{\lambda}_1 \geq \hat{\lambda}_2 \geq \cdots \geq \hat{\lambda}_p$ are the eigenvalues of the $\frac{1}{N-1} X^T X$ matrix. From this follows

$$\begin{aligned} \hat{t}_i^T \hat{t}_j &= \hat{p}_i^T X^T X \hat{p}_j = (N-1)\, \hat{p}_i^T \left(\hat{\lambda}_1 \hat{p}_1 \hat{p}_1^T + \hat{\lambda}_2 \hat{p}_2 \hat{p}_2^T + \cdots + \hat{\lambda}_p \hat{p}_p \hat{p}_p^T \right) \hat{p}_j \\ &= \left\{ \begin{array}{l} 0, \text{ for } j \neq i \\ (N-1)\, \hat{\lambda}_i, \text{ for } j = i, \end{array} \right. \qquad \text{(C.7)} \end{aligned}$$

i.e.

$$\hat{T}_{\text{PCA}}^T \hat{T}_{\text{PCA}} = (N-1)\,\text{diag}\left(\hat{\lambda}_i\right). \tag{C.8}$$

A factor model

The basic aim of PCA is normally to summarize the useful information in $X \approx \hat{T}_{\text{PCA}}\hat{P}^T$ and leave the noise in a matrix of residuals E. Assuming an underlying latent variable vector $\tau = \begin{bmatrix} \tau_1 & \tau_2 & \cdots & \tau_a \end{bmatrix}^T$, we may thus introduce the factor model

$$\begin{aligned} X &= T_{\text{PCA}}\hat{P}^T + E = \begin{bmatrix} t_1 & t_2 & \cdots & t_a \end{bmatrix} \begin{bmatrix} \hat{p}_1^T \\ \hat{p}_2^T \\ \vdots \\ \hat{p}_a^T \end{bmatrix} + E \\ &= t_1\hat{p}_1^T + t_2\hat{p}_2^T + \ldots + t_a\hat{p}_a^T + E, \end{aligned} \tag{C.9}$$

where $1 \leq a \leq p$ is the number of principal components that one decides to use. An ordinary LS solution will now result in (C.4) above.

Singular value decomposition

We can also find estimates $\hat{T}_{\text{PCA}}$ and $\hat{P}$ by a singular value decomposition of X as

$$\begin{aligned} X &= USV^T = \begin{bmatrix} U_{\text{signal}} & U_{\text{noise}} \end{bmatrix} \begin{bmatrix} S_{\text{signal}} & 0 \\ 0 & S_{\text{noise}} \end{bmatrix} \begin{bmatrix} P^T \\ V_{\text{noise}}^T \end{bmatrix} \\ &= U_{\text{signal}}S_{\text{signal}}\hat{P}^T + U_{\text{noise}}S_{\text{noise}}V_{\text{noise}}^T = \hat{T}_{\text{PCA}}\hat{P}^T + \hat{E}. \end{aligned} \tag{C.10}$$

The number of components

The decision on the number of components a to use may be done on the basis of the eigenvalues $\hat{\lambda}_i$ introduced above. The total sample variance is equal to

$$\begin{aligned} \hat{\Sigma} &= \frac{1}{N-1}\,\text{trace}\left(X^TX\right) = \text{trace}\left(\hat{P}_p\hat{\Lambda}_p\hat{P}_p^T\right) \\ &= \text{trace}\left(\hat{\Lambda}_p\hat{P}_p^T\hat{P}_p\right) = \text{trace}\left(\hat{\Lambda}_p\right) = \hat{\lambda}_1 + \hat{\lambda}_2 + \cdots + \hat{\lambda}_p, \end{aligned} \tag{C.11}$$

and consequently the proportion of total variance due to (explained by) the kth principal component is

$$\begin{pmatrix} \text{proportion of total} \\ \text{sample variance} \\ \text{due to the } k\text{th} \\ \text{principal component} \end{pmatrix} = \frac{\hat{\lambda}_k}{\hat{\lambda}_1 + \hat{\lambda}_2 + \cdots + \hat{\lambda}_p}. \tag{C.12}$$

When PCA is used in principal component regression (PCR), the number of components can be found through validation against an independent data set (see below).

C.2 Principal component regression

Ordinary linear regression

Ordinary linear regression is the statistical methodology for estimating values of one or more response variables $y_1, y_2, \ldots, y_m$ from a collection of regressor variables $x_1, x_2, \ldots, x_p$. Assuming centered data, we thus want to find the parameter matrix B in

$$y^T = \xi^T B + \psi, \tag{C.13}$$

or with the variables collected in Y and X matrices in

$$Y = XB + \Psi, \tag{C.14}$$

and the well known least squares solution is (e.g. Johnson and Wichern, 1992)

$$\hat{B}^{\mathrm{LS}} = \left(X^T X\right)^{-1} X^T Y. \tag{C.15}$$

Principal component regression

With a large number of variables in X and a limited number of samples, we will experience a large variance in $\hat{B}^{\mathrm{LS}}$ determined by the ordinary LS solution. In many cases, however, the X variables are highly collinear, and the principal components of X may then be used to obtain a regularized solution. We thus use that $X \approx \hat{T}_{\mathrm{PCA}} \hat{P}^T$ and obtain

$$Y = \hat{T}_{\mathrm{PCA}} \hat{P}^T B + \Psi = \hat{T}_{\mathrm{PCA}} \hat{B}_T + \Psi, \tag{C.16}$$

with the LS solution

$$\hat{B}_T^{\mathrm{PCR}} = \left(\hat{T}_{\mathrm{PCA}}^T \hat{T}_{\mathrm{PCA}}\right)^{-1} \hat{T}_{\mathrm{PCA}}^T Y. \tag{C.17}$$

Since $\hat{P}^T \hat{P} = I$ and $\hat{T}_{\mathrm{PCA}} = X\hat{P}$, we have $\hat{y}^T = \hat{\tau}^T \hat{B}_T^{\mathrm{PCR}} = \xi^T \hat{P} \hat{B}_T^{\mathrm{PCR}}$, and we thus finally find the principal component regression (PCR) estimator

$$\hat{B}^{\mathrm{PCR}} = \hat{P} \left(\hat{P}^T X^T X \hat{P}\right)^{-1} \hat{P}^T X^T Y. \tag{C.18}$$

The number of components to use in PCR can be found through validation, preferably against an independent data set.

C.3 Partial least squares regression

Introduction

In PCR we form estimates of the score vectors in $\hat{T}_{\text{PCA}}$ according to (C.4) as

$$\hat{t}_1 = X\hat{p}_1 = x_1\hat{p}_{11} + x_2\hat{p}_{21} + \cdots + x_p\hat{p}_{p1}, \tag{C.19}$$

etc., and we then use the scores as regressor variables. However, it may well be that principal components that explain a lot of the variation in the X data, explain little of the Y data, and in that case the corresponding parameters in $\hat{B}^{\text{PCR}}$ will be small. The inclusion of such principal components will contribute little to the solution of the regression problem, and since also the small $\hat{B}^{\text{PCR}}$ parameters must be determined, they may in fact do more harm than good by increasing the variance in $\hat{B}^{\text{PCR}}$. This is a well known problem also in the ordinary LS case (e.g. Ljung, 1987,1999).

Wolds iterative PLSR algorithm for one y-variable

The iterative partial least squares regression (PLSR) algorithm for one y-variable was originally developed by Wold et al. (1983). The score variables $\hat{t}_1, \hat{t}_2, \ldots, \hat{t}_a$ are also here weighted sums of the x-variables, but with other weights then in the PCR solution. We thus have

$$\hat{t}_1 = X\hat{v}_1 = x_1\hat{v}_{11} + x_2\hat{v}_{21} + \cdots + x_p\hat{v}_{p1}, \tag{C.20}$$

etc., and in sum (C.4) is replaced by

$$\hat{T}_{\text{W}} = X\hat{V}. \tag{C.21}$$

As in PCR we find the number of components to be used through validation.

Assuming centered data, we will find that the loadings matrix $\hat{P}$ in (C.18) is replaced by a weighting matrix $\hat{W}_{\text{PLS}}$. In the Wold algorithm $\hat{W}_{\text{PLS}}$ for centered data is found as follows (essentially following Martens and Næs (1989)):

1. Use the "local model" $X = yw_1^T + E_w$ and find the scaled LS solution

   $$\hat{w}_1 = c_1 X^T y, \tag{C.22}$$

   such that $\hat{w}_1^T\hat{w}_1 = 1$, i.e.

   $$c_1 = \left(y^T X X^T y\right)^{-1/2}. \tag{C.23}$$

   (As we will find below, $\hat{w}_1$ plays the same role as the first loading vector $\hat{p}_1$ in the PCR method, only that this choice of $\hat{w}_1$ maximizes the covariance between the linear combination $X\hat{w}_1$ and y).

2. Use the "local model" $X = t_1\hat{w}_1^T + E_t$ and find the LS solution (since $\hat{w}_1^T\hat{w}_1 = 1$)

$$\hat{t}_1 = X\hat{w}_1 = c_1 XX^T y. \tag{C.24}$$

3. Estimate the loadings p_1 using the "local model" $X = \hat{t}_1 p_1^T + E_p$, which gives the LS solution

$$\hat{p}_1 = \left(\hat{t}_1^T\hat{t}_1\right)^{-1} X^T\hat{t}_1 = c_1^{-1}\left(y^T XX^T XX^T y\right)^{-1} X^T XX^T y. \tag{C.25}$$

4. Estimate the loading q_1 using the "local model" $y = \hat{t}_1 q_1 + e_q$, which gives the LS solution

$$\hat{q}_1 = \left(\hat{t}_1^T\hat{t}_1\right)^{-1} y^T\hat{t}_1 = c_1^{-1}\left(y^T XX^T XX^T y\right)^{-1} y^T XX^T y. \tag{C.26}$$

5. Create new data residuals

$$X_1 = X - \hat{t}_1\hat{p}_1^T \tag{C.27}$$

and

$$y_1 = y - \hat{t}_1\hat{q}_1. \tag{C.28}$$

6. Repeat step 1 to 5 using X_1 and y_1, and determine $\hat{t}_2$, $\hat{p}_2$ and $\hat{q}_2$, and repeat again until a factors $\hat{t}_1$, $\hat{t}_2$, ... , $\hat{t}_a$ etc. have been found. The number of factors to be used must be determined through validation.

7. The final estimator is

$$\hat{b}^{\text{PLSR}} = \hat{W}_{\text{PLS}}\left(\hat{P}_{\text{W}}^T\hat{W}_{\text{PLS}}\right)^{-1}\hat{q}, \tag{C.29}$$

where

$$\hat{W}_{\text{PLS}} = \begin{bmatrix} \hat{w}_1 & \hat{w}_2 & \cdots & \hat{w}_a \end{bmatrix}, \tag{C.30}$$

$$\hat{P}_{\text{W}} = \begin{bmatrix} \hat{p}_1 & \hat{p}_2 & \cdots & \hat{p}_a \end{bmatrix} \tag{C.31}$$

and

$$\hat{q} = \begin{bmatrix} \hat{q}_1 & \hat{q}_2 & \cdots & \hat{q}_a \end{bmatrix}^T. \tag{C.32}$$

It can be shown (Helland, 1988) that $\hat{V}$ in (C.21) is expressed in $\hat{W}_{\text{PLS}}$ and $\hat{P}_{\text{W}}$ so that

$$\hat{T}_{\text{W}} = X\hat{W}_{\text{PLS}}\left(\hat{P}_W^T\hat{W}_{\text{PLS}}\right)^{-1}. \tag{C.33}$$

From this follows that $\hat{P}$ in the PCR estimator is replaced by $\hat{W}_{\text{PLS}}\left(\hat{P}_{\text{W}}^T\hat{W}_{\text{PLS}}\right)^{-1}$, and the PCR estimator (C.18) is therefore replaced by

$$\begin{aligned}\hat{b}^{\text{PLSR}} &= \hat{W}_{\text{PLS}}\left(\cdot\right)^{-1}\left(\left(\cdot\right)^{-T}\hat{W}_{\text{PLS}}^T X^T X\hat{W}_{\text{PLS}}\left(\cdot\right)^{-1}\right)^{-1}\left(\cdot\right)^{-T}\hat{W}_{\text{PLS}}^T X^T y \\ &= \hat{W}_{\text{PLS}}\left(\hat{W}_{\text{PLS}}^T X^T X\hat{W}_{\text{PLS}}\right)^{-1}\hat{W}_{\text{PLS}}^T X^T y, \end{aligned} \tag{C.34}$$

i.e. the final estimator can be expressed by use of only the $\hat{W}_{\text{PSL}}$ matrix in addition to the X and y data.

Remark 21 *The scaling factor c_1 is not quite necessary (Helland, 1988), but it is a part of the Wold algorithm.*

Remark 22 *It is also possible to use the same y vector for all factors, and determine only new data matrices X_1, X_2, ..., X_{a-1} (e.g. Manne, 1987).*

Remark 23 *The score vectors in the Wold algorithm are orthogonal, i.e. $\hat{t}_i^T\hat{t}_j = 0$ for all $j \neq i$.*

Remark 24 *The scores $\hat{t}_i$ and loadings $\hat{p}_i$ do not appear in the final estimator (C.33). They are, however, valuable interpretation tools used in the chemometrical practice (e.g. Esbensen et al., 1994).*

Remark 25 *There exist also a PLSR algorithm for several y-vectors, see e.g. Martens and Næs (1989) and Høskuldsson (1996).*

Martens iterative PLSR algorithm for one y-variable

Martens (1987) has developed an alternative PLSR algorithm, with non-orthogonal score vectors. The resulting weighting matrix $\hat{W}_{\text{PLS}}$ is, however, the same as in the Wold algorithm, and it also plays the role of $\hat{V}$ in (C.21). This means that (C.33) is replaced by

$$\hat{T}_{\text{M}} = X\hat{W}_{\text{PLS}}, \tag{C.35}$$

while the PLSR estimator is the same as given in (C.34).

Non-iterative PLSR algorithm for one y-variable

Di Ruscio (1998) has shown that the PLSR estimator (C.34) can be determined non-iteratively as

$$\hat{b}^{\text{PLSR}} = K_a\left(K_a^T X^T X K_a\right)^{-1} K_a^T X^T y, \tag{C.36}$$

where K_a is a Krylov matrix (e.g. Golub and Loan, 1983) for the pair (X^TX, X^Ty),

$$K_a = \left[\begin{array}{cccc} X^Ty & X^TXX^Ty & \left(X^TX\right)^2 X^Ty & \cdots & \left(X^TX\right)^{a-1} X^Ty \end{array} \right]. \quad \text{(C.37)}$$

He further showed that the weight matrix $\hat{W}_{PLS}$ in (C.34) is given by the QR decomposition

$$K_a = \hat{W}_{\text{PLS}} R_1, \quad \text{(C.38)}$$

where R_1 is an upper triangular $a \times a$ matrix.

Bibliography

Anderson B.D.O. (1985), *Identification of scalar errors-in variables models with dynamics*, Automatica, Vol. 21, No. 6, pp. 709-716

Anderson B.D.O. and J.B. Moore (1989), *Optimal Control: Linear Quadratic Methods*, Prentice-Hall, New Jersey

Ansley C.F. and R. Kohn (1986), *Prediction mean squared error for state space models with estimated parameters*, Biometrika, 73, 2, pp. 476-473

Åström and Wittenmark (1990), *Computer-Controlled Systems: Theory and Design*, Prentice-Hall, New Jersey.

Belsley, D.A. (1991), *Conditioning Diagnostics: Collinearity and Weak Data in Regression*, John Wiley & Sons, New York

Berntsen, H. (1988), *Utvidet Kalmanfilter og multivariabel kalibrering*, Report STF48 A88019, SINTEF, Trondheim, Norway

Budman, H.M., C. Webb, T.R. Holcomb and M. Morari (1992), *Robust inferential control for a packed-bed reactor*, Ind. Eng. Chem. Res., 31, pp. 1665-1679

Chou C.T. and M. Verhaegen (1997), *Subspace algorithms for the identification of multivariable dynamic errors-in-variables models*, Automatica, Vol. 33, No. 10, pp. 1857-1869

Dayal S. and J.F. MacGregor (1997), *Recursive exponentially weighted PLS and its applications to adaptive control and prediction*, J. Proc. Contr., Vol. 7 No. 3, pp. 169-179

Di Ruscio, D. (1997), A method for identification of combined deterministic-stochastic systems, in *Applications of Computer Aided Time Series Modeling*, M. Aoki and A.M. Havenner, Eds., Springer- Verlag, New York

Di Ruscio (1998), *The partial least squares algorithm: A truncated Cayley-Hamilton series approximation used to solve the regression problem*, Modeling, Identification and Control, Vol. 19, No. 3, pp. 117-140

Doyle J.C. and G. Stein (1979), *Robustness with observers*, IEEE Transactions on Automatic Control, Vol. AC-24, No. 4, pp. 607-611

Ergon R. and D. Di Ruscio (1997), *Dynamic system calibration by system identification methods*, Proc. Fourth European Control Conference (EEC'97), Brussels, Belgium, CD-ROM

Ergon, R. (1998a), *Dynamic system multivariate calibration by system identification methods*, Modeling, Identification and Control, Vol. 19, No. 2, pp 77-97

Ergon, R. (1998b), Dynamic system calibration: The low primary output sampling rate case, *Modeling, Identification and Control*, Vol. 19, No. 2, pp. 99-107

Ergon, R. (1998c), *Dynamic system multivariate calibration*, Chemometrics and Intelligent Laboratory Systems, *Vol.* 44, pp. 135-146

Ergon, R. (1999), *On primary output estimation by use of secondary measurements as input signals in system identification*, IEEE Transactions on Automatic Control, Vol. 44, No. 4, pp. 821-825

Ergon, R. and M. Halstensen (1999), *Dynamic system multivariate calibration applied on acoustic data with low Y sampling rate*, 6th Scandinavian Symposium on Chemometrics: SSC6, Porsgrunn, Norway

Esbensen K., S. Schönkopf, T. Midtgaard and D. Guyot (1994), *Multivariate Analysis in Practice*, Camo ASA, Trondheim, Norway

Esbensen K., B. Hope, T.T. Lied, M. Halstensen, T. Gravermoen and K. Sundberg (1999), *Acoustic chemometrics for fluid flow quantifications-II: A small constriction will go a long way,* Journal of Chemometrics, 13, pp. 1-29

Faanes H., C. Gjermundbo, V. Gundersen and K. Tvedt (1997), *Statisk og dynamisk modell for forsøksekstruder ved Borealis*, student project under supervision by R. Ergon, Høgskolen i Telemark, Porsgrunn, Norway

Frank P.M. (1990), *Fault Diagnosis in Dynamic Systems Using Analytical and Knowledge-based Redundancy - A Survey and Some New Results*, Automatica, Vol. 26, No. 3, pp. 459-474

Franklin, G.F., J.D. Powell and M.L. Workman (1990), *Digital Control of Dynamic Systems*, Addison-Wesley, Mass.

Friedland, B. (1986), *Control System Design: An Introduction to State-Space Methods*, McGraw-Hill, New York

Gelb A., Ed. (1974), Applied Optimal Estimation, MIT Press, Mass.

Golub G.H., and C.F. Loan (1983), *Matrix Computations,* The John Hopkins University Press, Maryland

Goodwin G.C. and R.L. Payne (1977), *Dynamic System Identification: Experiment Design and Data Analysis*, Academic Press, New York

Grace A., A.J. Laub, J.N. Little and C.M. Thompson, *Control System Toolbox for use with Matlab*, The MathWorks Inc., Mass.

Grewal, M.S. and A.P. Andrews (1993), *Kalman Filtering: Theory and Practice*, Prentice Hall, New Jersey

Harnett, M.K., G. Lightbody and G.W. Irwin (1998), *Dynamic inferential estimation using principal components regression (PCR)*, Chemometric and Intelligent Laboratory Systems 40, pp. 215-224

Harnett, M.K., G. Lightbody and G.W. Irwin (1999), *Identification of state models using principal components analysis*, Chemometric and Intelligent Laboratory Systems 46, pp. 181-196

Helland I.S. (1988), *On the structure of partial least squares regression*, Communications in statistics, 17(2), pp. 581-607

Ho B. and R. Kalman (1966), *Efficient construction of linear state variable models from input/output functions*, Regelungstechnik, 14, pp. 545-548

Hoerl A.E. and R.W. Kennard (1970), *Ridge regression: Biased estimation for nonorthogonal problems*, Technometrics, Vol. 12, No. 1, pp. 55-67

Høskuldsson, A. (1996), *Prediction Methods in Science and Technology*, Thor Publishing, Copenhagen

Isaksen A. (1993), *Identification of ARX-models subject to missing data*, IEEE Transactions on Automatic Control, Vol. 38, No. 5, pp. 813-819

Johansson R. (1993), *System Modeling and Identification*, Prentice Hall, New Jersey

Johnson R.A. and D.W. Wichern (1992), *Applied Multivariate Statistical Analysis*, Prentice-Hall, New Jersey

Joseph, B. and C.B. Brosilow (1978), *Inferential control of processes*, AIChE Journal, Vol. 24, No. 3, pp. 485-509

Kailath T. (1980), *Linear Systems*, Prentice-Hall, New Jersey

Karstang T. (1997), *Report DSR-RES.DOC*, Norsk Hydro, Forskningssenteret, Porsgrunn, Norway

Karstang T. (1999), *Personal comment*

Kung S. (1978), *A new identification and model reduction algorithm via singular value decomposition*, Proc. 12th Asilomar Conf. on Circuits, Systems and Computers, Pacific Grove, Ca. pp. 705-714

Lewis, F.L. (1986), *Optimal Estimation: With an Introduction to Stochastic Control Theory*, Wiley, New York

Lewis, F.L. (1992), *Applied Optimal Control & Estimation: Digital Design and Implementation,* Prentice Hall, New Jersey

Ljung, L. (1978), *Convergence analysis of parametric identification methods*, IEEE Transactions on Automatic Control, Vol. AC-23, pp. 770-783

Ljung L. (1987), *System Identification: Theory for the User*, Prentice Hall, New Jersey

Ljung L. (1995), *System Identification Toolbox for use with Matlab*, The MathWorks Inc., Mass.

Ljung L. (1995), *System Identification*, Technical Report LiTH-ISY-R-1763, Linköping University, Sweden

Ljung L. (1999), *System Identification: Theory for the User*, Second Edition, Prentice Hall, New Jersey

Lunze J. (1992), *Feedback control of large-scale systems*, Prentice Hall International (UK), Hemel Hempstead

Manne R. (1987), *Analysis of two partial-least-squares algorithms for multivariate calibration*, Chemometrics and Intelligent Laboratory Systems, 2, pp. 187-197

Martens H. (1987), *A general partial least squares calibration algorithm*, NCC Note STAT/35/87, The Norwegian Computer Center, Oslo

Martens H. and Tormod Næs (1989), *Multivariate Calibration*, John Wiley & Sons, New York

Mejdell T. and S. Skogestad (1989), *Estimate of process output from multiple secondary measurements*, Proc. American Control Conference, pp. 2112-2121

Moore B.C. (1981), *Principal component analysis in linear systems: Controllability, observability and model reduction*, IEEE Transactions on Automatic Control, Vol. AC-26, pp. 17-31

Ogata K. (1987), *Discrete-Time Control Systems*, Prentice-Hall, Englewood Cliffs, New Jersey

Patton R.J., P.M. Frank and R.N. Clark (1989), *Fault Diagnosis in Dynamic Systems: Theory and Application*, Prentice Hall International, Hertfordshire, Great Britain

Qin S.J. and T.J. McAvoy (1992), *A data-based process modeling approach and its applications*, IFAC Dynamics and Control of Chemical Reactors (DYCORD+92), Maryland

Rasmussen J. (1983), *Skills, rules, and knowledge; Signals, signs, and symbols, and other distinctions in human performance models*, IEEE Transactions on Systems, Man, and Cybernetics, Vol. SMC-13, No. 3, pp. 257-266

Ricker N.L. (1988), *The use of biased least-squares estimators for parameters in discrete-time pulse-response models,* Ind. Eng. Chem. Res., 27, pp. 343-350

Roorda B. and C. Heij (1995), *Global total least squares modeling of multivariable time series*, IEEE Transactions on Automatic Control, Vol. 40, No.1, pp. 50-63

Rouse W.B., J.M. Hammer and C.M. Lewis (1988), *On capturing human skills and knowledge: Algorithmic approaches to model identification*, IEEE Transactions on Systems, Man, and Cybernetics, Vol. 91, No. 3, pp. 558-573

Seborg D.E., T.F. Edgar and D.A. Mellichamp (1989), *Process Dynamics and Control*, John Wiley & Sons, New York

Shaked U. (1983), *Optimal nearly singular estimation of continuous linear stationary uniform rank systems*, International Journal of Control, Vol. 38, pp. 275-317

Shaked U. (1985), *Explicit solution to the singular discrete-time stationary linear filtering problem*, IEEE Transactions on Automatic Control, Vol. AC-30, No. 1, pp. 34-47

Sjöberg J., T. McKelvey and L. Ljung (1993), *On the use of regularization in system identification*, IFAC 12th Triennial World Congress, Sidney, Australia, pp. 75-80

Sjöberg J., and L. Ljung (1995), *Overtraining, regularization and searching for a minimum, with application to neural networks*, International Journal of Control, Vol. 62, No. 6, 1391-1407

Söderström T. and Petre Stoica (1989), *System Identification*, Prentice Hall, Cambridge

Söderström (1981), *Identification of stochastic linear systems in presence of input noise,* Automatica, Vol. 17, No. 5, pp. 713-725

Tikhonov, A.N. and V.Y. Arsenin (1977), *Solutions of Ill-Posed Problems*, V.H. Winston & Sons, Washington, D.C.

Tylee J.L. (1983), *On-line failure detection in nuclear power plant instrumentation*, IEEE Transactions on Automatic Control, Vol. AC-28, pp. 406-415

Van Overshee P. and B. De Moor (1996), *Subspace Identification for Linear Systems*, Kluwer Academic Publishers, Dordrecht, The Netherlands

Wikström C, C. Albano, L. Eriksson, H. Fridén, E. Johansson, Å. Nordahl, S. Rännar, M. Sandberg, N. Kettaneh-Wold and S. Wold (1998), *Multivariate process and quality monitoring applied to an electrolysis process. Part II. Multivariate time-series analysis of lagged latent variables*, Chemometrics and Intelligent Laboratory Systems, 42, pp. 233-240

Wilhelmsen J.O. (1998), *Styring og overvåking av plastrørproduksjon*, M.Sc. thesis under supervision by R. Ergon, Høgskolen i Telemark, Porsgrunn, Norway

Wise B.M. (1991), *Adapting Multivariate Analysis for Monitoring and Modeling Dynamic Systems*, Ph.D. dissertation, University of Washington, Washington

Wise B.M. and N.L. Ricker (1992), *Identification of finite response models by principal components regression: Frequency-response properties*, Process Control and Quality, 4, pp. 77-86

Wise B.M., B.R. Holt, N.B. Gallagher and S. Lee (1995), *A comparison of neural networks, non-linear biased regression and a genetic algorithm for dynamic model identification*, Chemometrics and Intelligent Laboratory Systems, 30, pp. 81-89

Wold S., H. Martens and H. Wold (1983), The multivariate calibration problem in chemistry solved by the PLS method, *Proc. Conf. Matrix Pencils* (A. Ruhe, B. Kågström, eds.), March 1982, *Lecture Notes in Mathematics*, Springer Verlag, Heidelberg, pp. 286-293

Wold S. (1993), *Discussion: PLS in chemical practice*, Technometrics, Vol. 35, No. 2, pp. 136-139